The preparation and use of sterically hindered organotin compounds

Brown, Paul

Award date:
1989

Awarding institution:
University of Bath

THE PREPARATION AND USE OF STERICALLY HINDERED ORGANOTIN COMPOUNDS.

Submitted by Paul Brown B.Sc.

For the degree of Ph.D.
of the University of Bath.
1989

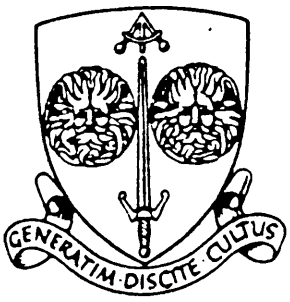

Department of Chemistry
University of Bath

Supervisor: Dr. K.C. Molloy

ProQuest LLC
789 East Eisenhower Parkway
P.O. Box 1346
Ann Arbor, MI 48106-1346

CONTENTS.

ABBREVIATIONS USED THROUGHOUT THIS THESIS.

Me	=	Methyl.
Et	=	Ethyl.
nPr	=	n-Propyl.
iPr	=	i-Propyl.
nBu	=	n-Butyl.
tBu	=	t-Butyl.
Cy	=	Cyclohexyl.
Bn	=	Benzyl.
Ph	=	Phenyl.
Mes	=	Mesityl.
(Tsi)	=	Tris(trimethylsilyl)methyl.
Ac	=	Acetyl.
EFG	=	Electric field gradient.
IS	=	Isomer shift.
QS	=	Quadrupole splitting.

ABSTRACT.

The preparation, characterisation and reaction chemistry of sterically hindered organotin halides has been investigated and their possible use as synthons for novel ring and cage chalcogenides explored. Sterically hindered organotin halides $RR'SnX_2$ (R = R' = iPr, neophyl; R = Ph, R' = tris(trimethylsilyl)methyl; X = Cl, Br) and $RSnBr_3$ (R = iPr, tris(trimethylsilyl)methyl) have been synthesised either by halogen cleavage from a mixed tetraorganotin compound, or by the direct addition of the carbanion of a sterically hindered organic substituent to a tin(IV) halide (R_2SnX_2: R = tBu, mesityl; X = Cl, Br). The latter route yields a dihalotetraorganodistannane XR_2SnSnR_2X for R = 2,4,6-tri-i-propylphenyl and X = Br for which the structure has been determined crystallographically. The attempted aqueous hydrogen halide cleavage of benzyl groups from dibenzyl[tris(trimethylsilyl)methyl]tin chloride yields two products, $(Tsi)Bn_2SnOSiMe_3$ and $(Tsi)Bn_2SnCH_2CH{=}C(SiMe_3)_2$, both of which have been structurally characterised. The postulated mechanism for the formation of these products is discussed.

The reaction of the synthesised organotin halides with sodium sulphide yields tetraorganohexachalcogenatetrastannaadamantanes $[RSnS(X_{0.5})]_4$ (R = nBu, iPr; X = O, S), tetraorganodithiadistannetanes $(RR'SnS)_2$ [R = R' = tBu, 2,4,6-tri-i-propylphenyl; R = Ph, R' = tris(trimethylsilyl)methyl] and hexaorganotrithiatristanninanes $(R_2SnS)_3$ [R = nBu and iPr]. The structure of phenyl[tris(trimethylsilyl)methyl]stannathiane has been determined crytallographically. The

hydrolysis of dihalotetraorganodistannoxanes yields mixed tetraorganooxathiadistannetanes RR'SnO(S)SnRR' [R = R' = nBu, tBu, iPr; R = phenyl, R' = tris(trimethylsilyl)methyl]. From the aerial oxidation of a postulated tetraorganothiadistannirane intermediate tetra[2,4,6-tri-i-propylphenyl]oxathiadistannetane has been synthesised and the structure determined crystallographically. Variable temperature Mossbauer data are reported for four organotin chalcogenides.

The use of sterically hindered diorganotin oxides to facilitate the introduction of oligomeric tin oxide units into cyclic boronate systems is reported. Two types of product, $tBu_2Sn[OBR(OH)]_2$ (R = Ph, mesityl) and tricyclo $\{tBu_2Sn(OH)_2[(tBu_2SnO)_2OBR]\}$ (R = Ph, mesityl) have been isolated from reactions between di-t-butyltin oxide and arylboronic acids. An example of each class has been structurally characterised.

ACKNOWLEDGEMENTS.

I would like to extend my sincere thanks to Dr. K.C. Molloy for his continued advice and undying support during my period of research. I would also like to express particular thanks to Dr. M.F. Mahon for the considerable quantity of crystallographic data detailed in this thesis. Thanks should also be extended to Mr. D.F. Wood for all nmr data, Mr. A.K. Carver for elemental analysis and Mr. C. Cryer for mass spectrometric data.

Furthermore I would like to extend my appreciation to all the academic and technical staff and particularly to my postgraduate colleagues in Bath University Chemistry Department for their assistance and support during my period of study.

In addition I am indebted to P. Kelt for her skill, patience and efficiency in the 'proof reading' of the text incorporated in this thesis.

Finally, my heartfelt gratitude should be extended to my parents, my brother and Sue for their continued support and encouragement throughout the 'ups and downs' encountered during the course of this work.

CHAPTER 1

ORGANOTIN CHEMISTRY: A SYNTHETIC, SPECTROSCOPIC AND STRUCTURAL REVIEW.

1.1 Introduction

Recent years have brought about a distinct increase in the interest shown in tin chemistry. Tin chemistry is wide-ranging, from inorganic oxides and halides through a whole chemical spectrum to a comprehensive array of synthetically useful organometallic compounds.

Tin, as an element, is the fourth member of Group IV in the periodic table. Two oxidation states, IV and II, are known, the former being the most stable in common with the earlier members of Group IV. As a result tin(IV) chemistry is the type most commonly occurring in the literature.

Industrial usage of tin is far-reaching, incorporating both inorganic and organometallic tin compounds, in a diverse cross-section of applications. The increased interest in the usage of tin compounds has resulted in an annual tin consumption of approximately 160,000 tonnes by 1980, of which nearly a quarter is composed of organotin applications.

1.2 Synthetic Preparation of Organotin Compounds

A most widely used precursor in organotin chemistry is the organotin halide R_nSnX_{4-n}. Several synthetic methods are available for the preparation of these compounds. The most commonly used industrial route is the Kocheshkov comproportionation[1,2] of a tetraorganotin with anhydrous tin(IV) chloride (equations 1-3).

$$3R_4Sn + SnCl_4 \rightarrow 4R_3SnCl \quad (1)$$

$$R_4Sn + SnCl_4 \rightarrow 2R_2SnCl_2 \quad (2)$$

$$R_4Sn + 3SnCl_4 \rightarrow 4RSnCl_3 \quad (3)$$

The above method is successful in cases where a symmetrical tetraorganotin is easily available. In other instances, especially in the case of sterically hindered organic moieties, a wide variety of organometallic reagents (metal = Li, Na, K, Mg, Al, Hg, etc.) may be reacted with anhydrous tin(IV) chloride, (equations 4 and 5) to produce the required organotin halide.

$$2RLi + SnCl_4 \rightarrow R_2SnCl_2 + 2LiCl \quad (4)$$

$$2RMgCl + SnCl_4 \rightarrow R_2SnCl_2 + 2MgCl_2 \qquad (5)$$

Having produced the required organotin halide, an extensive array of reaction chemistry is available, as shown in Scheme 1.[3]

1.3 Structural Variations in Organotin Compounds

Organotin compounds display a wide array of varying structural geometries, necessitated by the coordination range observed in organotin(IV) containing units (figures 1 and 2).

The lowest coordination number observed for organotin(IV) systems is three. In this instance only one example is at present known, in the form of a highly hindered stannaethene[4] (I).

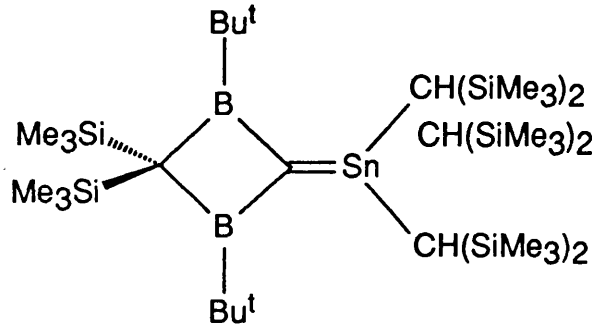

(I)

The expected planarity of the above compound is not observed and a 61° twist is present across the C=Sn double bond. However, the C=Sn bond length of 2.025Å, is consistent with that calculated for the $H_2C=SnH_2$ system.[5]

In contrast to the above unique example, for coordination number four a multitude of compounds, all displaying tetrahedral geometry,

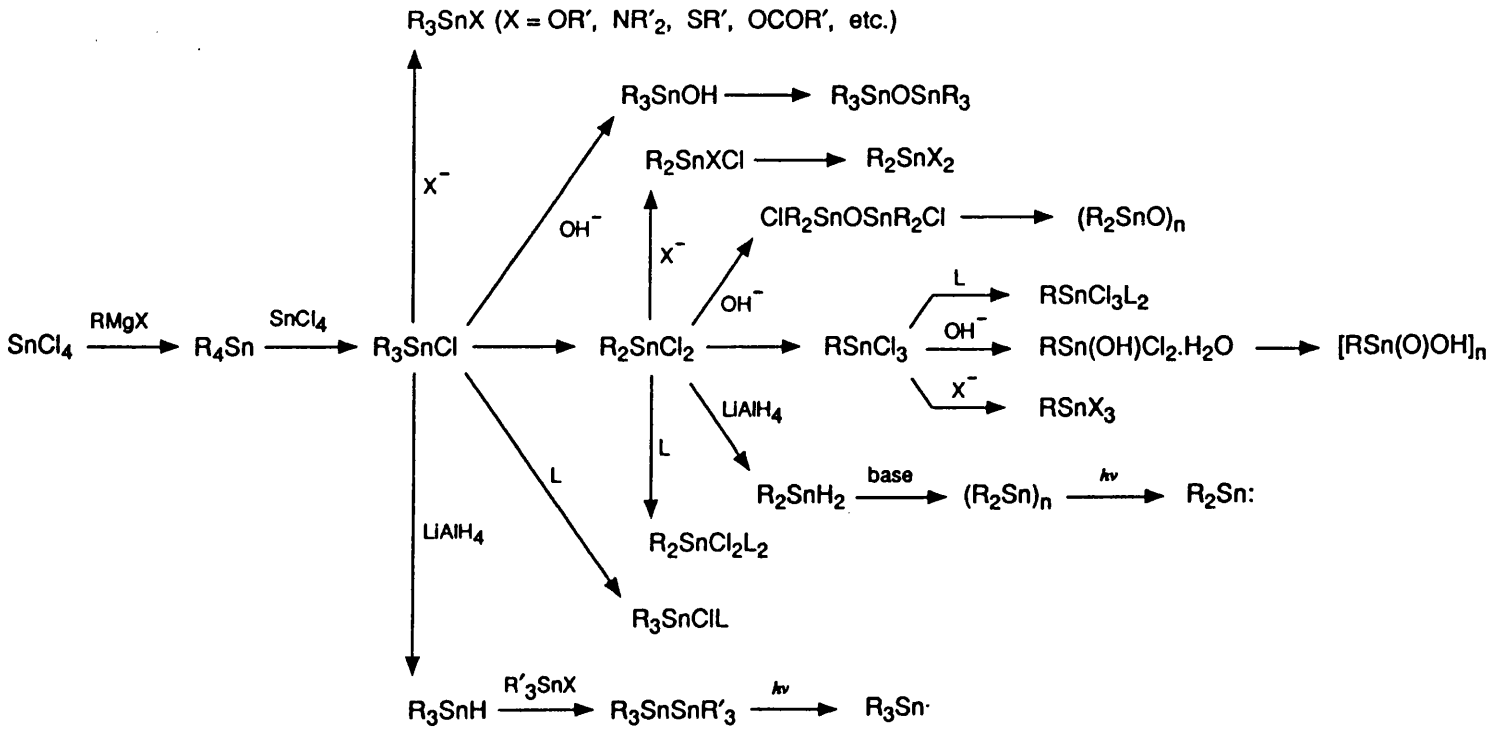
R3SnX (X = OR', NR'2, SR', OCOR', etc.)
SnCl4
RMgX
R4Sn
SnCl4
R3SnCl
X-
OH-
R3SnOH
R3SnOSnR3
R2SnXCl
R2SnX2
X-
OH-
ClR2SnOSnR2Cl
(R2SnO)n
R2SnCl2
L
RSnCl3L2
OH-
RSnCl3
RSn(OH)Cl2.H2O
[RSn(O)OH]n
X-
RSnX3
LiAlH4
L
R2SnH2
base
(R2Sn)n
hν
R2Sn:
LiAlH4
L
R2SnCl2L2
R3SnClL
R3SnH
R'3SnX
R3SnSnR'3
hν
R3Sn·

Scheme 1.

Coordination Number 4 - Tetrahedral.

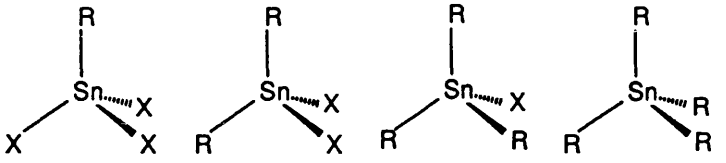

$RSnX_3$ R_2SnX_2 R_3SnX R_4Sn

Coordination Number 5 - Trigonal Bipyramidal.

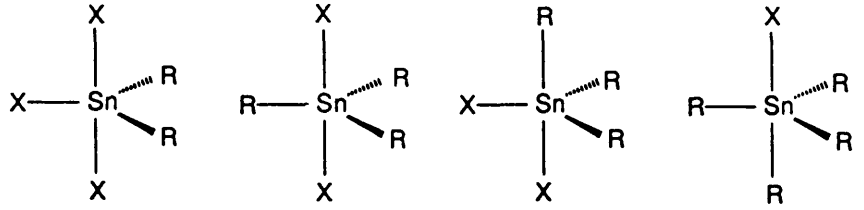

cis-R_2SnX_3 *trans*-R_3SnX_2 *cis*-R_3SnX_2 R_4SnX

Coordination Number 5 - Square Pyramidal.

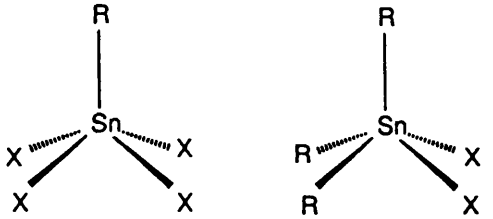

$RSnX_4$ R_3SnX_2

Figure 1: Structural Geometries of Organotin(IV) Compounds.

Coordination Number 6 - Octahedral.

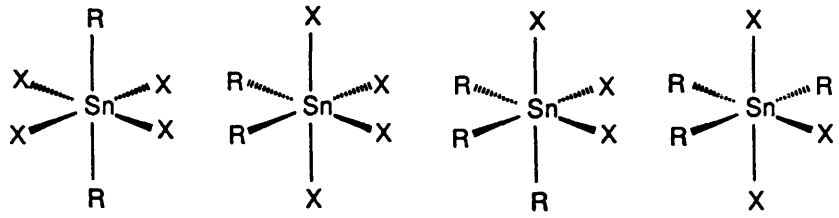

trans-R_2SnX_4 *cis*-R_2SnX_4 *fac*-R_3SnX_3 *mer*-R_3SnX_3

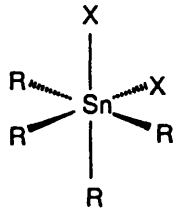

R_4SnX_2

Coordination Number 7 - Pentagonal Bipyramidal.

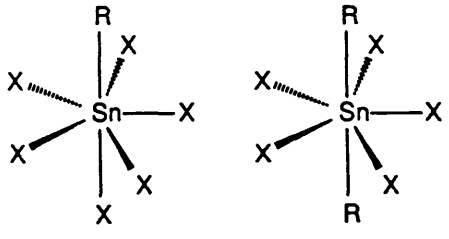

$RSnX_6$ R_2SnX_5

Figure 2: Structural Geometries of Organotin(IV) Compounds.

are known to occur. For tetraorganotins, many instances of both symmetric, e.g. p-$CH_3SC_6H_4)_4Sn$[6] and unsymmetric, e.g. Ph_3Sn(cyclopent-2-enyl),[7] can be noted. As well as R_4Sn compounds a whole range of substituted organotin compounds can be found, displaying four-coordinate geometry at tin. Suitable instances of substituted tri, di and monoorganotin compounds are given in the following examples: Ph_3Sn(1-pyrrolethio-carboxylate),[8] bis(2,4,6-tri-t-butylphenyl)dichlorotin[9] and methyltriiodotin.[10]

For coordination number five, two basic structural geometries are observed, i.e. trigonal bipyramidal and square pyramidal. These two structural types are synonymous with AB_5 five-coordinate systems, as detailed in Berry's pseudorotation mechanism,[11] where a square pyramidal structure acts as a slightly higher energy intermediate in the conversion of one trigonal bipyramidal structure to another. In organotin chemistry, examples of both structural types are available, but the most prolific is the trigonal bipyramidal.

Very few examples of five-coordinate tetraorganotins are known as a result of the poor Lewis acidic nature of the central tin, however, in compounds such as (2-carbomethoxy-1,4-cyclohexadien-1-yl)trimethyltin[12] (II), the carbonyl oxygen in the carbomethoxy grouping, forms an intramolecular tin-oxygen coordination bond, yielding the five-coordinate structure.

For multiple heteroatom substitution at tin, instances of structural isomerism increase. For substituted triorganotin compounds, the *trans* isomer is by far the most common structural form, e.g. triphenyltin chloride-ε-caprolactam.[13] The *trans* isomer is most

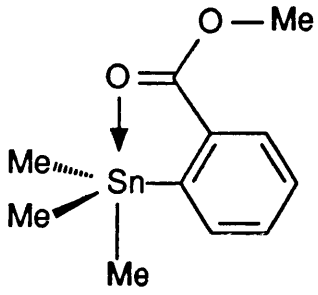

(II)

favoured when the axial substituents are of a highly electronegative nature (i.e. Cl and O in the triphenyltin chloride-ε-caprolactam example). In contrast, the *cis* isomer is favoured in cases where the R and X substituents display similar electronegativities, as shown in $\{[(CN)_2C_2S_2]SnPh_3\}(Me_4N)$.[14] In the case of the *mer* isomer, as yet no examples have been substantiated by X-ray crystallography, although based on Mossbauer spectral evidence, it has been proposed that [$Ph_3Sn(O_2C(C_6H_4)N_2R')$ R' = 4-hydroxynaphthyl],[15] is an authentic example. Further heteroatom substitution also yields examples of five-coordinate structures, for diorganotin compounds, e.g. di-n-butyltin-3-thiopropionate[16] and monoorganotin compounds, e.g. $PhClSnS(CH_2)_2O(CH_2)_2S$.[17] In the case of the former, only examples displaying *cis* geometry with respect to R are known.

Examples of square pyramidal, five-coordinate organotin compounds are far less common than the trigonal bipyramidal examples. One recent example displays an anionic tin compound held in a square pyramidal array, by two approximately isobidentate ethane-1,2-dithiolate ligands (III) for R = nBu and Ph.[18] A second instance of the square pyramidal geometry is Bn_3Sn(pyridine-N-oxide-2-thiol) for Bn = benzyl,[19] where

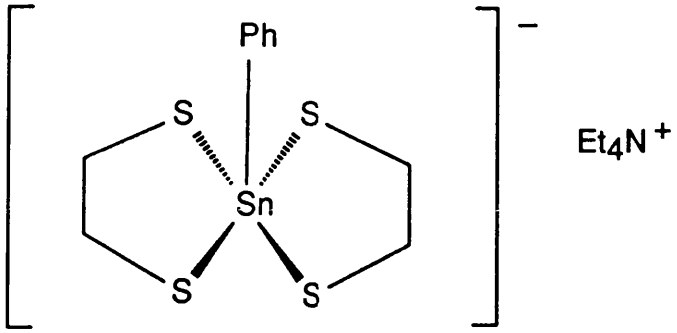

(III)

an anisobidendate ligand restricts the geometry at tin, resulting in a benzyl group attaining an apical position in the square pyramidal array.

In the case of coordination number six, octahedral geometry, both distorted and undistorted, is exclusive for organotin(IV) compounds. For tetraorganotins, only one six-coordinate example is at present known, bis[3(2-pyridyl)-2-thienyl-C,N]diphenyltin (IV),[20] in which the two Sn-X moieties display a *cis* geometric arrangement. As in the five-coordinate tetraorganotin example, intramolecular Sn-X coordination bonds exist between the poorly Lewis acidic tin and the heteroatom present (in this case X = N) in the organic substrate.

For six-coordinate triorganotin compounds only one example of each of the *fac* and *mer* isomers are known. In the case of the *fac* isomer, the known example employs a tridentate, tris(pyrazolyl)borate ligand, to bind the facial sites in tris(pyrazolyl)borate(trimethyl)tin[21] (V). The only known example of the *mer* isomer is Ph_3SnOAc[22] (figure 3). In contrast to the monomeric *fac* isomer, this example displays a polymeric chain structure with acetate bridges between the

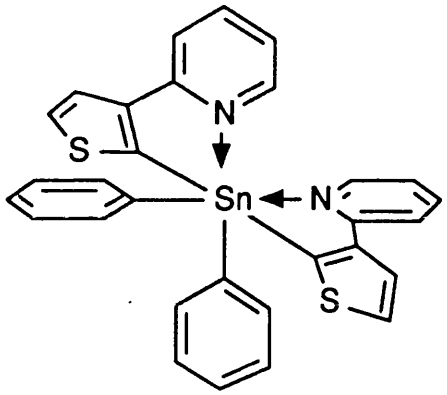

(IV)

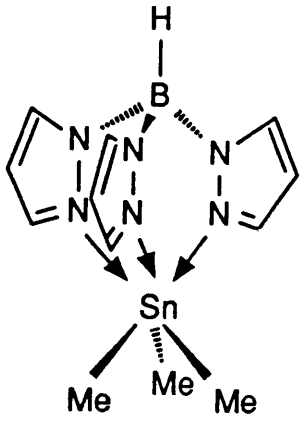

(V)

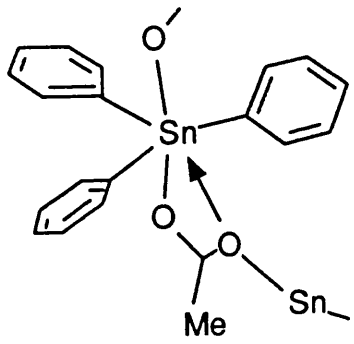

Figure 3: *mer* Structural Geometry of Triphenyltin Acetate.

triorganotin units. The phenomenon that results in the formation of the *mer* geometry is a solid state effect by which an acetate oxygen as well as providing the backbone of the polymer, also forms a relatively long intramolecular dative bond (2.349Å) to the triorganotin unit, resulting in three Sn-O bonds in a *mer* structural array.

For diorganotin compounds, a plethora of six-coordinate structures have been cited in the literature. Of these, the *trans* isomer is by

far the most common structural array, although examples of the *cis* isomer are well known, e.g. *trans*-bis(2-aminopyridinium)dimethyltetrachlorostannate[23] and *cis*-1,10-phenanthrolinedichlorodi-n-butyltin.[24] Six-coordinate examples of monoorganotin compounds are also encountered in the literature, e.g. $BuSn(OMe)Cl_2.CoCl(salen)$ salen = N,N'-ethylenebis(salicylideneaminato),[25] where the highly Lewis acidic tin attracts coordinative bonding from the oxygen atoms in the salen adduct.

The highest known coodination state for organotin(IV) compounds is seven. The structural geometry adopted by the known examples is pentagonal bipyramidal. Examples of seven-coordinate structures are known for monoorganotin, e.g. $PhSn(OSCNCH=CHCH=CH)_3$[26] and diorganotin, e.g. $Ph_2Sn(dapa)$ (H_2dapa) = 2,6-diacetylpyridinebis(2-aminobenzoylhydrazone),[27] type compounds.

1.4 Applications of Spectroscopic Techniques in Organotin Chemistry.

1.4.1 ^{119}Sn NMR Spectroscopy.

Natural tin exhibits three nmr active nuclei ^{115}Sn (0.34%), ^{117}Sn (7.57%) and ^{119}Sn (8.58%), all possessing a nuclear spin of I = 1/2. Of these, ^{119}Sn is the chosen isotope for nmr determination, due to its superior relative receptivity (4.44×10^{-3} with respect to ^{1}H) and its comparatively high natural abundance, particularly in comparison with ^{115}Sn. The chemical shift range for ^{119}Sn nmr is approximately

3000 ppm and is referenced against tetramethyltin at 0 ppm (figure 4). Many general reviews on ^{119}Sn nmr have been published,[28-31] encompassing reviews of both techniques and theoretical principles, as well as listing chemical shifts for a large variety of tin(IV) and tin(II) compounds. Additionally, two books on multinuclear nmr are also available incorporating chapters on ^{119}Sn nmr.[32,33] Complementary to solution state nmr is the technique of cross polarisation magic angle (CPMAS) solid state nmr. Although a new technique, many reviews are now available detailing both associated theoretical and practical problems as well as giving results from the systems already investigated.[34-55] Solid state investigations of organotin compounds have recently been carried out and several references are cited in the literature.[56-61]

The chemical shift for a compound gives insight into the composition and is also highly indicative of structural aspects of the compound in question. In general it is found that for increasing coordination number, an upfield shift in the ^{119}Sn nmr is observed. For an increase in coordination number, precise chemical shift ranges are not encountered, as variation in substitution at tin masks some of the effects resulting from the coordination change. However, for a related series of compounds a four to five-coordination change results in an upfield shift of between 60 and 150 ppm. For coordination changes of five to six and six to seven, upfield shifts of between 130 to 200 ppm and approximately 100 ppm respectively, are observed.[62] Examples of ^{119}Sn nmr chemical shifts for compounds of varying coordination are given in table 1.

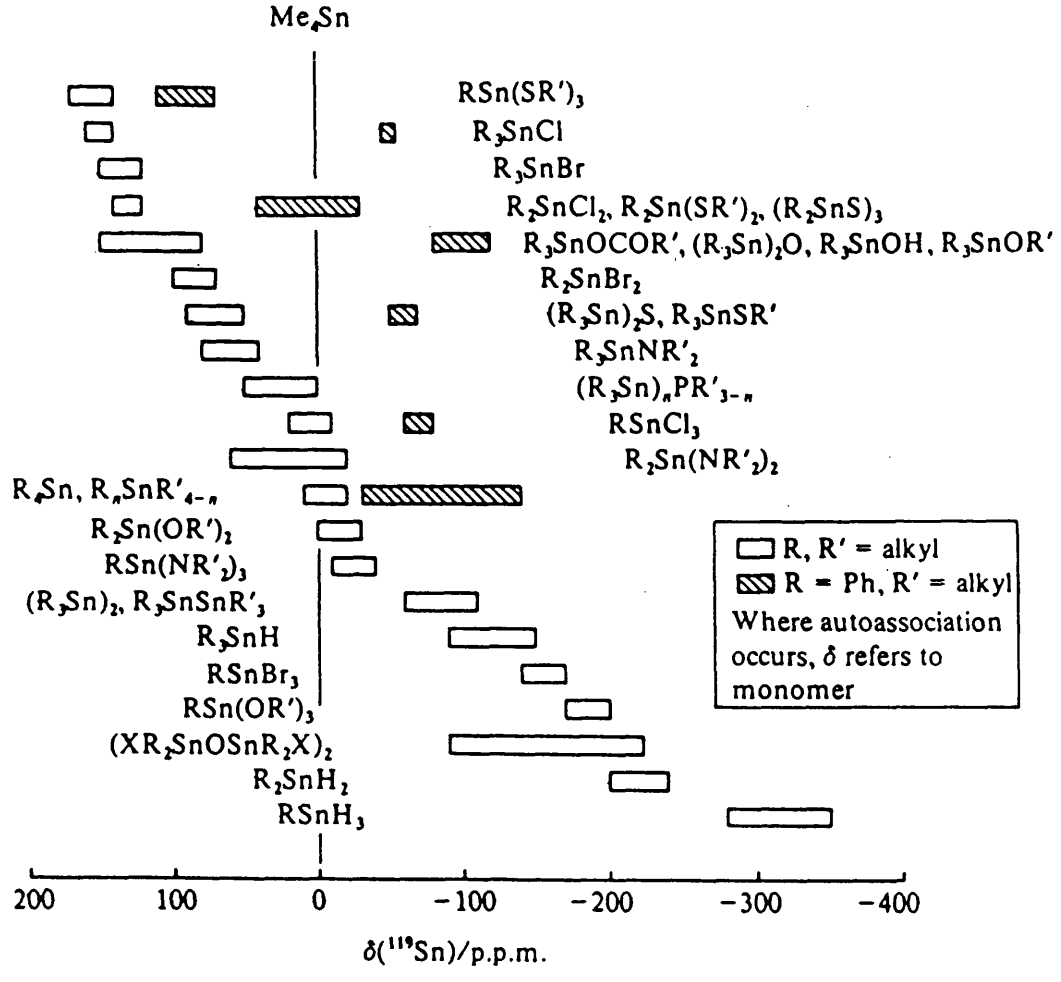

Figure 4: ^{119}Sn Chemical Shifts in Organotin Compounds.

Table 1: $\delta(^{119}Sn)$ Values for Organotin Compounds of Varying Coordination.

Compound	Geometry	$\delta(^{119}Sn)$[a]	Reference
Ph_3SnI	4 coordinate tetrahedral	-112.8	62
$Ph_3Snedtc$[b]	5 coordinate *cis* tbp[c]	-189.8	63
$Ph_3SnI.py$[d]	5 coordinate *trans* tbp[c]	-236.6	63
$PhSnCl(mdtc)_2$[e]	6 coordinate octahedral	-361	64
$Ph_2SnR(acac).C_6H_6$[f,g]	7 coordinate pbp[h]	-602	64

[a] = ppm.

[b]edtc = N,N-diethyldithiocarbamate.

[c]tbp = trigonal bipyramidal.

[d]py = pyridine.

[e]mdtc = N,N-dimethyldithiocarbamate.

[f]R = 1-(2-pyridylazo)-2-naphtholate.

[g]acac = acetylacetonate.

[h]pbp = pentagonal bipyramidal.

From the examples shown it can be seen that an increase in coordination results in an upfield chemical shift. Theoretical reasoning dictates that for a higher coordination geometry at tin an increase in the electron density on the tin atom results, causing shielding and a subsequent upfield nmr chemical shift.

Increases in the coordination at tin can be brought about as a result of a synthetic strategy to produce a required high coordination species. However, the use of coordinating solvents, e.g. pyridine, dimethylsulphoxide (DMSO), acetone etc., in the nmr solutions of tin compounds displaying a strongly Lewis acidic centre, will result in the formation of an *in situ* adduct, resulting in an increase in the coordination number and a subsequent upfield shift in the observed nmr chemical shift. This effect is exemplified by nmr solution studies of Me_3SnCl, where a +159 ppm chemical shift is observed for solutions utilising non-coordinating solvents like carbon tetrachloride compared to the -9 ppm chemical shift when pyridine is used. The adducts formed in these solutions can frequently be isolated and the structures confirmed by X-ray crystallography.[65]

For tin compounds, variations in the concentrations of the solutions examined often results in a phenomenon called 'auto-association'. For association to take place, the molecule needs to possess strongly Lewis basic substituents capable of dative bonding with the Lewis acidic tin. This effect is observed in nmr solution studies over a concentration range, for $CDCl_3$ (non-coordinating solvent) solutions of organotin compounds like $Me_3Sn(O_2CH)$.[66] As the concentration of the solution increases, an upfield chemical shift

will occur because of the formation of five-coordinate chain structures (figure 5).

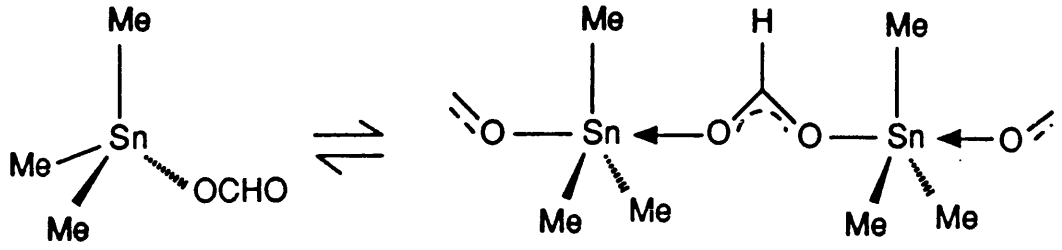

Figure 5: Autoassociation in Trimethyltin Formate.

Strong association also occurs in organotin alkoxides, where the oxygen in the alkoxide moiety acts as a strong Lewis base. However, if the Lewis basic nature of the heteroatom is reduced (e.g. organotin thiolates), then no association takes place and four-coordinate, tetrahedral species are observed in solution throughout the concentration range. However, in some examples, even with a highly Lewis basic heteroatom, the presence of sterically hindered organic substituents (e.g. tBu etc.), can prevent association, as shown in the case of mono-, di- and tri-n-butyltin alkoxides (table 2).

Variations in chemical shift so far discussed have all resulted from an alteration of the coordination sphere at tin and the resultant structural change. However, other comparatively small shift variations are observed, as a result of substituent changes at tin. It is known that high electron density at tin causes shielding resulting in an upfield shift in the nmr. It therefore follows that for increasingly electronegative substituents, electron density at tin will be diminished and a downfield chemical shift observed. This effect is

Table 2: ^{119}Sn Chemical Shifts* for Mono, Di and Tri n-Butyltin Alkoxides.

R	$(nBu)_3Sn(OR)$	$(nBu)_2Sn(OR)_2$	$(nBu)Sn(OR)_3$
Et	+86	-154	-432
tBu	+60	-31	-199

* = ppm.

observed experimentally for most organic and heteroatom substituents[28,66-70] (figure 6). In the case of unsaturated organic systems, e.g. phenyl, allyl, vinyl etc. a sharp upfield shift is observed in comparison to related saturated organotin compounds. The reason for this is thought to be associated with the degree of polarisability of the organic moiety causing shielding at tin and a resultant upfield chemical shift. For multiple substitution of electronegative groups on tin it might be assumed that a linear increase in deshielding would occur. This however is not the case and the largest downfield shift is seen to occur for n = 1 or 2 in a $R_{4-n}SnX_n$ type compound[68,71,72] (figure 7). The exact reasons for this are not as yet fully understood.

If an environment is accorded where, due to geometric constraints, the bond angles at tin are caused to vary from their ideal polyhedral value, a change in the chemical shift will result. Such a phenomenon is observed when tin is incorporated into a ring system. If the chemical shifts for some organotin ring systems are analysed, it can be seen that as ring strain increases, the variation from ideal for the tetrahedral angles increase and so a downfield shift is observed, in the ^{119}Sn nmr spectrum[73-75] (table 3).

For ^{119}Sn nmr, as with chemical shift, considerable structural information can be derived from coupling constant data. A large array of information is available detailing spin-spin coupling between ^{119}Sn and other spin active nuclei, although instances involving ^{1}H and ^{13}C are by far the most frequent. Recent nmr investigations on coupling constant values have yielded correlations between the angular geometry

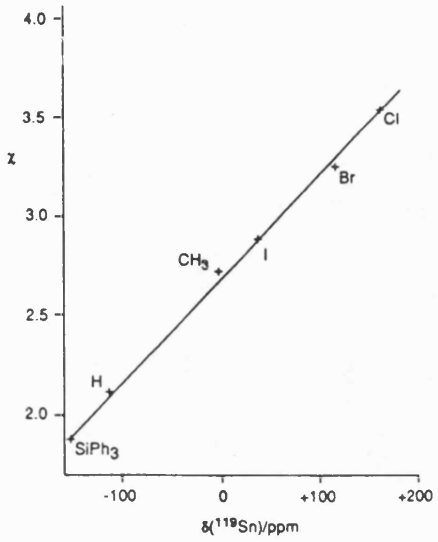

Figure 6: Dependence of ^{119}Sn Chemical Shifts (ppm) Upon Pauling Electronegativity (χ) of Substituent, for Some Me_3SnX Compounds.

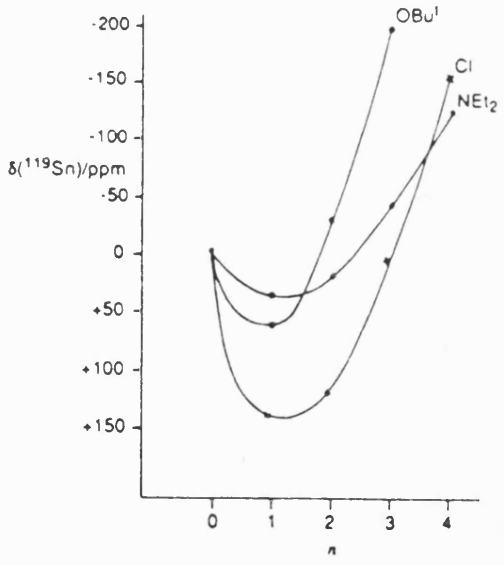

Figure 7: ^{119}Sn Chemical Shifts (ppm) for Unassociated n-Butyltin Compounds, $Bu_{4-n}SnX_n$ as a Function of n.

Table 3: ^{119}Sn Chemical Shifts* for Some Diorganostanna-Cycloalkanes and Thiocycloalkanes

Compound	δ	Compound	δ
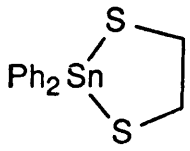	+78	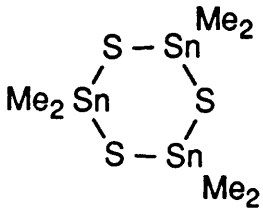	+129
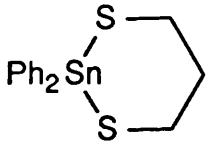	+28.5	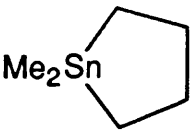	+53.5
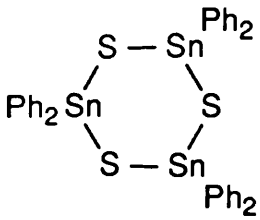	+19.5	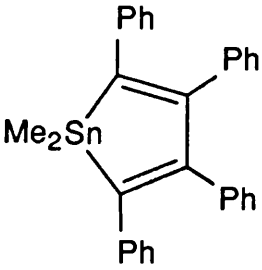	+52
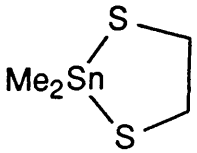	+190	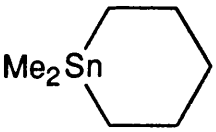	-42.5
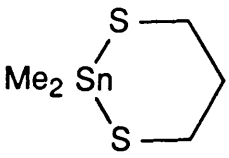	+149		

* = ppm.

at tin and the magnitude of the observed J value. One such example has yielded this type of relationship for the $^{2}J(^{119}Sn-^{1}H)$ coupling constant in methyltin compounds.[76] In the report, 25 examples were tested resulting in two empirical correlations being tendered (equations 7 and 8).

$$\theta = 0.0161(^{2}J)^{2} - 1.32(^{2}J) + 133.4 \quad (7)$$

$$\theta = 0.0105(^{2}J)^{2} - 0.799(^{2}J) + 122.4 \quad (8)$$

θ = C-Sn-C bond angle.

For the compounds tested, only two failed to conform with the former equation. In the cases of Me_2SnCl_2 and Me_2SnBr_2, when recorded in a range of solvents, the angular relationship with $^{2}J(Sn-H)$, always conformed with the latter equation.

As with $^{2}J(^{119}Sn-^{1}H)$, several relationships have been observed to exist between the angular geometry at tin and $^{1}J(^{119}Sn-^{13}C)$ coupling constants. In the recent literature, two reports have been produced postulating two empirical relationships based on the angular geometric variation at tin and the resultant diversity in the values of $^{1}J(^{119}Sn-^{13}C)$.[77,78] The former is a report on the solid state nmr spectroscopic analysis of methyltin polymers, which yields the following empirical relationship (equation 9).

$$[J] = 11.4(\theta) - 875 \quad (9)$$

The second report details $CDCl_3$ solution nmr results for a varied range of n-butyltin compounds, which generate the following empirical correlation (equation 10).

$$[J] = (9.99 \pm 0.73)\theta - (746 \pm 100) \qquad (10)$$

A known correlation also exists between the magnitude of the $^1J(^{119}Sn-^{13}C)$ coupling constant and C-Sn-C bond angle in stannacycloalkanes.[31]

The theoretical basis for these angular correlations is reported as being directly dependent on the degree of *s*-character in the Sn-C bond.[63] From this it can be seen to follow that for increases in coordination number for compounds like the *trans* trigonal bipyramidal $Ph_3SnCl.py$, where the equatorially disposed phenyl groups are bonded via an sp^2 array of orbitals at tin, a larger coupling constant than would be observed for the tetrahedral Ph_3SnCl, will result. A similar effect is observed for changes in the organic group on tin from an sp^2 hybridised phenyl group to an sp^3 hybridised alkyl group. For this change the degree of *s*-character in the Sn-C bond will decrease resulting in a reduction in the magnitude of the observed coupling constant. This is exemplified by the $^1J(^{119}Sn-^{13}C)$ coupling constants observed for nBu_3SnCl and Ph_3SnCl where respective values of 338.7 and 614.7 Hz are obtained.

1.4.2 Mossbauer Spectroscopy.

Mossbauer spectroscopy is principally associated with the two isotopes, ^{57}Fe and ^{119}Sn, however since the discovery of the Mossbauer effect in 1957,[79] more than thirty isotopes have been found to display the effect.[80] In the 31 years since the discovery, a vast array of books[81-88] and reviews[89-100] have been published, detailing the theoretical and chemical applications of the Mossbauer effect.

Mossbauer spectroscopy as a technique depends on transitions between nuclear energy levels as a result of absorbed or emitted γ-rays. To obtain an energy range of γ-rays a Doppler effect is induced on the γ-ray source, yielding an energy range according to the Doppler formula (equation 10).

$$\Delta E = (v/c)E_{\gamma} \qquad (10)$$

ΔE = change in energy of γ photon

v = velocity of source relative to absorber

c = velocity of light

E_{γ} = energy of γ-rays prior to Doppler perturbation

For different compounds of an isotope, differences in the extranuclear environment result in changes in the nuclear energy levels. The perturbed energy levels necessitate different energies for absorbance and transmittance of γ-rays, resulting in changes in the observed spectrum. Perturbation of nuclear energy levels by extranuclear

electrical effects are referred to as hyperfine interactions. Two measured parameters in Mossbauer spectroscopy arise from these hyperfine interactions, i.e. isomer shift and quadrupole splitting.

The isomer shift occurs as a result of electrostatic interactions between the charge distribution of the nucleus and those electrons, whose probability functions predict will have a finite chance of spatial incidence with the nucleus. The resultant effect is a slight perturbation of the ground and excited nuclear energy levels of the compound relative to those of the free nucleus.

From classical first-order perturbation theory, it is possible to calculate isomer shift from the s-electron overlap at the nucleus (equation 11).

$$\delta = \frac{K\delta R}{R}\{[\psi(0)_a]_a^2 - [\psi(0)_s]_s^2\} \qquad (11)$$

$[\psi(0)_a]_a^2$ = total s-electron density in the absorber

$[\psi(0)_s]_s^2$ = total s-electron density in the source

K = constant for a given isotope

$\frac{\delta R}{R}$ = change in the nuclear radius between ground and excited states.

Due to an s-electron dependence, it is found that isomer shift is a very sensitive technique for the detection of variations in oxidation state at tin, arising from a decrease in the population of the 5s-subshell for an increase in oxidation state. The range of isomer shift values is from -0.61 to +4.69 mms^{-1}, with a boundary between tin(IV) and tin(II) oxidation states taken as being +2.10 mms^{-1}, the isomer

shift for α-tin. However, ambiguities of structure do occur for compounds with isomer shifts of comparable value to that of the assumed boundary. This is exemplified by compounds like $[(Me_3Si)_2CH]_2Sn{\rightarrow}Cr(CO)_5$[101] with an isomer shift value of 2.21 mms^{-1}. In this compound dative bond formation through electron donation from tin results in a lowering of the isomer shift value from a distinct tin(II) to a *pseudo* tin(IV) species.

Isomer shift values also show sensitivity to changes in the electronegativities of the attached substituents. This is exemplified for the tin tetrahalides, for which increasing electronegativity of the halogen results in a decrease in the isomer shift value from SnI_4 at 1.47 mms^{-1} to SnF_4 at -0.27 mms^{-1}. [102-104] (For SnF_4 an unusually large decrease in the isomer shift occurs not only through electronegativity effects but also as a result of an extended fluorine bridged structural network.) The decrease in isomer shift is also observed for an increase in the electronegativity of the organic group. This is exemplified by the series nPr_3SnCl,[105] Me_3SnCl,[106] Ph_3SnCl[107] and $(C_6F_5)_3SnCl$[108] where the observed isomer shifts gradually decrease from 1.62 to 1.21 mms^{-1}.

The quadrupole splitting is generated as a result of interactions between the electric field gradient (EFG) tensor, resulting from a non-cubic extranuclear geometry and the quadrupole of a non-spherical nucleus. The consequence of this effect is a partial degeneracy removal of $I > 1/2$ nuclear energy states (figure 8). The partially degenerate $I = 3/2$ energy level is responsible for the typical two line spectrum observed for low symmetry tin compounds. From the

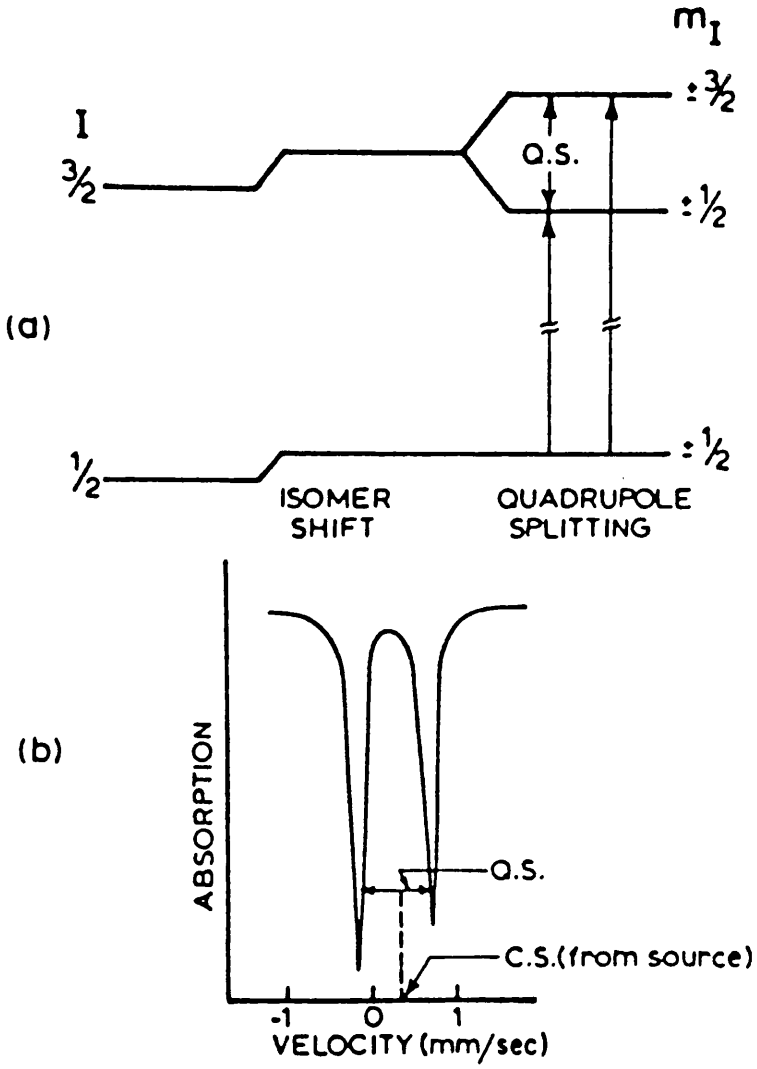

Figure 8: Nuclear Energy Levels, the Isomer Shift and Quadrupole Splitting for I_{gr} = 1/2, I_{ex} = 3/2 and the Resultant Mossbauer Spectrum.

spectrum the two required parameters can be measured, where the quadrupole splitting is the separation between the two observed peaks and the isomer shift is the point equidistant between them. The EFG tensor is a measure of the distortion of the ligand field and hence of the electron distribution, surrounding the object atom. Therefore, in cases of totally spherical substitution at the object atom, no EFG tensor results and hence no quadrupole splitting is observed. However, for other situations where an EFG tensor does occur, quadrupole splitting will be observed. The magnitude of the quadrupole splitting for ^{119}Sn is given by the following relationship (equation 12).

$$\Delta E_Q = E_{3/2} - E_{1/2} = \frac{e^2qQ}{2}\left(1+\frac{\mu^2}{3}\right)^{1/2} \qquad (12)$$

$E_{3/2}$ = energy of $m_I = \pm 3/2$

$E_{1/2}$ = energy of $m_I = \pm 1/2$

e = electronic charge

μ = asymmetry parameter

The asymmetry parameter μ is related to the three principal moments of the EFG tensor (equation 13).

$$\mu = \frac{|(\delta^2V/\delta y^2 - (\delta^2V/\delta x^2)|}{(\delta^2V/\delta x^2)} \qquad (13)$$

The value of the quadrupole splitting gives a valuable, if not always unequivocal, insight into the structural geometry at tin. Correlations

between the observed quadrupole splitting and the structural geometry at tin can be noted (table 4).

Theoretical models have been postulated to try to predict the quadrupole splitting values for changing geometry at tin. By the application of point-charge approximations for each of the substituents directly bonded to tin, and the use of molecular point-group symmetry, the major trends for quadrupole splitting values for varying structural type, have been determined. For example, in the case of octahedral R_2SnL_4 systems the quadrupole splitting value for the *trans* isomer would be expected to be twice that for the *cis* isomer; $RSnL_5$ and *cis* R_2SnL_4 systems should have equivalent quadrupole splitting values and for tetrahedral geometry an R_2SnL_2 system should display a quadrupole splitting value 1.6 times that expected for $RSnL_3$ and R_3SnL cases.[100,116] Important discrepancies occur between the theoretical and observed values for quadrupole splitting, because of the inability of the ionic, highly symmetrical model to mimic real organotin structures that are covalently bonded and frequently display low symmetry, distorted geometries.

An alternative method for the theoretical calculation of quadrupole splitting values for diorganotin compounds can be obtained by the use of the model published by Bancroft and Sham.[117] In this model the organic substituents are assumed to be the sole cause of the quadrupole splitting. From this theory an expression is presented for quadrupole splitting in terms of the partial quadrupole splitting of the two organic substituents (R) and the C-Sn-C bond angle ($180°-2\theta$) (equation 14).

Table 4: Quadrupole Splitting Values Obtained for ^{119m}Sn Mossbauer Spectroscopic Analysis of Organotin Compounds.

Compound	QS[a]	Geometry	Reference
$Et_3SnC{\equiv}CH$	1.22	R_4Sn	109
$Ph_2Sn(C_6F_5)_2$	1.11	$R_2R'_2Sn$	110
$MeSn(C_6F_5)_3$	1.14	RR'_3Sn	110
$(Ph_3Sn)_2S$	1.17	R_3SnX	111
nBu_2SnO	2.10	R_2SnX_2	112
$Ph_3Sn[O_2CC_6H_4(N_2R)\text{-}o]$[b]	2.36	*cis*-R_3SnX_2	15
$Ph_3Sn[O_2CC_6H_4(N_2R')\text{-}o]$[c]	2.31	*cis*-R_3SnX_2	15
$Me_3SnCl.py$[d]	3.44	*trans*-R_3SnX_2	113
Me_3SnF	3.86	*trans*-R_3SnX_2	113
$Me_2Snoxin_2$[e]	1.98	*cis*-R_2SnX_4	114
$Ph_2Sn(NCS)_2.phen$[f]	2.34	*cis*-R_2SnX_4	115
$Ph_2SnCl_2.phen$[f]	3.37	*trans*-R_2SnX_4	115
$nBu_2Sn(NCS)_2.phen$[f]	4.18	*trans*-R_2SnX_4	115

[a] = mms^{-1}.

[b] R = 2-hydroxy-5-methylphenyl.

[c] R' = 2-hydroxynaphthyl.

[d] py = pyridyl.

[e] oxin = oxinate.

[f] phen = *o*-phenanthroline.

$$|QS| = 4(R)[1-3\sin^2\theta\cos^2\theta]^{1/2} \qquad (14)$$

The greatest accuracy is achieved for the model when the partial quadrupole splitting is much greater for the organic substituents than that exerted by the other attached groups. This occurs in the case of directly bonded oxygen, nitrogen and halogen bonded ligands.

A major effect in Mossbauer spectroscopy is the influence of the recoil-free fraction (f), on the observed Mossbauer effect. The recoil-free fraction is a dynamic effect resulting from the momentum transfer of an absorbed γ-ray. If the magnitude of the resultant recoil is comparable with the wavelength of the incoming γ-ray, then incoherent phasing of the absorbed and emitted γ-rays result in interference and a subsequent reduction of the observed Mossbauer effect. Therefore, in an unbounded system such as a gas or a liquid, recoil can take place freely, negating the Mossbauer effect. However, in a frozen gas or liquid, or in a solid, the object atoms are in a fixed matrix, resulting in a restricted recoil and allowing the Mossbauer effect to be observed.

Theory predicts that recoil-free fraction is linearly related to the area under the observed Mossbauer spectrum resulting in the following relationship being presented (equation 15).

$$A(T) \propto f(T) = \exp\{-4\pi^2\langle x^2\rangle\}{\lambda^2} \qquad (15)$$

(x^2) = Mean square amplitude of the vibration in the direction of emission of the γ-ray, averaged over the lifetime of the nuclear level involved in the γ-ray emission process.

λ = Wavelength of the Mossbauer transition.

Resultant plots of the natural logarithm of the normalised area ln[A(T)/A(78)] against T, should give straight lines with gradients dependent on the rate of decay of the resonance effect, giving rise to information on the intermolecular association of the investigated tin containing molecule.[118] Shallow slope values, from these experiments are proposed to arise from polymeric type systems, in which vibrations of the tin atom along the direction of polymer propagation are restricted.[119] The type of behaviour described is known to occur in systems where either linear or zig-zag polymeric arrays are displayed. Instances of these structures are found, for the former in $PhSnCl_3$.pyrazine and $(C_6H_{11})_3SnF$ and the latter in Ph_3SnF and $(C_6H_{11})_2SnCl_2$. Steep slopes are found in instances of loosely polymeric 'S'-type or helical arrays, or in cases of monomeric structures. In these systems only small restrictions are exerted on the tin containing unit allowing effective vibration of the tin through three dimensions. Instances of these systems are observed in $Ph_3Sn(NCS)$ and $(C_6H_{11})_3Sn(O_2CMe)$ for the 'S'-type polymer, $(Ph_3Sn)_2NCN$ for the helical polymer and Ph_3SnCl and $(C_6H_{11})_3SnBr$ as examples of monomeric structures.

1.4.3 Infra-Red Spectroscopy of Organotin Compounds.

Three major reviews on the use of infra-red spectroscopy in organotin chemistry have been produced.[120-122] Applications of infra-red spectroscopy are largely twofold. Firstly, an infra-red spectrum is highly characteristic and stands as good evidence for repeated preparation and purity. The second application of infra-red is derived from the sensitivity of the technique to structural change. An example of this occurs for the infra-red spectra of Me_3SnBr and Me_3SnOH. Tetrahedral geometry is observed for Me_3SnX (for X = Cl, Br and I), giving rise to symmetric and asymmetric Sn-C stretches, observed at 506-516 cm^{-1} and 528-536 cm^{-1}, respectively.[123] However, for Me_3SnOH, the structural geometry is a *trans* trigonal bipyramidal arrangement, with a planar Me_3Sn- unit, resulting in the symmetric Sn-C stretch no longer inducing a change in dipole moment resulting in an infra-red inactive stretching mode.[124,125]

For certain types of substituted organotin compounds, highly characteristic stretching frequencies are observed in the infra-red spectrum. This is exemplified by the Sn-H stretching frequency in tin hydrides where a single, intense peak is displayed in the observed spectrum, at approximately 1820 cm^{-1}. By monitoring changes in the intensity of the peak, valuable information on reaction progress and the kinetics of the reaction in question can be obtained. Other examples of characteristic Sn-X stretches are given in table 5.

Table 5: Characteristic Sn-X Stretches in Organotin Infra-red Spectroscopy.

Compound	Assignment	Frequency[a]	Reference
Ph_3SnH	Sn-H stretch	1825	126
Bu_2SnH_2	Sn-H stretch	1835	127
$(Me_2SnO)_n$	Sn-O-Sn stretch	580	128
$(Ph_3Sn)_2O$	Sn-O-Sn stretch	777	129-131
$(ClMe_2Sn)_2O$	Sn-O-Sn stretch	576,600	128
$(Ph_2SnS)_3$	Sn-S-Sn as. stretch	343,371	132
	Sn-S-Sn sym. stretch	303,321	
Ph_3SnBr	Sn-Br stretch	225	133
nPr_3SnCl	Sn-Cl stretch	336	134
$Et_3SnSn(nPr)_3$	Sn-Sn ax. deformation	194	135
Ph_4Sn	Sn-Ph vibration	1070	136

[a] = cm^{-1}.

1.5 Structural Variations in Inorganic and Organometallic Solids

Structural investigations of inorganic and organometallic compounds have yielded the widest possible array of structural classes available. Simplistic examples of monomeric and dimeric inorganic species are the B_4Cl_4 monomer[137] and the Nb_2Cl_{10} dimer.[138] Further structural expansion occurs for two-dimensional layer arrays, depicted in the carbon allotrope, graphite and also in a wide variety of boron nitrides. Expansion to three-dimensional lattice structures give rise to the most complex crystalline arrays encountered. Examples of these are typified for octahedral geometry, by the heteropoly molybdates and tungstates and for tetrahedral arrangements by the feldspars and zeolites. Zeolites, both natural and synthetic have generated large interest in both research and industrial environments, giving rise to a dramatic increase in the applications available.[139] As adsorption materials, zeolites are widely used for separations, drying agents and as gas scavengers. In ion-exchange the applications of zeolites cover a diverse range of areas as illustrated by their usage in the removal of metal ions from aqueous systems, radioisotope recovery from solution and regeneration of synthetic kidney dialysate by the removal of toxins. The largest area of zeolite usage, however, is as catalysts, with industrial applications in areas exemplified by alkylation, methanation, carbon monoxide oxidation and synthetic gasoline production.

For tin compounds, wide varieties of lattice types are observed. Most of the extensive lattice arrangements encountered are for

inorganic tin species, as seen for SnI_4, which displays the zinc-blende structural modification. However, for organotin compounds, as yet, the vast majority display much smaller oligomeric arrays. For many organotin compounds, in the solid state, intermolecular association gives rise to chain structures, exemplified by $Me_3SnOSOR$ (R = Me[140,141] or $CH_2C{\equiv}CH$[142]), $Bn_3SnOCOMe$[143] and Me_3SnCN.[144] For these examples, *trans* trigonal bipyramidal arrangements are observed, with the direction of chain propagation occurring through the *trans* axial sites. In a chain array, the nature of the ligand substituent controls the shape of the chain backbone, as seen in the quoted examples where the CN ligand in the latter case enforces a linear structure, while the others present helical or zig-zag arrangements. The type of substituents in the tin units can drastically alter the degree of association in chain type structures. If sterically large groups are used, either in the ligand or in the organic moieties, then association will be reduced. This effect is observed in $Cy_3SnOCOMe$[145] (Cy=cyclohexyl), where the bulk of the cyclohexyl unit reduces association to almost zero, resulting in slightly distorted tetrahedral units being present in the solid state. Association can also be removed by the use of weakly coordinating ligands e.g. dimethyldithiocarbamate, where intermolecular coordination is reduced in preference to intramolecular association. This results in the formation of discrete entities[146] rather than the chain type polymeric structures found in comparable strongly coordinating systems. Other chain structures are observed for R_2SnX_2 type compounds, e.g. Et_2SnCl_2 and Et_2SnBr_2,[147] where a distorted octahedral geometry, with

intermolecular halide bridges, constitutes the chain array.

Increased complexity in organotin structures occurs in the form of ring formation. A wide variety of ring sizes are observed in the plenitude of examples cited in the literature. As with association, two major effects are observed for the control of ring size. Firstly, control can be exerted by the use of sterically demanding substituents, where ring size decreases as the steric bulk increases (VI, VII).[148-150]

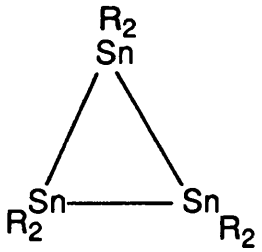

R = 2,6 - Diethylphenyl

(VI)

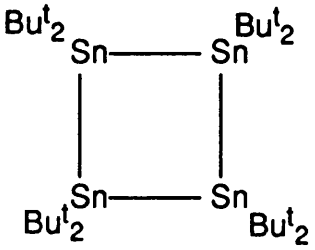

(VII)

Other types of ring systems present in organotin chemistry are the tin-heteroatom arrays. For tin-oxygen systems, extensive steric hindrance is required to restrict R_2SnO compounds to distinct ring structures as exemplified by $(tBu_2SnO)_3$[151] (VIII), $[(2,6\text{-}Et_2C_6H_3)_2SnO]_3$[148] and $[(2,4,6\text{-}Me_3C_6H_2)_2SnO]_3$.[152] For R_2SnO systems with unhindered organic substituents, amorphous sheet structures of polymeric tin oxides occur. Ring formation in tin-heteroatom systems most commonly occurs for the lower members of the chalkogens, i.e. S, Se and Te. For these, chain and sheet formation are only rarely found, with ring systems of varying sizes dominating the structural behaviour. Thus, the choice of heteroatom bonded to tin can be used as a second method of promoting ring in preference to

chain formation. The variation in ring size is not observed to change with variation of chalkogen but can be seen to be controlled through steric constraints. This phenomenon is exemplified by $(tBu_2SnS)_2$[153] (**IX**) and $(Me_2SnS)_3$[154] (**X**).

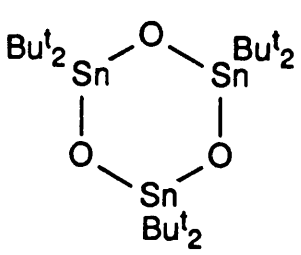

(**VIII**)

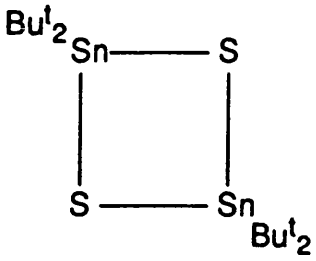

(**IX**)

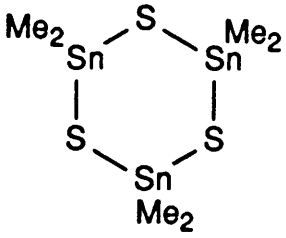

(**X**)

From ring systems, by inter-ring association, two-dimensional 'ladder' structures can be obtained. This type of structure seems to proliferate in compounds where a Lewis basic heteroatom is present in the ring system (e.g. oxygen) and where steric hindrance is low allowing close molecular association. Examples of this type of structure are $[CliPr_2SnOSniPr_2(OH)]$[155] (figure 9) and $[RSnO(O_2CC_6H_{11})_2RSn(O_2CC_6H_{11})_3]_2$ (R = nBu[156] and Me[157]).

Further structural complexity occurs, when three-dimensional cage and cluster, structures are considered. Literature examples are available, displaying simple, highly symmetrical cage structures, for example the adamantane $[(C_6F_5)Sn]_4S_6$[158] and cubane $(PhSnP)_4$[159] type cages. Less common cage structures are also in evidence, as exemplified by the structures of $[(CH_3)_2Sn]_6P_2$[160] (figure 10) and the tin(II) compound $(tBuN)_6Si_2Sn_2$[161] (**XI**).

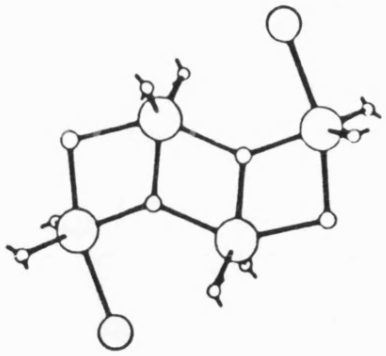

Figure 9: Asymmetric Unit of 1-Chloro-3-hydroxo-1,1,3,3-tetra-i-propylstannoxane.

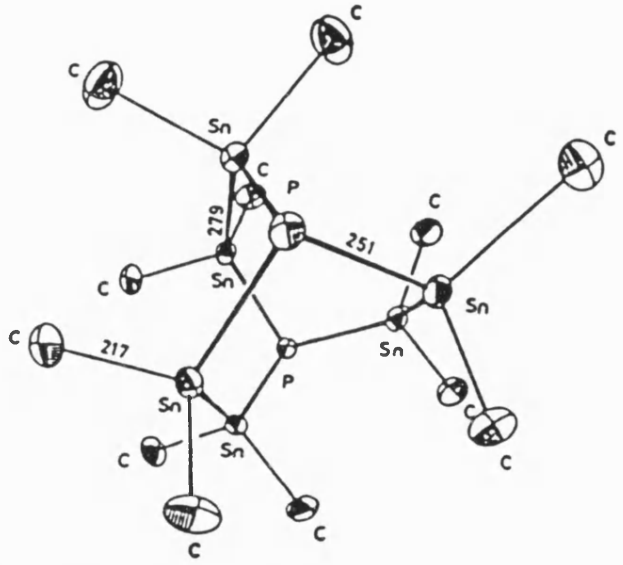

Figure 10: ORTEP Plot of $[(CH_3)_2Sn]_6P_2$.

In organotin chemistry more extensive arrays occur as a result of the combination of either rings or ladders, containing tin units with strongly Lewis basic substituents. The known 'drum' structures can be viewed as resulting from a cyclisation of ladder type structures, forming a staggered cyclic bi-layer stannoxane array. Structures of

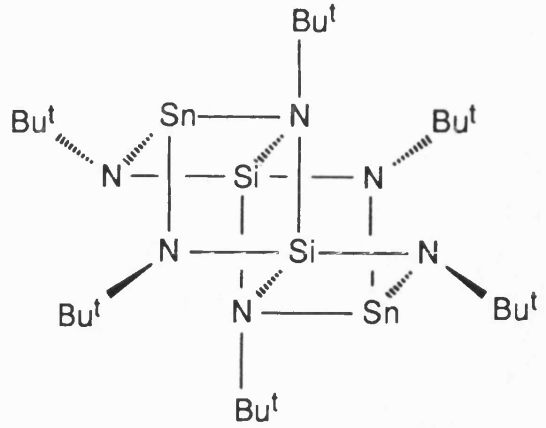

(XI)

this type are exemplified by [nBuSnO(O$_2$CR)]$_6$.C$_6$H$_6$[156] (figure 11) for R = C$_5$H$_9$ or C$_6$H$_{11}$ and [PhSnO(O$_2$CC$_6$H$_{11}$)]$_6$.[162]

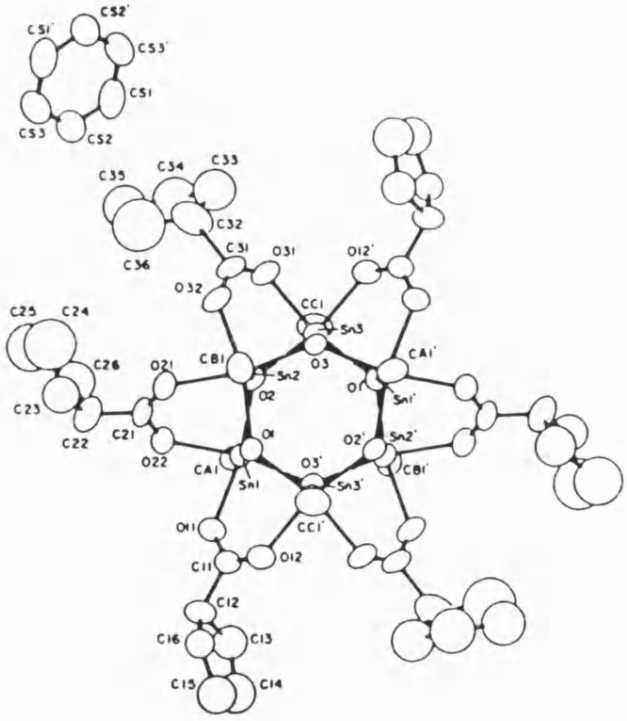

Figure 11: Asymmetric Unit of [nBuSn(O)O$_2$CC$_5$H$_9$]$_6$.C$_6$H$_6$.

A modified 'drum' type structure is also known, where effectively a

hydrolysis stage has cleaved the drum into two parts, leaving an oxygen capped cluster as the resultant cage $([nBuSn(OH)O_2PPh_2)_3O][Ph_2PO_2]$[163] (figure 12).

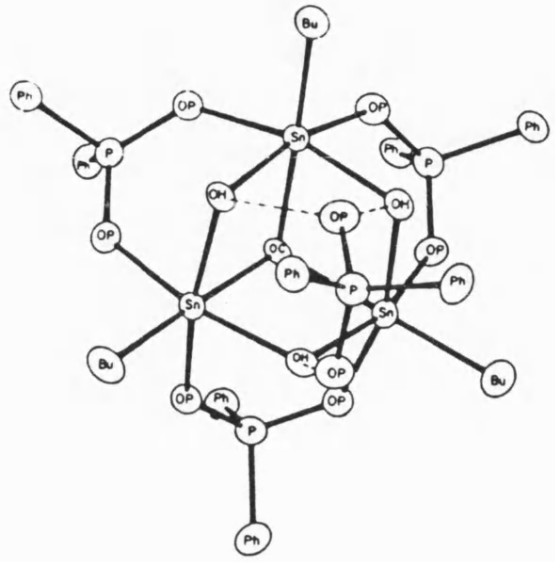

Figure 12: Asymmetric Unit of $[(nBuSn(OH)O_2PPh_2)_3O][Ph_2PO_2]$.

For organotin compounds three-dimensional crystalline networks are rare. One of the few examples known is an extensive polymer of $(Me_3Sn[Co(CN)_6])_\infty$[164] containing trigonal bipyramidal *trans* $R_3Sn(CN)_2$ units.

The use of zeolites is dependent on the extensive porous crystalline networks produced from the silicon oxide tetrahedral monomers. In contrast, the structures so far encountered in organotin chemistry, although interesting, are not as yet able to mimic the desirable properties displayed by the zeolites.

1.6 Projected Aims of This Research.

To produce new materials capable of fulfilling roles comparable with those realised for example in zeolite chemistry, synthetic strategies are required to control and manipulate the construction of the molecular architecture. This can schematically be viewed in terms of three distinct synthetic stages: ring formation, combining rings into cages and finally linking cages of a desired diameter into a network lattice (scheme 2).

In the short term it is necessary to concentrate effort into providing synthetic routes for the preparation of the basic ring systems, incorporating strong Lewis acid sites and to understand the extent of the control available in determining ring size. This thesis sets out to examine these effects with respect to ring systems incorporating tin. By the use of a mixture of steric hindrance and heteroatom variation in the ring system it should be possible to restrict polymer or sheet formation and promote the formation of discrete two or three-dimensional entities. This control would allow synthesis of ring systems (possibly of a controllable size) from diorganotin precursors, or the corresponding cage structures from monoorganotin progenitors where the three active functionalities on tin could be used in the direct formation of three-dimensional arrays.

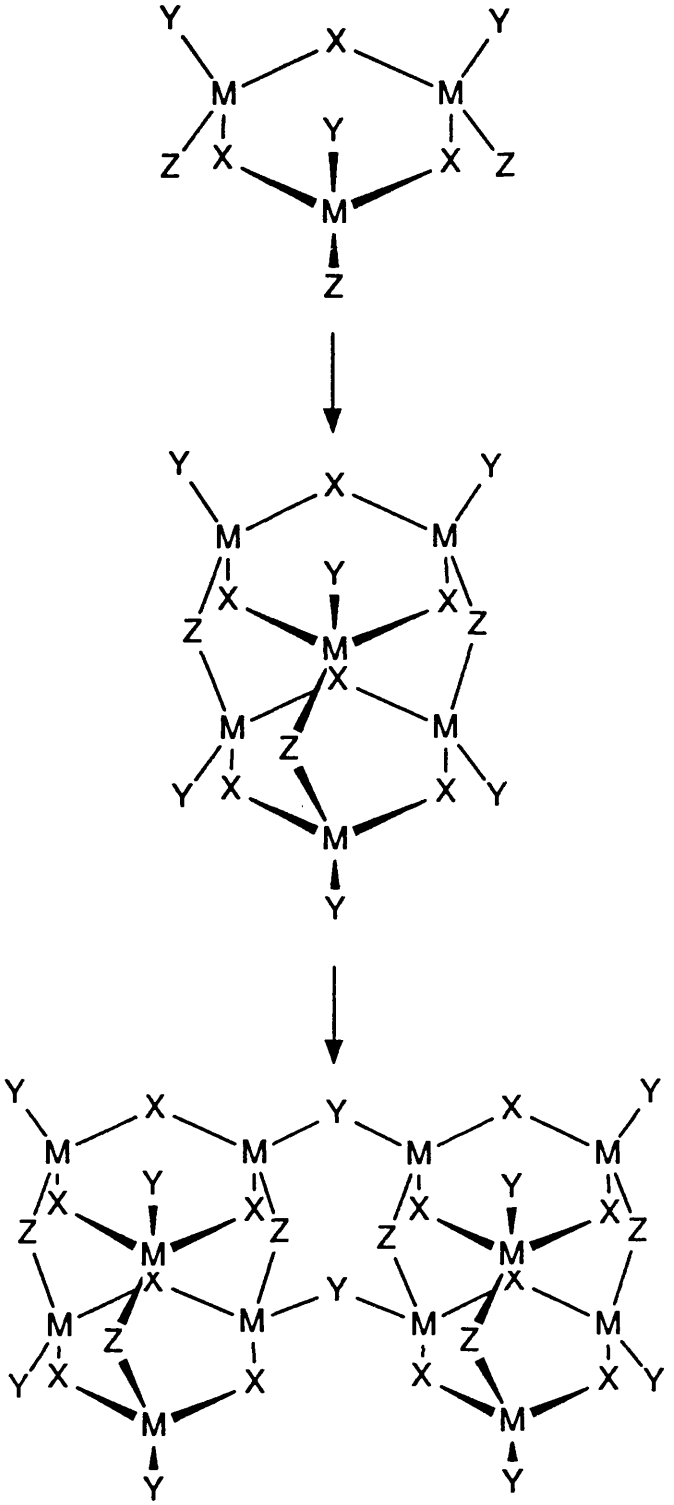

Scheme 2.

CHAPTER 2.

APPROACHES TO STERICALLY HINDERED MONO- AND DIORGANOTIN COMPOUNDS.

2.1 Introduction.

One of the methods for controlling structure in organotin compounds, discussed in chapter 1 was the inclusion of restrictive sterically hindered groups on tin to inhibit association of molecular units. The importance of this strategy is exemplified by the successful synthesis of compounds (I)[4], (XII)[165] and (XIII)[166], where the application of extremely bulky substituents on tin restricts further chemical attack, favouring oligomers with respect to polymers and kinetically stabilising reactive multiple bonds.

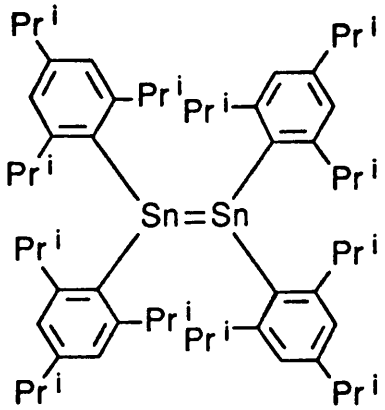

(XII)

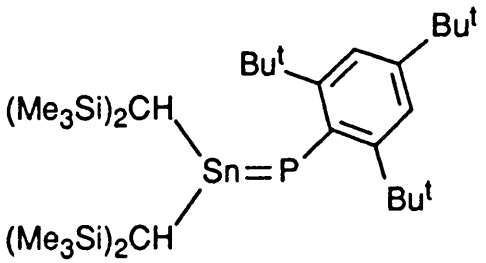

(XIII)

By the use of sterically hindered organotin halides as precursors further synthetic procedures can then be envisaged to produce rings and cages of restricted size.

Classical preparative techniques for organotin halides are based on the application of two types of synthetic methodology. The most widely used industrial route is the Kocheshkov comproportionation of a tetraorganotin with anhydrous tin(IV) chloride[1]. (see equations 1-3) This reaction can be controlled by reagent stoichiometry to yield a dominant organotin halide product. This methodology contrasts sharply with the direct reaction of a carbanion with anhydrous tin(IV) chloride, where a spectrum of products irrespective of reagent stoichiometry is obtained. The former preparation is usually satisfactory for systems where the tetraorganotin can be made in high purity, usually by reaction of an excess of its carbanion with anhydrous tin(IV) chloride. However, even in instances of tetraorganotin compounds where organic moieties of moderate steric hindrance are required, problems are encountered. This is exemplified for the preparation of tetraneophyltin.[167] By the standard synthetic route of excess neophyl Grignard reagent reacting with anhydrous tin(IV) chloride a mixture composed of 44% trineophyltin chloride and 8% tetraneophyltin is obtained. This obviously is unsuitable as a method for the preparation of the required tetraorganotin precursor for the comproportionation stage.

The second favoured synthetic route is the direct reaction between an organometallic reagent and anhydrous tin(IV) chloride in the correct stoichiometric ratio. Again, in this technique the major

problem encountered is the purification of the reaction product for cases where products of mixed stoichiometry are obtained. As the steric hindrance of the organic moiety increases, so preferential product formation is seen to occur. This phenomenon is exemplified by the direct reaction of t-butyl Grignard reagent and anhydrous tin(IV) chloride in which di-t-butyltin dichloride is the major isolated product.[168] For instances of extreme steric hindrance as in the reaction between 2,4,6-tri-t-butylphenyl ('super mesityl') lithium and anhydrous tin(IV) chloride it is found that the bis-addition is still the preferred stoichiometry resulting in the exclusive formation of the bis-aryltin dihalide.[9] This result suggests that except for massively sterically hindered groups, preparative synthetic routes based upon direct alkylation or arylation would appear to be of limited synthetic value for the formation of monoorganotin trihalides.

The aim of the synthetic procedures detailed in this chapter was to prepare sterically hindered mono- and diorganotin halides in high purity by the application of structured synthetic routes.

2.2 Results and Discussion.

2.2.1 Alkyltin Halides.

In an attempt to overcome the problems incurred during comproportionation type reactions the property of selective organic group cleavage by a halogen[169] was investigated. For organic moieties

of varying nature the relative ease of cleavage has been found to be Ph > Bn > vinyl > Me > Et > nPr > nBu.[170] The theoretical basis for the ease of cleavage is thought to be directly related to the degree of stabilisation in the leaving anion. However, in certain systems, for instance trimethyl(trifluoromethyl)tin, it is found that chlorine will preferentially cleave methyl groups rather than the more stable trifluoromethyl anion.[171] This effect is thought to be related to the bond strength existing between tin and the attached groups resulting in selectivity of cleavage.

Solvent effects are also known to display a large influence on the halogen cleavage reaction mechanism.[172,173] If highly polar solvents e.g. methanol, dimethylformamide, dimethylsulphoxide, acetic acid etc. are used, it is conceivable that the solvent will be the strongest nucleophile in the reaction mixture. The result of this will be that the solvent will preferentially complex with tin resulting in an expansion of coordination to a trigonal bipyramidal geometry at the metal. For the now *trans* disposed organic group the bond to tin is weakened and the halogen cleavage reaction will proceed by an electrophilic attack at carbon via an open S_E2 transition state (figure 13). However, in instances where non-polar solvents e.g. toluene, carbon tetrachloride, cyclohexane etc. are used in the reaction, then the halogen will be the strongest nucleophile present resulting in nucleophilic attack at tin and the halogen cleavage reaction will proceed via the formation of a cyclic S_E2 transition state (figure 14).

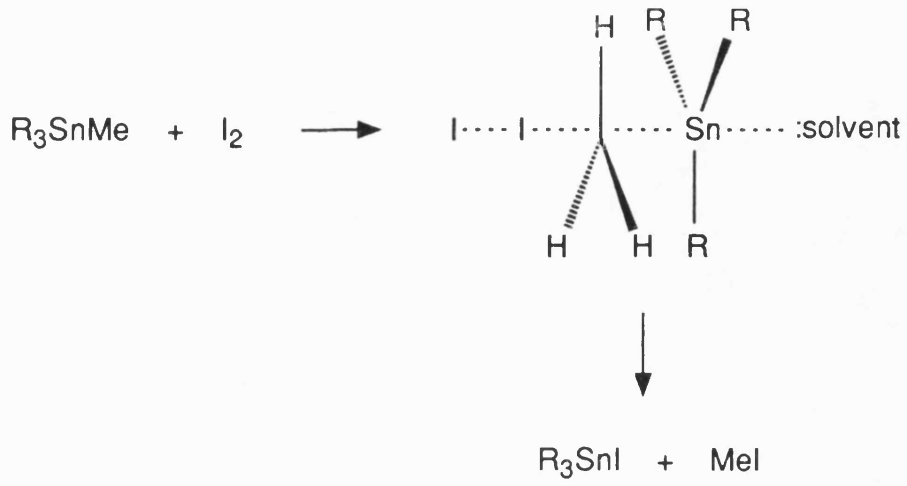

Figure 13: Halogen Cleavage of a Mixed Tetraorganotin Via a Solvent Activated Open S_E2 Transition State.

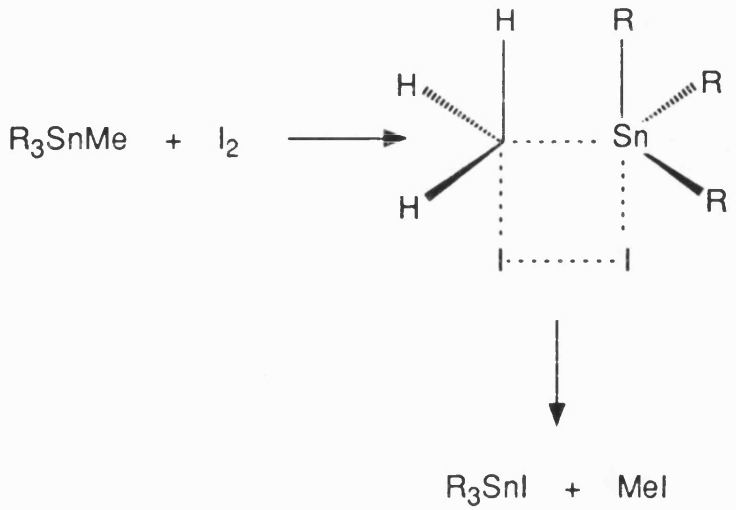

Figure 14: Halogen Cleavage of a Mixed Tetraorganotin Via a Halogen Activated Cyclic Transition State.

For different halogens variations in the ability to cleave organic groups from tin are observed. In the case of iodine the cleavage of organic groups is usually restricted to mono-substitution,[174] however, for bromine or chlorine multiple group cleavage is often observed for higher stoichiometric halogen additions.

For the preparation of dialkyltin dihalides it was envisaged that aryl groups could be utilised as coordination site blocking groups, thereby enabling the introduction of the required number of sterically demanding alkyl groups to be made by the stoichiometric addition of an alkylating agent to a commercially available diaryltin dihalide starting material, for instance diphenyltin dichloride. Selective halogen cleavage of the reactive Sn-Ph bond could then be applied to generate the appropriate mono- or diorganotin product. For the dialkyltin dihalide preparations alkyl Grignard reagents were chosen as the alkylating species (equation 16).

$$2RMgX + Ph_2SnCl_2 \rightarrow Ph_2R_2Sn + 2MgX_2 \qquad (16)$$

For R = i-propyl and neophyl.

After purification of the tetraorganotin product, dropwise addition of a stoichiometric amount of bromine (chloroform solution) at room temperature was employed to cleave the phenyl groups from tin (equation 17).

$$Ph_2R_2Sn + 2Br_2 \rightarrow R_2SnBr_2 + 2PhBr \qquad (17)$$

For R = i-propyl and neophyl.

Distillation of the crude product to remove phenyl bromide resulted in high purity dialkyltin dihalides being produced in good yields. This route was used for the preparation of dineophyl and di-i-propyltin dibromide. By the direct attack of i-propyllithium on anhydrous tin(IV) chloride, Prince[175] managed to isolate di-i-propyltin dichloride in approximately 30% yield compared to the overall yield of 78% obtained for the preparation of di-i-propyltin dibromide detailed above.

For the preparation of di-t-butyltin dichloride the direct, stoichiometric reaction between the t-butyl Grignard reagent and anhydrous tin(IV) chloride was employed (equation 18).

$$2tBuMgCl + SnCl_4 \rightarrow tBu_2SnCl_2 + 2MgCl_2 \qquad (18)$$

This route was chosen as a result of two important features of t-butyltin halide preparations. Firstly, tri-t-butyltin chloride is only made in very poor yield from the direct attack of an excess of the t-butyl Grignard reagent and anhydrous tin(IV) chloride. The synthetic route adopted in the literature necessitates the use of the more reactive organotin fluorides to obtain workable yields of tri-t-butyltin chloride.[168] The second feature making the direct synthesis possible is the extreme instability at room temperature of mono-t-butyltin trichloride which rapidly disproportionates into tin(II) chloride and t-butyl chloride (equation 19).[176]

$$tBuSnCl_3 \rightarrow SnCl_2 + tBuCl \qquad (19)$$

As a result, the major isolable product obtained from the direct reaction of the t-butyl Grignard reagent and tin(IV) chloride is di-t-butyltin dichloride. However the yield obtained from this reaction after purification (36%) is still not totally satisfactory.

As for diorganotin dihalides, the halogen cleavage methodology was chosen for the preparation of sterically hindered monoorganotin trihalides. To make the aryl-blocked alkyltriphenyltin precursor an alkyl halide was reacted with triphenyltin lithium[177] (equations 20 and 21).

$$Ph_3SnCl + 2Li \rightarrow Ph_3SnLi + LiCl \quad (20)$$

$$Ph_3SnLi + RX \rightarrow Ph_3RSn + LiX \quad (21)$$

R = i-propyl.

After subsequent purification of the product, halogen cleavage of the phenyl groups from tin was achieved with a stoichiometric amount of bromine (chloroform solution) (equation 22) analogous to the above diorganotin dihalide preparation.

$$Ph_3RSn + 3Br_2 \rightarrow RSnBr_3 + 3PhBr \quad (22)$$

R = i-propyl.

This synthetic procedure was successfully employed for the preparation of i-propyltin tribromide in a high overall yield (74%).

2.2.2 Aryltin Halides.

For the preparation of aryltin halides the synthetic approaches available are rather more limited than for alkyltin halides. For cases of mixed aryl tin compounds selective aryl cleavage by halogen is generally not observed. However, the usual group cleavage order with halogen can be altered under certain circumstances, as observed in the work of Jousseaume and Villeneuve.[178] In this research, trialkylmonoaryltin compounds were synthesised where the aryl functionality contained an *ortho* substituent displaying a strongly Lewis basic heteroatom in either an α or β position to the aryl ring. It was found that under normal halogen cleavage conditions the accepted order of bond cleavage was reversed and an alkyl group was selectively cleaved by the incoming halogen. The mechanistic basis for this observation is that the Lewis basic substituent in the aryl functionality associates with tin in an intramolecular manner, forming a *pseudo* trigonal bipyramidal geometry at tin. As a result, one of the alkyl groups is coerced into being *trans* disposed to the associated Lewis basic group resulting in bond weakening and thus becomes the preferential position for electrophilic halogen attack (figure 15). A similar observation was made by Kuivila et al.[179] for preferential group cleavage in unsymmetrical tetraalkyltin compounds.

In this work, highly sterically hindered alkyl-substituted aryl groups were the type investigated e.g. 2,4,6-trimethylphenyl (mesityl) and 2,4,6-tri-i-propylphenyl, and so *trans* directed cleavage reactions of the type described above are not feasible. As a result, the direct

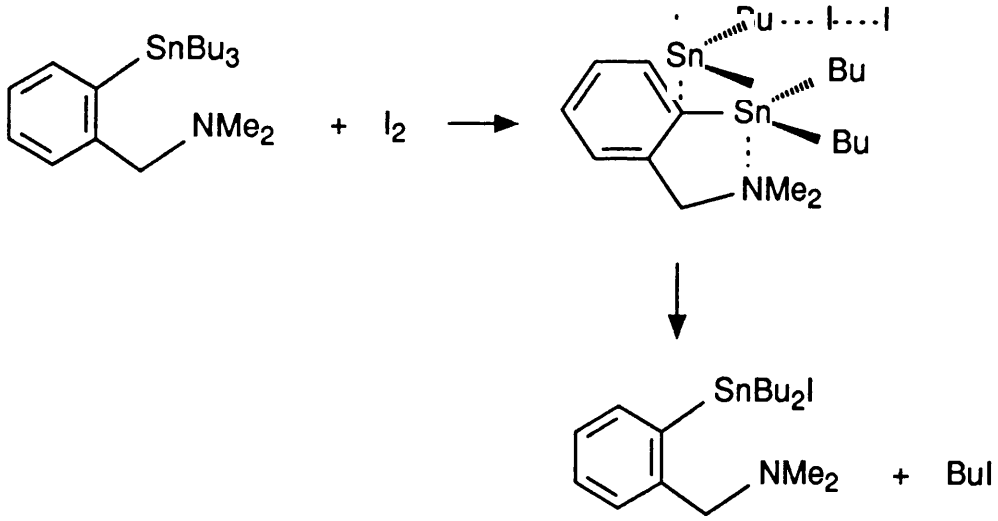

Figure 15: Reversal of Selectivity in S_E2 Cleavage of Mixed Tetraorganotin Compounds by Iodine.

reaction between tin(IV) chloride and either an aryl Grignard reagent (equation 23) or an aryllithium reagent (equation 24) was employed.

$$2RMgX + SnCl_4 \rightarrow R_2SnCl_2 + 2MgXCl \qquad (23)$$

R = 2,4,6-trimethylphenyl.

$$2RLi + SnCl_4 \rightarrow R_2SnCl_2 + 2LiCl \qquad (24)$$

R = 2,4,6-trimethylphenyl.

R = 2,4,6-tri-i-propylphenyl.

The yield of pure products obtained from these reactions was limited, possibly due to by-product formation, but enough of the desired product was obtained to enable further synthesis to take place.

By the use of an organolithium reagent the preparation of dimesityltin dichloride was attempted, from which the required product was isolated in high purity by recrystallisation (21%). The preparation of dimesityltin dichloride was also attempted using a Grignard reagent substitution reaction (equation 23). By this route a slightly better yield was obtained (30%). However, instead of obtaining the pure dichloride, due to the use of mesityl bromide as the Grignard reagent precursor in reaction with tin(IV) chloride, halogen scrambling occurred resulting in the formation of a complete range of the possible halogen containing products.

The evidence for the mixed halogen species was observed in the ^{119}Sn nmr spectrum, where three peaks with an approximately equal difference in chemical shift were observed. From the previous synthetic preparation of dimesityltin dichloride, using exclusively chlorine containing species, the ^{119}Sn nmr chemical shift was observed to be -51.6 ppm. As a result, in the mixed halide product the peak observed at -52.4 ppm can be assigned to the dichloride. The slight difference observed in the two values for the chemical shift is most likely caused by a difference in the concentration of the two nmr samples. From the diorganotin dihalide examples cited in the literature it can be observed that for a change in the halogen substituent on tin from chloride to iodide an upfield shift in the ^{119}Sn nmr spectrum is observed e.g. Me_2SnCl_2 +140 ppm, Me_2SnBr_2 +70 ppm and Me_2SnI_2 -159 ppm.[180] On this basis the observed chemical shift values for the mixed halide product were assigned as shown in table 6. From the ^{119}Sn nmr spectrum the relative intensities of the peaks

Table 6: ^{119}Sn NMR[a] Data for Mixed Halogen Dimesityltin Dihalides.

Component	Proportion in product[b]	$\delta(^{119}Sn)$
Mes_2SnCl_2	3	-52.4
$Mes_2SnBrCl$	30	-97.8
Mes_2SnBr_2	67	-148.2

[a] = ppm.

[b] = %.

observed allowed a weighted prediction of the expected elemental analysis to be made. The theoretical values for the elemental analysis were in good agreement with the experimentally obtained values.

Using the mixed halogen product the synthesis of mesityltin trihalide was attempted using a Kocheshkov comproportionation type reaction with tin(IV) chloride[1] (equation 25).

$$Mes_2SnX_2 + SnCl_4 \rightarrow 2MesSnX_{3-n}Cl_n \qquad (25)$$

The required product was obtained and due to the nature of the dimesityltin dihalide precursor, also contained a full range of the possible halogen containing products. As with the dimesityltin dihalide sample the ^{119}Sn nmr spectrum was assignable to the mixture with four peaks corresponding to the full array of possible halogen species. From examples of monoorganotin trihalides cited in the literature assignments of the observed peaks can be made. As in the diorganotin dihalide examples, an upfield shift is observed for changes in halogen substitution from chloride to iodide in monoorganotin trihalides e.g. $MeSnCl_3$ +21 ppm, $MeSnBr_3$ -165 ppm and $MeSnI_3$ -699.5 ppm.[180,181] In the literature the chemical shift value for $PhSnCl_3$ is reported as being -60.5 ppm providing further evidence for the assignment of the observed peak at -85.5 ppm as being $MesSnCl_3$. On this basis the observed chemical shift values for the mixed halide product were assigned as shown in table 7. As before, weighted values for the theoretical elemental analysis obtained from the relative peak intensities gave good agreement with the values obtained

Table 7: ^{119}Sn NMR[a] Data for Mixed Halogen Mesityltin Trihalides.

Component	Proportion in product[b]	$\delta(^{119}Sn)$
$MesSnCl_3$	41	-85.5
$MesSnBrCl_2$	44	-150.1
$MesSnBr_2Cl$	14	-219.7
$MesSnBr_3$	2	-294.2

[a] = ppm.

[b] = %.

experimentally.

By the use of an extremely bulky organic moiety e.g. 2,4,6-tri-i-propylphenyl, it was surmised that monoorganotin trihalides might be prepared by a direct stoichiometric reaction between the organolithium reagent and anhydrous tin(IV) halide (equation 24). In the attempted preparation of the two analogous aryltin trihalides unexpected products were obtained. From the 1:1 reaction of 2,4,6-tri-i-propylphenyllithium and anhydrous tin(IV) chloride a colourless oil that defied all efforts of purification was obtained. This crude product, assumed to be the required 2,4,6-tri-i-propylphenyltin trichloride, was then used in the attempted preparation of (2,4,6-tri-i-propylphenyl)thiastannane, $(RSnS_{1.5})_n$. However, from this reaction the product obtained proved to be tetra(2,4,6-tri-i-propylphenyl)-oxathiadistannetane, $R_2SnO(S)SnR_2$ (full details in chapter 3).

A subsequent attempt to try to identify the intermediate halide in the above by the analogous preparation of 2,4,6-tri-i-propylphenyltin tribromide, yielded a product similar to that obtained in the attempted 2,4,6-tri-i-propylphenyltin trichloride preparation, based on the similarities observed in their infra-red spectra. From this reaction however, a solid product was isolated which, upon recrystallisation, yielded a highly crystalline material. From the ^{119}Sn nmr spectrum the presence of a $^1J(^{117}Sn-^{119}Sn)$ = 5212 Hz indicated the existence of a tin-tin bond. Elemental analysis of the compound confirmed the composition as 1,2-dibromo-1,1,2,2-tetra(2,4,6-tri-i-propylphenyl)distannane (**1**).

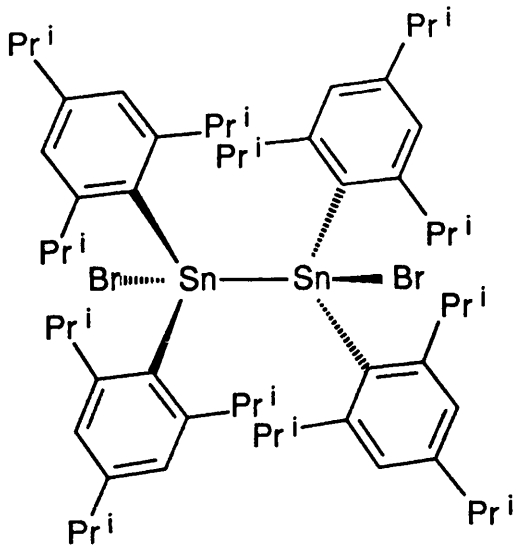

(1)

Masamune et al.[165] prepared the chloride analogue of (1) and reported complex ^{1}H and ^{13}C nmr spectra resulting from the extreme steric hindrance generated by the presence of the 2,4,6-tri-i-propyl-phenyl groups. This observation is borne out by our own nmr spectroscopic investigations which indicate a high degree of inequivalence in the environments accorded to the i-propyl groups. By the use of a 2d ^{1}H-COSY-90 nmr experiment more information can be obtained from a correlation of the methyl and methine signals in the i-propyl groups (figure 16 and table 8). In the methine region of the spectrum six multiplets are observed. From the ^{1}H-COSY correlation plot it can be seen that three of the methine multiplets are uniquely coupled to differing methyl signals, indicating that although the i-propyl groups are in different environments, free rotation is possible resulting in the equivalence of the methyl signal for

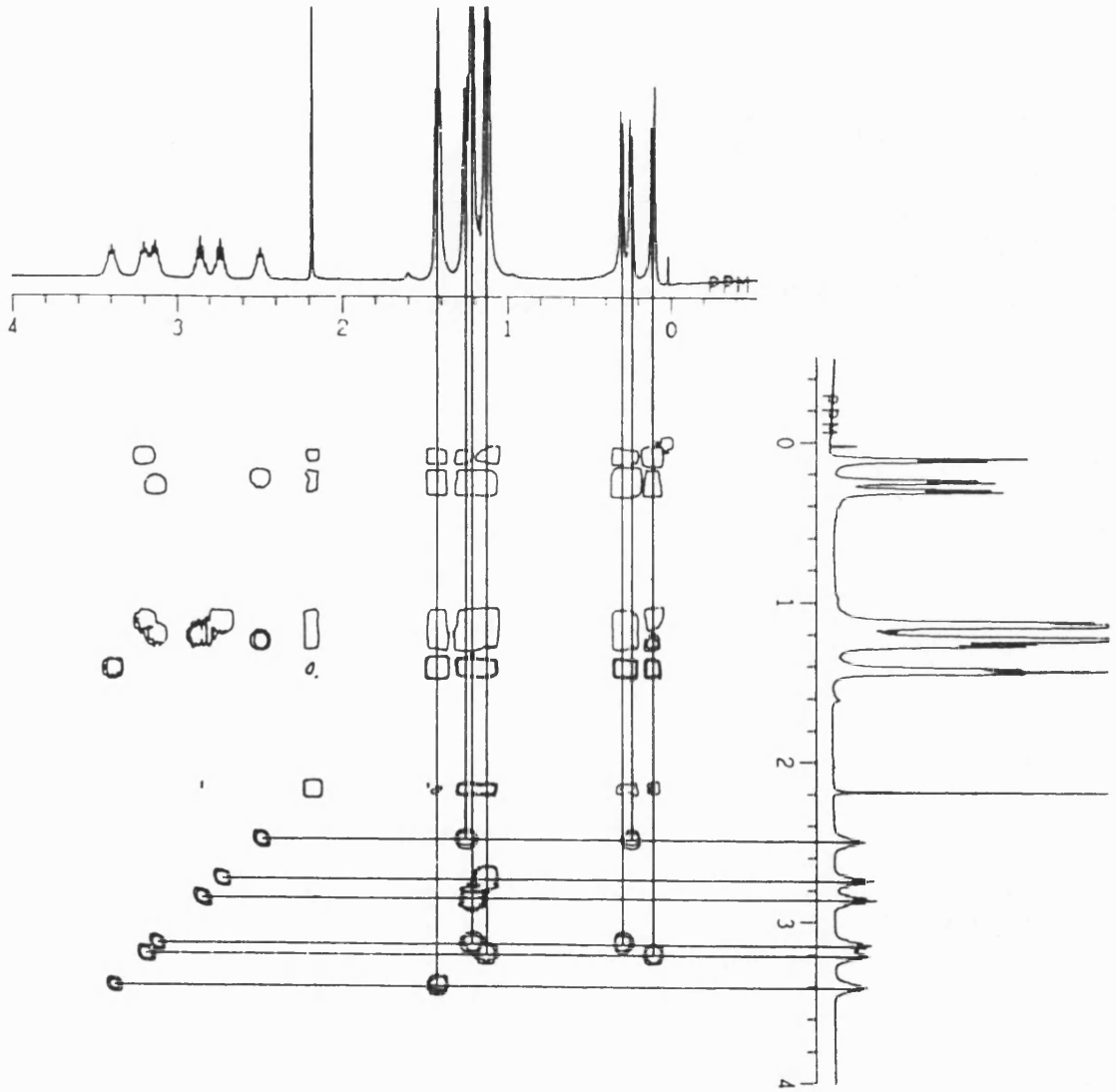

Figure 16: 2d ^{1}H-COSY-90 NMR Experiment for 1,2-Dibromo-1,1,2,2-tetra-(2,4,6-tri-i-propylphenyl)distannane (**1**).

Table 8: Correlations Between the ^{1}H NMR Chemical Shift Values[a] Obtained for the Methyl and Methine Environments in the i-Propyl Groups in 1,2-Dibromo-1,1,2,2-tetra(2,4,6-tri-i-propylphenyl)distannane (**1**).

δ[(CH$_3$)C*H*]	δ[(C*H*$_3$)CH]
2.50, multiplet, 2H	0.25, doublet, 6H
	1.27, doublet, 6H
2.72, multiplet, 2H	1.13, triplet[b], 12H (of 18H signal)
2.86, multiplet, 2H	1.23, doublet, 12H (of 18H signal)
3.14, multiplet, 2H	0.31, doublet, 6H
	1.23, doublet, 6H (of 18H signal)
3.21, multiplet, 2H	0.11, doublet, 6H
	1.13, triplet[b], 6H (of 18H signal)
3.40, multiplet, 2H	1.44, triplet[b], 12H

[a] = ppm.

[b] = The observed triplet most likely occurs as a result of the superimposition of two slightly differing doublets.

specific i-propyl moieties. For the other three methine multiplets couplings are observed for two distinct methyl environments in which one of the pair of signals is shifted markedly upfield by approximately 1 ppm compared to the usual chemical shift expected for i-propyl methyl groups. This observation would seem to suggest that not only is rotation of the i-propyl groups severely restricted, but also the environment accorded to one methyl group is shielded, possibly by the close proximity of a neighbouring aryl ring current. To try to induce rotation to the i-propyl groups an elevated temperature ^{1}H nmr spectrum was recorded at 55°C. However, no change occurred in the spectrum except for a slight reduction in peak resolution.

In the work of Weidenbruch et al.[9] during the preparation of bis(2,4,6-tri-t-butylphenyl)tin dichloride two products were obtained. One product was the expected bis-aryltin dichloride: the other, however, had undergone a protic rearrangement of one of the 2,4,6-tri-t-butylphenyl groups resulting in bond formation to tin via one of the t-butyl moieties to form [2-methyl-2-(3,5-di-t-butylphenyl)propyl]-[2,4,6-tri-t-butylphenyl]tin dichloride. From the nmr data obtained on this compound increased complexity was observed for the t-butyl region in the ^{1}H and ^{13}C nmr spectra compared to that seen in the nmr spectra of the bis-aryltin dichloride. Initially it was postulated that the complexity observed for the i-propyl region in the nmr spectra of (**1**) could be due to a similar type of rearrangement taking place in the 2,4,6-tri-i-propylphenyl groups. However, the absence of an inverted methylene signal in the 135 DEPT ^{13}C nmr spectrum indicated that

conventional tin-aryl bond formation was present.

After recrystallisation from acetone a suitably high quality crystal sample of (1) was obtained enabling a single crystal X-ray structure determination to be made. An ORTEP plot of the structure of (1) can be seen in figure 17. Selected bond lengths and angles are given in table 9 and full crystal data is available in Appendix II. For the crystal sample used the cell geometry was monoclinic with a $P2_1/n$ space group.

From the literature several structures are cited detailing tin-tin bond distances. In instances of low steric hindrance exemplified by hexaphenyldistannane[162] and 1,2-dichloro-1,1,2,2-tetramethyl-distannane[163] the bond lengths quoted at 2.780(4)Å and 2.770(2)Å respectively are considerably shorter than in (1) [2.841(1)Å]. However, in sterically hindered instances exemplified by 1,2-dichloro-1,1,2,2-tetra[bis(trimethylsilyl)methyl]distannane[164] and 1,2-dibromo-1,1,2,2-tetra(pentacarbonylmanganio)distannane[165] the tin-tin bond lengths of 2.844(1)Å and 2.885(1)Å are almost equal to the equivalent bond length observed in (1). From the examples given it would seem that the tin-tin bond length is dependent on the degree of steric hindrance present in the molecule. Therefore in the first two examples where only small organic substituents are present the observed tin-tin bond length is relatively short. However, in the case of the latter two examples and in (1), where large sterically demanding organic substituents are present an expansion of the tin-tin bond length results to reduce the molecular interactions.

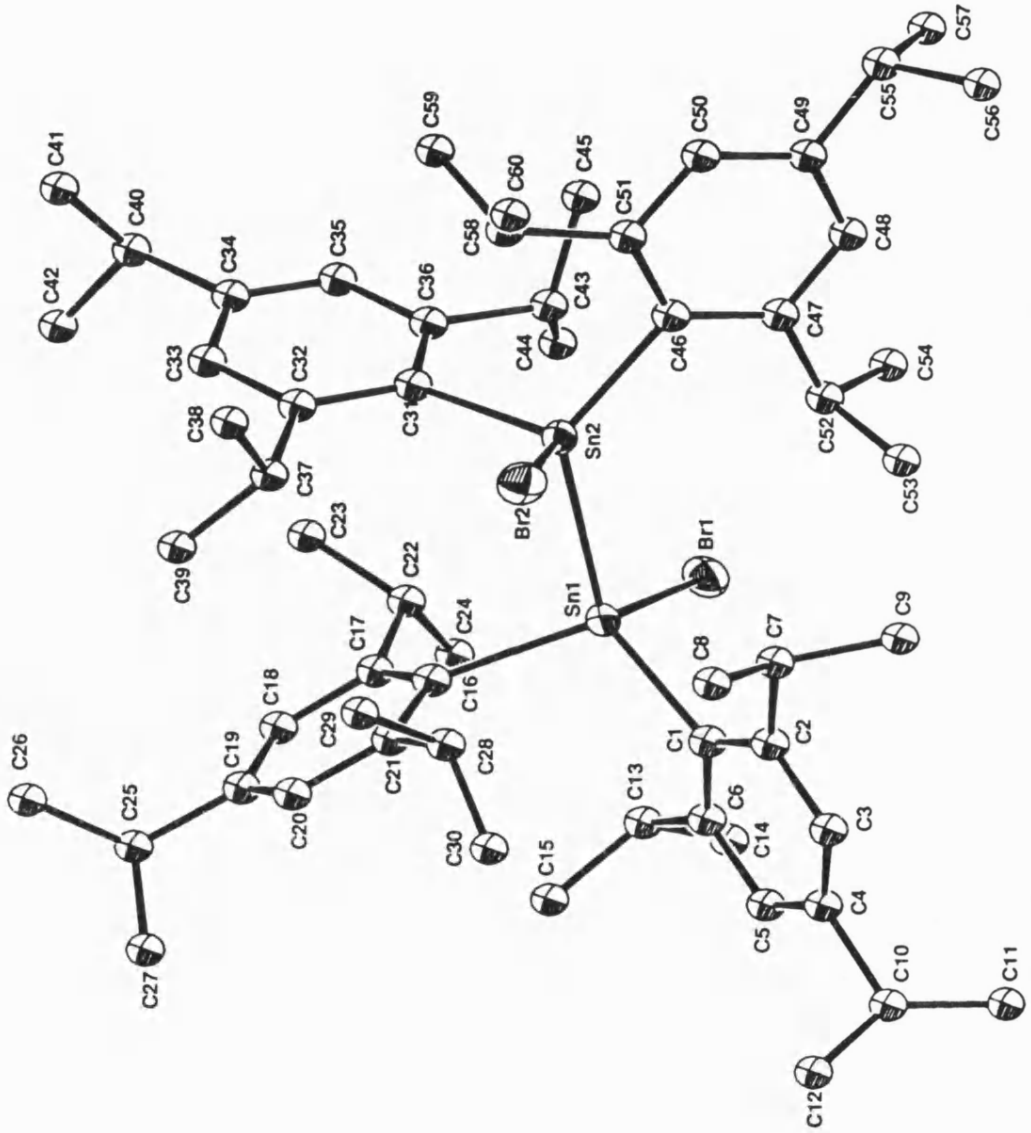

Figure 17: ORTEP Plot of 1,2-Dibromo-1,1,2,2-tetra(2,4,6-tri-i-propylphenyl)distannane (1).

Table 9: Bond Lengths[a] and Angles[b] for 1,2-Dibromo-1,1,2,2-tetra-(2,4,6-tri-i-propylphenyl)distannane (**1**).

Sn1 -Sn2	2.841(1)	Br1 -Sn1 -Sn2	99.8(1)
Sn1 -Br1	2.551(1)	C1 -Sn1 -Sn2	135.2(3)
Sn1 -C1	2.191(10)	C16 -Sn1 -Sn2	104.6(3)
Sn1 -C16	2.202(10)	C1 -Sn1 -Br1	99.0(3)
Sn2 -Br2	2.537(1)	C16 -Sn1 -Br1	113.6(3)
Sn2 -C31	2.201(10)	C16 -Sn1 -C1	104.4(4)
Sn2 -C46	2.179(9)	Br2 -Sn2 -Sn1	98.2(1)
		C31 -Sn2 -Sn1	105.0(3)
		C46 -Sn2 -Sn1	131.8(3)
		C31 -Sn2 -Br2	115.8(3)
		C46 -Sn2 -Br2	99.9(3)
		C46 -Sn2 -C31	106.5(4)
		Br1 -Sn1 -Sn2 -Br2	161.6(6)

[a] = Å.

[b] = °.

In the literature other examples are cited for compounds of slightly different structural type which display tin-tin bonds. In a series of 1,1,2,2-tetraphenyldistannyldiacetates[186] due to the bidentate chelating nature of the acetate groups across the tin-tin bond, the ring formation restricts the tin-tin bond length because of increasing ring strain that results on bond lengthening. In these compounds the tin-tin bond length is shorter, ranging from 2.691(1)Å in the actetate to 2.711(1)Å in the trichloroacetate derivative in comparison to that observed in (1).

For organotin halide systems of low steric hindrance, halide bridged, six-coordinate distorted octahedral structures are obtained as exemplified by the linear polymeric chain structures found in Et_2SnX_2 (for X = Cl, Br and I).[187] However, as the steric hindrance is increased so the structures simplify to monomeric four-coordinate tetrahedral arrays as observed for bis(2,4,6-tri-t-butylphenyl)tin dichloride.[9] In the case of dihalotetraorganodistannane structures a similar trend is observed. For 1,2-dichloro-1,1,2,2-tetramethyl-distannane a helical double chain six-coordinate structure, bridged through chlorines, is found. In the case of (1) and for the other sterically hindered dihalotetraorganodistannane examples already cited, monomeric four-coordinate species are observed due to the extreme steric bulk preventing any possible coordinative bonding.

In (1) a group of angular effects are also observed as a result of the steric hindrance present in the molecule. Firstly, it is observed that two distinct types of Sn-Sn-C bond angles are present in the molecule. In the case of both C1-Sn1-Sn2 and C46-Sn2-Sn1 angles of

135.2(3)° and 131.8(3)° respectively are found in comparison to the complementary angles C16-Sn1-Sn2 and C31-Sn2-Sn1, for which angles of 104.6(3)° and 105.0(3)° respectively, are observed. It would seem that this phenomenon results from a minimum energy array produced in the molecule to reduce the steric interactions of the bulky organic moieties. A second angular effect observed in (1) is a rotation about the central axis of the molecule resulting in an imperfect *trans* arrangement for the bromine substituents [Br1-Sn1-Sn2-Br2 161.6(6)°]. Again it would appear that this occurs to effect a reduction in the steric interactions of the organic moieties.

From the crystal structure of (1) the reasons for the complexity of the ^{1}H and ^{13}C nmr spectra observed for the i-propyl substituents can be readily rationalised. By the use of the Insight™ interactive molecular graphics software on an Evans and Sutherland PS330 computer graphics system the stereo image of the structure of (1) was observed. By rotation of the molecule on the display monitor it could be seen that the four *para* and two of the *ortho* substituted i-propyl groups (C7-C8-C9 and C52-C53-C54) were virtually unhindered allowing free rotation of the group and thus equivalence of signals in the nmr spectra.

For the remaining six i-propyl units it was apparent that one methyl group per moiety was accorded a position in close proximity to an adjacent aryl ring system while the other was oriented into free space. This observation confirms the reason previously suggested for the inequivalence of the methyl groups in six of the i-propyl moieties as seen in the nmr spectra. Having identified the i-propyl groups

affected by this phenomenon the distances between the aryl ring plane and the closest methyl groups could then be obtained from the crystal data and are given in table 10. From the data presented it can be seen that the distances observed are short enough to result in the protons on the methyl groups in question to be affected by the ring current of the aryl ring thus resulting in the shielding effect observed in the ^1H nmr spectrum.

The preparation of compound (1) is thought to proceed by the intermediate formation of the bis-aryltin dihalide. At this stage two differing types of reaction could occur which would lead to the same end product. One possible route would involve another 2,4,6-tri-i-propylphenyllithium unit undergoing a lithium/halogen exchange reaction with a diaryltin dihalide unit resulting in the formation of a diaryltinhalido lithium species. The tin lithium reagent would then react with a second diaryltin dihalide unit forming the tin-tin bonded structure. (equations 26 to 28)

$$2RLi + SnX_4 \rightarrow R_2SnX_2 + 2LiX \qquad (26)$$

$$R_2SnX_2 + RLi \rightarrow R_2SnXLi + RX \qquad (27)$$

$$R_2SnXLi + R_2SnX_2 \rightarrow XR_2SnSnR_2X + LiX \qquad (28)$$

(1)

R = 2,4,6-tri-i-propylphenyl.

Table 10: Through Space Distances* for the Six Close Proximity Methyl Moieties to the Mean Plane of the Appropriate Aryl Ring Systems.

Carbon Atom in Methyl Group	Aryl Ring	Through Space Distance
C15	C16 -C21	3.542
C23	C31 -C36	3.597
C30	C1 -C6	3.479
C39	C16 -C21	3.572
C45	C46 -C51	3.529
C59	C31 -C36	3.805

* = Å.

Alternatively the 2,4,6-tri-i-propylphenyllithium could react as a base with the diaryltin dihalide resulting in the required ditin formation but with the resultant side products differing from those obtained by the previous mechanism (equation 29).

$$2R_2SnX_2 + 2RLi \rightarrow XR_2SnSnR_2X + 2LiX + R_2 \qquad (29)$$

(1)

The latter of the two reaction routes is mirrored in the preparative route employed by Masamune et al.[165] where lithium naphthalenide is employed as a strong base for the coupling of the two diaryltin dihalide units, resulting in the formation of the tin-tin bond. Without further evidence regarding the nature of the side products no full conclusion can be drawn as to the reaction mechanism for the formation of (1).

This reaction however, serves to highlight the extreme difficulties faced when trying to introduce, in a controlled manner, precise numbers of organic groups onto tin by direct substitution methods.

2.2.3 Tris(trimethylsilyl)methyltin Halides.

From the synthetic routes so far discussed it becomes apparent that the synthetic methodology based on direct substitution reactions for the preparation of monoorganotin compounds is extremely limited due to the tendency for multiple group substitutions to occur. This tendency

can be averted by the use of organic moieties with such a high degree of steric hindrance that it becomes physically impossible for the bis-substituted product to form. By the use of the extremely hindered tris(trimethylsilyl)methyl moiety it was hoped that the targeted tris(trimethylsilyl)methyltin trihalides might be synthesised. [The tris(trimethylsilyl)methyl moiety is commonly refered to as (Tsi) and hereafter in the text this abbreviation will be used.]

The first preparative strategy used for the attempted synthesis of these compounds was analogous to that used in the preparation of i-propyltin tribromide. However, for the formation of the alkyl-triaryltin precursor a reversal of reaction roles was undertaken. In the preparation of i-propyltriphenyltin, triphenyltin lithium was reacted with i-propyl bromide. In the preparation of (Tsi)triphenyltin the synthetic route adopted by Glockling et al.[168] was used, where (Tsi)lithium was synthesised[169] and reacted with triphenyltin chloride yielding the required product (2) (equations 30 and 31).

$$[(CH_3)_3Si]_3CH + CH_3Li \rightarrow [(CH_3)_3Si]_3CLi + CH_4\uparrow \quad (30)$$

$$[(CH_3)_3Si]_3CLi + Ph_3SnCl \rightarrow [(CH_3)_3Si]_3CSnPh_3 + LiCl \quad (31)$$

(2)

From the above reaction (Tsi)triphenyltin could be obtained in the pure form by successive recrystallisations from either ethanol or acetonitrile to remove the unwanted hexaphenyldistannane by-product. This method of purification proved very costly in terms of yield and

so in repeated preparations of (Tsi)triphenyltin the pure product was not isolated, but reacted in an impure state and purified at a later stage. The hexaphenyldistannane by-product occurs as a result of (Tsi)lithium behaving both as a base and as a nucleophile in the reaction with triphenyltin chloride (equations 32 and 33).

$$[(CH_3)_3Si]_3CLi + Ph_3SnCl \rightarrow [(CH_3)_3Si]_3CCl + Ph_3SnLi \quad (32)$$

$$Ph_3SnCl + Ph_3SnLi \rightarrow Ph_3SnSnPh_3 + LiCl \quad (33)$$

For the attempted preparation of (Tsi)tin tribromide, direct bromination of (2) under the same conditions as used for previous aryl halogen cleavage reactions was attempted. From this reaction the required (Tsi)tin tribromide was not obtained, instead phenyl(Tsi)tin dibromide (3) was formed (equation 34).

$$[(CH_3)_3Si]_3CSnPh_3 + 3Br_2 \rightarrow \underset{(3)}{([(CH_3)_3Si]_3C)PhSnBr_2} + 2PhBr + Br_2 \quad (34)$$

At this stage it was considered that steric hindrance was the barrier to the final halogenation stage and so an analogous chlorination of (2) was attempted. With chlorine it was hoped that the smaller Van der Waals radius of the chlorine atom would lower the steric hindrance encountered by the incoming halogen. However, bubbling chlorine gas through a solution of (2) in carbon tetrachloride only resulted in the formation of the chlorine analogue

of (3) (equation 35).

$$[(CH_3)_3Si]_3SnPh_3 + xsCl_2 \rightarrow \{[(CH_3)_3Si]_3\}PhSnCl_2 + 2PhCl \quad (35)$$

(4)

This preparative route yielded the compound shown, but by nmr investigation it was observed that minor peaks were present in the (Tsi) methyl region of the ^1H and ^{13}C nmr spectra giving rise to the suspicion that as well as halogen cleavage of the phenyl groups secondary attack was also occurring on the (Tsi) group.

In an attempt to cleave the final phenyl group from tin in the above reaction sequence, more forceful electrophilic bromination conditions were employed using anhydrous iron tribromide as a catalyst for the reaction. Under these conditions the required (Tsi)tin trihalide was produced with limited success. The major limitation of the technique was the poor reproducibility of the reaction results. For two successive small scale reactions (0.0034 mole) under the same conditions, from one the required (Tsi)tin tribromide (5) was obtained while from the second only starting material (2) was recovered. On attempted scale up of the reaction (0.0086 mole) again only starting material was recovered.

A second problem encountered in this synthesis was the necessity for halogen containing entities of exclusively one halogen type to be present in the reaction mixture. In the synthesis, bromine and iron tribromide were employed as the halogenation system, however the solvent used initially was carbon tetrachloride. The product obtained

from this reaction was a range of both simple and mixed (Tsi)tin trihalides, occurring due to the presence of both chlorine and bromine containing species in the reaction mixture. Evidence for this was obtained from the ^{119}Sn nmr spectrum (table 11) and chemical ionisation mass spectrometry. The agreement between the theoretical and experimentally derived mixed isotope clusters for high mass fragments in the mass spectrum can be seen in figure 18. By use of the peak intensities from the ^{119}Sn nmr spectrum a weighted theoretical elemental analysis was calculated for the mixed halide system giving good agreement with the experimentally obtained values.

A second method which was attempted for the synthesis of (Tsi)tin tribromide was the direct addition of (Tsi)lithium to anhydrous tin(IV) bromide (equation 36).

$$[(CH_3)_3Si]_3CLi + SnBr_4 \rightarrow [(CH_3)_3Si]_3CSnBr_3 + LiBr \quad (36)$$

(5)

After recrystallisation from acetonitrile a white crystalline solid was obtained. The results from ^{119}Sn nmr, ^{119m}Sn Mossbauer spectroscopy and chemical ionisation mass spectrometry are consistent both with the expected properties and the spectroscopic results previously obtained for (Tsi)tin tribromide prepared by an earlier synthetic route. However, the ^{1}H and ^{13}C nmr spectra and elemental analysis results were inconsistent with the expected product. In the ^{1}H and ^{13}C nmr spectra it would be expected to observe just one major signal in each. (A very small signal would also be expected for the

Table 11: ^{119}Sn NMR[a] Data for Mixed Halogen Tris(trimethylsilyl)tin Trihalides.

Component	Proportion in product[b]	$\delta(^{119}Sn)$
$(Tsi)SnBrCl_2$	10	-100.5
$(Tsi)SnBr_2Cl$	41	-167.9
$(Tsi)SnBr_3$	49	-237.1

[a] = ppm.

[b] = %.

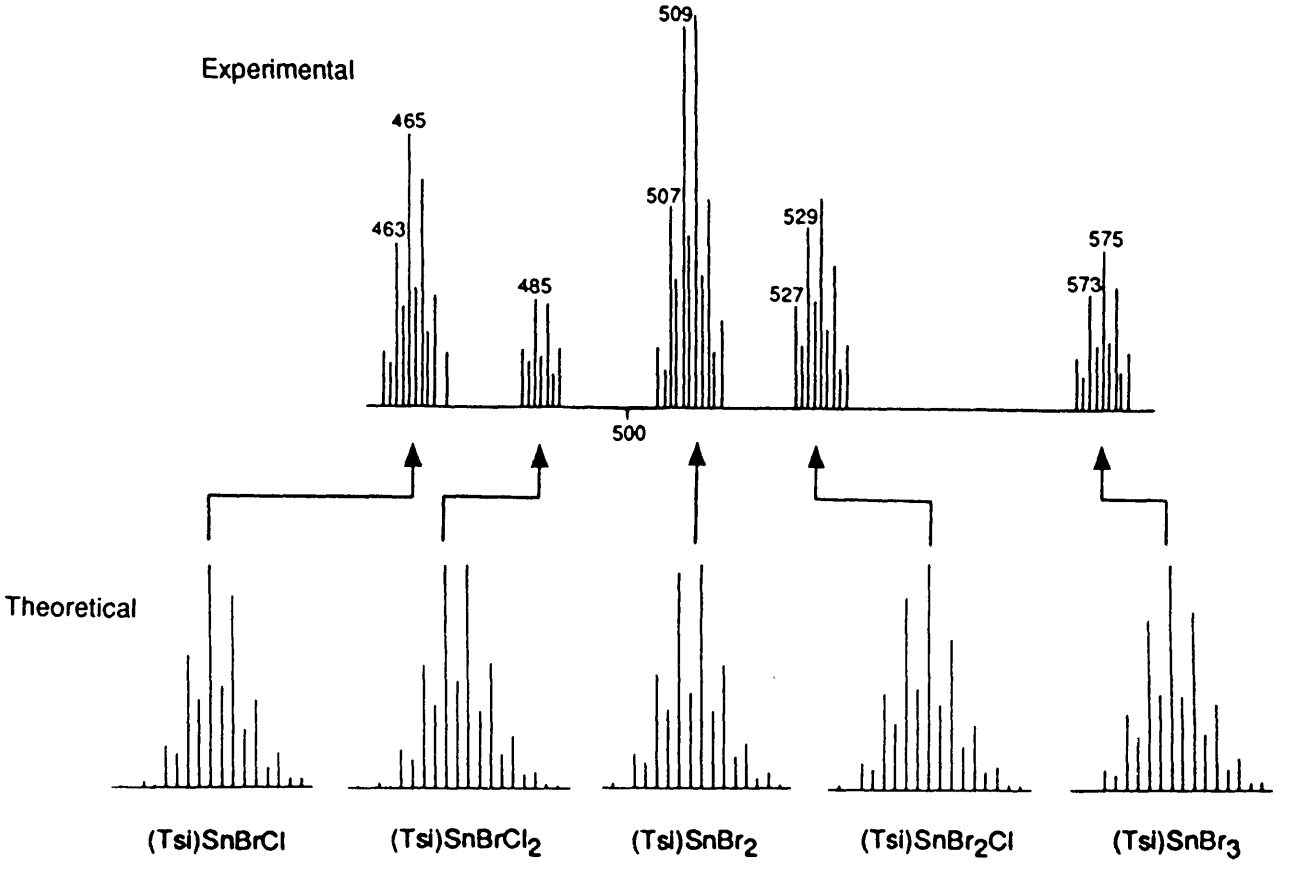

Figure 18: Comparison of the Theoretical and Experimental High Mass Fragments for Tin Halide Systems.

tertiary carbon in the ^{13}C nmr spectrum.) However, three major signals were observed in both spectra. This observation is consistent with that reported by Glockling et al.[88] for the product obtained from the reaction between (Tsi)lithium and anhydrous tin(IV) chloride, where three peaks were reported in the ^{1}H nmr spectrum. In this example, only one signal was present in the ^{13}C nmr spectrum and the elemental analysis values obtained experimentally were in reasonable agreement with the calculated values for (Tsi)tin trichloride.

In an attempt to clarify the observed results, the product was repurified by a second recrystallisation from acetonitrile. From this, two batches of a white crystalline solid were obtained. From the elemental analyses it was apparent that the compositions of the two products were very different (1st batch C 25.90%; H 6.11% and 2nd batch C 37.00%; H 8.86%). From ^{119}Sn nmr spectroscopy and chemical ionisation mass spectrometry the spectra obtained were similar for both batches. However, for the second product, the signal intensities of the high mass fragments in the mass spectrum and the signal intensity in the ^{119}Sn nmr spectrum were significantly diminished for the same mass of sample, indicating a reduction in the tin content, which would also account for the comparatively high carbon content observed in the elemental analysis figures. For the second product a simplification was also observed in the ^{1}H and ^{13}C nmr spectra with one signal being dominant in both. In contrast to what had been previously observed for other (Tsi)tin compounds, no $^{3}J\{[(^{13}CH_3)_3Si]_3C-^{117,119}Sn\}$ coupling constant was in evidence in the ^{13}C nmr spectrum. From these results it was hypothesised that in the

second product only a very small proportion of the material incorporated any tin containing species. For the observed signal in the ^{13}C spectrum however, due to the chemical shift position being coincidental with that for (Tsi) methyl carbons and also due to the presence of a $^{1}J[(^{13}CH_3)_3-^{29}Si]$ coupling constant it was evident that the major component of the second product was a (Tsi) based non-tin containing compound. The identity of the major component was deduced from the elemental analysis to be (Tsi) bromide (Found C 37.00%; H 8.86% and Calculated C 38.56%; H 8.74%).

From the evidence available it would appear that the products obtained fom the direct reaction between (Tsi)lithium and anhydrous tin(IV) bromide are the required (Tsi)tin tribromide and (Tsi) bromide in approximately a 50% mixture. A third minor impurity was also observed but its identity as yet is unknown. The origin of the (Tsi) bromide is unclear, however it is conceivable that a lithium/bromine exchange reaction could take place between (Tsi)lithium and tin(IV) bromide followed by a reductive elimination of lithium bromide to yield tin(II) bromide. This would be consistent with the absence of tin containing impurities as all the inorganic salt by-products would be removed during the recrystallisation process (equations 37 and 38).

$$[(CH_3)_3Si]_3CLi + SnBr_4 \rightarrow [(CH_3)_3Si]_3CBr + LiSnBr_3 \quad (37)$$

$$LiSnBr_3 \rightarrow LiBr + SnBr_2 \quad (38)$$

A second method by which (Tsi) bromide might be produced in the reaction is if (Tsi)tin tribromide is itself unstable and disproportionates to give (Tsi) bromide and tin(II) bromide (equation 39).

$$(Tsi)SnBr_3 \rightarrow (Tsi)Br + SnBr_2 \qquad (39)$$

A precedent for this type of disproportionation is available in the literature for t-butyltin trichloride which decomposes at room temperature yielding t-butyl chloride and tin(II) chloride (equation 19).[176]

Having obtained only limited success in the preparation of (Tsi)tin trihalides by either the direct addition of a (Tsi) anion to anhydrous tin(IV) halide or by the selective cleavage of aryl groups using either standard or catalysed halogenation conditions, a change of approach was sought. The methodology of selective group cleavage with halogen was maintained but a benzyl substituted (Tsi)tin compound was targeted as an intermediate followed by selective cleavage of the benzyl groups from tin instead of the phenyl groups which had previously proved only partially successful. In the literature it is cited that phenyl groups are preferentially cleaved in comparison with benzyl groups.[170] However, by the use of benzyl groups it was hoped to find that steric hindrance at tin would be relaxed as a result of the inclusion of a methylene unit between tin and the phenyl ring. The compound chosen to be used in this work as a precursor was dibenzyl-(Tsi)tin chloride (**6**) which was prepared by the reaction of

(Tsi)lithium with dibenzyltin dichloride (equation 40).

$$[(CH_3)_3Si]_3CLi + Bn_2SnCl_2 \rightarrow \underset{(6)}{\{[(CH_3)_3Si]_3C\}Bn_2SnCl} + LiCl \quad (40)$$

(Bn = benzyl.)

The spectra obtained for (6) were totally consistent with the expected product. In the ^1H nmr spectrum the signal obtained for the methylene protons in the benzyl group was a quartet with intensities in the ratio 1:4:4:1. This array is cited in the literature as resulting from an AB two proton system where the chemical shift difference between the two protons is approximately equal to the geminal coupling constant. The actual chemical shifts of the two protons cannot be directly obtained by measurement from the spectrum but have to be calculated using the following expression (equation 41).

$$\delta_A - \delta_B = [(\nu_4 - \nu_1)(\nu_3 - \nu_2)]^{1/2} = w \quad (41)$$

δ_A = origin position of the A proton.

δ_B = origin position of the B proton.

ν_x = chemical shift of line x.

The midpoint of the four line system is given by equation 42, and from a combination of these two expressions the origin positions for the two protons can be calculated (equations 43 and 44).

$$r = 1/2(\nu_3 + \nu_2) \quad (42)$$

$$\delta_A = r + 1/2w \quad (43)$$

$$\delta_B = r - 1/2w \quad (44)$$

r = midpoint of the four-line system.

By the use of the above expressions the chemical shifts for the geminal protons are δ_A = 2.83 ppm and δ_B = 2.89 ppm, generating a chemical shift difference of 15.4 Hz compared to the geminal coupling constant of 12 Hz.

The first halogen cleavage reaction attempted on (**6**) was bromine (chloroform solution) addition under standard conditions (equation 45).

$$Bn_2(Tsi)SnCl + xsBr_2 \rightarrow (Tsi)SnBr_2Cl + 2BnBr \quad (45)$$

However, by this method no cleavage of the benzyl groups occurred. Instead, two reactions took place, the first being the exclusively *para* directed electrophilic attack of bromine on the aryl ring, the second being the halogen exchange between bromine and chlorine on tin. The compound resulting from this reaction was di-(*para*-bromobenzyl)-(Tsi)tin bromide (**7**) (equation 46).

$$[(C_6H_5)CH_2]_2(Tsi)SnCl + xsBr_2 \rightarrow [p\text{-}Br(C_6H_4)CH_2]_2(Tsi)SnBr + 2HX \quad (46)$$

(**7**)

The spectroscopic data obtained on (7) is as expected for the compound obtained. In the ^1H nmr spectrum the AB quartet is again observed with the origin chemical shifts for the geminal protons calculated from equations 41 to 44 at δ_A = 2.69 ppm and δ_B = 2.75 ppm generating a chemical shift difference of 16.75 Hz compared to the geminal coupling constant of 12 Hz. On analysing the aryl region of the proton spectrum the *para* substitution has brought about a simplification of the spectrum resulting in two doublets displaying weak secondary long range coupling around the ring. The $J_{1,2}$ coupling constant for the ring protons is 8.4 Hz.

Due to the lack of success of a system based on electrophilic attack at the aryl group it was decided to investigate nucleophilic attack at tin using hydrogen bromide, which could result in the required benzyl cleavage generating toluene as the by-product (equation 47). In the reaction, an aqueous solution of hydrogen bromide and a diethyl ether solution of (6) were stirred together at room temperature.

$$Bn_2(Tsi)SnCl + HBr_{(aq)} \rightarrow (Tsi)SnBr_2Cl + 2(C_6H_5)CH_3 \qquad (47)$$

This reaction however, did not occur. Instead three compounds were isolated from the reaction, the first dibenzyl(Tsi)trimethylsiloxy-stannane (8), the second 1,1-bis(trimethylsilyl)-3-[dibenzyl(Tsi)-stannyl]prop-1-ene (9) and some unreacted starting material (6) (equation 48).

$$2Bn_2(Tsi)SnCl + 3HBr_{(aq)} \rightarrow (6) + (8) + (9) \quad (48)$$

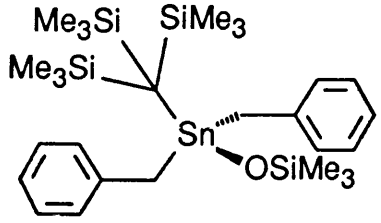

(8)

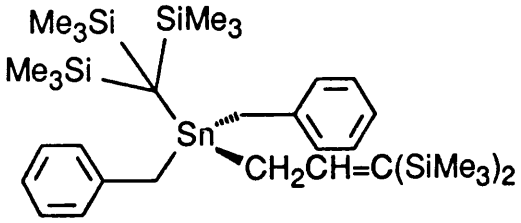

(9)

Compound (8) was characterised by its ^{1}H and ^{13}C nmr spectra, with no unusual features in evidence except for the singlet observed for the methylene protons in the benzyl groups as opposed to the quartet usually expected for the benzyl AB two proton system. It is not clear just by examination of models of the molecule as to why the two protons have become apparently equivalent. From the ^{29}Si nmr spectrum two signals are observed at 6.4 and -1.2 ppm, indicative of the two silicon environments expected for the proposed structure. The downfield signal can be assigned to the trimethylsiloxy moiety and displays a $^{2}J[(CH_3)_3{}^{29}SiO-{}^{117,119}Sn]$ of 58.0 Hz (unresolved) while the upfield signal assigned to the (Tsi) moiety displays a $^{2}J\{[(CH_3)_3{}^{29}Si]_3C-{}^{117,119}Sn)$ of 36.7 Hz (unresolved). In the infra-red spectrum of (8) a strong peak can be observed at 980 cm^{-1} which is highly characteristic of a non-bridging Sn-O-$SiMe_3$ system.[190,191]

A single crystal X-ray structure determination of compound (8) confirmed the proposed structure as can be seen in the ORTEP plot given in figure 19. Selected bond lengths and angles are given in

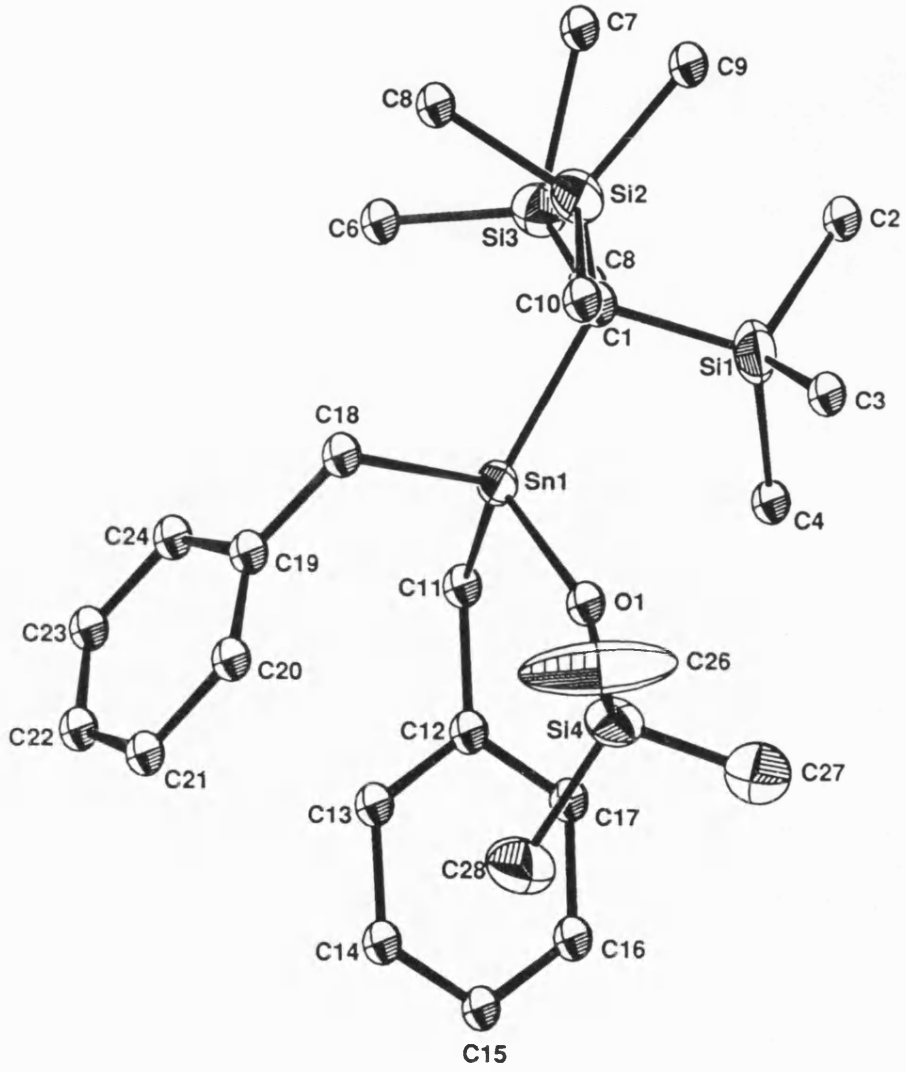

Figure 19: ORTEP Plot of Dibenzyl[tris(trimethylsilyl)methyl]-trimethylsiloxystannane (8).

table 12 and full crystal data are available in Appendix III. For the crystal sample used the cell geometry was monoclinic with a $P2_1/a$ space group. In the literature very few examples are available for comparison with the observed crystal structure. In the one analogous example available reported by Harrison et al.[192] high disorder was present in the unit cell precluding the solution of the crystal structure for triphenylsiloxytriphenyltin. A second example cited in the literature is the structural determination of di-1,3-(trimethylsiloxy)-1,1,3,3-(tetramethyl)distannoxane by Okawara et al.[193], however structural details are only given for the bond lengths in the bridged, dimeric distannoxane unit.

In the structure presented it can be seen that the tetrahedral array at tin is slightly distorted due to the relaxation of steric hindrance by the inclusion of the oxygen between the tin and the trimethylsilyl group and also by the presence of methylene groups between tin and the phenyl rings. As a result the molecule possesses a 'piano stool' type of appearance as the three pendular substituents have all oriented themselves away from the bulky (Tsi) group.

A comparison can be made for the tin-oxygen-silicon unit with the analogous lead system, triphenylsiloxytriphenyllead, as detailed by Harrison et al.[192] In this system longer metal-oxygen and silicon-oxygen bonds were observed compared to those present in (8) [Si-O 1.87(3)Å and Pb-O 2.01(3)Å compared to Si-O 1.63(1)Å and Sn-O 1.93(1)Å] as well as an expansion of the bond angle present in the unit [Si-O-Pb 142(1)° compared to Si-O-Sn 159.2(7)°].

For compound (9) the spectra obtained were more complex. Nmr

Table 12: Bond Lengths[a] and Angles[b] for Dibenzyl[tris(trimethylsilyl)-methyl]trimethylsiloxystannane (8).

Sn1 -C1	2.17(1)	Si4 -O1 -Sn1	159.2(7)
Sn1 -C11	2.17(2)	C1 -Sn1 -O1	106.7(5)
Sn1 -C18	2.17(2)	C11 -Sn1 -O1	105.9(5)
Sn1 -O1	1.93(1)	C18 -Sn1 -O1	103.3(6)
Si4 -O1	1.63(1)	C11 -Sn1 -C1	115.6(5)
		C18 -Sn1 -C1	113.3(6)
		C18 -Sn1 -C11	111.0(6)
		C12 -C11 -Sn1	115(1)
		C19 -C18 -Sn1	113(1)

[a] = Å.

[b] = °.

data for the benzyl and (Tsi) groups were as expected from previous examples, including the usual quartet for the methylene protons in the benzyl groups. The origin chemical shifts for the geminal protons can be calculated from equations 41 to 44 giving values of δ_A = 2.58 ppm and δ_B = 2.69 ppm generating a chemical shift difference of 29.0 Hz compared to the geminal coupling constant of 12.0 Hz. In this molecule the intensities of the quartet of signals is in the ratio 1:2:2:1. This is characteristic of a system where the difference in the chemical shifts of the AB protons is larger than the geminal coupling constant, as observed in the calculated values.

For the newly-formed alkenyl moiety three groups of signals are observed. The first group consists of two singlets at 0.07 and 0.12 ppm with integral ratios of 9H corresponding to the two trimethylsilyl groups occupying the bis-substituted C(1) positions of the prop-1-ene chain. The second two groups of signals are seen to be coupled to each other (7.9 Hz), one being a doublet at 2.19 ppm the other a triplet at 6.79 ppm with integral ratios of 2H and 1H respectively. These two groups of signals are generated by the propenyl protons on the C(2,3) positions.

For the ^{13}C nmr all peaks are totally assignable within the proposed structure, however uncertainties are raised by some of the observed signals. The uncertainties arise as a result of the the two most downfield signals corresponding to the C(1) and C(2) propenyl signals at 141.38 and 154.55 ppm respectively. The first surprising fact about these two signals is that from a standard ^{13}C nmr experiment the signal intensity of the bis-silyl substituted C(1)

carbon is only 33% lower than the intensity of the proton substituted C(2) carbon. This would seem to contradict the observations of Seyferth et al.[194] for the 1,1,2,2-tetramethyl-3,4-bis(trimethylsilyl)-1,2-disilacyclobut-3-ene system. In order to obtain sufficiently intense signals for the bis-silyl substituted ring carbons a pulse delay had to be incorporated into the nmr experiment to counteract the poor relaxation properties of the system. No explanation is readily forthcoming to clarify this observation. A second surprising observation concerning these two peaks is the equivalence of the ^{117,119}Sn couplings to both the C(1) and C(2) carbons at 37.4 Hz. Again no obvious explanation is available for this phenomenon.

From the ^{29}Si nmr spectrum three signals are observed at -0.9, -1.8 and -10.0 ppm as expected for the proposed structure. The most upfield shifted signal at -10.0 ppm arises from the *trans* trimethylsilyl C(1) substituent while the signal at -1.8 ppm arises from the analogous *cis* substituent. The signal at -0.9 ppm arises from the (Tsi) moiety and displays a $^{2}J([(CH_3)_3{}^{29}Si]_3C\text{-}^{117,119}Sn)$ of 30.5 Hz (unresolved).

A single crystal X-ray structure determination confirmed the proposed structure of (9), as can be observed in the ORTEP plot given in figure 20. Selected bond angles and bond lengths are given in table 13 and full crystal data are available in Appendix IV. For the crystal sample used the cell symmetry was triclinic with a $P\bar{1}$ space group.

In the structure of (9) a slightly distorted tetrahedral array is present at tin. The overall appearance of the molecule is reminiscent of (8) where to attain steric relaxation the pendular benzyl groups

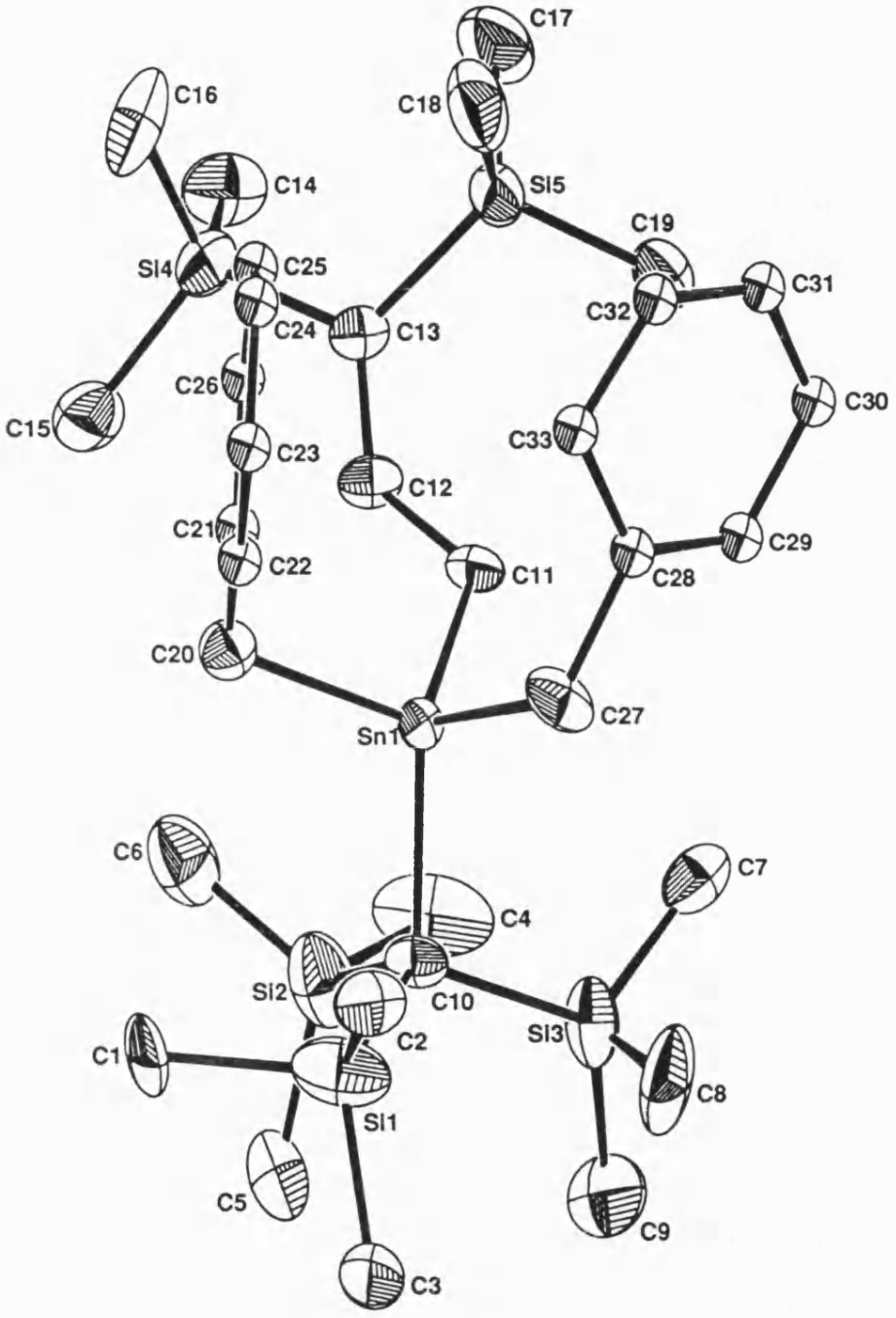

Figure 20: ORTEP Plot of 1,1-Bis(trimethylsilyl)-3-(dibenzyl[tris-(trimethylsilyl)methyl]stannyl)prop-1-ene (**9**).

Table 13: Bond Lengths[a] and Angles[b] for 1,1-Bis(trimethylsilyl)-3-{dibenzyl[tris(trimethylsilyl)methyl]stannyl}prop-1-ene (**9**).

Sn1 -C10	2.24(1)	C11 -Sn1 -C10	114.5(5)
Sn1 -C11	2.19(1)	C20 -Sn1 -C10	110.7(6)
Sn1 -C20	2.24(2)	C27 -Sn1 -C10	108.9(6)
Sn1 -C27	2.21(1)	C20 -Sn1 -C11	106.4(6)
C11 -C12	1.47(2)	C27 -Sn1 -C11	108.2(6)
C12 -C13	1.35(2)	C27 -Sn1 -C20	107.8(6)
Si4 -C13	1.85(2)	C12 -C11 -Sn1	116(1)
Si5 -C13	1.92(2)	C13 -C12 -C11	130(1)
		C12 -C13 -Si4	117(1)
		C12 -C13 -Si5	123(1)
		Si5 -C13 -Si4	119.4(8)
		C21 -C20 -Sn1	112(1)
		C28 -C27 -Sn1	115(1)
		Sn1 -C11 -C12 -C13	130.5

[a] = Å.

[b] = °.

and the allylic substituent are oriented away from the (Tsi) moiety thereby reducing the steric interactions. Similarly a 'piano stool' type appearance is again observed for the molecule.

In the allylic unit a double bond of length 1.35(2)Å is observed which is very similar in length to that found in ethylene (1.33Å). However, the bond distance between C11-C12 of 1.47(2)Å is shorter than a standard alkane carbon-carbon bond of approximately 1.54Å indicating a small increase in the bond order. In the allylic unit, C11, C12, C13, Si4 and Si5 are all planar and except for a slight expansion of the C13-C12-C11 bond angle to 130° all the other angles appear to approximate to those found in a typical alkene where sp^2 orbital mixing results in 120° bond angles.

In the literature only two examples of allyltin compounds have previously been investigated by single crystal X-ray diffraction. In the structure of triphenylallyltin reported by Ganis et al.[195] the bond lengths present in the allyl unit are 1.37(3)Å and 1.26(3)Å which are very short in comparison to standard alkane and alkene bond lengths. In the report it was theorised that $\sigma_{<Sn-C>}$-π conjugation was responsible for the decrease in the bond lengths in the allyl group. The evidence for this theory is largely based on the angle of tin away from the plane of the allyl substituents. In this example the torsional angle is either 108° or 97° (dependent on the conformer chosen) which is in good agreement with the theoretically calculated value of 90°[196] for maximum $\sigma_{<Sn-C>}$-π conjugation. In (**9**) the torsional angle for tin away from the plane of the allylic group is 134.5° which would lead to very low $\sigma_{<Sn-C>}$-π conjugation possibly

explaining the reason for (**9**) appearing more like an alkene than the hypothesised $\sigma_{\langle Sn-C\rangle}$-$\pi$ conjugated allylic system in triphenylallyltin.

In the second allyltin structure determination also by Ganis et al.[7] for cyclopent-2-enyltriphenyltin the allyl linkage displays bond lengths [1.52(4)Å and 1.35(4)Å] similar to those observed in (**9**) in comparison with the extreme bond shortening observed in triphenylallyltin. In this compound the torsional angles for tin away from the allylic plane are 111° and 92° (dependent on conformer) again giving a good alignment with the π-system for possible $\sigma_{\langle Sn-C\rangle}$-$\pi$ conjugation. In this system it is claimed that due to the incorporation of the allyl unit into a ring system any bond shortening would be opposed by ring strain. This would result in slight elongation of the optimum minimum bond length resulting from $\sigma_{\langle Sn-C\rangle}$-$\pi$ conjugation.

If $\sigma_{\langle Sn-C\rangle}$-$\pi$ conjugation is believed to be taking place in these compounds it should be possible to postulate a reason as to why this does not occur in (**9**). One possibility is that steric hindrance restricts the angle through which the tin atom can align with the allyl π-system thus removing the possible interaction responsible for $\sigma_{\langle Sn-C\rangle}$-$\pi$ conjugation. A second possibility is that a certain amount of electron density is back-donated from the π-system in the allyl unit into low lying empty *d*-orbitals on the silicons of the trimethylsilyl substituents. This would have the effect of lowering the electron density of the π-system thus negating the $\sigma_{\langle Sn-C\rangle}$-$\pi$ conjugation.

In an attempt to gain some insight into the mechanism by which these two rather surprising compounds were formed the synthesis was

repeated using dry hydrogen chloride gas bubbled through a solution of (**6**) in dichloromethane over a two-hour period. From this reaction only starting material was recovered, implicating the roles of water and/or diethyl ether in the formation of compounds (**8**) and (**9**). The exact mechanism of the reactions taking place is currently uncertain, although some speculations can be made as to the source of the novel moieties observed in the reaction products.

To synthesise compounds (**8**) and (**9**) the formation of several new sub-units has to be theorised. In compound (**8**) the only difference in comparison with starting material (**6**) is the presence of the trimethylsiloxy residue which must originate from a cleaved (Tsi) moiety from another molecule of starting material. Likewise with compound (**9**) only one group differs between the starting material (**6**) and the required product which in this instance is the appearance of the 1,1-bis(trimethylsilyl)prop-1-enyl moiety. The preparation of this residue poses the most awkward mechanistic questions as to its source.

On examination the group can be broken down into two more basic units i.e. a bis(trimethylsilyl)methyl moiety and a C_2 carbon backbone. The presence of the bis(trimethylsilyl)methyl unit accounts for the remains of the (Tsi) group from where the trimethylsilyl residue in compound (**8**) originated. The C_2 fragment can only come from one source in the reaction mixture and that is the diethyl ether as this is the only component encompassing an accessible C_2 unit. A general overview of the synthetic pathways occurring in the preparation of compounds (**8**) and (**9**) is given in scheme 3.

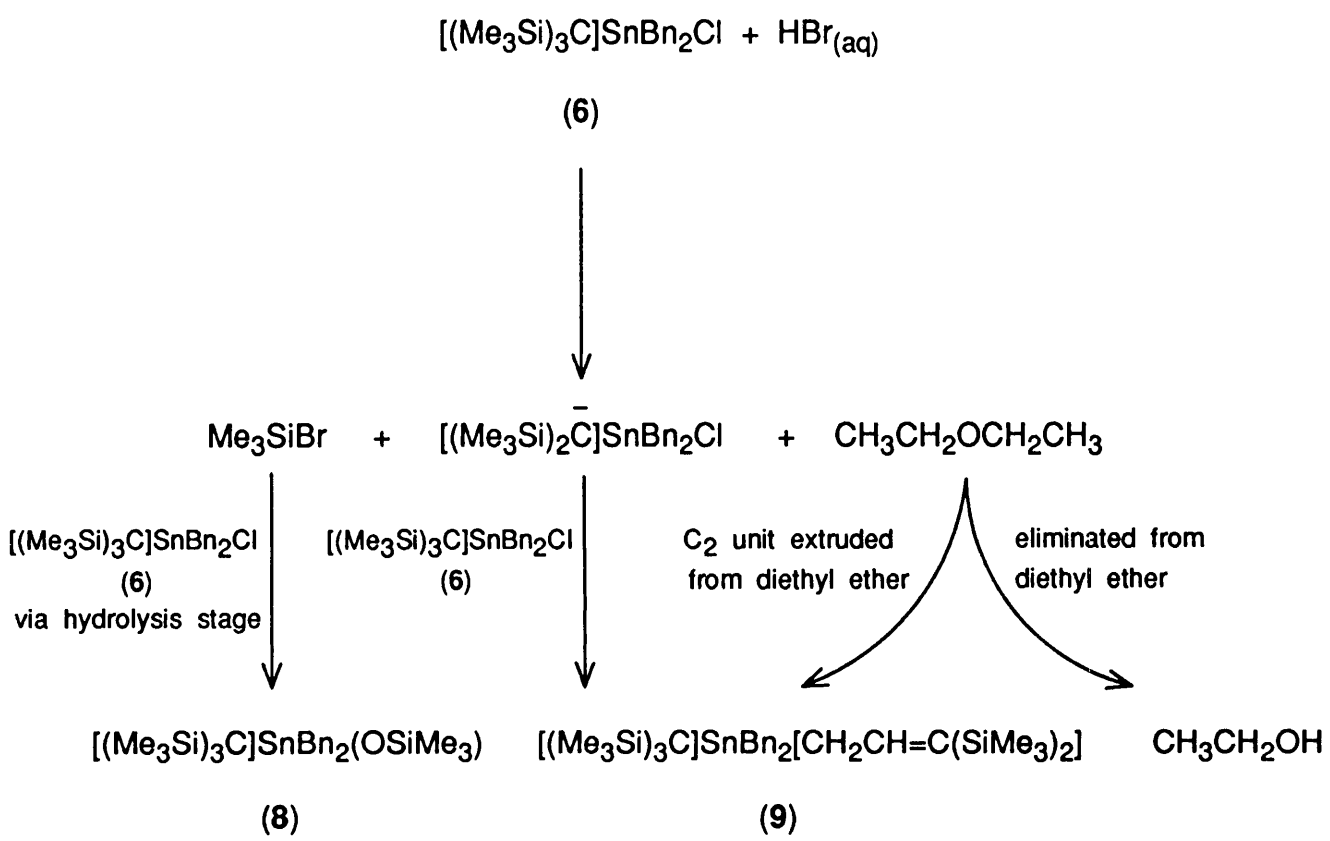

Scheme 3: An Overview of the Synthetic Routes Present in the Reaction Between Dibenzyl-[tris(trimethylsilyl)methyl]tin Chloride (**6**) and Aqueous Hydrogen Bromide.

Therefore to obtain the C_2 unit, a room temperature cleavage of diethyl ether has to be surmised. This could occur through the initial formation of a coordination bond between the oxygen of the ether and the Lewis acidic centre at tin, followed by the elimination of chloride which initially would yield a triorganotin alkoxide unit. A standard ether cleavage at this stage would yield a tin-oxygen bonded species which is not observed. However, if a rearrangement were to take place analogous to the Steven's rearrangement, a system would be created where a tin-carbon bonded species would occur and with a successive elimination of ethanol a potentially active C_2 ethenyl functionality bonded to tin, would be produced (figure 21).

The foreseeable problems with this mechanism are firstly the extreme steric hindrance present impeding the approach of the diethyl ether and thus reducing the likelihood of the formation of the initial coordination bond to tin. Secondly, having achieved the tin-ether bonded system the usual method by which a Steven's rearrangement is initiated is to remove a proton from the α-carbon (with respect to oxygen) to form a ylide, by the use of a strong base. The reaction conditions in this instance were acidic necessitating a modified ylide initiation stage to effect the rearrangement. A third question arising from this approach is that having produced an alkene moiety the presence of hydrogen bromide in the reaction conditions would be expected to yield some bromoethyl species in the reaction products resulting from the hydrobromination of the ethenyl system. However, no hydrobrominated species was isolated in the reaction products.

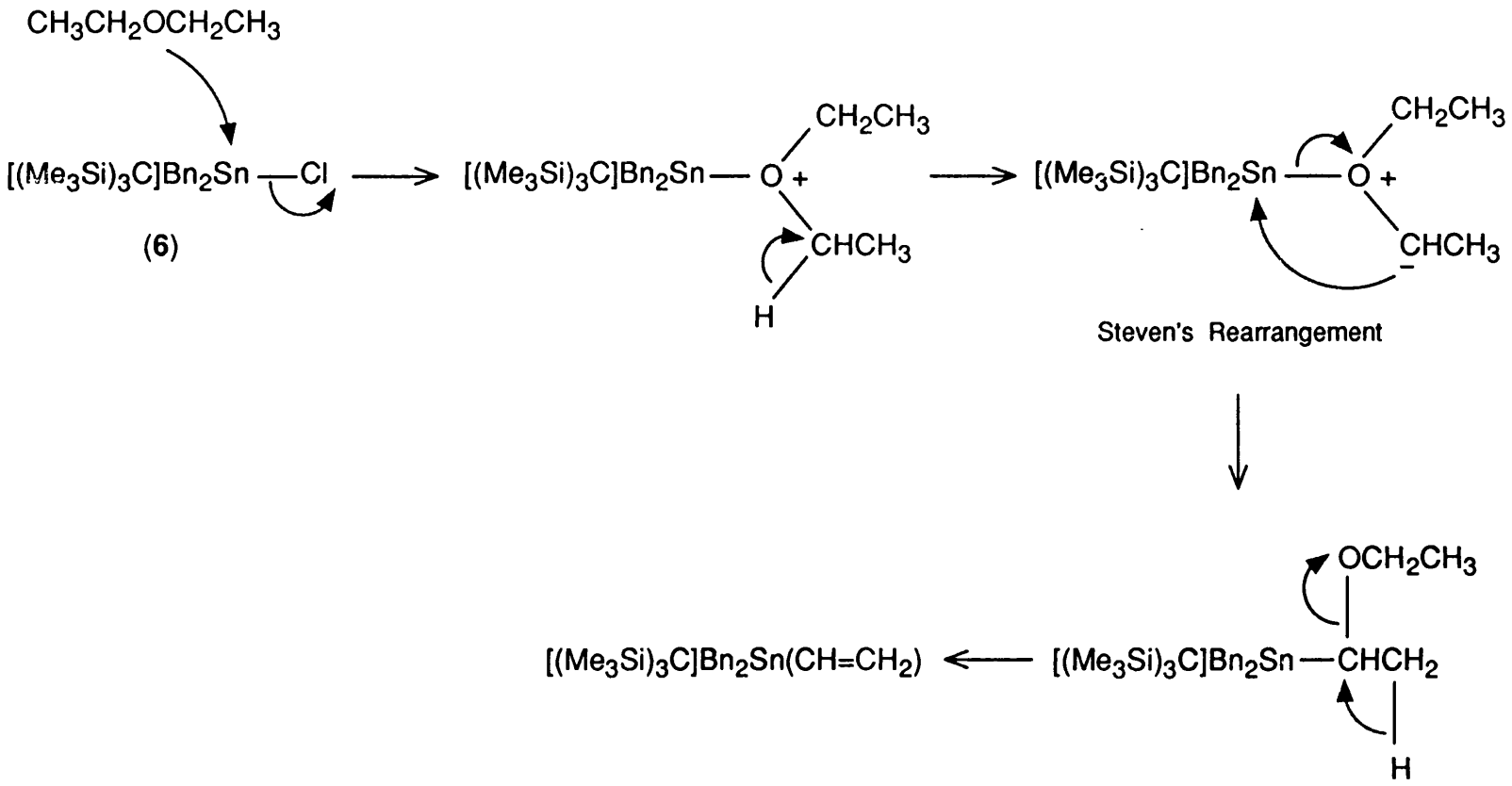

Figure 21: Formation of {Dibenzyl[tris(trimethylsilyl)]stannyl}ethene from a Steven's Rearrangement of Diethyl Ether at Tin.

Having created a suitably active C_2 group on tin the next process required is to analyse the reaction chemistry of the (Tsi) moiety from which the other residues required for the preparation of compounds (8) and (9) arise. On the basis of the reaction conditions present it is reasonable to assume that the (Tsi) derived residues will result from bromide attack on (6). In the starting material (6) two possible sites are available for the bromide nucleophilic attack to occur, the first being at a silicon in the (Tsi) unit and the second being at tin. By the first route a possible mechanism can be suggested for the production of a carbene which, on reaction with the ethenyl moiety, could give rise to the required propenyl group. Likewise with the second alternative the formation of the propenyl unit can be mechanistically predicted, but in this instance a (Tsi) anion is the active species involved in the attack on the ethenyl moiety.

By the first route the initial bromide attack would generate trimethylsilyl bromide and a sterically hindered carbanion. To produce a carbene from this system a possible intermediate might be a hindered stannene resulting from the elimination of chloride from tin, assuming that neither hydrolysis due to the aqueous conditions nor halogen exchange at tin, has occurred. From the stannene the required carbene may occur as a result of a double bond fission to produce the required carbene and dibenzylstannylene (figure 22). The dibenzylstannylene produced would be immediately hydrolysed to dibenzyltin oxide. The inert oxide would then take no further part in the synthesis and would probably not be observed in the reaction products due to its

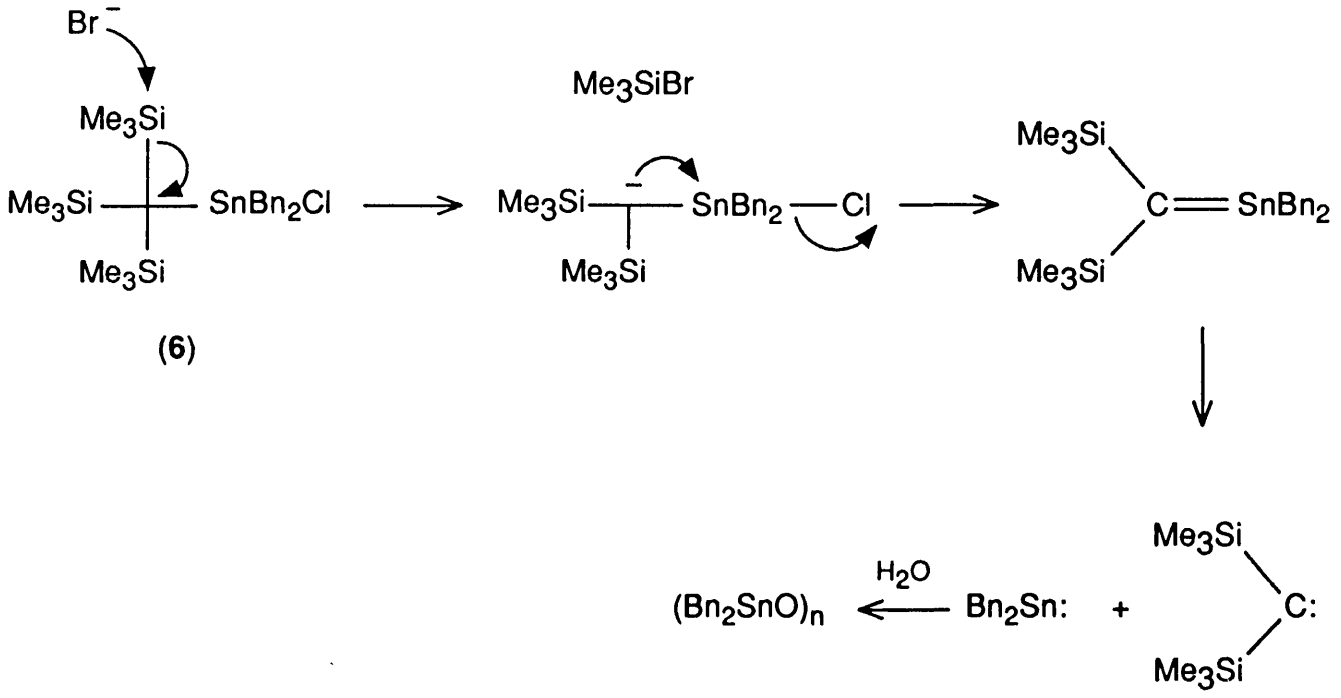

Figure 22: The Indirect Synthesis of Bis(trimethylsilyl)methyl Carbene from Bromide Attack at Silicon in Dibenzyl[tris(trimethylsilyl)methyl]tin Chloride (**6**).

insolubility in organic solvents and hence subsequent loss during purification. The ensuing reaction between the carbene and the ethenyl double bond could then proceed via a cyclopropyl intermediate followed by a steric relaxation induced 1,2-protic shift to produce the propenyl functionality required (figure 23).

The shortcomings of the explanation for the latter stage of the reaction are numerous. For instance, literature preparations of the bis(trimethylsilyl)methyl carbene are known but they involve either the photolysed or pyrolysed (400°C) extrusion of nitrogen from bis(trimethylsilyl)diazomethane.[197] From the same literature source it is also stated that having prepared the carbene a rearrangement is seen to take place forming a silene due to methyl migration from silicon to carbon, thus influencing the nature of the products obtained from further syntheses. Further inconsistencies arise when considering the very short predicted lifetimes of both the proposed carbene and its stannene precursor in the environment accorded by the reaction conditions i.e. water, oxygen and hydrogen bromide. The probability of the carbene being formed and also being present in the reaction mixture long enough to react with the ethenyl double bond as opposed to the other species present would be expected to be small.

In the second mode of attack by the bromide anion, dibenzyltin dihalide and the (Tsi) anion would be the two resultant products. The dibenzyltin dihalide might be hydrolysed by the reaction conditions present generating dibenzyltin oxide which as before would be lost in the purification process (figure 24). From the earlier reaction of starting material (**6**) and diethyl ether an ethenyl substituted

$[(Me_3Si)_3C]Bn_2Sn[CH_2CH{=}C(SiMe_3)_2]$

(9)

Figure 23: Bis(trimethylsilyl)methyl Carbene Attack on {Dibenzyl[tris(trimethylsilyl)methyl]stannyl}ethene.

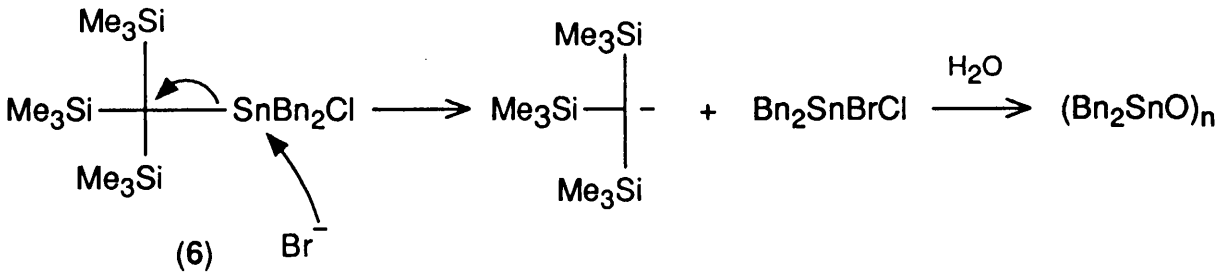

Figure 24: Formation of the Tris(trimethylsilyl)methyl Anion from Bromide Attack at Tin in Dibenzyl[tris(trimethylsilyl)methyl]tin Chloride (**6**).

tetraorganotin was produced (figure 21). If a (Tsi) anion addition to the ethenyl double bond took place it would most likely occur via an initial protonation of the C(2) position on the ethenyl system followed by the nucleophilic addition of the (Tsi) anion to the C(1) position. If a nucleophilic bromide attack then occurred at one of the trimethylsilyl groups on the (Tsi) moiety the subsequent anion could attack at the C(2) position resulting in the formation of a cyclopropyl unit with a subsequent loss of a hydride moiety (figure 25). Once the ring system is obtained, as previously explained, by way of a steric relaxation induced 1,2-protic shift, it could be opened to yield the required propenyl moiety (figure 23).

As with the previous mechanism several questions arise concerning the feasibilty of this mechanism. Firstly, as with the carbene the stability of the (Tsi) anion must be debatable under the acidic conditions present in the reaction. Secondly, during the addition of the (Tsi) anion to the double bonded ethenyl system, competition between the postulated addition and direct hydrobromination would occur resulting in the formation of some brominated species in the reaction mixture. A third contestable point from this mechanism is the method by which the cyclopropyl intermediate is formed. In the mechanism an anion is produced which attacks at the C(1) position on the ethenyl system eliminating a hydride moiety. This step seems unlikely as the anion would most likely protonate in the acidic environment. Additionally, even if the anion was stable enough for a nucleophilic attack to occur, then the lack of a good leaving group at the C(1) position would make the proposed step less likely.

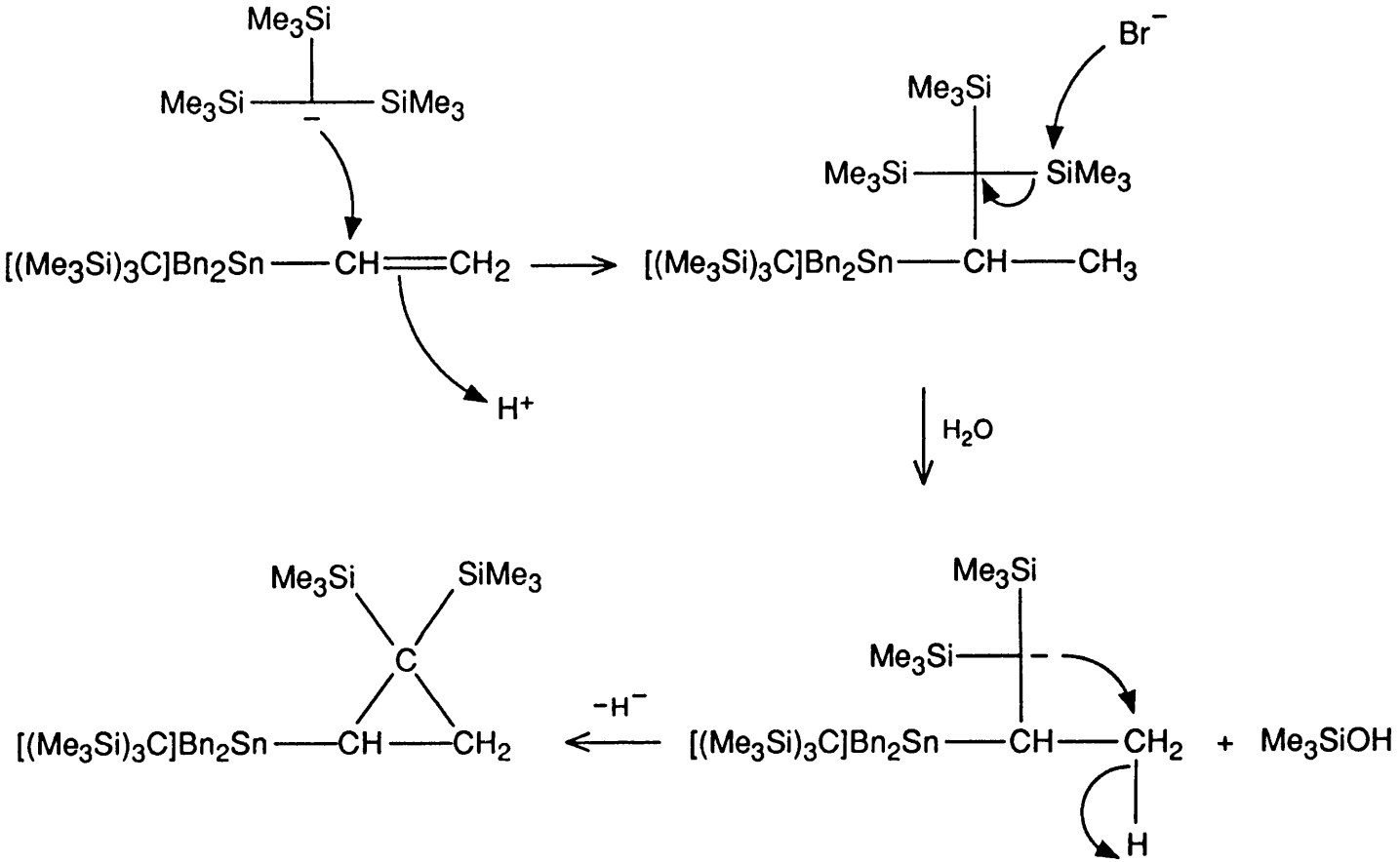

Figure 25: Tris(trimethylsilyl)methyl Anion Attack on {Dibenzyl[tris(trimethylsilyl)methyl]stannyl}ethene.

From both of the postulated mechanisms trimethylsilyl bromide is generated during the preparation of the required compound (9). By the reaction of trimethylsilyl bromide with another molecule of (6), probably via a hydrolysis stage, the preparative route to (8) can be surmised.

The ideas suggested in this text for the mechanism by which compound (9) is formed leave many questions unanswered. Obviously in the reaction medium, complex systems are invoked which may be unravelled with further investigation. At this stage however, conclusions as to the nature of the chemistry taking place are only speculative.

2.3 Experimental.

Di-i-propyldiphenyltin. To prepare the i-propyl Grignard reagent, i-propyl bromide (64.2g, 0.436 mole) in dry diethyl ether (1l) was added dropwise with stirring to magnesium turnings (10.3g, 0.424 mole) in dry diethyl ether (500ml). An exothermic reaction resulted and the reaction mixture was allowed to stir at room temperature for 4 hr. No magnesium remained at this stage. To this solution diphenyltin dichloride (50g, 0.145 mole) in dry diethyl ether (400ml) was added dropwise. Again an exothermic reaction occurred and stirring at room temperature was continued for 2 hr. resulting in the formation of a clear yellow diethyl ether solution and a heavy precipitate of inorganic salts. To decompose excess Grignard reagent, dilute hydrochloric acid was added with caution and the organic phase separated from the two-phase system. Resultant washings with diethyl ether were combined and dried over anhydrous sodium sulphate. *In vacuo* solvent removal from the organic phase yielded a yellow oil. The crude product was distilled at reduced pressure yielding a colourless oil. (43.9g, 84%), b.p. 108°C/0.2 mm.

I.R. [(cm^{-1}) liquid film]: 3075; 3060; 3025; 2970; 2950; 2875; 1585; 1485; 1470; 1435; 1210; 1160; 1085; 1010; 995; 880; 740; 715; 665; 515; 460; 410; 280.

^1H NMR [δ(ppm) $CDCl_3$ solution]: 1.45 [d,12H,$(CH_3)_2CH$]; 1.87 [m,2H, $(CH_3)_2CH$]; 7.31 and 7.49 [m,10H,C_6H_5]; $^3J[(C^1H_3)_2CH-^{117,119}Sn]$ 69.6, 72.9 Hz.

^{13}C NMR [δ(ppm) $CDCl_3$ solution]: 15.53 [$(CH_3)_2CH$]; 21.90 [$(CH_3)_2CH$];

128.21 and 128.37 [*m,p*-C_6H_5]; 137.35 [*o*-C_6H_5]; 139.54 [*i*-C_6H_5];

$^1J[(CH_3)_2{}^{13}CH-^{117,119}Sn]$ 362, 388 Hz; $^2J[(^{13}CH_3)_2CH-^{117,119}Sn]$ 15 Hz (unresolved).

^{119}Sn NMR [δ(ppm) $CDCl_3$ solution]: -80.8.

^{119m}Sn Mossbauer (mms^{-1}): I.S.=1.38.

Analysis (%): Found C 60.30; H 6.94; Calculated for $C_{16}H_{24}Sn$: C 60.21; H 6.74.

Mass Spectrum [(m/z) E.I]: 317 [M - i-Pr]$^+$; 275; 197; 120; 58; 43.

Dineophyldiphenyltin. To prepare the neophyl Grignard reagent, neophyl chloride (15g, 0.089 mole) in dry diethyl ether (300ml) was added dropwise with stirring to magnesium turnings (2.4g, 0.099 mole) in dry diethyl ether (100ml). A grey, turbid solution resulted. The overall reaction was slow, resulting in heating to reflux being applied over a 4 hr. period to drive the reaction to completion. On cooling, excess magnesium was removed by filtering the Grignard reagent solution through a glass wool plug. To the stirred Grignard reagent solution diphenyltin dichloride (10g, 0.029 mole) in dry diethyl ether (200ml) was added dropwise. An exothermic reaction resulted on addition and to ensure completion of reaction the mixture was heated at reflux. After a 2 hr. period a clear yellow diethyl ether solution and a heavy precipitate of inorganic salts resulted. To decompose excess Grignard reagent, dilute hydrochloric acid was added with caution and the organic phase separated from the two-phase system. Resultant washings with diethyl ether were combined and dried over anhydrous sodium sulphate. *In vacuo* solvent removal from the

organic phase yielded a light yellow oil. Purification of the oil by distillation even at 235°C (oil bath temperature)/0.3 mm was unsuccessful and so the crude reaction product was used directly in further syntheses. (11.21g, 72%)

I.R. [(cm^{-1}) liquid film]: 3075; 3040; 2980; 2950; 1610; 1590; 1500; 1490; 1450; 1440; 1390; 1370; 1285; 1195; 1080; 1040; 1005; 915; 780; 740; 710; 620; 565; 460; 260.

^{1}H NMR [δ(ppm) $CDCl_3$ solution]: 1.23 {s,12H,[$(C_6H_5)(CH_3)_2C$]CH_2}; 1.54 {s,4H,$(C_6H_5)(CH_3)_2C$]CH_2}; 7.16 [m,20H,C_6H_5]; ^{2}J[$(C_6H_5)(CH_3)_2CC'H_2$-^{117,119}Sn] 52.8 Hz (unresolved).

^{13}C NMR [δ(ppm) $CDCl_3$ solution]: 31.59 {[$(C_6H_5)(CH_3)_2C$]CH_2]; 32.73 and 37.85 {[$(C_6H_5)(CH_3)_2$]CH_2}; 125.17 [o-C_6H_5, neophyl]; 125.39 [p-C_6H_5, neophyl]; 127.83 and 127.96 [m-C_6H_5, neophyl and Ph; p-C_6H_5, Ph]; 136.58 [o-C_6H_5, Ph]; 141.42 [i-C_6H_5, Ph]; 150.82 [i-C_6H_5, neophyl]; ^{1}J[$(C_6H_5)(CH_3)_2C'^{13}CH_2$-^{117,119}Sn] 348.1, 363.5 Hz; ^{3}J[$(C_6H_5)('^{13}CH_3)_2CCH_2$-^{117,119}Sn] 37.5 Hz and 17.6 Hz (unresolved).

^{119}Sn NMR [δ(ppm) $CDCl_3$ solution]: -97.5.

^{119m}Sn Mossbauer (mms^{-1}): I.S.=1.34.

Analysis (%): Found C 71.70; H 6.83; Calculated for $C_{32}H_{36}Sn$: C 71.27; H 6.73.

Mass Spectrum [(m/z) C.I.]: 463 [M - Ph]$^+$; 407 [M - neophyl]$^+$; 352; 133; 119; 105; 91.

Di-i-propyltin Dibromide. To a stirred solution of di-i-propyl-diphenyltin (42g, 0.117 mole) in chloroform (200ml) at room temperature, a solution of bromine (37.4g, 0.234 mole) in chloroform

(200ml) was added dropwise. Total decolourisation of the bromine solution resulted after stirring for a period of 18 hr. *In vacuo* removal of the chloroform produced a pale orange oil. Distillation of the crude product at reduced pressure yielded two fractions, the first being phenyl bromide (b.p. 18°C/0.18 mm) and secondly the di-i-propyltin dibromide. (39.8g, 93%), b.p. 46-48°C/0.18 mm.

I.R. [(cm^{-1}) liquid film]: 2960; 2880; 1470; 1400; 1380; 1205; 1180; 1100; 1010; 935; 880; 530; 505; 410; 280.

^1H NMR [δ(ppm) $CDCl_3$ solution]: 1.46 [d,12H,$(CH_3)_2CH$]; 2.31 [m,2H,$(CH_3)_2CH$]; $^3J[(C^1H_3)_2CH-^{117,119}Sn]$ 124.3, 130.0 Hz.

^{13}C NMR [δ(ppm) $CDCl_3$ solution]: 20.33 [$(CH_3)_2CH$]; 31.37 [$(CH_3)_2CH$].

^{119}Sn NMR [δ(ppm) $CDCl_3$ solution]: 95.2

^{119m}Sn Mossbauer (mms^{-1}): I.S.=1.69; Q.S.=3.41.

Analysis (%): Found C 19.90; H 3.94; Calculated for $C_6H_{14}Br_2Sn$: C 19.76; H 3.87.

Mass Spectrum [(m/z) C.I.]: 364 $[M]^+$; 321 $[M - i\text{-}Pr]^+$; 285 $[M - Br]^+$; 242; 199; 120.

Dineophyltin Dibromide. To a stirred solution of dineophyldiphenyltin (16.3g, 0.030 mole) in chloroform (50ml) at room temperature, a solution of bromine (9.7g, 0.061 mole) in chloroform (100ml) was added dropwise. Total decolourisation of the bromine solution resulted after stirring for a period of 6 hr. *In vacuo* removal of the chloroform yielded a tan coloured oil. Distillation of the crude product at reduced pressure yielded a first fraction of phenyl bromide however, as with the dineophyldiphenyltin precursor, even at high temperatures

no higher fraction was obtained. As a result the residual liquors were used for spectral analysis. (10.1g, 62%)

I.R. [(cm^{-1}) liquid film]: 3100; 3075; 3045; 2980; 1610; 1590; 1505; 1480; 1455; 1395; 1380; 1285; 1205; 1085; 1040; 780; 760; 740; 715; 570; 255.

^{1}H NMR [δ(ppm) $CDCl_3$ solution]: 1.38 {s,12H,[$(C_6H_5)(CH_3)_2C$]CH_2}; 1.96 {s,4H,[$(C_6H_5)CH_3)_2$]CH_2}; 7.26 {m,10H,[$(C_6H_5)(CH_3)_2C$]CH_2};

^{2}J[$(C_6H_5)(CH_3)_2CC'H_2$-^{117,119}Sn] 53.1 Hz (unresolved);

^{4}J[$(C_6H_5)(C'H_3)_2CCH_2$-^{117,119}Sn] 7.5 Hz (unresolved).

^{13}C NMR [δ(ppm) $CDCl_3$ solution]: 31.66 and 38.44 {[$(C_6H_5)(CH_3)_2C$]CH_2}; 47.13 {[$(C_6H_5)(CH_3)_2C$]CH_2}; 125.01 and 126.43 [*o,p*-C_6H_5]; 128.61 [*m*-C_6H_5]; 148.88 [*i*-C_6H_5]; ^{1}[$(C_6H_5)(CH_3)_2C'^{13}CH_2$-^{117,119}Sn] 380, 395 Hz ; ^{3}J[$(C_6H_5)(^{13}CH_3)_2CCH_2$-^{117,119}Sn] 25 Hz and 35Hz (unresolved).

^{119}Sn NMR [δ(ppm) $CDCl_3$ solution]: 22.8.

^{119m}Sn Mossbauer: I.S.=1.54; Q.S.=2.72.

Analysis (%): Found C 43.80; H 4.85; Calculated for $C_{20}H_{26}Br_2Sn$: C 44.08; H 4.81.

Mass Spectrum [(m/z), C.I.]: 465 [M - Br]$^+$; 411 [M - neophyl]$^+$; 133; 91.

Di-t-butyltin Dichloride. To prepare the t-butyl Grignard reagent, freshly distilled t-butyl chloride (106.6g, 1.15 mole) in dry tetrahydrofuran (900ml) was added with stirring, to magnesium turnings (28g, 1.15 mole) (activated with 0.2ml iodomethane) in dry tetrahydrofuran (100ml). After a brief initiation period a mildly exothermic reaction resulted and the reaction allowed to stir at room

temperature for 4 hr. The Grignard reagent solution, prior to further usage, was filtered via a glass wool plug to remove any excess magnesium followed by a dropwise addition to a solution of anhydrous tin(IV) chloride (119.9g, 0.46 mole) in 60-80 petrol (2l) at 0°C. A highly exothermic reaction occurred generating large amounts of the tin(IV) chloride ditetrahydrofuranate, which necessitated heating the mixture to reflux for 4 hr to ensure the completion of the required Grignard substitution reaction. To decompose excess Grignard reagent, dilute hydrochloric acid was added with caution followed by the addition of saturated ammonium chloride solution to encourage the formation of a two-phase system. After separation the aqueous phase was washed repeatedly with diethyl ether. The collective organic fractions were dried over anhydrous sodium sulphate followed by *in vacuo* solvent removal to yield a bright yellow oil. The crude product was distilled at reduced pressure yielding a pale yellow coloured oil that solidified at room temperature. (42.3g, 36.3%), b.p. 52-54°C/0.4 mm.

I.R. [(cm^{-1}) liquid film]: 2975; 2940; 2860; 1470; 1370; 1180; 1020; 800; 340.

^{1}H NMR [δ(ppm) $CDCl_3$ solution]: 1.47 [s,18H,$(CH_3)_3C$]; ^{3}J[$(C'H_3)_3C$-$^{117,119}Sn$] 112.1, 117.2 Hz.

^{13}C NMR [δ(ppm) $CDCl_3$ solution]: 29.16 [$(CH_3)_3C$]; 45.18 [$(CH_3)_3C$].

^{119}Sn NMR [δ(ppm) $CDCl_3$ solution]: 53.9.

^{119m}Sn Mossbauer (mms^{-1}): I.S.=1.72; Q.S.=3.02.

Analysis (%): Found C 31.68; H 6.19; Calculated for $C_8H_{18}Cl_2Sn$: C 31.63; H 5.97.

i-Propyltriphenyltin. To prepare triphenyltin lithium, triphenyltin chloride (40g, 0.104 mole) in dry tetrahydrofuran (120ml) was added in a dropwise manner to ultrasound-cleaned lithium shot (3.6g, 0.519 mole) in dry tetrahydrofuran (120ml) at room temperature. After 5 hr. stirring an intense dark green colouration was present in the solution. After stirring for a further 15 hr. the excess lithium was filtered off by passing the solution through a glass wool plug. The dark green triphenyltin lithium solution was then added in a dropwise manner to a solution of i-propyl bromide (12.8g, 0.104 mole) in dry tetrahydrofuran (120ml) at room temperature, resulting in a further darkening of the reaction mixture. *In vacuo* solvent removal yielded a black oil. Organic solvent extraction using a diethyl ether/water two-phase system yielded a nearly colourless diethyl ether phase which was dried over anhydrous sodium sulphate. *In vacuo* solvent removal yielded an off-white crystalline solid which was purified by recrystallisation from a mixture of chloroform/ethanol. (33.4g, 82%), m.p. 81-82°C.

I.R. [(cm^{-1}) KBr disc]: 3075; 3025; 2975; 2940; 2860; 1480; 1430; 1075; 1020; 995; 990; 750; 740; 695; 655; 495; 440; 260.

^{1}H NMR [δ(ppm) $CDCl_3$ solution]: 1.45 [d,6H,$(CH_3)_2CH$]; 2.07 [m,1H, $(CH_3)_2CH$]; 7.32 and 7.54 [m,15H,C_6H_5]; ^3J[$(C^1H_3)_2CH$-^{117,119}Sn] 77.5, 80.2 Hz.

^{13}C NMR [δ(ppm) $CDCl_3$ solution]: 16.74 [$(CH_3)_2CH$]; 21.73 [$(CH_3)_2CH$]; 128.44 [*p*-(C_6H_5)]; 128.77 [*m*-(C_6H_5)]; 137.36 [*o*-(C_6H_5)]; 138.82 [*i*-(C_6H_5)]; ^2J[$(^{13}CH_3)_2CH$-^{117,119}Sn] 17.6 Hz (unresolved); ^{2}[*o*-($^{13}C_6H_5$)-^{117,119}Sn] 33.1 Hz (unresolved); ^3J[*m*-($^{13}C_6H_5$)-^{117,119}Sn] 88.1 Hz (unresolved); ^4J[*p*-($^{13}C_6H_5$)-^{117,119}Sn] 17.6 Hz (unresolved).

^{119}Sn NMR [δ(ppm) $CDCl_3$ solution]: -105.1.

^{119m}Sn Mossbauer (mms^{-1}): I.S.=1.22.

Analysis (%): Found C 64.31; H 5.60; Calculated for $C_{21}H_{22}Sn$: C 64.17; H 5.64.

i-Propyltin Tribromide. To a stirred solution of i-propyltriphenyltin (15g, 0.038 mole) in chloroform (250ml) at room temperature a solution of bromine (18.31g, 0.115 mole) in chloroform (100ml) was added dropwise. Total decolourisation of the bromine solution occurred after stirring for a period of 15 hr. *In vacuo* removal of the chloroform yielded a grey oil. Distillation of the crude product at reduced pressure yielded the expected phenyl bromide and a second higher boiling point fraction of the required i-propyltin tribromide. (14g, 91%), b.p. 43°C/0.3 mm.

I.R. [(cm^{-1}) liquid film]: 2975; 2950; 2925; 2860; 1460; 1395; 1375; 1195; 1150; 1095; 1005; 505; 400; 270.

^{1}H NMR [δ(ppm) $CDCl_3$ solution]: 1.48 [d,6H,$(CH_3)_2CH$]; 2.88 [m,1H, $(CH_3)_2CH$]; $^3J[(C'H_3)_2CH-^{117,119}Sn]$ 215.9, 230.5 Hz.

^{13}C NMR [δ(ppm) $CDCl_3$ solution]: 19.82 [$(CH_3)_2CH$]; 41.78 [$(CH_3)_2CH$]; $^2J[(^{13}CH_3)_2CH-^{117,119}Sn]$ 41.8 Hz (unresolved).

^{119}Sn NMR [δ(ppm) $CDCl_3$ solution]: -115.3.

^{119m}Sn Mossbauer (mms^{-1}): I.S.=1.41; Q.S.=1.81.

Analysis (%): Found: C 9.19; H 1.81; Calculated for $C_3H_7Br_3Sn$: C 8.98; H 1.76.

Dimesityltin Dichloride. To prepare mesityllithium, mesityl bromide (5g, 0.025 mole) in dry tetrahydrofuran (30ml) was added dropwise with stirring to a solution of n-butyllithium (1.6g, 10.3ml of a 2.4M solution in hexane, 0.025 mole) in dry tetrahydrofuran (65ml) at -78°C. After initial decolourisation of the pale yellow n-butyllithium solution an intense white precipitate formed. Stirring at -78°C was continued for a period of 3 hr. To the stirred slurry anhydrous tin(IV) chloride (3.2g, 0.013 mole) in dry n-hexane (100ml) was added dropwise. At -78°C no apparent reaction was seen to take place however at approximately 0°C the quantity of the white precipitate diminished markedly. After 15 hr. stirring a pale yellow solution and a small quantity of a white precipitate resulted. To ensure completion of reaction the mixture was heated to reflux for a 2 hr. period. After cooling and *in vacuo* solvent removal the residue was redissolved in chloroform and filtered to remove any inorganic side products. On solvent removal, an off-white solid resulted, which was recrystallised from ethyl acetate/60-80 petrol (1.1g, 21%), m.p. 172-173°C.

I.R. [(cm^{-1}) KBr disc]: 3025; 2985; 2925; 2860; 1600; 1560; 1450; 1410; 1380; 1300; 1045; 855; 710; 595; 555; 345; 320.

^1H NMR [δ(ppm) $CDCl_3$ solution]: 2.28 [s,6H, *p*-$(CH_3)_3C_6H_2$]; 2.54 [s,12H, *o*-$(CH_3)_3C_6H_2$]; 6.93 [s,4H, *m*-$(CH_3)_3C_6H_2$]; ^4J[*o*-$(C'H_3)_3C_6H_2$-$^{117,119}Sn$] 9.2 Hz (unresolved); ^4J[*m*-$(CH_3)_3C_6'H_2$-$^{117,119}Sn$] 36.3 Hz (unresolved).

^{13}C NMR [δ(ppm) $CDCl_3$ solution]: 21.08 [*p*-$(CH_3)_3C_6H_2$]; 24.68 [*o*-$(CH_3)_3C_6H_2$]; 129.55 [*m*-$(CH_3)_3C_6H_2$]; 139.15 [*i*-$(CH_3)_3C_6H_2$]; 141.38 [*p*-$(CH_3)_3C_6H_2$]; 143.53 [*o*-$(CH_3)_3C_6H_2$]; ^2J[*o*-$(CH_3)_3{}'^3C_6H_2$-$^{117,119}Sn$] 59.5 Hz (unresolved); ^3J[*m*-$(CH_3)_3{}'^3C_6H_2$-$^{117,119}Sn$] 77.1 Hz

(unresolved); $^{3}J[o\text{-}(^{13}CH_3)_3C_6H_2\text{-}^{117,119}Sn]$ 48.5 Hz (unresolved).

^{119}Sn NMR [δ(ppm) $CDCl_3$ solution]: -51.6.

^{119m}Sn Mossbauer (mms^{-1}): I.S.=1.33; Q.S.=2.65.

Analysis (%): Found C 50.30; H 5.27; Calculated for $C_{18}H_{22}Cl_2Sn$: C 50.50; H 5.20.

Dimesityltin Dihalides. To prepare the mesityl Grignard reagent, mesityl bromide (31.40g, 0.158 mole) in dry diethyl ether (90ml) was added dropwise with stirring, to previously activated magnesium turnings (3.88g, 0.160 mole) (0.2ml methyl iodide) in diethyl ether (10ml). The Grignard formation was very sluggish at ambient temperature and so gentle heating to 35°C (water bath) was implemented. After a period of 5 hr. at 35°C the excess magnesium was filtered off through a glass wool plug. The Grignard reagent solution was cooled to -20°C prior to the dropwise addition of anhydrous tin(IV) chloride (19.6g, 0.075 mole) in dry 60-80 petrol (250ml) which resulted in the formation of a dense white precipitate. After stirring at room temperature for 15 hr. the mixture was heated to reflux to ensure total reaction of the Grignard reagent. On cooling a light yellow solution with a white precipitate resulted. After removal of the solids by filtration the combined organic filtrates were reduced to a light yellow oil by *in vacuo* solvent removal. Trituration with 80-100 petrol yielded an off-white solid which was recrystallised from 80-100 petrol. (11.2g, 30%), m.p. 172-174°C.

I.R. [(cm^{-1}) KBr disc]: 3025; 2975; 2925; 2860; 1600; 1560; 1445; 1405; 1375; 1295; 1040; 855; 705; 590; 545; 335; 315.

Because of the mixed halide nature of the product the chemical shift values for ^{1}H and ^{13}C nmr are slightly confused due to differing environments which result from the changing nature of the halogen products. However, the nmr chemical shifts are very similar to those observed for the pure dimesityltin dichloride example detailed above.

^{119}Sn NMR [δ(ppm) $CDCl_3$ solution]: -52.4 [Mes_2SnCl_2]; -97.8 [$Mes_2SnBrCl$]; -148.1 [Mes_2SnBr_2].

^{119m}Sn Mossbauer (mms^{-1}): I.S.=1.38; Q.S.=2.52.

Analysis (%): Found C 42.70; H 4.42; Calculated for 3% $C_{18}H_{22}Cl_2Sn$: 30% $C_{18}H_{22}BrClSn$: 67% $C_{18}H_{22}Br_2Sn$ (% products taken from ^{119}Sn nmr integrals): C 43.25; H 4.44.

Mesityltin Trihalides. Anhydrous tin(IV) chloride (1.56g, 0.006 mole) was added to dimesityltin dihalide, from the above preparation (3g, 0.006 mole) at -5°C, under anaerobic conditions. After cooling to -196°C a partial vacuum was applied to the reaction tube prior to sealing. After attaining room temperature, the mixture was heated at 150°C for a 3 hr. period. On cooling an off-white solid formed which was recrystallised from 80-100 petrol. (3.2g, 70%), m.p. 74-74.5°C.

I.R. [(cm^{-1}) KBr disc]: 3030; 2975; 2930; 1600; 1560; 1450; 1385; 1300; 1255; 1045; 1020; 900; 865; 705; 595; 555; 370; 320; 285.

For the same reasons given for the dimesityltin dihalides the resolution in the ^{1}H and ^{13}C nmr spectra was poor and so values are quoted for the average chemical shifts for peaks of comparable derivation.

^{1}H NMR [δ(ppm) $CDCl_3$ solution]: 2.36 [s,3H, *p*-(CH_3)$_3C_6H_2$]; 2.69 [t,6H,

o-(CH_3)$_3$$C_6H_2$]; 7.02 [t,2H, *m*-($CH_3$)$_3$$C_6H_2$]; ^{4}J[*m*-($CH_3$)$_3$$C_6$'$H_2$-^{117,119}Sn] 57.5, ≈60, and 61.6 Hz (unresolved); ^{6}J[*p*-(C'H_3)$_3$$C_6H_2$-^{117,119}Sn] 7.9 Hz (unresolved).

^{13}C NMR [δ(ppm) $CDCl_3$ solution]: 21.18 [*p*-(CH_3)$_3$$C_6H_2$]; 43.18 [*o*-($CH_3$)$_3$$C_6H_2$]; 130.10 [*m*-($CH_3$)$_3$$C_6H_2$]; 143.30, 143.40 and 143.56 [*i,o,p*-(CH_3)$_3$$C_6H_2$]; ^{3}J[*m*-($CH_3$)$_3$$^{13}C_6H_2$-^{117,119}Sn] 116.8 Hz (unresolved); ^{3}J[*o*-($^{13}CH_3$)$_3$$C_6H_2$-^{117,119}Sn] 57.4 Hz (unresolved).

^{119}Sn NMR [δ(ppm) $CDCl_3$ solution]: -85.5 [$MesSnCl_3$]; -150.1 [$MesSnBrCl_2$]; -219.7 [$MesSnBr_2Cl$]; -294.2 [$MesSnBr_3$].

^{119m}Sn Mossbauer (mms^{-1}): I.S.=1.20; Q.S.=1.72.

Analysis (%): Found C 28.60; H 2.93; Calculated for 41% $C_9H_{11}Cl_3Sn$: 44% $C_9H_{11}Cl_2BrSn$: 14% $C_9H_{11}ClBr_2Sn$: 2% $C_9H_{11}Br_3Sn$ (% products taken from ^{119}Sn nmr integrals): C 28.78; H 2.95.

Attempted preparation of (2,4,6-tri-i-propylphenyl)tin tribromide. To prepare 2,4,6-tri-i-propylphenyllithium, n-butyllithium (1.13g, 7.07ml of a 2.5M solution in hexane, 0.018mole) in dry tetrahydrofuran (50ml) was added dropwise to a stirred solution of 2,4,6-tri-i-propylphenyl bromide (5g, 0.018 mole) in dry tetrahydrofuran (25ml) at -78°C. After stirring for 1 hr. no apparent change had taken place and so the reaction mixture was warmed to -35°C upon which a white precipitate formed. However, with successive stirring the precipitate totally redissolved. After a further period of stirring for 1 hr. the reaction mixture was cooled to -78°C prior to further reaction. Anhydrous tin(IV) bromide (7.74g, 0.018 mole) in dry 60-80 petrol was added dropwise to the stirred reaction mixture at -78°C, resulting in a

series of colour changes from yellow, through orange and eventually yielding a white slurry on completion of addition. After warming to room temperature the reaction was stirred for a further 15 hr. period upon which a beige oily precipitate remained. The mixture was heated gently to reflux for 2 hr. after which *in vacuo* solvent removal yielded a light brown oily product. Trituration with acetone followed by recrystallisation also from acetone yielded a highly crystalline white solid [1,2-dibromo-1,1,2,2-tetra(2,4,6-i-propylphenyl)-distannane (1). (1.8g, 17%), m.p. 180-181°C.

I.R. [(cm^{-1}) KBr disc]: 3050; 2975; 2880; 1600; 1560; 1465; 1415; 1390; 1365; 1265; 1100; 1070; 1055; 1010; 880; 800; 740; 640; 510; 385.

^{1}H NMR [δ(ppm) $CDCl_3$ solution]: 0.11 {d,6H, 2,4,6-[(CH_3)$_2$CH]$_3^a$$C_6H_2$); 0.25 {d,6H, 2,4,6-[($CH_3$)$_2$CH]$_3^b$$C_6H_2$); 0.31 {d,6H, 2,4,6-[($CH_3$)$_2$CH]$_3^c$-$C_6H_2$); 1.13 {[t,18H] 6H, 2,4,6-[(CH_3)$_2$CH]$_3^a$$C_6H_2$; 12H, 2,4,6-[($CH_3$)$_2$CH]$_3^d$$C_6H_2$); 1.23 {[d,18H] 6H, 2,4,6-[(CH_3)$_2$CH]$_3^c$$C_6H_2$; 12H, 2,4,6-[($CH_3$)$_2$CH]$_3^a$$C_6H_2$); 1.27 {d,6H, 2,4,6-[($CH_3$)$_2$CH]$_3^b$$C_6H_2$); 1.44 {t,12H, 2,4,6-[($CH_3$)$_2$CH]$_3^f$$C_6H_2$); 2.50 {m,2H, 2,4,6-[($CH_3$)$_2$C*H*]$_3^b$-$C_6H_2$) ; 2.72 {m,2H, 2,4,6-[($CH_3$)$_2$C*H*]$_3^d$$C_6H_2$); 2.86 {m,2H, 2,4,6-[($CH_3$)$_2$C*H*]$_3^a$$C_6H_2$); 3.14 {m,2H, 2,4,6-[($CH_3$)$_2$C*H*]$_3^c$$C_6H_2$); 3.21 {m,2H, 2,4,6-[($CH_3$)$_2$C*H*]$_3^a$$C_6H_2$); 3.40 {m,2H, 2,4,6-[($CH_3$)$_2$C*H*]$_3^f$$C_6H_2$); 6.85 {d,4H, 2,4,6-[($CH_3$)$_2$CH]$_3$$C_6$*H*$_2$); 6.94 {s,2H, 2,4,6-[($CH_3$)$_2$CH]$_3$-$C_6$*H*$_2$); 7.10 {s,2H, 2,4,6-[($CH_3$)$_2$CH]$_3$$C_6$*H*$_2$).

^{13}C NMR [δ(ppm) $CDCl_3$ solution]: 22.54, 22.80, 23.09, 23.81, 23.97, 25.33, 25.66, 26.43 and 27.73 {2,4,6-[(*C*H$_3$)$_2$CH]$_3$$C_6H_2$); 34.19, 37.33, 39.86 and 41.81 {2,4,6-[(CH_3)$_2$*C*H]$_3$$C_6H_2$); 122.15, 122.93, 123.42 and

123.97 {2,4,6-[$(CH_3)_2CH]_3$*m*-C_6H_2); 141.58 and 145.76 {2,4,6-[$(CH_3)_2CH]_3$ *i*-C_6H_2); 150.63, 152.38, 153.61, 154.75 and 155.201 {2,4,6-[$(CH_3)_2CH]_3$ *o,p*-C_6H_2).

^{119}Sn NMR [δ(ppm) $CDCl_3$ solution]: -118.3; $^1J(^{117}Sn$-$^{119}Sn)$ 5212.4 Hz.

^{119m}Sn Mossbauer (mms^{-1}): I.S.=1.54; Q.S.=2.23.

Analysis (%): Found C 59.50; H 7.84; Calculated for $C_{60}H_{92}Br_2Sn_2$: C 59.53; H 7.66.

Mass Spectrum [(m/z) E.I.]: 605 {M-[Br($iPr_3C_6H_2)_2$Sn])$^+$; 526; 480; 321; 202; 189; 91; 43.

Attempted preparation of (2,4,6-tri-i-propylphenyl)tin trichloride.

The attempted preparation of 2,4,6-tri-i-propylphenyltin trichloride followed the same synthetic route as the above for the corresponding bromide. However, the crude end product, a colourless oil, defied all attempts to obtain a crystalline product and so was used directly in its impure state in further synthesis.

I.R. [(cm^{-1}) liquid film]: 3040; 2960; 2930; 2875; 1600; 1560; 1460; 1420; 1385; 1365; 1320; 1265; 1100; 1070; 1060; 1020; 945; 860; 745; 720; 655; 520; 400; 320.

[Tris(trimethylsilyl)methyl]triphenyltin (2). To prepare (Tsi)lithium, methyllithium (0.57g, 18.6ml of a 1.4M solution in diethyl ether, 0.026 mole) in dry diethyl ether (45ml) was added with stirring to a solution of (Tsi)H (5g, 0.025 mole) in dry tetrahydrofuran (50ml) resulting in the formation of a yellow coloured solution. For a 6 hr. period the mixture was heated to reflux

resulting in the formation of a dark orange solution which was allowed to cool before the next addition. Triphenyltin chloride (9.5g, 0.022 mole) in dry tetrahydrofuran (40ml) was added dropwise to the dark orange (Tsi)lithium solution resulting in a discharge of the orange colouration. After 15 hr. stirring at room temperature the orange colouration returned. To ensure completion of reaction the mixture was heated to reflux for 7 hr. after which *in vacuo* solvent removal yielded an orange oil. Trituration with ethanol generated an off-white solid which on recrystallisation from acetonitrile yielded a colourless crystalline product. (4.2g, 33.6%), m.p. 184°C.

I.R. [(cm^{-1}), KBr disc]: 3075; 3050; 2990; 2960; 2900; 1485; 1430; 1270; 1260; 1250; 1075; 855; 840; 800; 735; 705; 680; 660; 620; 460; 260.

^{1}H NMR [δ(ppm) $CDCl_3$ solution]: 0.25 (s,27H,[$(CH_3)_3Si]_3C$); 7.31 and 7.66 [m,15H,C_6H_5]; $^{2}J[(C^{1}H_3)_3{}^{29}Si]$ 6.23 Hz.

^{13}C NMR [δ(ppm) $CDCl_3$ solution]: 6.10 ([$(CH_3)_3Si]_3C$); 128.25 [*m*-C_6H_5]; 128.54 [*p*-C_6H_5]; 137.95 [*o*-C_6H_5]; 141.61 [*i*-C_6H_5]; $^{1}J[(^{13}CH_3)_3{}^{29}Si]$ 50.7 Hz; $^{3}J([(^{13}CH_3)_3Si]_3C{}^{117,119}Sn)$ 15.4 Hz (unresolved); $^{2}J[o\text{-}^{13}C_6H_5{}^{117,119}Sn]$ 37.5 Hz (unresolved); $^{3}J[m\text{-}^{13}C_6H_5{}^{117,119}Sn]$ 52.8 Hz (unresolved).

^{119}Sn NMR [δ(ppm) $CDCl_3$ solution]: -98.4; $^{1}J[i\text{-}^{13}C_6H_5{}^{119}Sn]$ 482.1 Hz; $^{2}J([(CH_3)_3{}^{29}Si]_3C{}^{119}Sn)$ 39.6 Hz.

^{119m}Sn Mossbauer (mms^{-1}): I.S.=1.23.

Analysis (%): Found C 58.10; H 7.45; Calculated for $C_{28}H_{42}Si_6Sn$: C 57.83; H 7.28.

Phenyl[tris(trimethylsilyl)methyl]tin Dibromide (3). To a stirred solution of (2) (1g, 0.0017 mole) in chloroform (10ml) at room temperature, a solution of bromine (0.83g, 0.0052 mole) in chloroform (20ml) was added dropwise. After stirring for a period of 17 hr. at room temperature, the solution retained the reddish-brown colouration of excess bromine in solution. *In vacuo* solvent removal yielded a reddish-brown slurry which on washing with n-hexane yielded a white solid. Recrystallisation from acetonitrile yielded a colourless crystalline product. (0.46g, 45%), m.p. 191°C.

I.R. [(cm^{-1}) KBr disc]: 3060; 3050; 2975; 2950; 2900; 1480; 1430; 1260; 1065; 1000; 845; 800; 730; 720; 695; 680; 665; 625; 450; 250.

^{1}H NMR [δ(ppm) $CDCl_3$ solution]: 0.42 {s,27H,[$(CH_3)_3Si]_3C$}; 7.45 and 7.83 [m,5H,C_6H_5]

^{13}C NMR [δ(ppm) $CDCl_3$ solution]: 5.12 {[$(CH_3)_3Si]_3C$}; 23.09 {[$(CH_3)_3Si]_3C$}; 129.06 [*m*-C_6H_5]; 130.58 [*p*-C_6H_5]; 134.77 [*o*-C_6H_5]; 143.30 [*i*-C_6H_5]; $^{1}J[(^{13}CH_3)_3-^{29}Si]$ 52.9 Hz; $^{3}J\{[(^{13}CH_3)_3Si]_3C-^{117,119}Sn\}$ 26.5 Hz (unresolved); $^{2}J[o-^{13}C_6H_5-^{117,119}Sn]$ 63.9 Hz (unresolved); $^{3}J[m-^{13}C_6H_5-^{117,119}Sn]$ 77.1 Hz (unresolved); $^{4}J[p-^{13}C_6H_5-^{117,119}Sn]$ 17.6 Hz (unresolved).

^{29}Si NMR [δ(ppm) $CDCl_3$ solution]: 0.7; $^{2}J\{[(CH_3)_3{}^{29}Si]_3C-^{117,119}Sn\}$ 51.8 Hz (unresolved).

^{119}Sn NMR [δ(ppm) $CDCl_3$ solution]: -39.5.

^{119m}Sn Mossbauer (mms^{-1}): I.S.=1.45; Q.S.=2.42.

Analysis (%): Found C 33.00; H 5.72; Calculated for $C_{16}H_{32}Br_2Si_3Sn$: C 32.73; H 5.72.

Phenyl[tris(trimethylsilyl)methyl]tin Dichloride (**4**). Chlorine gas was bubbled through a stirred solution of an impure mixture of (2) and hexaphenylditin (1:1.8) (6.21g) in carbon tetrachloride (50ml). Colour changes from yellow to red to cloudy white and finally back to yellow took place during the 3 hr. chlorine addition. To remove excess chlorine gas from the carbon tetrachloride solution nitrogen gas was passed through the reaction mixture. After *in vacuo* solvent removal recrystallisation from a mixture of methanol/ethanol yielded a colourless needle-shaped crystalline solid. (1.35g, 81%), m.p. 150-152°C.

I.R. [(cm^{-1}) KBr disc]: 3080; 3060; 2950; 2920; 1490; 1275; 1265; 1080; 1010; 865; 845; 810; 740; 725; 705; 695; 675; 460; 350.

^{1}H NMR [δ(ppm) $CDCl_3$ solution]: 0.41 {s,27H,[$(CH_3)_3Si]_3C$}; 7.49 and 7.82 [m,5H,C_6H_5].

^{13}C NMR [δ(ppm) $CDCl_3$ solution]: 4.99 {[$(CH_3)_3Si]_3C$}; 32.89 {[$(CH_3)_3Si]_3C$}; 129.29 [*m*-C_6H_5]; 130.78 [*p*-C_6H_5]; 134.67 [*o*-C_6H_5]; 143.40 [*i*-C_6H_5]; ^1J[($^{13}CH_3)_3$-^{29}Si] 72.7 Hz; ^3J{[($^{13}CH_3)_3Si]_3C$-$^{117,119}Sn} 26.5 Hz (unresolved); ^2J[*o*-$^{13}C_6H_5$-^{117,119}Sn] 63.9 Hz (unresolved); ^3J[*m*-$^{13}C_6H_5$-^{117,119}Sn] 79.4 Hz (unresolved); ^4J[*p*-$^{13}C_6H_5$-^{117,119}Sn] 17.6 Hz (unresolved).

^{119}Sn NMR [δ(ppm) $CDCl_3$ solution]: 17.1.

^{119m}Sn Mossbauer (mms^{-1}): I.S.=1.36; Q.S.=2.42.

Analysis (%): Found C 37.90; H 6.53; Calculated for $C_{16}H_{32}Cl_2Si_3Sn$: C 38.57; H 6.47.

Tris(trimethylsilyl)methyltin Tribromide (5). To a stirred slurry of (2) (1.11g, 0.0019 mole) and iron tribromide (0.7g) in bromoform (30ml) at room temperature, a solution of bromine (0.92g, 0.0058 mole) in bromoform (20ml) was added dropwise. After 15 hr stirring a reddish brown to dark brown colour change had taken place. The brown slurry was poured carefully onto ice and extracted using bromoform. The combined bromoform washings were dried over anhydrous sodium sulphate and following *in vacuo* solvent removal, the resultant brown slurry was recrystallised from ethanol to give a white crystalline solid. (0.65g, 58%).

^{119}Sn NMR [δ(ppm) C_6D_6 solution]: -236.8.

^{119m}Sn Mossbauer (mms^{-1}): I.S.=1.39; Q.S.=1.56.

Analysis (%): Found C 20.85; H 4.74; Calculated for $C_{10}H_{27}Br_3Si_3Sn$: C 20.36; H 4.61.

In a similar preparation of (5) carbon tetrachloride was used as the reaction solvent resulting in halogen scrambling taking place. By ^{119}Sn nmr spectroscopyand chemical ionisation mass spectrometry the resultant product was shown to embrace the whole spectrum of possible trihalide products. Further evidence for the mixture of products was provided by a weighted analysis based on the ratios of the products in the mixture obtained from the ^{119}Sn nmr spectrum.

I.R. [(cm^{-1}) KBr disc]: 2990; 2960; 2910; 1415; 1270; 1260; 860; 835; 800; 715; 685; 660; 630; 350.

^{119}Sn NMR [δ(ppm) $CDCl_3$ solution]: -100.5 [(Tsi)$SnBrCl_2$]; -167.9 [(Tsi)$SnBr_2Cl$]; -237.1 [(Tsi)$SnBr_3$].

Analysis (%): Found C 21.56; H 5.09; Calculated for 10% $C_{10}H_{27}BrCl_2Si_3Sn$; 41% $C_{10}H_{27}Br_2ClSi_3Sn$ and 49% $C_{10}H_{27}Br_3Si_3Sn$: C 21.39 ; H 4.86.

Mass Spectrum [(m/z) C.I.]: 575 [(Tsi)$SnBr_3$, M - Me]$^+$; 531 [(Tsi)$SnBr_2Cl$, M - Me]$^+$; 509 [(Tsi)$SnBr_3$, M - Br]$^+$; 485 [(Tsi)$SnBrCl_2$, M - Me]$^+$; 465 [(Tsi)$SnBr_2Cl$, M - Br]$^+$; 293; 281; 267; 231; 217; 201; 73.

Tris(trimethylsilyl)methyltin Tribromide (5). Methyllithium (0.38g, 12.4ml of a 1.4M solution in diethyl ether, 0.017 mole) in dry diethyl ether (15ml) was added with stirring to a solution of (Tsi)H (4.0g, 0.017 mole) in dry tetrahydrofuran (30ml). After heating the mixture to reflux for a period of 6 hr. the reaction mixture had turned dark orange in colour. Following cooling the (Tsi)lithium solution was added dropwise to a solution of anhydrous tin(IV) bromide (6.8g, 0.016 mole) in dry 60-80 petrol (60ml). On addition a yellow oily residue resulted. After stirring at room temperature for 15 hr. the reaction mixture was heated to reflux for 2 hr. to ensure total reaction of the lithium reagent. On cooling *in vacuo* solvent removal generated an orange oil which on the addition of ethanol produced a white solid. Recrystallisation from acetonitrile yielded a white crystalline solid product (sublimes > 200°C).

I.R. [(cm^{-1}) KBr disc]: 2990; 2960; 2910; 1415; 1300; 1265; 1255; 840; 790; 705; 675; 655; 615; 300.

^{1}H NMR [δ(ppm) C_6D_6 solution]: 0.45 {s,27H,[(CH_3)$_3$Si]$_3$C); ^{2}J[(C^1H_3)$_3$-^{29}Si] 6.2 Hz.

^{13}C NMR [δ(ppm) C_6D_6 solution]: 5.02 {[$(CH_3)_3Si]_3C$}; ^1J[$(^{13}CH_3)_3-^{29}Si$] 50.7 Hz; ^4J[$[(^{13}CH_3)_3Si]_3C-^{117,119}Sn$) 37.5 Hz (unresolved).

^{119}Sn NMR [δ(ppm) C_6D_6 solution]: -236.9.

^{119m}Sn Mossbauer (mms^{-1}): I.S.=1.36; Q.S.=1.55.

Analysis (%): Found C 28.5; H 6.94; Calculated for $C_{10}H_{27}Br_3Si_3Sn$: C 20.40; H 4.60. [(Tsi) bromide major contaminant causing high analysis results, see discussion.]

Mass Spectrum [(m/z) C.I.]: 575 $[M - Me]^+$; 509 $[M - Br]^+$; 297; 231; 217; 201; 143; 73.

Dibenzyl[tris(trimethylsilyl)methyl]tin chloride (**6**). Methyllithium (0.57g, 18.6ml of a 1.4M solution, 0.026 mole) was added with stirring to a solution of (Tsi)H (5g, 0.022 mole) in dry tetrahydrofuran (43ml). After a period of 6 hr. reflux the reaction mixture had turned dark orange. Following cooling a solution of dibenzyltin dichloride (7.2g, 0.019 mole) in dry tetrahydrofuran (40ml) was added dropwise to the (Tsi)lithium solution. After addition the dark orange colour had been discharged leaving a light yellow solution. The mixture was heated gently at reflux for 15 hr. resulting in the formation of a white solid. After cooling *in vacuo* solvent removal yielded a cloudy yellow oil. Extraction of the oil using a chloroform/water system, followed by drying over anhydrous sodium sulphate and *in vacuo* solvent removal yielded a clear yellow oil. Trituration with ethanol, followed by recrystallisation from chloroform/acetonitrile yielded two products, the first a white purely organic solid containing only benzyl groups and a second white highly crystalline solid (**6**). (4.85g,

41%), m.p. 132-134°C.

I.R. [(cm^{-1}) KBr disc]: 3090; 3070; 3040; 2960; 2910; 1605; 1500; 1455; 1270; 1260; 1215; 1125; 1060; 1040; 910; 860; 810; 790; 765; 705; 680; 665; 625; 570; 560; 450; 330.

^{1}H NMR [δ(ppm) $CDCl_3$ solution]: 0.42 (s,27H,[$(CH_3)_3Si]_3C$); 2.85 [q,4H, $(C_6H_5)CH_2$]; 6.88 and 7.16 [m,10H, $(C_6H_5)CH_2$].

^{13}C NMR [δ(ppm) $CDCl_3$ solution]: 5.19 ([$(CH_3)_3Si]_3C$); 12.62 ([$(CH_3)_3Si]_3C$); 30.94 [$(C_6H_5)CH_2$]; 124.75 [*p*-$(C_6H_5)CH_2$]; 128.22 [*m*-$(C_6H_5)CH_2$]; 128.54 [*o*-$(C_6H_5)CH_2$]; 137.91 [*i*-$(C_6H_5)CH_2$]; $^1J[(^{13}CH_3)_3{-}^{29}Si]$ 50.7 Hz; $^3J([(^{13}CH_3)_3Si]_3C{-}^{117,119}Sn)$ 19.8 Hz (unresolved); $^1J[(C_6H_5)^{13}CH_2{-}^{117,119}Sn]$ 290.8, 304.0 Hz; $^3J[o$-$(^{13}C_6H_5)CH_2{-}^{117,119}Sn]$ 30.9 Hz (unresolved); $^4J[m$-$(^{13}C_6H_5)CH_2{-}^{117,119}Sn]$ 17.6 Hz (unresolved); $^5J[p$-$(^{13}C_6H_5)CH_2{-}^{117,119}Sn]$ 22.0 Hz (unresolved).

^{119}Sn NMR [δ(ppm) $CDCl_3$ solution]: 69.0.

^{119m}Sn Mossbauer (mms^{-1}): I.S.=1.08; Q.S.=2.18.

Analysis (%): Found C 50.70; H 7.48; Calculated for $C_{24}H_{41}ClSi_3Sn$: C 50.75; H 7.28.

Di-p-bromobenzyl[tris(trimethylsilyl)methyl]tin Bromide (7). A solution of bromine (0.79g, 0.0049 mole) in chloroform (10ml) was added dropwise to a stirred solution of (6) (1.4g, 0.0025 mole) in chloroform (10ml) at room temperature. After 15 hr. stirring decolourisation of the solution had not occurred and so the reaction mixture was heated to reflux for 8 hr. *In vacuo* solvent removal yielded a tan solid which, when recrystallised from ethanol/

chloroform, produced white highly crystalline platelets. (1.57g, 82%), m.p. 173°C.

I.R. [(cm^{-1}) KBr disc]: 2980; 2960; 2900; 1590; 1485; 1410; 1270; 1260; 1210; 1185; 1120; 1075; 1020; 850; 805; 765; 715; 685; 665; 625; 560; 470.

^1H NMR [δ(ppm) $CDCl_3$ solution]: 0.30 {s,27H,[$(CH_3)_3Si]_3C$}; 2.74 [q,4H, $(BrC_6H_4)CH_2$]; 6.57 and 7.16 [m,8H, $(BrC_6H_4)CH_2$].

^{13}C NMR [δ(ppm) $CDCl_3$ solution]: 5.29 {[$(CH_3)_3Si]_3C$}; 12.70 {[$(CH_3)_3Si]_3C$}; 30.49 [$(BrC_6H_4)CH2$]; 118.55 [*p*-$(BrC_6H_4)CH_2$]; 129.97 [*o*-$(BrC_6H_4)CH_2$]; 131.23 [*m*-$(BrC_6H_4)CH_2$]; 137.20 [*i*-$(BrC_6H_4)CH_2$]; $^1J[(BrC_6H_4)^{13}CH_2$-$^{117,119}Sn]$ 275.5, 286.5 Hz; $^3J[o$-$(Br^{13}C_6H_4)CH_2$-$^{117,119}Sn]$ 28.6 Hz (unresolved); $^4J[m$-$(Br^{13}C_6H_4)CH_2$-$^{117,119}Sn]$ 17.6 Hz (unresolved).

^{119}Sn NMR [δ(ppm) $CDCl_3$ solution]: 54.3.

^{119m}Sn Mossbauer (mms^{-1}): I.S.=1.50; Q.S.=2.20.

Analysis (%): Found C 37.10; H 5.42; Calculated for $C_{24}H_{39}Br_3Si_3Sn$: C 37.43; H 5.10.

Dibenzyl[tris(trimethylsilyl)methyl]trimethylsiloxystannane (8) and *1,1-bis(trimethylsilyl)-3-(dibenzyl[tris(trimethylsilyl)methyl]-stannyl)prop-1-ene* (9). A solution of hydrogen bromide (1.37g, 0.017 mole) in water (20ml) was added dropwise to a stirred solution of (6) (3.2g, 0.0056 mole) in diethyl ether (50ml) at room temperature. After stirring for 18 hr. the two-phase reaction mixture was separated and the combined diethyl ether washings dried over anhydrous sodium sulphate. *In vacuo* solvent removal yielded a yellow oil which on

solution in a chloroform/acetonitrile solution, produced an off-white solid. A secondary recrystallisation in the same solvent system yielded two solid products as well as a small amount of unreacted starting material. (8), m.p. 117°C and (9), m.p. 98-99°C.

Compound (8).

I.R. [(cm^{-1}) KBr disc]: 3080; 3060; 3030; 2960; 2900; 1600; 1545; 1495; 1450; 1260; 1245; 1205; 1100; 1055; 1025; 980; 900; 850; 830; 795; 750; 690; 670; 650; 610; 545; 435; 285.

^{1}H NMR [δ(ppm) $CDCl_3$ solution]: -0.17 [s,9H,$(CH_3)_3SiO$]; 0.37 {s,27H, [$(CH_3)_3Si]_3C$); 2.71 [s,4H,$(C_6H_5)CH_2$]; 7.16 [m,10H,$(C_6H_5)CH_2$]; ^2J[$(C^1H_3)_3$-^{29}SiO] 6.4 Hz; ^2J[[$(C^1H_3)_3$-^{29}Si]$_3$C) 6.2 Hz; ^2J[$(C_6H_5)C^1H_2$-^{117,119}Sn] 67.8, 71.1 Hz.

^{13}C NMR [δ(ppm) $CDCl_3$ solution]: 3.47 [$(CH_3)_3SiO$]; 5.38 {[$(CH_3)_3Si]_3C$) ; 11.36 {[$(CH_3)_3Si]_3C$); 30.62 [$(C_6H_5)CH_2$]; 124.45 [*p*-$(C_6H_5)CH_2$]; 128.44 [*m*-$(C_6H_5)CH_2$]; 128.54 [*o*-$(C_6H_5)CH_2$]; 139.24 [*i*-$(C_6H_5)CH_2$]; ^1J[[$(^{13}CH_3)_3$-^{29}Si]$_3$C) 52.9 Hz; ^3J[[$(^{13}CH_3)_3Si]_3C$-^{117,119}Sn) 17.6 Hz (unresolved); ^1J[$(C_6H_5)^{13}CH_2$-^{117,119}Sn] 321.7, 334.9 Hz; ^3J[*o*-$(^{13}C_6H_5)CH_2$-^{117,119}Sn] 28.6 Hz (unresolved); ^5J[*p*-$(^{13}C_6H_5)CH_2$-^{117,119}Sn] 19.8 Hz (unresolved).

^{29}Si NMR [δ(ppm) $CDCl_3$ solution]: -1.2 {[$(CH_3)_3Si)_3C$); 6.4 [$(CH_3)_3SiO$]; ^2J[[$(CH_3)_3{}^{29}Si]_3C$-^{117,119}Sn) 36.7 Hz (unresolved); ^2J[$(CH_3)_3{}^{29}SiO$-^{117,119}Sn] 58.0 Hz (unresolved).

^{119}Sn NMR [δ(ppm) $CDCl_3$ solution]: -10.2.

^{119m}Sn Mossbauer (mms^{-1}): I.S.=1.24; Q.S.=1.42.

Analysis (%): Found C 52.20; H 8.27; Calculated for $C_{27}H_{50}OSi_4Sn$: C 52.17; H 8.11.

Compound (**9**).

I.R. [(cm^{-1}) KBr disc]: 3090; 3060; 3030; 2960; 2910; 1605; 1540; 1500; 1460; 1270; 1260; 1215; 1040; 905; 860; 845; 760; 705; 685; 665; 650; 615; 560; 485; 460; 445.

^{1}H NMR [δ(ppm) $CDCl_3$ solution]: 0.07 and 0.12 {s,18H, [$(CH_3)_3Si]_2C=CHCH_2$}; 0.36 {s,27H,[$(CH_3)_3Si]_3C$); 2.19 {d,2H, [$(CH_3)_3Si]_2C=CHCH_2$}; 2.64 [q,4H,$(C_6H_5)CH_2$]; 6.56 {t,1H, [$(CH_3)_3Si]_2C=CHCH_2$}; 6.76 and 7.09 [m,10H,$(C_6H_5)CH_2$]; ^{2}J({[$(C'H_3)$-$^{29}Si]_2C=CHCH_2$) 6.59 and 6.23 Hz; ^{2}J({[$(C'H_3)_3$-$^{29}Si]_3C$) 5.87 Hz; ^{2}J({[$(CH_3)_3Si]_2C=CHC'H_2$-$^{117,119}Sn$) 61.6, 63.9 Hz.

^{13}C NMR [δ(ppm) $CDCl_3$ solution]: 0.97 and 2.27 {[$(CH_3)_3Si]_2C=CHCH_2$}; 5.93 {[$(CH_3)_3Si]_3C$); 24.49 [$(C_6H_5)CH_2$]; 25.17 {[$(CH_3)Si]_2C=CHCH_2$}; 123.90 [*p*-$(C_6H_5)CH_2$]; 128.18 [*o*-$(C_6H_5)CH_2$]; 128.54 [*m*-$(C_6H_5)CH_2$]; 138.66 [*i*-$(C_6H_5)CH_2$]; 141.38 {[$(CH_3)_3Si]_2C$=CCHCH$_2$); 154.55 {[$(CH_3)_3Si]_2C=CHCH_2$}; ^{1}J({[$(^{13}CH_3)_3$-$^{29}Si]_3C$) 50.3 Hz; ^{3}J({[$(^{13}CH_3)_3Si]_3C$ -$^{117,119}Sn$) 13.6 Hz (unresolved); ^{1}J[$(C_6H_5)^{13}CH_2$-$^{117,119}Sn$] 248.0, 257.8 Hz; {[$(CH_3)_3Si]_2C=CH^{13}CH_2$-$^{117,119}Sn$) 266.7, 271.08 Hz; ^{3}J[*o*-$(^{13}C_6H_5)CH_2$-$^{117,119}Sn$] 22.4 Hz (unresolved); ^{4}J[*m*-$(^{13}C_6H_5)CH_2$-$^{117,119}Sn$] 13.6 Hz (unresolved); ^{5}J[*p*-$(^{13}C_6H_5)CH_2$] 17.7 Hz (unresolved); ^{2}J({[$(CH_3)_3Si]_2C=^{13}CHCH_2$-$^{117,119}Sn$) 37.4 Hz (unresolved); ^{3}J({[$(CH_3)_3Si]_2{}^{13}C$=CHCH$_2$-$^{117,119}Sn$) 37.4 Hz (unresolved).

^{29}Si NMR [δ(ppm) $CDCl_3$ solution]: -10.0 {*trans*-[$(CH_3)_3Si]_2C=CHCH_2$}; -1.8 {*cis*-[$(CH_3)_3Si]_2C=CHCH_2$}; -0.9 {[$(CH_3)_3Si]_3C$); ^{2}J({[$(CH_3)_3{}^{29}Si]_3C$-$^{117,119}Sn$) 30.5 Hz (unresolved).

^{119}Sn NMR [δ(ppm) $CDCl_3$ solution]: -30.9.

^{119m}Sn Mossbauer (mms^{-1}): I.S.=1.40; Q.S.=0.39.

Analysis (%): Found C 55.25; H 8.88; Calculated for $C_{33}H_{62}Si_5Sn$: C 55.20; H 8.70.

Mass Spectrum [(m/z) C.I.]: 703 $[M - Me]^+$; 627 $[M - Bn]^+$; 533 $[M - (Me_3Si)_2C{=}CHCH_2]^+$; 457; 217; 201; 91; 73.

CHAPTER 3.

PREPARATIVE STRATEGIES FOR THE SYNTHESES OF NOVEL, EXCLUSIVE AND MIXED ORGANOCHALCOGENASTANNANE SYSTEMS.

3.1 Introduction.

In chapter two the strategies for the preparation of sterically hindered organotin halide systems were explored. As was previously discussed the steric hindrance of the substituents on tin is very important when attempting to restrict the prepared species to oligomeric units as opposed to polymeric systems during the preparation of substituted organotin compounds. A second method by which the degree of polymerisation can be controlled in organotin syntheses is by the use of poorly coordinating species as the heteroatom substituents. This phenomenon is exemplified in the structures of the dimethylchalcogenastannanes where six-membered boat arrays are observed for the sulphur,[154,198] selenium[199] and tellurium[200] derivatives which are trimeric. In contrast to this observation is the proposed structure of dimethyltin oxide for which a highly associated, polymeric, amorphous solid is postulated. Examples recently published by Holmes et al.[201] display two structures showing the sharp contrast between the highly associating nature of oxygen compared to the lower members of Group VI. In the two structures shown, bidentate ligands are used in both cases. The first uses the

mixed chalcogenide mercaptoethanolate ligand (figure 26) and the second the dimercaptomaleonitrile ligand (figure 27).

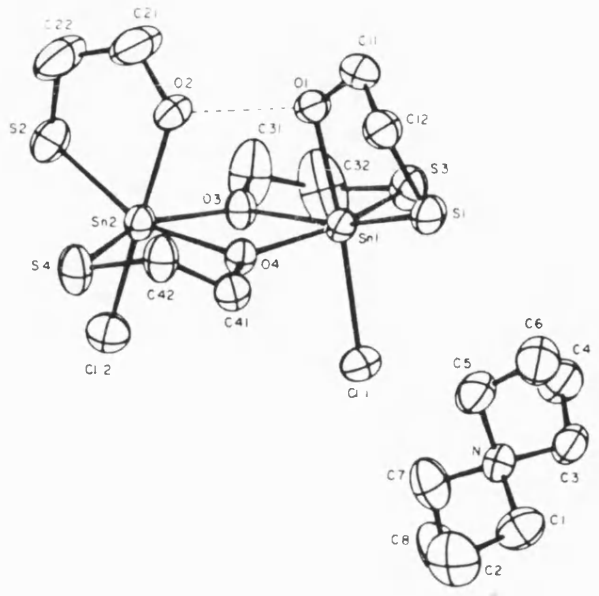

Figure 26: ORTEP Plot of $[(C_2H_4OS)_2SnCl]_2[H][Et_4N]$. The Interaction of the Proton with O1 and O2 is Indicated by a Dotted Line.

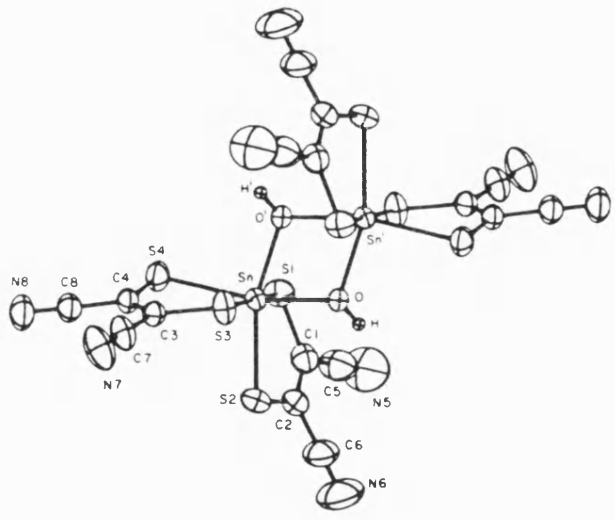

Figure 27: ORTEP Plot of the Anion of $\{[(CN)_2C_2S_2]_2SnOH)_2[Et_4N]_2$.

In the first structure two environments are exhibited for oxygen, one where coordinative and σ-bonding are displayed for the oxygen incorporated into the central four-membered ring system and the second being a hydrogen-bonded system where a proton is trapped between two oxygens. In this structure it can also be seen that the sulphurs play no part in any type of coordinative bonding. In the second structure again no coordinative bonding is observed for the sulphurs in the dimercaptomaleonitrile ligands and the four-membered ring at the centre of the structure is composed of two hydroxyl groups bonding the two tin units into a four-membered ring system.

The contrasting association properties of the members of Group VI have also been highlighted in a series of papers recently published by Davies et al.[202-204] In these reports the structures of dioxastannolanes, oxathiastannolanes and dithiastannolanes in differing physical states are compared by the use of solution and solid state ^{119}Sn nmr and where possible, single crystal X-ray diffraction studies. With the dioxastannolanes five-coordinate, dimeric, 'ladder' type structures are observed in solution compared to the infinite six-coordinate, highly associated structures found in the solid state. In the case of the oxathiastannolanes five-coordinate dimeric species are again obtained in solution resulting from coordination through oxygen to tin. However, in this instance in the solid state a five-coordinate polymeric structure is observed. The intermonomeric distance between tin and sulphur is below the predicted Van der Waals distance, but even if classed as a coordination bond it only generates a very weakly associated six-coordinate system. For the

dithiastannolanes monomeric four-coordinate systems are observed in the solution state. In the solid state for small organic substituents on tin, five-coordinate linear polymers are observed. However, for organic substituents of greater hindrance than methyl, pseudo monomeric six-coordinate systems are observed. In these instances extremely weak six-coordination occurs where the intermonomeric tin-sulphur distance is slightly lower than the predicted Van der Waals distance.

Several classical techniques for the preparation of organo-chalcogenastannanes are detailed in the literature[205-209] (equations 49 to 51).

$$2R_3SnCl + Na_2X \rightarrow (R_3Sn)_2X + 2NaCl \quad (49)$$

X = S, Se and Te

$$(R_3Sn)_2O + H_2S \rightarrow (R_3Sn)_2S + H_2O \quad (50)$$

$$(Ph_3Sn)_2O + CS_2 \rightarrow (Ph_3Sn)_2S + COS \quad (51)$$

As well as these general preparative routes several other methods have been employed to yield novel chalcogenastannane products[158,200,210-215] (equations 52 to 60).

$$2Mes_2SnCl_2 + 2Na_2S \rightarrow (Mes_2SnS)_2 + 4NaCl \quad (52)$$

$$4(C_6F_5)SnCl_3 + 6(Me_3Si)_2S \rightarrow [(C_6F_5)SnS_{1.5}]_4 + 12Me_3SiCl \quad (53)$$

$$3Me_2SnCl_2 + 3H_2Se \rightarrow (Me_2SnSe)_3 + 6HCl \quad (54)$$

$$3Me_2SnCl_2 + 3NaHTe \rightarrow (Me_2SnTe)_3 + 3NaCl + 3HCl \quad (55)$$

$$2ClMe_2SnSnMe_2Cl + 2NaHTe \rightarrow Te(Me_2SnSnMe_2)_2Te + 2NaCl + 2HCl \quad (56)$$

$$3(tBu_2Sn)_4 + 8X \rightarrow 4(tBu_2Sn)_3X_2 \quad (57)$$

X = S, Se and Te

$$I(tBu_2Sn)_4I + H_2X \rightarrow (tBu_2Sn)_4X + 2HI \quad (58)$$

X = S, Se and Te

$$3Me_2SnH_2 + 2X \rightarrow (Me_2Sn)_3X_2 + 3H_2 \quad (59)$$

X = Se and Te

$$2(iPr_2SnCl)_2X + Na_4SnX_4 \rightarrow [(iPr_2Sn)_2X_3]_2Sn + 4NaCl \quad (60)$$

X = S and Se

By the use of the sterically hindered products prepared in chapter two and by the application of some of the synthetic routes detailed above, an attempt was made to prepare ring and cage organochalcogenastannanes of controlled structure. In all the examples detailed so far only single chalcogenide species have been incorporated into the compounds. By the use of structured synthetic approaches it was hoped that mixed chalcogenastannanes might be produced displaying structures intermediate between polymers and small rings depending on the nature

of the incorporated chalcogens. The results of these synthetic attempts are described in this chapter.

3.2 Results and Discussion.

3.2.1 Diorganochalcogenastannanes.

Following standard techniques a selection of diorganochalcogenastannanes were prepared both for the structural interest inherent in this class of compounds and also for use in further syntheses which will be discussed later. To prepare the thiastannanes the standard reaction conditions of sodium sulphide nonahydrate reacting with a diorganotin dihalide were employed (equation 61).

$$nRR'SnCl_2 + xsNa_2S \rightarrow (RR'SnS)n + 2nNaCl \quad (61)$$

n = 2.

R = R' = t-butyl (**10**) and 2,4,6-tri-i-propylphenyl (**11**).

R = phenyl and R' = (Tsi) (**12**).

n = 3.

R = R' = n-butyl (**13**) and i-propyl (**14**).

For the products prepared all the spectra obtained were consistent with the proposed structures. In the case of 2,4-diphenyl-2,4-di[tris(trimethylsilyl)methyl]-1,3-dithia-2,4-distannetane (**12**) a single crystal X-ray structural determination was carried out. The

ring structure obtained was a dimeric four-membered ring array as can be seen in the ORTEP plot of the crystal structure given in figure 28. Selected bond lengths and angles are given in table 14 and full crystal data are available in Appendix V. The crystal sample used displayed triclinic cell symmetry with a *P*1 space group.

The structure contains a four-membered tin-sulphur ring with almost equivalent tin-sulphur bond distances [2.457(6)Å and 2.438(6)Å]. This structure is more reminiscent of the structure of 2,2,4,4-tetra-t-butyl-1,3-diselena-2,4-distannetane than the analogous 2,2,4,4-tetra-t-butyl-1,3-dithia-2,4-distannetane (10) reported by Puff et al.[153] In the diselenadistannetane structure the tin-selenium bond distances are exactly equal at 2.55Å, whereas in the dithia-distannetane structure the tin-sulphur bond distances are reported as 2.49Å and 2.38Å. It would seem from these structures that with two highly sterically hindered t-butyl groups on tin the equalisation of bond distances for a tin-sulphur system cannot be attained. This occurs as a result of an increase in the tin-tin distance required to relax the steric strain across the ring in the dimeric unit. The resultant effect is a partial change in the system from the behaviour expected in a purely dimeric array to that expected for a system displaying two coordinatively bonded monomers (figure 29). For (12), although a (Tsi) group is present on tin providing extreme steric hindrance, the presence of the phenyl group means the two distinct groups can align themselves across the dimer resulting in reduced overall steric strain. This results in a reduction in the overall steric hindrance compared to the di-t-butyl example enabling the tin-

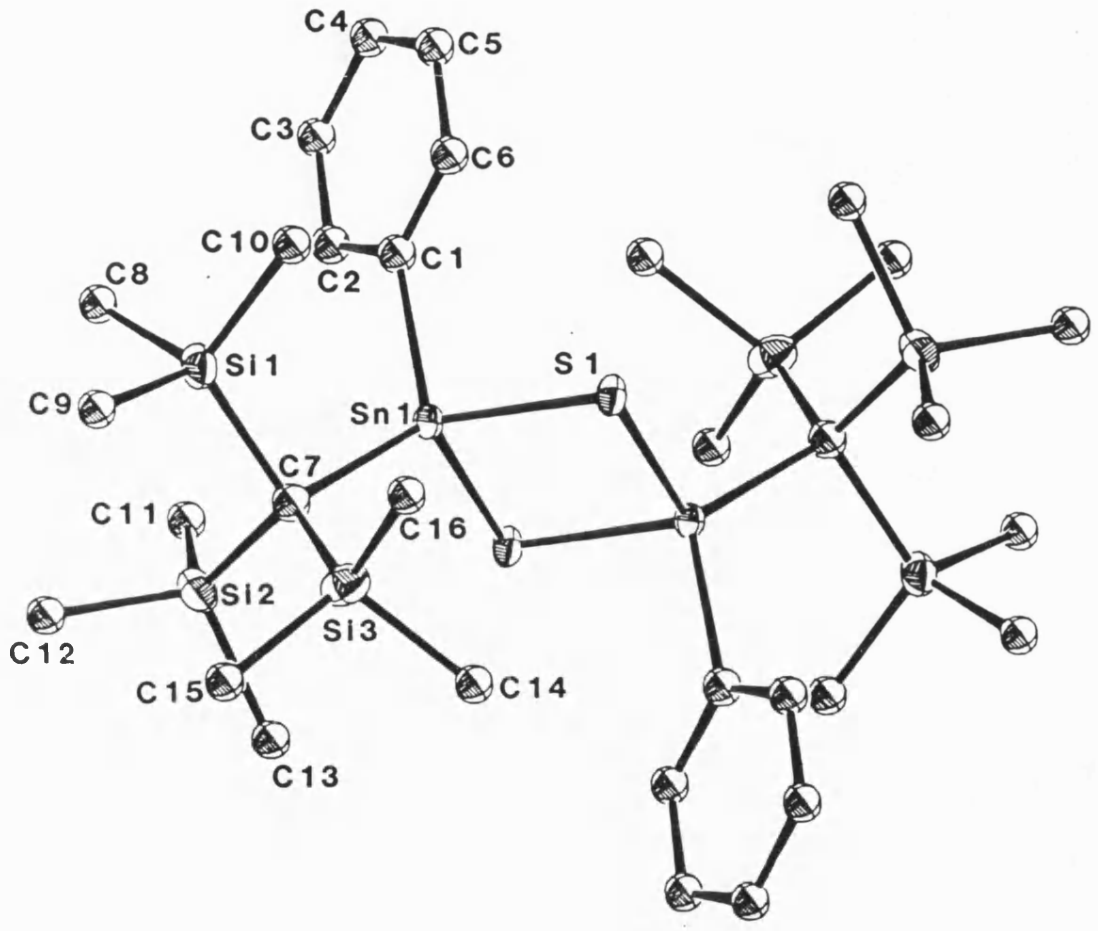

Figure 28: ORTEP Plot of the Dimeric Ring Structure of 2,4-Diphenyl-2,4-[tris(trimethylsilyl)methyl]-1,3-dithia-2,4-distannetane (12).

Table 14: Bond Lengths[a] and Angles[b] for 2,4-Diphenyl-2,4-[tris-(trimethylsilyl)methyl-1,3-dithia-2,4-distannetane (12).

Sn1 -S1	2.457(6)	Sn1 -S1 -Sn1'	92.0(5)
Sn1'-S1	2.438(6)	C1 -Sn1 -S1	107.6(5)
Sn1 -C1	2.153(17)	C7 -Sn1 -S1	114.8(6)
Sn1 -C7	2.242(25)	C7 -Sn1 -C1	118.8(8)
Sn1 -Sn1	3.323(3)		

[a] = Å.

[b] = °.

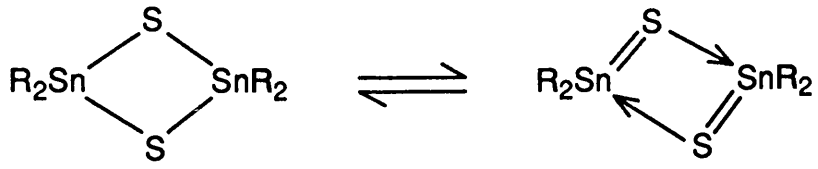

Figure 29: Structural Variation for the Conversion of a Dimeric Symmetrically Bonded Array to a Monomeric Coordinated System.

sulphur bond distances to equalise. This effect is imitated by the purely dimeric tetra-t-butyldiselenadistannetane system where the longer tin-selenium bond helps to reduce the steric interactions between the t-butyl groups.

As well as the preparation of the organothiastannanes, hexaphenyltriselenatristanninane [$(Ph_2SnSe)_3$] (**15**) was prepared from the reaction between sodium hydrogenselenide[216] and diphenyltin dichloride (equation 62).

$$3Ph_2SnCl_2 + 3NaHSe \rightarrow (Ph_2SnSe)_3 + 3NaCl + 3HCl \qquad (62)$$

The yellow crystals obtained were used for detailed ^1H, ^{13}C, ^{77}Se and ^{119}Sn nmr investigations. From the ^{119}Sn nmr spectrum the usual $^2J(^{117/119}Sn-^{119}Sn)$ could be observed at 235 Hz as well as $^1J(^{77}Se-^{119}Sn)$ at 1318.4 Hz. This latter value was confirmed in the

^{77}Se nmr, which also displayed $^{1}J(^{77}Se-^{117}Sn)$ at 1260.3 Hz.

3.2.2 2,2,4,4-Tetra[2,4,6-tri-i-propylphenyl]-1,3-oxathia-2,4-distannetane (16).

As previously stated in chapter two, from the attempted preparation of 2,4,6-tri-i-propylphenyltin trichloride by the stoichiometric reaction of 2,4,6-tri-i-propylphenyllithium and anhydrous tin(IV) chloride, an impure oil was obtained. On the assumption that the required monoorganotin trihalide had been formed the impure product was heated at reflux with three equivalents of sodium sulphide in ethanol. Following purification the true identity of the product and by implication, the organotin halide progenitor, only became apparent after a X-ray structure determination was carried out. Initially, the identity of the product was determined as 2,2,4,4-tetra(2,4,6-tri-i-propyl)-1,3-dithia-2,4-distannetane (11). All the spectra were consistent with this assignment, however, the elemental analysis was slightly at variance with the proposed formulation (found C = 65.30; H = 8.49; calculated for $C_{60}H_{92}S_2Sn_2$: C = 64.64; H = 8.32). During the solution of the X-ray crystal structure it was found that the thermal parameters for one of the proposed sulphurs were excessively high and that the bonds to tin were too short. From this evidence the presence of oxygen was postulated and on recalculation of the theoretical elemental analysis values (calculated for $C_{60}H_{92}OSSn_2$: C = 65.58; H = 8.44) it became apparent that the isolated product was in fact

2,2,4,4-tetra(2,4,6-tri-i-propylphenyl)-1,3-oxathia-2,4-distannetane (**16**).

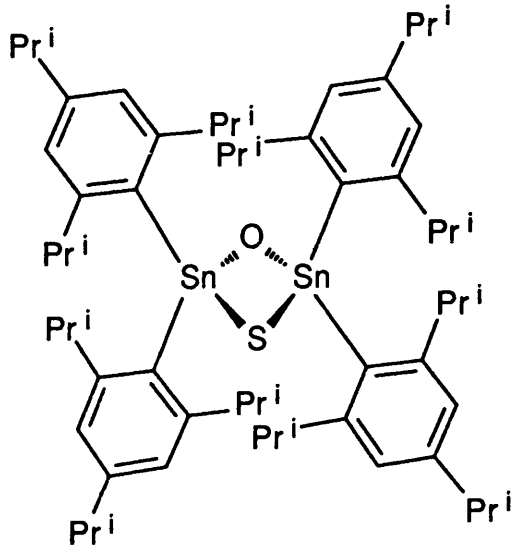

(**16**)

The spectroscopic data obtained for (**16**) were consistent with the known structure. In the ^{1}H nmr spectrum inequivalences in the observed signals were apparent. The theoretically predicted spectrum for a 2,4,6-tri-i-propylphenyl group would give rise to two distinct sets of signals for both the methyl and methine protons, in a 2:1 ratio for the *ortho* and *para* substituted i-propyl groups. However, in the observed spectrum three sets of signals in a 1:1:1 ratio were seen. This observation suggests that inequivalence in the i-propyl groups is occurring probably as a result of hindrance of free rotation. This phenomenon was also observed in the ^{1}H nmr spectrum of 1,2-dibromo-1,1,2,2-tetra(2,4,6-tri-i-propylphenyl)distannane (**1**), however the inequivalence effect is much reduced in the spectrum of (**16**). In the ^{13}C nmr spectrum increased complexity compared to the theoretical spectrum is also observed for the same reason. In the ^{119}Sn nmr

spectrum, as well as the signal observed for (**16**) a trace of a second component is also observed at -48.2 ppm (8% intensity). This signal is attributable to a small amount of 2,2,4,4-tetra(2,4,6-tri-i-propyl-phenyl)-1,3-dithia-2,4-distannetane (**11**) obtained from the reaction.

As already stated, the correct formulation of (**16**) was obtained from a single crystal X-ray structure determination. The structure obtained was a monomeric, four-membered ring array as can be seen in the ORTEP plot given in figure 30. Selected bond lengths and angles are given in table 15 and full crystal data is available in Appendix VI. The crystal sample used possessed a unit cell of monoclinic geometry with a $P2_1/a$ space group.

In the crystal structure of (**16**) the tin-sulphur bond distances are equal in length [2.439(4)Å and 2.435(4)Å] as essentially are the two tin-oxygen bond lengths [2.042(8)Å and 2.026(8)Å]. Due to the presence of mixed chalcogen species the four-membered ring is distorted from pure rhombic, the distortion, however, being different in nature to that observed in tetra-t-butyldithiadistannetane (**10**) structure (figure 31).

In compound (**16**) the tin-oxygen bond lengths are long in comparison with the observed distances in other sterically hindered diorganotin oxide systems. For the six-membered ring systems of di-t-butyltin oxide and di-t-amyltin oxide the tin-oxygen bond lengths are between 1.95Å and 1.98Å.[151] One explanation for this could be the increased steric interactions occurring for bulky organic substituents across the ring in a four-membered system in comparison to those exerted in

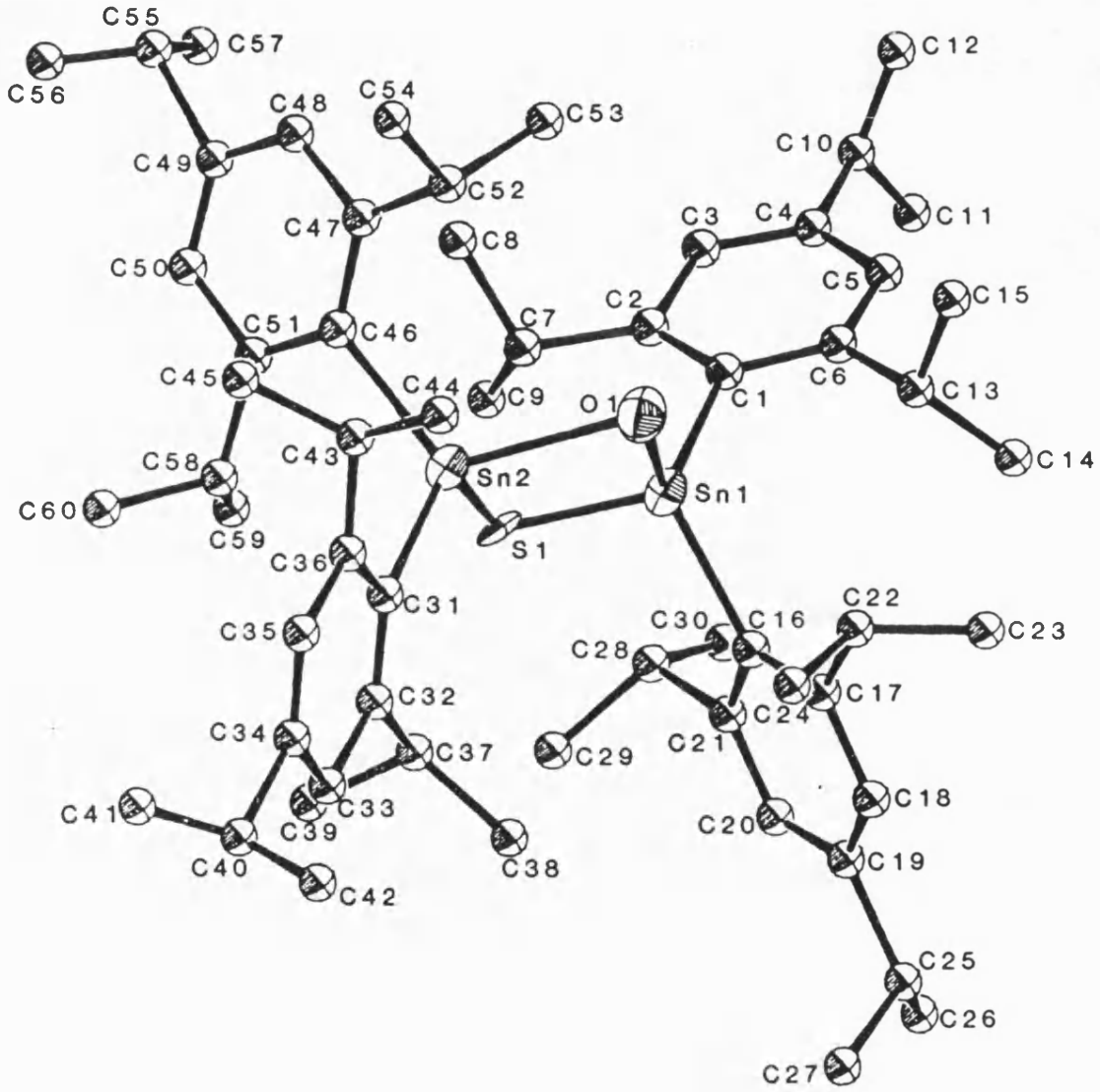

Figure 30: ORTEP Plot of 2,2,4,4-Tetra[2,4,6-tri-i-propylphenyl]-1,3-oxathia-2,4-distannetane (**16**).

Table 15: Bond Lengths[a] and Angles[b] for 2,2,4,4-Tetra(2,4,6-tri-i-propylphenyl)-1,3-oxathia-2,4-distannetane (**16**).

Sn1 -S1	2.439(4)	O1 -Sn1 -S1	88.6(3)
Sn2 -S1	2.435(4)	O1 -Sn2 -S1	89.1(2)
Sn1 -O1	2.042(8)	Sn2 -S1 -Sn1	80.6(1)
Sn2 -O1	2.026(8)	Sn2 -O1 -Sn1	101.7(4)
Sn1 -C1	2.164(15)	C1 -Sn1 -S1	113.1(4)
Sn1 -C16	2.166(14)	C1 -Sn1 -O1	114.4(5)
Sn2 -C31	2.186(13)	C16 -Sn1 -S1	114.7(4)
Sn2 -C46	2.148(13)	C16 -Sn1 -O1	103.7(4)
Sn1 -Sn2	3.154(1)	C31 -Sn2 -S1	113.9(3)
		C31 -Sn2 -O1	115.9(4)
		C46 -Sn2 -S1	118.0(4)
		C46 -Sn2 -O1	105.3(4)
		C16 -Sn1 -C1	118.2(6)
		C46 -Sn2 -C31	112.4(5)

[a] = Å.

[b] = °.

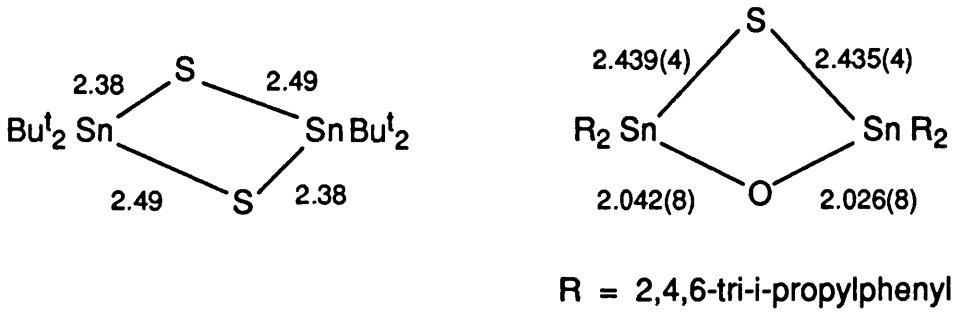

Figure 31: Differing Aspects of Distortion from Pure Rhombic in the Four-membered Ring Arrays in Tetra-t-butyldithia-distannetane (**10**) and Tetra[2,4,6-tri-i-propylphenyl]-oxathiadistannetane (**16**).

the six-membered examples. This would result in an increase in the tin-tin distance with a subsequent elongation of the tin-oxygen bonds in (**16**). A second explanation could be apportioned to the presence of mixed chalcogen species in the oxathiadistannetane ring. Any decrease in bond length for tin-oxygen compared to tin-sulphur bonds will cause a reduction in the Sn-S-Sn bond angle which would result in an increase in ring strain. Therefore to relax ring strain the tin-oxygen bond lengths would elongate to allow a larger angle to occur.

From the structure small differences are observed in the carbon-tin bond data for the two tin atoms present in the structure. For Sn1 the tin-carbon bond distances are equal [2.16(2)Å and 2.17(1)Å] with the C16-Sn1-C1 bond angle [118.2(6)°] correlating with the expected value for a slightly distorted tetrahedral system resulting from the steric hindrance of the organic substituents. However, in the case of Sn2 the

bond distances to the adjacent carbon atoms are slightly dissimilar [Sn2-C31 2.19(1)Å and Sn2-C46 2.15(1)Å] and the bond angle is reduced compared to the analogous angle for Sn1 [112.4(5)°]. From the ORTEP plot of the crystal structure it is not clear as to the reasons for these inconsistencies except to say that the molecule displays extreme steric hindrance and thus the structure is probably perturbed in order to relax the steric interactions. In the literature no instances of other organic substituted group IV metal, mixed chalcogen, ring systems are available for comparison with the above structure.

From further results obtained (see chapter two section 2.2.2) it now seems likely that the active intermediate in the impure oil used in the above preparation was 1,2-dichloro-1,1,2,2,-tetra(2,4,6-tri-i-propylphenyl)distannane. On this evidence a postulated mechanism for the production of (16) is via the initial formation of a thiadistannirane three-membered ring array, 2,2,3,3-tetra(2,4,6-tri-i-propylphenyl)-1-thia-2,3-distannirane (17) from the reaction of one mole equivalent of sodium sulphide with 1,2-dichloro-1,1,2,2-tetra-(2,4,6-tri-i-propylphenyl)distannane (equation 63).

$$ClR_2SnSnR_2Cl + Na_2S \rightarrow R_2Sn(S)SnR_2 + 2NaCl \qquad (63)$$

(17)

R = 2,4,6-tri-i-propylphenyl.

Having formed the thiadistannirane, by the conditions present in the reaction of heating at reflux in ethanol in the presence of oxygen, it is assumed that oxygen is inserted into the tin-tin bond forming (16)

(equation 64).

$$R_2Sn(S)SnR_2 + [O] \rightarrow R_2SnO(S)SnR_2 \quad (64)$$

(16)

R = 2,4,6-tri-i-propylphenyl.

However, as was observed in the ^{119}Sn nmr spectrum, a small amount of the diorganodithiadistannetane (**11**) was also produced in the reaction. This indicates a competition taking place between the insertion of oxygen and the insertion of sulphur, the latter most likely obtained by an extrusion process from sodium sulphide. In this reaction it would seem that the insertion of oxygen is by far the most facile process as indicated by the ratio of the two products in the reaction mixture [92% of (**16**) : 8% of (**11**)].

In an attempt to confirm the thiadistannirane intermediate the anaerobic sulphidation of 1,2-dibromo-1,1,2,2-tetra(2,4,6-tri-i-propylphenyl)distannane (**1**) was carried out using sodium sulphide nonahydrate in ethanol. From the reaction the thiadistannirane was not observed; instead the dominant species isolated from the reaction was 2,2,4,4-tetra(2,4,6-tri-i-propylphenyl)-1,3-dithia-2,4-distannetane (**11**) (equation 65 and 66).

$$BrR_2SnSnR_2Br + Na_2S \rightarrow R_2Sn(S)SnR_2 + 2NaBr \quad (65)$$

(1) **(17)**

$$R_2Sn(S)SnR_2 + [S] \rightarrow (R_2SnS)_2 \quad (66)$$

(17) (11)

R = 2,4,6-tri-i-propylphenyl.

From this reaction again it can be postulated that the reaction proceeded via a thiadistannirane intermediate. However, in this instance due to the absence of oxygen the sole insertion reaction taking place into the tin-tin bond was that resulting from the extrusion of sulphur from sodium sulphide, yielding the observed tetraorganodithiadistannetane (**11**).

The spectroscopic data obtained were consistent with the proposed structure. In this instance the ^1H and ^{13}C nmr spectra simplified to that theoretically predicted for the 2,4,6-tri-i-propylphenyl system. This most likely occurs due to further elongation of the tin-tin distance across the ring resulting from the inclusion of a second sulphur moiety, allowing free rotation of the i-propyl groups to occur in the 2,4,6-tri-i-propylphenyl system. In the ^{119}Sn nmr spectrum a trace contaminant (2%) was observed to give a signal of chemical shift coincident with that observed for (**16**). This leads to the suggestion that a trace of oxygen entered the reaction vessel at some stage during the reaction allowing a competition to be set up for the possible insertion species into the thiadistannirane intermediate. As was observed in the preparation of (**16**) the insertion of oxygen is a more facile reaction resulting in the immediate reaction of any oxygen present with the tin-tin bond upon thiadistannirane formation.

In the above preparations of (**16**) and (**11**) it is speculated that the reaction proceeds via a thiadistannirane (**17**) intermediate prior to tin-tin bond cleavage, either by oxygen to give (**16**), or by extrusion of sulphur from sodium sulphide to yield (**11**). In the preparation of (**11**), under anaerobic conditions, it is conceivable that the reaction could be halted upon formation of the thiadistannirane intermediate by the use of one mole equivalent of the sulphiding species. This, however, is inpracticable when using sodium sulphide nonahydrate, due to the variable sulphide content resulting from the hygroscopic nature of the reagent. An alternative reagent that could be used instead of sodium sulphide is hexamethyl-disilathiane. This can be produced in good yields from the reaction reported by Harpp and Steliou[217] between hexamethyldisilazane and hydrogen sulphide with imidazole as a catalyst (equation 67).

$$[(CH_3)_3Si]_2NH + H_2S + \text{imidazole (1\%)} \rightarrow [(CH_3)_3Si]_2S + NH_3 \quad (67)$$

By the use of this reagent it can be speculated that a more controlled stoichiometric addition to (**1**) could be made, resulting in the formation of the required thiadistannirane (**17**) (equation 68). This as yet is speculation and awaits further investigation.

$$\underset{(1)}{BrR_2SnSnR_2Br} + [(CH_3)_3Si]_2S \rightarrow \underset{(17)}{R_2Sn(S)SnR_2} + 2(CH_3)_3SiBr \quad (68)$$

R = 2,4,6-tri-i-propylphenyl.

In the literature, examples of three-membered homocyclic ring systems are known for the Group IV metals. Crystallographic evidence is reported for the existence of examples for silicon,[218,219] germanium[220] and tin.[148] However, for three-membered chalcogen substituted, heterocyclic ring systems examples become less frequent on descending group IV. For silicon, several different three-membered ring arrays are reported including both monosila- and disila-substituted oxiranes[221,222] and thiiranes.[223,224] For these compounds single crystal X-ray structural evidence is available to confirm the proposed structures. For germanium, instances of three-membered heterocyclic ring systems are far less common with chalcogen examples being limited to the monogerma- and digerma- substituted thiiranes[225] and the selenadigermirane.[225] No examples of monogerma- or digerma-substituted oxiranes have as yet been produced. Structural information so far obtained for the germanium examples is restricted to nmr spectroscopic and mass spectrometric evidence as no single crystal X-ray structure determinations have as yet been successfully carried out. In the case of tin, no three-membered heterocyclic ring systems have as yet been isolated indicating the increase in the instability encountered for small ring formation in the lower members of group IV.

3.2.3 Structured Synthesis of 2,2,4,4-Tetraorgano-1,3-oxathia-2,4-distannetanes.

Having prepared 2,2,4,4-tetra(2,4,6-tri-i-propylphenyl)-1,3-oxathia-2,4-distannetane (**16**) from the reaction of a dihalotetraorganodistannane with sodium sulphide in the presence of oxygen a more structured synthetic route to compounds of the same type was formulated. The postulated methodology was to start with a dihalide and initially convert it through to the partial hydrolysis product, a dihalotetraorganodistannoxane. From these compounds it was proposed that on reaction with sodium sulphide further examples of the tetraorganooxathiadistannetanes might be produced (equations 69 and 70).

$$2RR'SnX_2 + 2OH^- \rightarrow XRR'SnOSnRR'X + H_2O + 2X^- \quad (69)$$

$$XRR'SnOSnRR'X + Na_2S \rightarrow RR'SnO(S)SnRR' + 2NaX \quad (70)$$

R = R' = n-butyl (**18**) and i-propyl (**19**).

R = phenyl and R' = (Tsi) (**20**).

X = chloride and bromide.

In the case of the partial hydrolysis of di-t-butyltin dichloride the hydrated form, di-t-butylchlorotin hydroxide is obtained instead of the distannoxane (equation 71).

$$tBu_2SnCl_2 + OH^- \rightarrow tBu_2SnCl(OH) + Cl^- \quad (71)$$

The reagents used in the hydrolysis reactions of the diorganotin dihalides were the standard conditions cited in the literature of a halogen removal by the use of an organic base, in this instance triethylamine in ethanol.[226]

The spectra obtained for products arising from the above reactions were consistent with the proposed structures. For the dihalotetra-organodistannoxanes an oxygen and halogen bridged dimer[227] is usually the assigned structure. This dimeric system gives rise to two non-equivalent five-coordinate tin environments (figure 32).

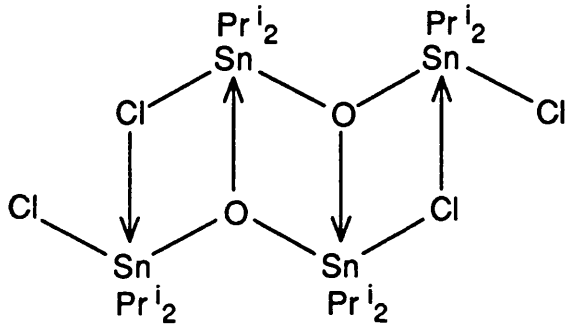

Figure 32: The Dimeric Oxygen and Halogen Bridged Array Present in Dihalotetraorganodistannoxanes.

As a result of the inequivalence of the two tin environments increased complexity would be expected to be observed in the ^1H and ^{13}C nmr spectra as well as two signals in the ^{119}Sn nmr spectrum. This occurs in both the 1,3-dichloro-1,1,3,3-tetra-n-butyl and 1,3-dibromo-1,1,3,3-tetra-i-propyldistannoxanes (**18**) and (**19**). However, in the case of 1,3-dichloro-1,3-diphenyl-1,3-di(Tsi)distannoxane (**20**) single environments are observed in the appropriate spectra. Differences are

also observed in both the Mossbauer and infra-red spectra. For compounds (**18**) and (**19**), quadrupole splitting values are recorded in the Mossbauer spectra that are indicative of the expected five-coordinate environments for tin [(**18**)[82] Q.S.= 3.24 mms^{-1} and (**19**) Q.S.= 3.16 mms^{-1}]. In the case of (**20**) the quadrupole splitting value obtained is more typical of a four-coordinate system (Q.S.= 2.18 mms^{-1}).

In the infra-red spectra of (**18**) and (**19**) two intense broad peaks are observed in the 530-650 cm^{-1} region of the spectra that are usually assigned to vibrations associated with the Sn-O-Sn unit for the dimeric dihalotetraorganodistannoxane system.[122] For (**20**) only one low intensity band is observed in the 530-650 cm^{-1} region. If the infra-red data available for the four-coordinate monomeric hexaorgano-distannoxanes are analysed it can be seen that the bands assigned to the Sn-O-Sn unit occur at between 750-800 cm^{-1} and 400 cm^{-1} respectively, for the asymmetric and symmetric stretches.[122] No direct assignments of bands can be made in these regions in the infra-red spectrum of (**20**) due to band congestion resulting from other infra-red active moieties in the molecule. However, bands are present which along with the other spectroscopic data already discussed, suggests that a monomeric structure is present in this particular dihalotetra-organodistannoxane system. If, as suggested, a monomeric unit occurs for (**20**) it would be reasonable to assume that the steric hindrance accorded by the presence of a (Tsi) group is too great for association and thus formation of the dimer to occur.

One surprising result observed in the spectra of (**19**) occurs in the E.I. mass spectrum. Instead of seeing fragments in the spectrum confirming the presence of the 1,3-dibromo-1,1,3,3-tetra-i-propyl-distannoxane, a series of high mass clusters are observed which correspond to a di-i-propyltin oxide trimer with successive losses of i-propyl mass fragments. The highest bromine containing fragment is observed at m/z = 321 mass units, which corresponds to i-propyltin dibromide i.e. an i-propyl group loss from di-i-propyltin dibromide. To confirm these observations theoretical mixed isotope patterns were calculated which gave good agreement with the observed clusters. This observation suggests that a disproportionation type rearrangement is taking place in the mass spectrometer giving rise to the observed species (equation 72).

$$3(iPr_2SnBr)_2O \rightarrow (iPr_2SnO)_3 + 3iPr_2SnBr_2 \qquad (72)$$

(**19**)

For the product obtained from the attempted preparation of di-t-butylchlorotin hydroxide the spectra obtained are consistent with the proposed structure. Previous authors have suggested[3] that the steric hindrance accorded by the t-butyl groups to tin prevents the formation of the distannoxane unit. The reasons for the t-butyl substituted system staying as a hydroxide compared to the phenyl(Tsi) derivative where the monomeric distannoxane forms is not clear. However, from the crystallographic data for comparable pairs of diorganothiastannanes (section 3.2.1) it would be reasonable to assume

that due to a *trans*-arrangement of sterically hindered groups possible in the latter case, closer interactions are allowed between the two tin units enabling the formation of the distannoxane.

Having obtained suitably substituted precursors the next stage of the synthesis was the attempted preparation of the tetraorganooxathia-distannetanes via the reaction pathway shown in equation 70. By the sulphidation of (**20**), 2,4-diphenyl-2,4-(Tsi)-1,3-oxathia-2,4-distannetane (**21**) was prepared. The spectra obtained were consistent with a structural type analogous to that observed for (**16**). From the Mossbauer spectrum a quadrupole splitting value of 1.63 mms^{-1} was obtained. This value is consistent with the expected four-coordinate structural geometry at tin and compares favourably with the previously discussed four-coordinate monomeric example (**16**) (Q.S.= 1.90 mms^{-1}).

By the same synthetic route the preparations of the n-butyl (**22**), t-butyl (**23**) and i-propyl (**24**) analogues were attempted. From the spectroscopic data obtained it appeared that the structures present in these systems were far more complex than the monomeric four-coordinate structures observed for (**16**) and (**21**). For (**22**) the ^{1}H, ^{13}C and ^{119}Sn nmr spectra indicate non-equivalence in the environments accorded to both tin and the organic substituents. In the Mossbauer spectrum a value of 2.78 mms^{-1} is observed for the quadrupole splitting indicative of coordination greater than four at tin. This phenomenon is observed for the lower hindrance examples of the dihalotetra-organodistannoxanes where dimeric halogen and oxygen bridged structures are observed.

A further interesting feature of (22) arises from the elemental analysis and infra-red spectroscopic data. In the elemental analysis it is apparent that for the proposed structure the correlation between the experimentally and theoretically derived values is poor (found C 36.00; H 7.24; calculated for $C_{16}H_{36}OSSn_2$: C 37.40; H 7.06). However, by the inclusion of a molecule of water the theoretical values give good agreement with the experimentally determined results (calculated for $C_{16}H_{38}O_2SSn_2$: C 36.12; H 7.20). The presence of -OH stretching modes were also very apparent in the infra-red spectrum. From this formulation two structual arrays can be theorised. The first is the mono hydrated form of (22) and the second dihydroxytetra-n-butyl-distannathiane. Both proposed structures are feasible on the evidence available. For a hydrated form of (22) a ladder type structure is foreseeable where both tins would be accorded five-coordination, one by oxygen bridging from a neighbouring oxathiastannane unit, the second by association with a water molecule (figure 33).

In this structure all the spectroscopic data is satisfied except for a slight query over the types of stretching modes observed in the infra-red spectrum. By comparison with the infra-red spectra of other hydroxyl or water associated tin compounds certain conclusions can be made. In the infra-red spectrum of the dimeric n-butyldichlorotin hydroxide monohydrate, $[nBuSn(OH)Cl_2.H_2O]_2$ bands assignable to both associated water and bridging hydroxyl groups are observed. For the associated water a very broad band is observed at approximately 3200 cm^{-1} whereas for the bridging hydroxyl moieties three bands can be assigned at 3400 cm^{-1} for the O-H stretch, 1000 cm^{-1} for the O-H

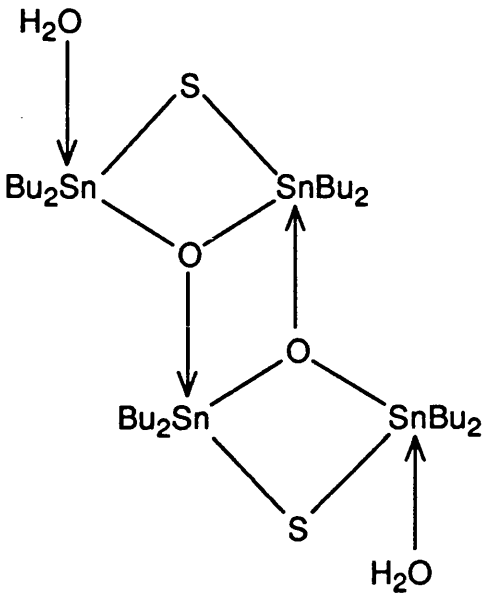

Figure 33: Dimeric Associated Array Postulated for 2,2,4,4-Tetra-n-butyl-1,3-oxathia-2,4-distannetane Monohydrate (22).

deformation and some poorly resolved bands between 600 and 500 cm^{-1} which are assignable to the Sn-O-Sn stretches. Similar observations are made for the bridging hydroxyl groups in the infra-red spectrum of di-t-butylchlorotin hydroxide at 3460 cm^{-1}, 975 cm^{-1} and 535/500 cm^{-1} respectively. By comparison with these spectra it would appear that the structure of (22) was more reminiscant of the hydroxyl bridged arrays rather than an associated water system, due to the presence of bands of similar appearance at 3460 cm^{-1}, 890 cm^{-1} and 645/580 cm^{-1}.

On the evidence presented a hydroxyl bridged structure similar to that proposed in figure 34 would seem to fit the observed spectral data. In this system the non-equivalence of the n-butyl groups would be maintained due to two five-coordinate environments being accorded

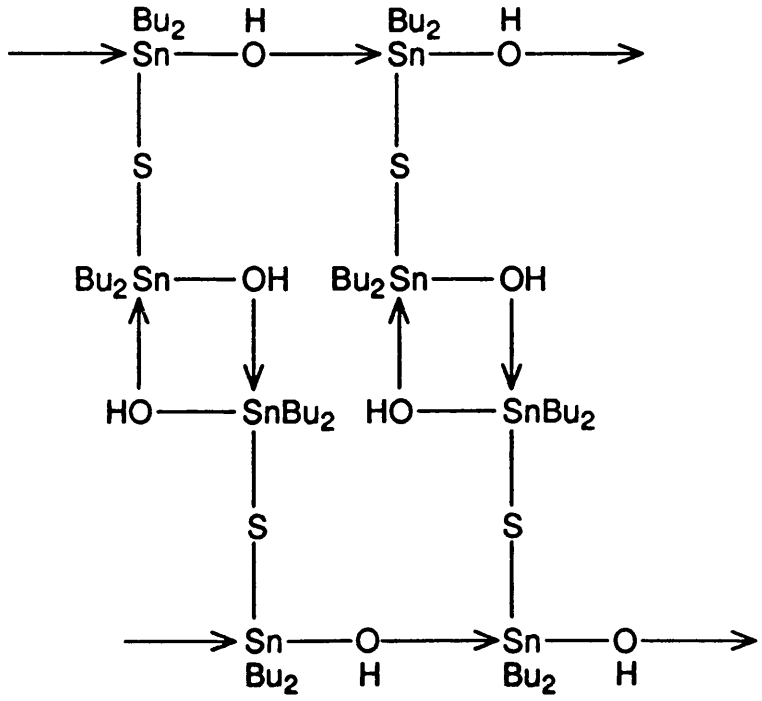

Figure 34: Hydroxyl Bridged Structure for 1,3-Dihydroxy-1,1,3,3-tetra-n-butyldistannathiane (22).

to tin in the postulated array.

For compound (23) spectroscopic details are limited as a result of poor solubility in most common solvents at room temperature. However, from the Mossbauer quadrupole splitting value of 2.71 mms^{-1} it would appear that the coordination at tin is greater than four. The values obtained experimentally by elemental analysis are in accord with the presence of two molecules of water per tetra-t-butyloxathiadistannetane unit (found C 35.20; H 7.39; calculated for $C_{16}H_{40}O_3SSn_2$: C 34.95; H 7.46). In this compound a very broad peak is observed at 3350 cm^{-1} for the O-H streching band in the infra-red spectrum. The

band position and overall shape is very reminiscent of the O-H stretch assigned to associated water in the infra-red spectrum of n-butyldichlorotin hydroxide monohydrate rather than the hydroxyl bridged system postulated for (22). From the limited evidence available a monomeric unit is proposed with a water molecule coordinated to each tin (figure 35).

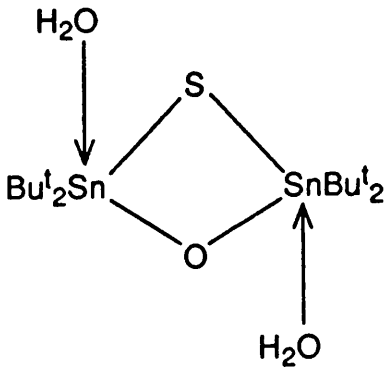

Figure 35: Postulated Dihydrated Structure for 2,2,4,4-Tetra-t-butyl-1,3-oxathia-2,4-distannetane (23).

From a molecular model of the proposed structure it is evident that the extreme steric hindrance present in the molecule prevents any further association with neighbouring oxathiadistannetane units, however, sufficient space appears to be present to allow the association of one molecule of water to each tin atom.

For compound (24) extreme problems were experienced in trying to isolate the reaction product in a pure state. One solid product that was isolated from the reaction mixture was characterised by the infra-red and ^{119}Sn nmr spectra as i-propylstannoic acid. This product is

assumed to have been formed by a redistribution reaction such as the one shown (equations 73 and 74), occurring during the attempted recrystallisation of the impure solid.

$$2iPr_2SnO(S)SniPr_2 + 2H_2O \rightarrow 2iPrSn(O)OH + 2iPr_3SnSH \quad (73)$$

(24)

$$2iPr_3SnSH \rightarrow iPr_3SnSSniPr_3 + H_2S \quad (74)$$

From the work undertaken so far the most convincing evidence for the formation of (24) is the Mossbauer spectrum of the impure solid where a quadrupole splitting value of 2.66 mms^{-1} is observed. This value is not coincident with that observed for i-propylstannoic acid (Q.S.= 1.73 mms^{-1}) but does compare favourably with the values already recorded for compounds (22) (Q.S.= 2.78 mms^{-1}) and (23) (Q.S.= 2.71 mms^{-1}). However, due to the poor yields gained from this reaction no further spectroscopic data was obtained.

3.2.4 Variable Temperature Mossbauer Spectral Study of Diorgano-chalcogenastannanes.

The variable temperature Mossbauer technique (detailed in chapter one section 4.2) was used to investigate the structural nature of 2,2,4,4-tetra-n-butyl-1,3-oxathia-2,4-distannetane monohydrate (22) by comparison with three compounds of known structural type. The experimental results are tabulated in tables 16-19 and the resultant

Table 16: Variable Temperature Mossbauer Data for 2,2,4,4,6,6-Hexa-n-butyl-1,3,5-trithia-2,4,6-tristanninane (13).

T*	Peak Area (A_T)	$\ln A_T/A_{78}$
78.5	3.026	0
85.0	2.596	-0.153
95.0	2.188	-0.324
105.0	1.667	-0.596
115.0	1.365	-0.796
125.0	0.993	-1.114
135.0	0.690	-1.479

* = K.

$\underline{a} = -d\ln A_T/dT \Rightarrow \underline{a} = 2.25 \times 10^{-2}\ K^{-1}$.

mass of sample used = 25.9 mg.

Table 17: Variable Temperature Mossbauer Data for Di-n-butyltin Oxide.

T*	Peak Area (A_T)	$\ln A_T/A_{78}$
78.6	3.522	0
85.0	3.391	-0.038
95.0	3.033	-0.149
105.0	2.686	-0.271
115.0	2.380	-0.392
125.0	2.213	-0.465
135.0	1.957	-0.587
145.0	1.731	-0.710

* = K.

$\underline{a} = -d\ln A_T/dT \Rightarrow \underline{a} = 1.26 \times 10^{-2}\ K^{-1}$.

mass of sample used = 24.3 mg.

Table 18: Variable Temperature Mossbauer Data for 2,2,4,4-Tetra-n-butyl-1,3-oxathia-2,4-distannetane Monohydrate (22).

T*	Peak Area (A_T)	$\ln A_T/A_{78}$
78.3	2.603	0
85.0	2.402	-0.080
95.0	2.062	-0.233
105.0	1.727	-0.410
115.0	1.444	-0.589
125.0	1.164	-0.805
135.0	0.921	-1.039
145.0	0.695	-1.320

* = K.

$a = -d\ln A_T/dT \Rightarrow a = 1.54 \times 10^{-2}\ K^{-1}$.

mass of sample used = 25.9 mg.

Table 19: Variable Temperature Mossbauer Data for 2,2,4,4-Tetra[2,4,6-tri-i-propylphenyl]-1,3-oxathia-2,4-distannetane (**16**).

T*	Peak Area (A_T)	$\ln A_T/A_{78}$
78.0	1.365	0
85.0	1.179	-0.146
95.0	0.979	-0.332
105.0	0.800	-0.534
115.0	0.618	-0.792
125.0	0.471	-1.064

* = K.

$\underline{a} = -d\ln A_T/dT \Rightarrow \underline{a} = 1.98 \times 10^{-2}\ K^{-1}$.

mass of sample used = 26 mg.

plots of $\ln A_T/A_{7\theta}$ against temperature are given in figure 36.

In the case of both 2,2,4,4,6,6-hexa-n-butyl-1,3,5-trithia-2,4,6-tristanninane (**13**) and 2,2,4,4-tetra(2,4,6-tri-i-propylphenyl)-1,3-oxathia-2,4-distannetane (**16**) the structures are known. 2,2,4,4,6,6-hexa-n-butyl-1,3,5-trithia-2,4,6-tristanninane (**13**) forms a trimeric six-membered ring structure which in the variable temperature Mossbauer experiment generates a line of steep gradient ($\underline{a}$ = 2.25 × 10^{-2} K^{-1}) resulting from discrete molecular entities in the solid state. For (**16**) a similar result is observed ($\underline{a}$ = 1.98 × 10^{-2} K^{-1}) because of the monomeric nature of the compound in the solid state as shown in the ORTEP plot of the crystal structure (figure 30). In contrast to the discrete systems already mentioned is di-n-buyltin oxide which is thought to form a highly associated reticulated structure. As can be seen, a much shallower slope is observed ($\underline{a}$ = 1.26 × 10^{-2} K^{-1}) indicative of the rigidly held polymeric system present in the compound.

In the case of (**22**) a line of intermediate slope ($\underline{a}$ = 1.54 × 10^{-2} K^{-1}) is observed indicative of an associated structure which is not as tightly bound as the restrictive polymeric system found in the di-n-butyltin oxide structure. This result would seem to vindicate the arguments so far put forward for an associated structure present in the tetraorganooxathiadistannetane examples containing less sterically demanding organic substituents.

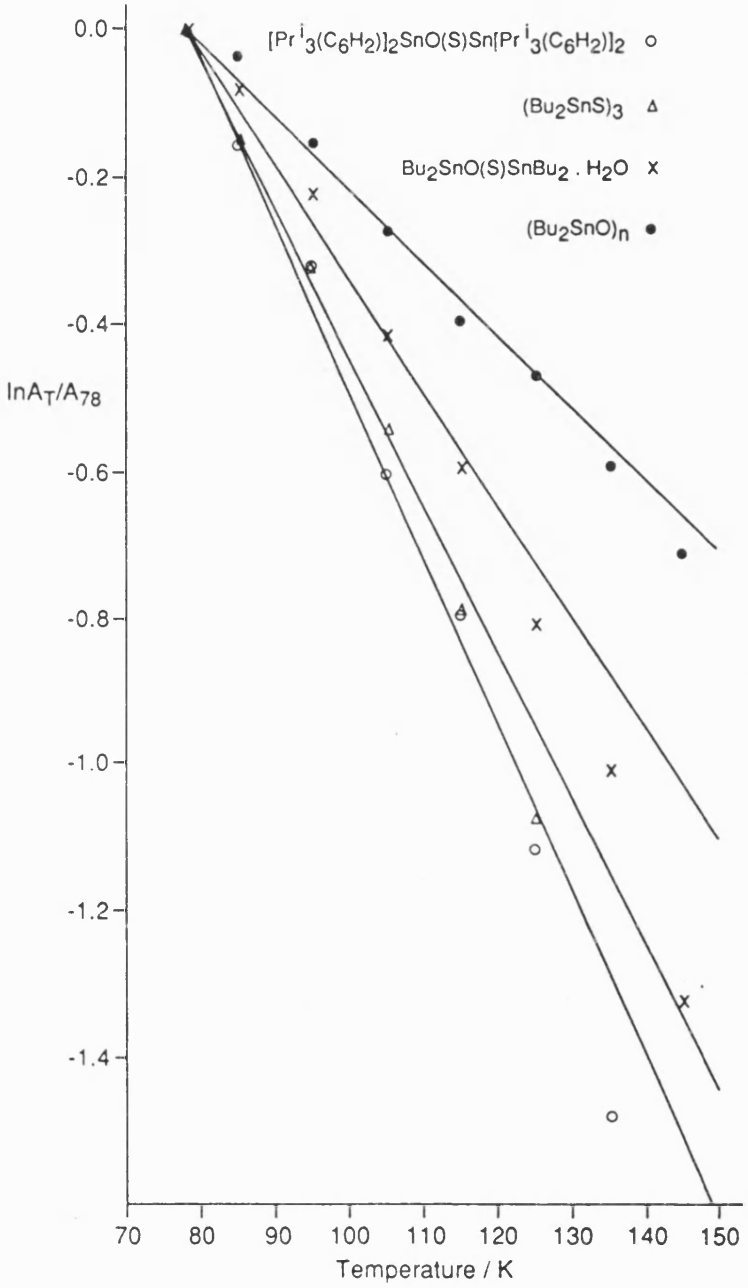

Figure 36: Plot of lnA_T/A_{78} vs Temperature/K for $(nBu_2SnS)_3$ (13), $(nBu_2SnO)_n$, $(nBu_2)SnO(S)Sn(nBu_2).H_2O$ (22) and $[iPr_3(C_6H_2)]_2SnO(S)Sn[iPr_3(C_6H_2)]_2$ (16).

3.2.5 Attempted Preparations of 1,3-Dihalo-1,1,3,3-tetraorgano-distannathianes.

A possible alternative route for the preparation of tetraorgano-oxathiadistannetanes is by the hydrolysis of a dihalotetraorgano-distannathiane. By this method compounds analogous to the previously prepared tetraorganooxathiadistannetanes might be produced with structural modifications resulting from the diminished association present in the reaction precursor.

The methodology used to try to prepare the dihalotetraorgano-distannathiane precursors was that reported by Davies and Harrison[228] where a disproportionation reaction between a diorganothiastannane and a diorganotin dihalide is used to prepare the required compound (equation 75).

$$nR_2SnX_2 + (R_2SnS)_n \rightarrow nXR_2SnSSnR_2X \qquad (75)$$

R = t-butyl and X = chloride.

R = i-propyl and X = bromide.

In the first attempted preparation tetra-t-butyldithiadistannetane (**10**) was heated with di-t-butyltin dichloride in the absence of solvent. To obtain a homogeneous melt from the two components the reaction temperature was held at 180°C for 3 hours. After purification a colourless, highly crystalline product was produced. In the ^1H and ^{13}C nmr spectra, sharp singlets were seen with well defined $^{117,119}Sn$ satellites indicating a high level of purity in the product. However,

from the results of the elemental analysis (Found C 31.00; H 6.03; Calculated for $C_{16}H_{36}Cl_2SSn_2$: C 33.79; H 6.38) and the ^{119}Sn nmr and Mossbauer spectra, doubt was raised as to the identity of the product. In the ^{119}Sn nmr spectrum six peaks were seen instead of the expected single environment and in the Mossbauer spectrum a singlet as well as the expected doublet was observed.

As a result of the highly crystalline nature of the product a single crystal X-ray structural determination was carried out. From this the true identity of the product was obtained. Instead of the expected dichlorotetra-t-butyldistannathiane the compound produced was the 2,2'-spirobi(4,4,6,6-tetra-t-butyl-1,3,5-trithia-2,4,6-tristanninane) (25). Full crystal data is available in Appendix VII.

In the work reported by Puff et al.[215] (25) was prepared by a different method to that used above and will be discussed later in full. Unfortunately, a single crystal X-ray structure determination was included in the report. As well as (25) the structural determinations for the i-propyl, sulphur and selenium analogues were also detailed in the same account. From these structures the two i-propyl analogues were shown to have tetragonal unit cells with $I4_1/a$ space groups compared to (25) where a monoclinic unit cell with a $C2/c$ space group was observed. In the refined crystal structures it was apparent that the i-propyl examples showed very different conformations to the t-butyl case. For our sample of (25) the crystal sample was shown to possess a triclinic unit cell with a $P\bar{1}$ space group. On this evidence it was hoped that the sample of (25) prepared above would display different molecular geometry, probably analogous

to the conformation observed in the i-propyl examples thus accounting for the differences in the crystal symmetries. However, on comparison, both structures appeared to be very similar except for slight differences observed in the arrangement of the t-butyl groups. The actual tin-sulphur skeletons of the two crystal samples were exactly superimposable. In the purification of the two samples different recrystallisation solvents were used which may have been responsible for different packing in the crystals thus giving rise to the different symmetries.

Having obtained the true identity of the product most of the inconsistencies previously observed in the spectral data could be explained. In the Mossbauer two environments would be expected, where the observed singlet is assignable to the spiro-tin and the doublet to the di-t-butyl substituted ring located tin atoms. The elemental analysis figures calculated for the spiro compound are also in good agreement with the values obtained experimentally (Calculated for $C_{32}H_{72}S_6Sn_5$: C 30.93; H 5.84).

One problem that remains unanswered is the complexity observed in the ^{119}Sn nmr spectrum shown in figure 37. In total six peaks are observed in the spectrum. The chemical shifts of the two most intense signals are assigned at 108.1 ppm to the t-butyl substituted tin and at 84.1 ppm for the SnS_4 tin atom. The observed chemical shifts agree with those cited in the literature by Puff et al.[215] for when (25) was prepared and characterised previously.

From the six peaks it would appear from the line shapes that two distinct types of tin environment are being observed. The peaks seen

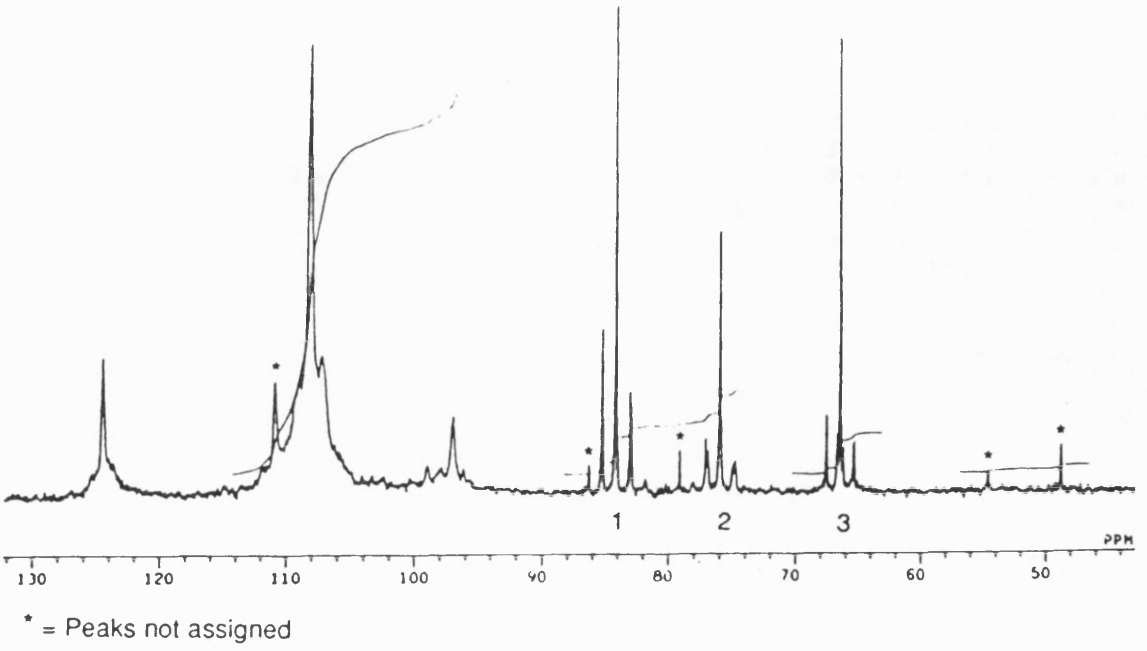

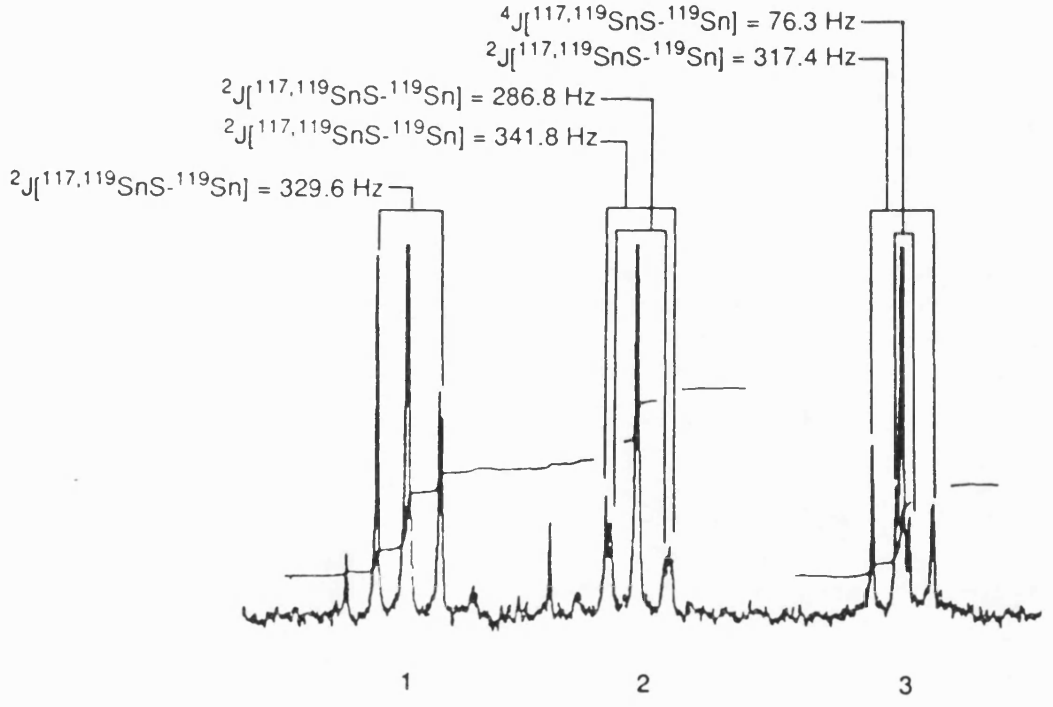

Figure 37: Solution State ^{119}Sn NMR of 2,2'-Spirobi(4,4,6,6-tetra-t-butyl-1,3,5-trithia-2,4,6-tristanninane) (25).

at 97.0, 108.1 and 124.5 ppm are very broad and no coupling details are observed. The reason for the line broadening is unclear however, incomplete proton decoupling of the t-butyl groups on tin is the most likely reason for this phenomenon. This evidence suggests that all three peaks arise from t-butyl substituted tin atoms. The identity of the peak at 124.5 ppm can be assigned as tetra-t-butyldithia-distannetane (**10**) on the basis of the chemical shift value of 124.1 ppm ($CDCl_3$ solution)[31] quoted in the literature. The second class of peaks occur at 66.5, 76.3 and 84.1 ppm and can be assigned to SnS_4 type tin environments. For these peaks the line width is narrow allowing satellites due to tin-tin coupling to be observed. For all three peaks unresolved $^2J(^{117,119}SnS\text{-}^{119}Sn)$ of values 317.4, 341.8 and 329.6 Hz respectively are observed with a second set of satellites also associated with the peak at 75.9 ppm of value 286.8 Hz. For the peak at 66.5 ppm a second set of satellites are observed which by the order of magnitude can be assigned to an unresolved $^4J(^{117,119}SnSSnS\text{-}^{119}Sn)$ with a value of 76.3 Hz.

From the data obtained by ^1H and ^{13}C nmr spectroscopy, elemental analysis and the X-ray structure determination, the compound appeared to be of high purity. From the spectral evidence it would thus appear that on long-term storage in solution the spiro compound breaks down to give other components one of which appears to be tetra-t-butyl-dithiadistannetane (**10**). (For ^1H and ^{13}C nmr investigations, solutions of the compounds are prepared and a spectrum recorded almost immediately. However, with the ^{119}Sn nmr investigation the solution would be stored and a spectrum recorded when the multinuclear nmr

probe became available and so a storage time of up to one week is usual.) If this hypothesis is correct it would seem reasonable to state that the spiro compound is in fact a thermodynamically unstable product and in the solution state the ring structure will break up to yield smaller more stable units. For (25) in the solid state a brown coloration results on extended exposure to light further supporting the theory that on prolonged storage the compound degrades to more thermodynamically stable species.

Without further investigation it is hard to assign with certainty the exact species present, however with the evidence obtained from the ^{119}Sn nmr spectrum some conclusions can be made as to the decomposition mechanism and the final products produced in this system. One species known to be produced in the reaction is tetra-t-butyldithiadistannetane (10) and for this to occur from (25) a ring fission would have to take place. If this disproportionation type reaction attained completion then the likely products yielded would be two mole equivalents of tetra-t-butyldithiadistannetane (10) and the 'stannic sulphide monomer' (equation 76).

$$\underset{(25)}{[(tBu_2Sn)_2S_3]_2Sn} \rightarrow \underset{(10)}{(tBu_2SnS)_2} + SnS_2 \qquad (76)$$

From the ^{119}Sn nmr spectrum it would appear that the intermediates for this reaction are also present in solution. For the disproportionation reaction to occur it can be hypothesised that initially bond cleavage occurs at one of the spiro-tin-sulphur bonds

which could be followed by an attack at a ring located tin to produce tetra-t-butyldithiadistannetane (**10**) (figure 38). Having removed one ring system a second ring cleavage would generate a second molecule of tetra-t-butyldithiadistannetane (**10**) and a 'stannic sulphide monomer' (figure 39). If at this stage a reaction were to occur between two of the primary ring cleavage residues (figure 38) and the 'stannic sulphide monomer' it is conceivable that a tri-spirocyclic species (**26**) would be produced (figure 40). Successive insertion of 'stannic sulphide monomers' into the propagating spirocyclic system would eventually lead to the production of what is essentially polymeric stannic sulphide. This result would seem to confirm observations made during the recrystallisation of an aged sample of (**25**) where a yellow solid which was apparently insoluble in organic solvents was filtered off prior to cooling.

The most conclusive evidence so far obtained for the production of (**26**) is from the assignment of the three outstanding peaks in the ^{119}Sn nmr spectrum (figures 37 and 40). To the ring located t-butyl substituted tins (type c) the peak at 97.0 ppm can be assigned due to the large line width resulting from the partially incomplete proton decoupling of the spectrum. In the case of the other two peaks coupling pathway information was used in the assignment. For the central tin (type a) both $^{2}J(^{117,119}SnS\text{-}^{119}Sn)$ and $^{4}J(^{117,119}SnSSnS\text{-}^{119}Sn)$ coupling pathways are possible. As a result of this the peak at 66.5 ppm can be assigned due to the observation of two sets of satellites of differing magnitude (317.4 and 76.3 Hz). For the last type of tin (type b) two sets of $^{2}J(^{117,119}SnS\text{-}^{119}Sn)$ to tin (type a

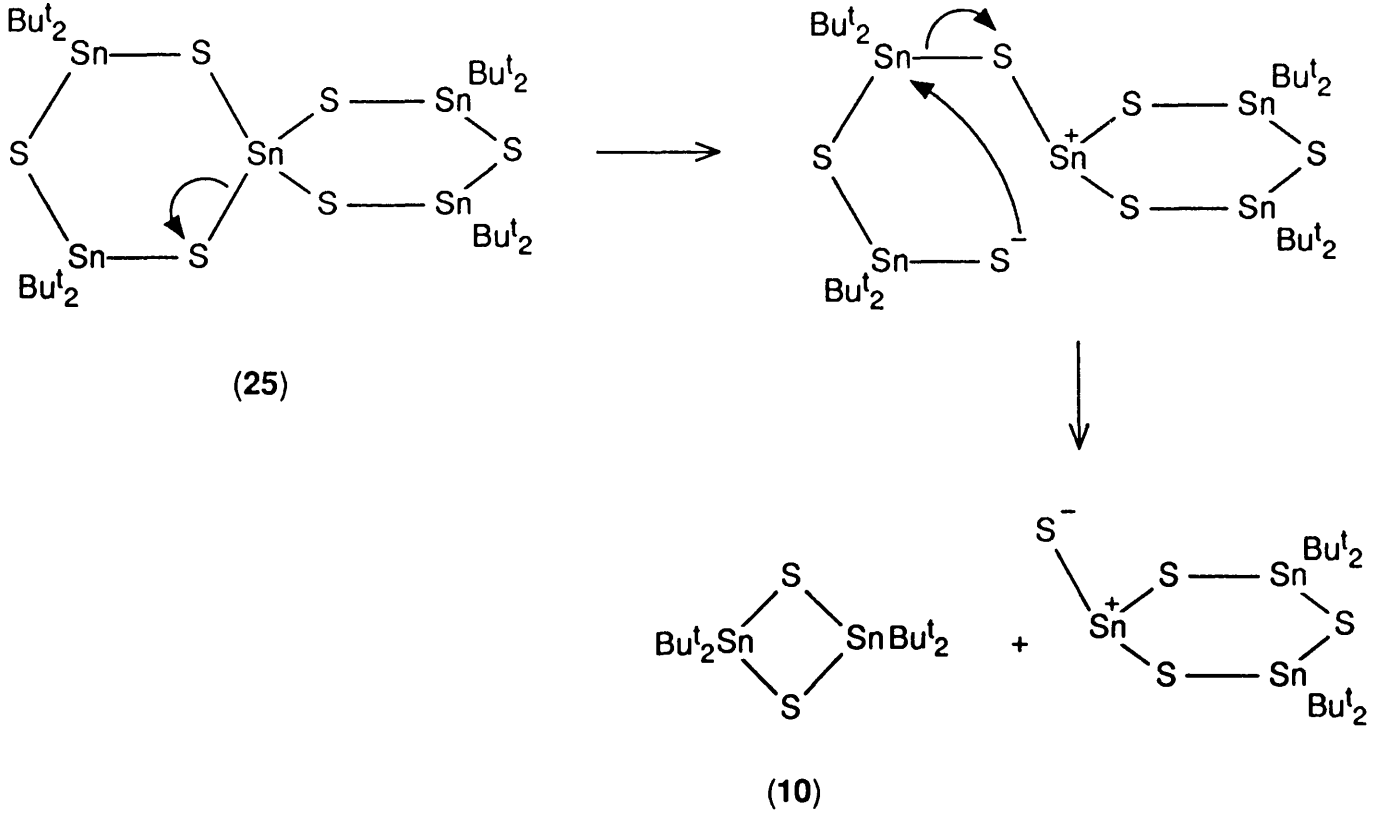

Figure 38: Primary Ring Fission of 2,2′-Spirobi(4,4,6,6-tetra-t-butyl-1,3,5-trithia-2,4,6-tristanninane) (**25**) Yielding 2,2,4,4-Tetra-t-butyl-1,3-dithia-2,4-distannetane (**10**).

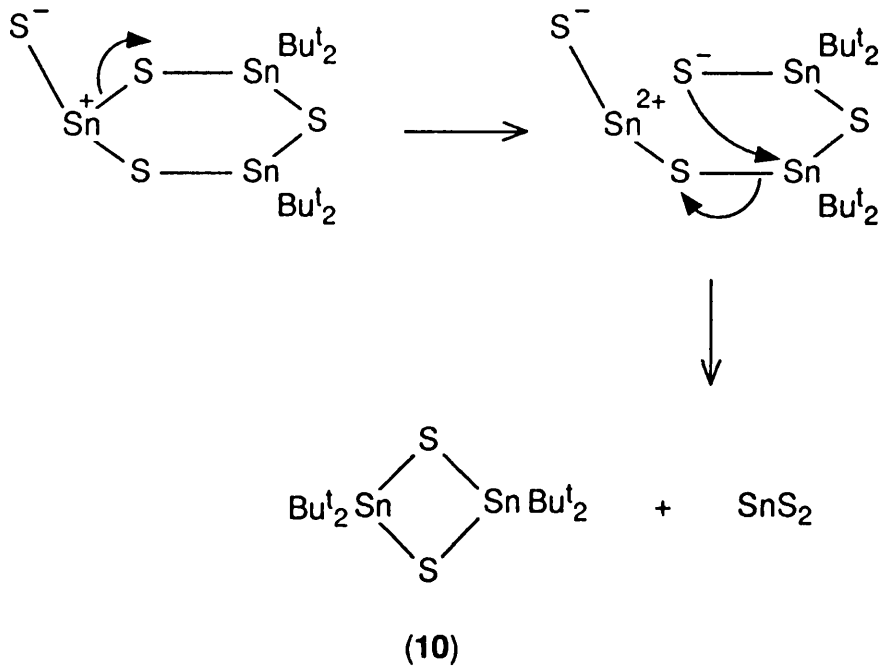

(10)

Figure 39: Secondary Ring Fission Yielding 2,2,4,4-Tetra-t-butyl-1,3-dithia-2,4-distannetane (**10**).

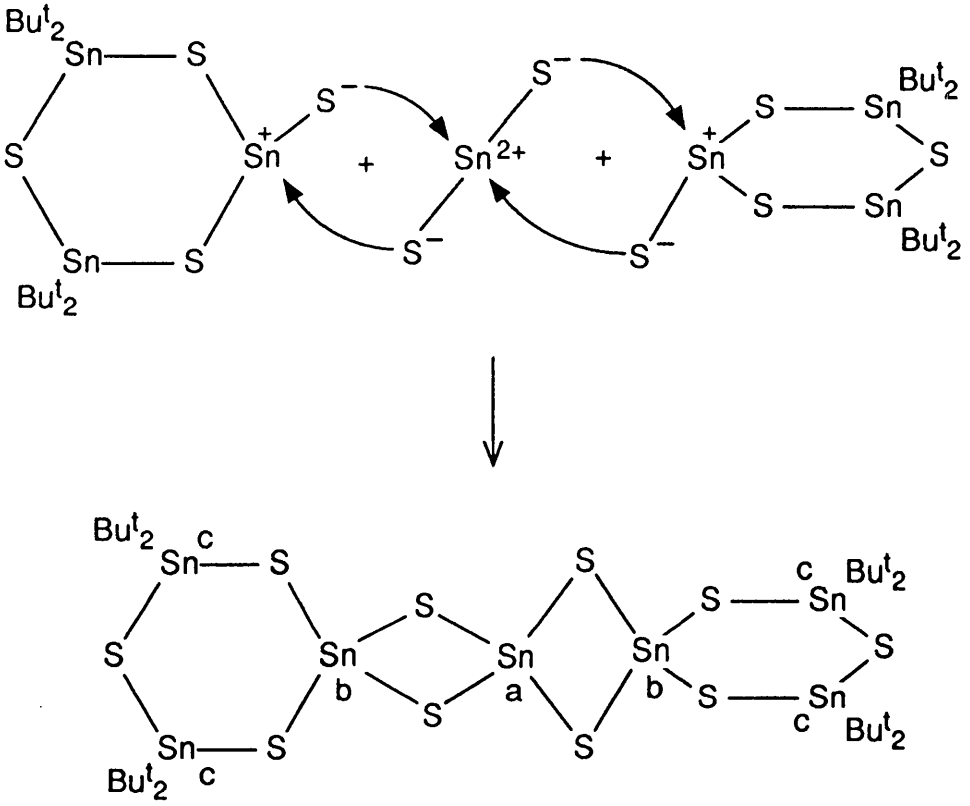

(26)

Figure 40: Formation of a Tri-spirocyclic Species (**26**) from the Fusion of Two Primary Ring Cleavage Residues and a 'Stannic Sulphide Monomer'.

and c) would be expected. However, the difference in value would only be small as is seen for the peak at 75.9 ppm where two types of satellites of similar value are observed (286.8 and 341.8 Hz).

The spiro compound is cited in the literature as having been previously prepared by two methods.[215,229] The first method employs heating tetra-t-butyldithiadistannetane (**10**) and sulphur together in a sealed tube while in the second the reaction between sodium tetrathiostannate and di-t-butyltin dichloride was used (equations 77 and 78).

$$5(tBu_2SnS)_2 + 4S \rightarrow 2[(tBu_2Sn)_2S_3]_2Sn + 2tBu_2S \quad (77)$$

(25)

$$4tBu_2SnCl_2 + 2Na_4SnS_4 \rightarrow [(tBu_2Sn)_2S_3]_2Sn + SnS_2 + 8NaCl \quad (78)$$

(25)

The exact reaction conditions employed for the production of (**25**) presented here are unclear as the synthetic methodology was designed as a stoichiometric disproportionation reaction for the preparation of dihalotetraorganodistannathianes. However, from the two previously known synthetic routes to this compound it would be reasonable to assume that the method of preparation quite closely followed the high temperature sealed tube reaction between tetra-t-butyldithia-distannetane (**10**) and elemental sulphur (equation 77).

From the reagents used in this preparation an equation can be suggested to satisfy the stoichiometry of the products obtained

(equation 79).

$$3(tBu_2SnS)_2 + tBu_2SnCl_2 \rightarrow [(tBu_2Sn)_2S_3]_2Sn + 2tBu_3SnCl \quad (79)$$

(25)

The by-product obtained from this reaction and the excess di-t-butyltin dichloride, both of which are soluble, would have been lost in the work-up of (25).

In an attempt to reduce the severity of the conditions the above preparation was repeated as a solution in toluene and heated at reflux for 1 hr. Following purification, on evidence obtained by ^{119}Sn nmr spectroscopy it became apparent that the major proportion of the product obtained was tetra-t-butyldithiadistannetane (**10**) starting material with some of (25) also present as an impurity.

The same pair of reaction conditions were also attempted for the i-propyl analogues. From both reactions whether carried out at 200°C in the absence of solvent or in toluene and heated to reflux for 1 hr the same product was isolated which from elemental analysis and the Mossbauer spectrum appeared to be the required 1,3-dibromo-1,1,3,3-tetra-i-propyldistannathiane (27) [Found C 23.50; H 4.58; Calculated for $C_{12}H_{28}Br_2SSn_2$: C 23.96; H 4.69. Mossbauer data (mms^{-1}): $(iPr_2BrSn)_2S$: I.S.= 1.68; Q.S.= 2.94. $(iPr_2SnS)_3$: I.S.= 1.51; Q.S.= 1.96. iPr_2SnBr_2: I.S.= 1.69; Q.S.= 3.41.]. However, from the ^1H, ^{13}C and ^{119}Sn nmr spectra multiplicity of peaks were observed. On investigation of the chemical shifts in the ^{119}Sn nmr it is apparent that the three peaks present correspond to (27) as well as equal

amounts of di-i-propyltin dibromide and hexa-i-propyltrithia-tristanninane (**14**). From this the conclusion can be made that initially the required compound is isolated which is stable in the solid state, however in solution a facile disproportionation occurs resulting in the formation of an equilibrium mixture composed of the product and its progenitors.

On the basis of this disproportionation in solution the results obtained for the attempted hydrolysis of (**27**) can be explained. Two methods were used for the hydrolysis experiments the first used sodium hydroxide with ethanol as the reaction solvent and the second used triethylamine in a mixture of ethanol and diethyl ether. From both reactions the only product isolated was 1,3-dibromo-1,1,3,3-tetra-i-propyldistannoxane (**19**). This can be explained by the fact that from the disproportionation reaction di-i-propyltin dibromide is produced and so the conditions in solution become the same as those previously described for the preparation of dihalotetraorganodistannoxanes (section 3.2.3). As the di-i-propyltin dibromide is converted to the distannoxane so the equilibrium of the disproportionation reaction constantly shifts until all of (**27**) is consumed (equations 80 and 81).

$$\underset{(27)}{(iPr_2SnBr)_2S} \rightarrow iPr_2SnBr_2 + \underset{(14)}{(iPr_2SnS)_3} \qquad (80)$$

$$2iPr_2SnBr_2 + 2OH^- \rightarrow \underset{(19)}{(iPr_2SnBr)_2O} + H_2O + 2Br^- \qquad (81)$$

A third reaction methodology was also tried in the attempt to prepare tetraorganooxathiadistannetanes. In the preparation of dihalotetraorganodistannoxanes one method by which these compounds can be prepared is by the disproportionation of a diorganotin oxide with a diorganotin dihalide.[230] By an analogous method using a diorganotin oxide and a diorganothiastannane it was hoped that the required tetraorganooxathiadistannetane would be produced. However, from the reaction between hexa-i-propyltrithiatristanninane (**14**) and 'di-t-butyltin dihydroxide' heated at reflux in benzene for 17 hours the only two products isolated on the evidence displayed in the infra-red spectra appeared to be tetra-t-butyldithiadistannetane (**10**) and di-i-propyltin oxide (equation 82).

$$2(iPr_2SnS)_3 + 6'tBu_2Sn(OH)_2' \rightarrow 3(tBu_2SnS)_2 + 6iPr_2SnO + 6H_2O \quad (82)$$

(**14**) (**10**)

From this reaction it could be suggested that a mechanism by which the chalcogen exchange occurs may proceed via an oxathiadistannetane intermediate with the insolubility of polymeric di-i-propyltin oxide acting as the driving force for a successive disproportionation reaction to occur. However, no other products apart from the two shown were isolated from the system and so any conclusions made are purely speculative.

3.2.6 Monoorganochalcogenastannanes.

Having already prepared diorganochalcogenastannanes from the reaction between diorganotin dihalides and a suitable chalcogenating agent, the analogous preparations of the monoorgano derivatives using a similar reaction methodology were attempted (equation 83).

$$4RSnX_3 + 6Na_2S \rightarrow (RSnS_{1.5})_4 + 12NaX \qquad (83)$$

For R = n-butyl (28) and i-propyl (29).

For X = bromide and chloride.

By the above reaction conditions the required products were obtained. The spectrocopic data were totally consistent with the proposed structures. For these type of compounds the structure normally observed is the adamantane cage array as exemplified by the tetramethyl and tetra(pentafluorophenyl) substituted tetraorgano-hexathiatetrastannaadamantanes.[158,231] The structures of both the n-butyl and i-propyl analogues (28) and (29) would be expected to be the same as the literature examples, however, spectroscopic data to confirm this proposal is limited. For (28) the product obtained from recrystallisation was a white powdery solid resisting all attempts to obtain a crystalline sample. However, from the ^{119}Sn nmr spectrum satellites were observed for the $^2J(^{117}Sn-^{119}Sn)$ of value 201.8 Hz. The normalised intensities of these satellites corresponded to 25% of the overall peak height. For each tin site in an adamantane cage array three contributions to the satellite intensities would be expected.

Theoretically for ^{117}Sn with a natural abundance of 7.6%, satellites of normalised overall intensities of 22.8% would be expected. As can be seen the theoretical value is in reasonable agreement with the experimentally observed figures. Further evidence for the structure of (28) is available from the Mossbauer spectrum (I.S.= 1.38 mms^{-1} and Q.S.= 1.44 mms^{-1}). When compared with the values obtained from the Mossbauer spectrum of the methyl analogue[232] (I.S.= 1.38 mms^{-1} and Q.S.= 1.40 mms^{-1}), for which the structure is known, it would seem reasonable to assume that both compounds displayed the same solid state adamantane type cage structure.

For (29) a highly crystalline product was obtained. By recrystallisation from ethyl acetate crystals were produced which appeared suitable for single crystal X-ray structure determination. However, from preliminary crystal analysis it was apparent that the crystals were all 'twinned', negating any attempts at full structure characterisation. In an attempt to obtain structural information on the compound ^{119}Sn nmr investigation was undertaken with a view to analysis of satellite intensities as described above. Unfortunately the compound in question proved to be nearly insoluble in any deuterated solvents available. As a result no structural information is available except to state that the Mossbauer spectrum for (29) (I.S.= 1.46 mms^{-1} and Q.S.= 1.40 mms^{-1}) is very similar both in isomer shift and quadrupole splitting to the analogous methyl example giving rise to the assumption that (29) also displays an adamantane cage structure.

To try and vary the structural characteristics of these types of compounds the preparation of a mixed chalcogen analogue was attempted. In this instance the primary hydrolysis product of n-butyltin trichloride (equation 84), the dimeric n-butyldichlorotin hydroxide monohydrate, was reacted with sodium sulphide (equations 85 and 86).

$$2nBuSnCl_3 \xrightarrow{air} [nBuSnCl_2(OH).H_2O]_2 + 2HCl \quad (84)$$

$$2[nBuSnCl_2(OH).H_2O]_2 + 4Na_2S \rightarrow [nBuSn(OH)S]_4 + 8NaCl + 4H_2O \quad (85)$$

$$[nBuSn(OH)S]_4 \rightarrow (nBuSnO_{0.5}S)_4 + 2H_2O \quad (86)$$

(30)

The spectroscopic data obtained on the product **(30)** was consistent with the proposed structure. The identity of the compound as the condensation product tetra-n-butyldioxatetrathiatetrastannaadamantane **(30)** rather than n-butylthiastannane hydroxide $\{[nBuSn(OH)S]_n\}$ is based upon the elemental analysis results (Analysis (%): Found C 22.28; H 4.36; Calculated for $C_4H_{10}OSSn$: C 21.36; H 4.48; Calculated for $C_4H_9O_{0.5}SSn$: C 22.26; H 4.20). In the solution state ^{119}Sn nmr spectrum a sharp singlet was observed at 142.9 ppm. As for **(28)** satellites were observed for $^2J(^{117}Sn-^{119}Sn)$ of 201.4 Hz. From the normalised overall intensities of 21.2% it can be concluded that as in **(28)** three ^{117}Sn atoms are contributing to the satellite intensities. As only a single tin environment is observed in the solution state as

shown by a singlet in the ^{119}Sn nmr spectrum it can again be postulated that the structure of (**30**) present in solution is of the adamantane cage type with a half share in two sulphurs and one oxygen accorded to each tin.

In the solid state, as reflected in its Mossbauer spectrum, a more complex structural array appears to be present. In the Mossbauer spectrum of a tetraorganohexathiatetrastannaadamantane cage system a narrow doublet would be expected as observed for (**28**) (Q.S.= 1.44 mms^{-1}) and (**29**) (Q.S.= 1.40 mms^{-1}). However, in (**30**) a narrow doublet is observed (Q.S.= 0.93 mms^{-1}) as well as the superimposition of a wider doublet (Q.S.= 2.28 mms^{-1}) (figure 41) indicating the presence of an additional species of coordination greater than four.

From these results it can be seen that the quadrupole splitting value for the narrow doublet is small compared to the values normally observed for a tetraorganohexathiatetrastannaadamantane. The reason for this is unclear from the evidence available. For the second wider doublet the observed quadrupole splitting value is comparable with that observed for n-butyldichlorotin hydroxide monohydrate (Q.S.= 2.31 mms^{-1}). Single crystal X-ray diffraction studies by Holmes et al.[201] have shown that a dimeric hydroxyl bridged structure is present in this compound. This result would seem to suggest that in the solid state, coordination bond formation through oxygen results in the formation of polymeric species which on dissolution are broken down forming monomeric entities. This type of phenomenon was observed by Davies et al.[204] for dimethyldithiastannolane where in the solid state a linear five-coordinate polymer is present, however, in solution the

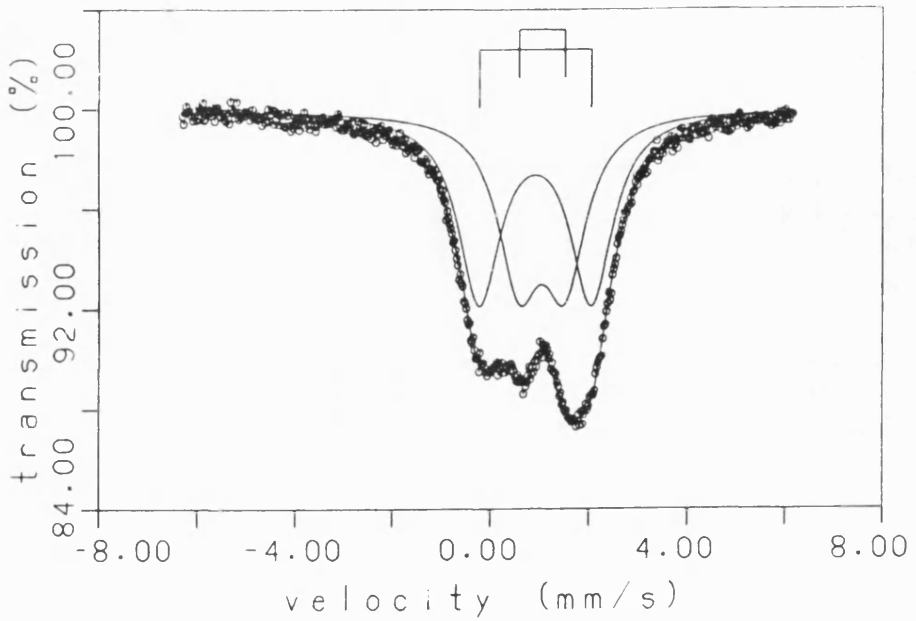

Figure 41: Mossbauer Plot of $\{[nBuSnO_{0.5}S]_4\}_n$ (**30**).

polymeric chain breaks down to give four-coordinate monomeric units. Without X-ray data to clarify the the solid state structure the exact details of the bonding taking place are unclear however, it can be surmised that a system similar to that shown in figure 42 may be present.

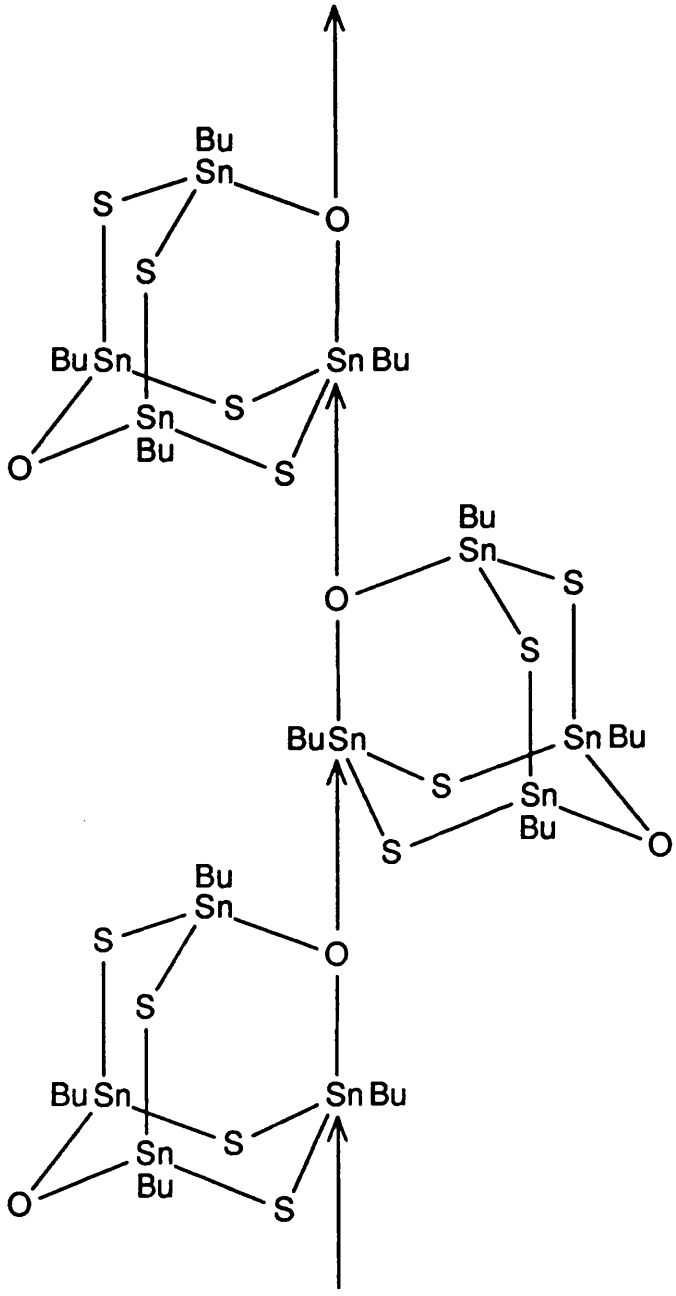

Figure 42: Polymeric Associated Array Postulated for the Solid State Structure of 2,4,6,9-Tetra-n-butyl-1,5-dioxa-3,7,8,10-tetrathia-2,4,6,9-tetrastannaadamantane (30).

3.3 Conclusion.

From the work investigated in this chapter certain conclusions can be drawn from the results obtained. For one synthetic methodology the precursor for the mixed chalcogen product was based around a system incorporating a single oxygen, e.g. a dihalotetraorganodistannoxane. From the subsequent sulphidation reactions, products were prepared where the newly formed sulphur linkages dictated the overall structural properties of the final compound. The structural arrays varied, from discrete monomeric rings for the compounds with bulky organic substituents to weakly associated polymeric/dimeric systems. The former type is exemplified by 2,2,4,4-tetra(2,4,6-tri-i-propyl-phenyl)-1,3-oxathia-2,4-distannetane (**16**) and the latter by 2,2,4,4-tetra-n-butyl-1,3-oxathia-2,4-distannetane monohydrate (**22**) (or its dihydroxy form 1,3-dihydroxy-1,1,3,3-tetra-n-butyldistannathiane). For (**22**) the actual structure has not been confirmed, however, if a dimeric array is present as suggested for the former or an associated polymeric array as theorised for the latter formulations, the degree of association is much reduced in comparison to the analogous di-n-butyltin oxide. The contrasting degree of association is reflected in the relative solubilities of the two compounds. For (**22**) it appears that if a polymeric array is present in the solid state it breaks down upon dissolution into dimeric units as observed in the nmr spectra. In contrast di-n-butyltin oxide is totally insoluble in organic solvents remaining as an amorphous, highly associated polymeric solid.

The second attempted approach was to use a weakly associated precursor containing a fixed number of the heavier chalcogen species e.g. 1,3-dibromo-1,1,3,3-tetra-i-propyldistannathiane (**19**) followed by hydrolysis to generate an associated system. By this route it would seem reasonable to assume that after hydrolysis the formation of oxygen linkages would dictate the structure present in the product. However, preparing the starting materials in this instance proved problematical. In the attempted synthesis of the dihalotetraorgano--distannathianes $(R_2SnX)_2S$, for the i-propyl analogue the compound was prepared and characterised, however a facile disproportionation occurred in solution negating its use in any further syntheses. For the t-butyl analogue an alternative product, 2,2'-spirobi(4,4,6,6-tetra-t-butyl-1,3,5-trithia-2,4,6-tristanninane) (**25**), resulted from the preparation. As a result only very limited progress was attained using this route.

On the basis of these results two future approaches can be postulated to attempt to overcome the problems incurred in the reaction methods detailed so far. The first would be to design oxygen based progenitors of a specific ring/sheet or 'open cage' structure with incorporated active centres suitable for further reaction. A suitable system would be a trihalotriorganotrioxatristanninane ring as in (**31**).

Very little information is known about the second hydrolysis products of monoorganotin trihalides, $RSn(OH)_2Cl$ (equation 87) which can be seen as precursors to compounds like (**31**) above.

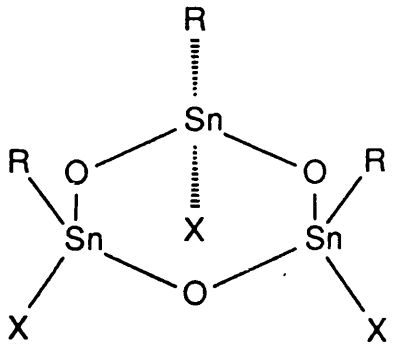

(31)

$$nRSnX_3 + 2nOH^- \rightarrow nRSn(OH)X_2 \rightarrow nRSn(OH)_2X + 2nX^- \quad (87)$$

In the literature Luijten reported that the monoorganohalotin dihydroxides can be formed from the reaction between an organotin trihalide and a stoichiometric amount of a suitable base which on heating condense to form 'glass-like' polymers of the general composition $[RSn(X)O]_n$[233] (equation 88).

$$nRSn(OH)_2X \rightarrow [RSn(X)O]_n + nH_2O \quad (88)$$

Structural details of these compounds are not known but it might be surmised that polymeric sheet arrays analogous to the low hindrance diorganotin oxides are present with inter-sheet halogen bridges. By further reaction of the halogens present in the structure with a range of bifunctional species, bridging of the sheet arrays would occur forming a pillared layer type material.

For the preparation of oligomeric arrays like (31) the use of bulky substituents could be used to limit the degree of association present

in the final product. Based on the use of sterically hindered organic moieties in the formation of oligomeric diorganotin oxides similar substituents could be used in this instance. The use of the bulkier halogens i.e. bromine and iodine as the halogen substituents would also increase steric hindrance in the system restricting polymer formation.

For the hydrolysis of tin halides aqueous base is the usual reagent used. However, with monoorganotin trihalides this route usually yields either the monoorganodichlorotin hydroxide monohydrate or the totally hydrolysed species, the stannoic acid. To control the degree of hydrolysis milder methods would need to be developed. One methodology that could be applied is a route analogous to that used by Honnick and Zuckerman[234] to prepare $Sn(OH)_2$ where trimethyltin hydroxide was used as the hydrolysis reagent. By analogy:

$$RSnCl_3 + R_3MOH \rightarrow RSn(OH)_2Cl + R_3MCl \qquad (89)$$

M = Si, Ge and Sn.

An alternative method for controlling the degree of hydrolysis would be to limit the accessability of the halogen substituents on tin by the use of a sterically hindered hydrolysis reagent. A possible example would be to use a sterically hindered silanol which as well as restricting the interaction with the tin halide system would also resist condensation of the reagent to a siloxane. A second mild method would be the atmospheric hydrolysis of a stannyl bis(amide) prepared from the stoichiometric reaction of lithium dimethylamide and a

monoorganotin trihalide (equations 90 and 91).

$$RSnX_3 + 2LiNMe_2 \rightarrow RSn(NMe_2)_2X + 2LiX \quad (90)$$

$$RSn(NMe_2)_2X \xrightarrow{air} RSn(OH)_2X + 2HNMe_2\uparrow \quad (91)$$

Having obtained the dihydroxide product a condensation reaction could then occur to yield the required sheet/ring array (**31**). A foreseeable problem in the preparation of these compounds is the formation of mixed isomers. Assuming the formation of a trimeric ring structure (**31**) the product can be isolated in two isomeric forms. In one instance all the halogens align on one side of the ring, however, a second isomer can also occur where both halogen and organic groups are present on one face of the ring.

Advances in the second approach for the attempted synthesis of cage systems would require the preparation of a more stable sulphur-based progenitor than the $[R_2SnX]_2S$ compounds described in this thesis. A suitable example still incorporating active halogen sites for further syntheses is (**32**). A possible precursor for (**32**) is a tetraorgano-hexathiatetrastannadamantane $(RSnS_{1.5})_4$ (chapter three section 3.2.6). A plausible route to (**32**) can be hypothesised by the use of a stoichiometric halogen cleavage of one of the tin-sulphur bonds present in the adamantane cage structure resulting in a partial cage opening (equation 92).

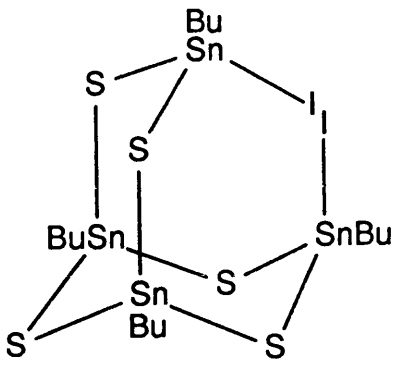

(32)

$$(RSnS_{1.5})_4 + I_2 \rightarrow [(RSnS_{1.5})_2(RSnSI)_2] + S \qquad (92)$$

(32)

A precedent for the above reaction was observed during research carried out in this thesis. In the attempted phenyl group cleavage from diphenyldi(Tsi)dithiadistannetane (12) using iodine the impure product obtained, although not fully characterised, appeared to be the ring cleaved phenyl(Tsi)tin diiodide as opposed to the expected diiododi(Tsi)dithiadistannetane (equation 93).

$$[Ph(Tsi)SnS]_2 + 2I_2 \rightarrow 2Ph(Tsi)SnI_2 + 2S \qquad (93)$$

Having synthesised the object precursor (32) controlled hydrolysis of the halide groups using similar reagents to those employed in the preparation of (31) could be applied to prepare oxygen linked cage systems. As with (31), in addition to hydrolysis, other bifunctional

reagents could be used to link the systems together enabling manipulation of the cavity size present in the subsequent oligomeric array to take place.

3.4 Experimental.

2,2,4,4,6,6-Hexa-n-butyl-1,3,5-trithia-2,4,6-tristanninane (**13**).

A slurry of di-n-butyltin dichloride (10g, 0.033 mole) and sodium sulphide nonahydrate (8.58g, based on a 30% Na_2S content, 0.033 mole) in ethanol (400ml) was heated at reflux over a 48 hr. period. After cooling, *in vacuo* solvent removal yielded an off-white solid. Organic solvent extraction of the solid using boiling toluene followed by *in vacuo* solvent removal yielded a light green oil which solidified on standing at room temperature. (5.9g, 68%)

I.R. [(cm^{-1}) liquid film]: 2960; 2930; 2880; 2860; 1465; 1420; 1380; 1180; 1155; 1080; 1050; 1025; 965; 880; 700; 680; 605; 435; 375; 335.

^1H NMR [δ(ppm) $CDCl_3$ solution]: 0.87 [t,6H,$CH_3(CH_2)_3$]; 1.37 [m,8H, $CH_3(CH_2)_3$]; 1.64 [m,4H,$CH_3(CH_2)_3$].

^{13}C NMR [δ(ppm) $CDCl_3$ solution]: 13.43 [$CH_3(CH_2)_3$]; 23.45 [$CH_3(CH_2)_2CH_2$]; 26.47 [$CH_3CH_2(CH_2)_2$]; 27.99 [$CH_3CH_2CH_2CH_2$]; ^1J[$CH_3(CH_2)_2{}^{13}CH_2$-$^{117,119}Sn$] 370.2, 387.8 Hz; ^2J[$CH_3CH_2{}^{13}CH_2CH_2$-$^{117,119}Sn$] 24.2 Hz (unresolved); ^3J[$CH_3{}^{13}CH_2(CH_2)_2$-$^{117,119}Sn$] 77.1 Hz (unresolved).

^{119}Sn NMR [δ(ppm) $CDCl_3$ solution]: 127.9; ^2J[^{117}SnS-^{119}Sn] 161.7 Hz.

^{119m}Sn Mossbauer (mms^{-1}): I.S.=1.42; Q.S.=1.96.

Analysis (%): Found C 36.40; H 7.22; Calculated for $C_{24}H_{54}S_3Sn_3$: C 36.26; H 6.85.

2,2,4,4-Tetra-t-butyl-1,3-dithia-2,4-distannetane (**10**).

The preparation of (**10**) followed the same synthetic route as for

2,2,4,4,6,6-hexa-n-butyl-1,3,5-trithia-2,4,6-tristanninane (**13**). The impure solid was recrystallised from ethanol/toluene yielding colourless needles. (1.9g, 44%), m.p. 168-172°C.

I.R. [(cm^{-1}) KBr disc]: 2960; 2925; 2860; 1465; 1395; 1365; 1165; 1020; 950; 810; 395; 355; 320.

^{1}H NMR [δ(ppm) $C_6D_5CD_3$ solution]: 1.25 [s,18H,$(CH_3)_3C$]; ^{3}J[$(C^1H_3)_3C$-^{117,119}Sn] 89.0 Hz (unresolved).

^{13}C NMR [δ(ppm) $C_6D_5CD_3$ solution]: 30.16 [$(CH_3)_3C$]; 38.86 [$(CH_3)_3C$].

^{119}Sn NMR [δ(ppm) $C_6D_5CD_3$ solution]: 121.3.

^{119m}Sn Mossbauer (mms^{-1}): I.S.=1.62; Q.S.=1.95.

Analysis (%): Found C 35.10; H 6.78; Calculated for $C_{16}H_{36}S_2Sn_2$: C 36.26; H 6.85.

2,2,4,4,6,6-Hexa-i-propyl-1,3,5-trithia-2,4,6-tristanninane (**14**). The preparation of (**14**) followed the same synthetic route as for 2,2,4,4,6,6-hexa-n-butyl-1,3,5-trithia-2,4,6-tristanninane (**13**). After extraction of the product into toluene and *in vacuo* solvent removal a colourless oil remained. Trituration of the oil with acetonitrile yielded a partially crystalline solid. (5.6g, 84%)

I.R. [(cm^{-1}) KBr disc]: 2960; 2940; 2870; 1460; 1385; 1370; 1200; 1160; 1090; 990; 925; 875; 520; 495; 375; 335.

^{1}H NMR [δ(ppm) $CDCl_3$ solution]: 1.39 [d,12H,$(CH_3)_2CH$]; 1.90 [m,2H, $(CH_3)_2CH$]; ^{3}J[$(C^1H_3)_2CH$-^{117,119}Sn] 97.5, 111.9 Hz.

^{13}C NMR [δ(ppm) $CDCl_3$ solution]: 21.02 [$(CH_3)_2CH$]; 27.18 [$(CH_3)_2CH$]; ^{1}J[$((CH_3)_2{}^{13}CH$-^{117,119}Sn] 383.4, 401.0 Hz; ^{2}J[$(^{13}CH_3)_2CH$-^{117,119}Sn] 13.3 Hz (unresolved).

^{119}Sn NMR [δ(ppm) $CDCl_3$ solution]: 116.4.

^{119m}Sn Mossbauer (mms^{-1}): I.S.=1.51; Q.S.=1.96.

Analysis (%): Found C 30.30; H 6.07; Calculated for $C_{18}H_{42}S_3Sn_3$: C 30.42; H 5.96.

2,2,4,4-Tetra[2,4,6-tri-i-propylphenyl]-1,3-dithia-2,4-distannetane (**11**). 1,2-dibromo-1,1,2,2-tetra(2,4,6-tri-i-propylphenyl)distannane (**1**) (0.43g, 0.00036 mole) and sodium sulphide nonahydrate (0.094g, based on a 30% Na_2S content, 0.00036 mole) were slurried in ethanol (25ml) in an oxygen free environment. The slurried mixture was heated to reflux for 17 hr. after which the initially colourless slurry had turned black. *In vacuo* solvent removal yielded a grey oil. The oil was redissolved in hot acetonitrile (previously nitrogen saturated) and filtered in an atmosphere of nitrogen. On cooling colourless crystals precipitated from solution. m.p. 210-212°C.

I.R. [(cm^{-1}) KBr disc]: 3050; 2970; 2940; 2880; 1600; 1565; 1465; 1420; 1385; 1365; 1270; 1095; 935; 875; 740; 385; 345; 310.

^{1}H NMR [δ(ppm) $CDCl_3$ solution]: 0.93 {d,12H,*o*-[$(CH_3)_2CH]_3C_6H_2$); 1.12 {d,6H,*p*-[$(CH_3)_2CH]_3C_6H_2$); 2.73 {m,2H,*p*-[$(CH_3)_2CH]_3C_6H_2$); 3.42 {m,4H, *o*-[$(CH_3)_2CH]_3C_6H_2$); 6.83 {s,4H,[$(CH_3)_2CH)_3C_6H_2$).

^{13}C NMR [δ(ppm) $CDCl_3$ solution]: 23.90 {*p*-[$(CH_3)_2CH]_3C_6H_2$); 24.75 {*o*-[$(CH_3)_2CH]_3C_6H_2$); 34.19 {*p*-[$(CH_3)_2CH]_3C_6H_2$); 36.52 {*o*-[$(CH_3)_2CH]_3C_6H_2$); 122.02 [*m*-C_6H_2]; 142.07 [*i*-C_6H_2]; 150.27 [*p*-C_6H_2]; 154.36 [*o*-C_6H_2]; ^{3}J{[$(CH_3)_2{}^{13}CH]_3C_6H_2$-^{117,119}Sn) 48.4 Hz (unresolved); ^{3}J[*m*-$^{13}C_6H_2$-^{117,119}Sn] 59.5 Hz (unresolved.

^{119}Sn NMR [δ(ppm) $CDCl_3$ solution]: -48.2; ^{2}J[^{117}*Sn*S-^{119}Sn] 177.0 Hz.

^{119m}Sn Mossbauer (mms^{-1}): I.S.=1.30; Q.S.=1.70.

Analysis (%): Found C 64.40; H 8.44; Calculated for $C_{60}H_{92}S_2Sn_2$: C 64.64; H 8.32.

2,4-Diphenyl-2,4-di[tris(trimethylsilyl)methyl]-1,3-dithia-2,4-distannetane (12). The preparation of (12) followed the same synthetic route as for 2,2,4,4,6,6-hexa-n-butyl-1,3,5-trithia-2,4,6-tristanninnane (13). The impure solid was recrystallised from ethyl acetate/toluene. (0.7g, 45%), m.p. 292-297°C.

I.R. [(cm^{-1}) KBr disc]: 3060; 2960; 2910; 1465; 1435; 1265; 1255; 1075; 1005; 850; 790; 740; 705; 685; 665; 620; 460; 360; 325.

^{1}H NMR [δ(ppm) $CDCl_3$ solution]: 0.12 (s,27H,[$(CH_3)_3Si]_3C$); 7.37 [m,3H, *m,p*-C_6H_5]; 7.88 [q,2H, *o*-C_6H_5].

^{13}C NMR [δ(ppm) $CDCl_3$ solution]: 5.29 ([$(CH_3)_3Si]_3C$); 128.05 [*m*-C_6H_5]; 128.86 [*p*-C_6H_5]; 136.13 [*o*-C_6H_5]; ^3J([$(^{13}CH_3)_3Si]_3C$-^{117,119}Sn) 22.0 Hz (unresolved).

^{119}Sn NMR [δ(ppm) $CDCl_3$ solution]: 41.8; ^2J[^{117}*Sn*S-^{119}Sn] 198.7 Hz.

^{119m}Sn Mossbauer (mms^{-1}): I.S.=1.39; Q.S.=1.69.

Analysis (%): Found C 41.88; H 7.23; Calculated for $C_{32}H_{64}S_2Si_6Sn_2$: C 41.83; H 7.02.

2,2,4,4,6,6-Hexaphenyl-1,3,5-triselena-2,4,6-tristanninane (15). For the preparation of sodium diselenide the preparative method of Klayman and Griffin[216] was used. To a stirred slurry of selenium (4.5g, 0.057 mole) in ethanol (150ml) at 0°C, sodium borohydride (1.44g, 0.038 mole) was added in small portions via a solid addition

tube. Together with a large evolution of hydrogen a dark brick-red coloration occurred in the solution. On completion of addition the solution was allowed to warm to room temperature until the evolution of hydrogen had ceased. Prior to further syntheses the brick-red solution was heated to reflux for 1½ hr. After cooling a solution of diphenyltin dichloride (6.5g, 0.019 mole) in ethanol (50ml) was added dropwise resulting in an immediate decolourisation of solution and the formation of a pale green solid. The solid was filtered off and extracted with hot ethyl acetate. After *in vacuo* solvent removal a yellow solid resulted which was recrystallised from ethyl acetate yielding bright yellow needles. (2.9g, 43%), m.p. 167-168°C.

I.R. [(cm^{-1}) KBr disc]: 3080; 3060; 3040; 1585; 1485; 1440; 1080; 1035; 1010; 740; 705; 455; 280; 260.

^{1}H NMR [δ(ppm) $CDCl_3$ solution]: 7.36 [m,6H, *m,p*-C_6H_5]; [q,4H, *o*-C_6H_5].

^{13}C NMR [δ(ppm) $CDCl_3$ solution]: 128.60 [*m*-C_6H_5]; 129.68 [*p*-C_6H_5]; 135.42 [*o*-C_6H_5]; 139.92 [*i*-C_6H_5]; ^{2}J[*o*-$^{13}C_6H_5$-^{117,119}Sn] 52.9 Hz (unresolved); ^{3}J[*m*-$^{13}C_6H_5$-^{117,119}Sn] 66.1 Hz (unresolved); ^{4}J[*p*-$^{13}C_6H_5$-^{117,119}Sn] 13.4 Hz (unresolved).

^{77}Se NMR [δ(ppm) $CDCl_3$ solution]: -451.0; ^{1}J[^{77}*Se*-^{117,119}Sn] 1260.3, 1318.4 Hz.

^{119}Sn NMR [δ(ppm) $CDCl_3$ solution]: -44.7; ^{2}J[^{117}*Sn*Se-^{119}Sn] 235.0 Hz.

^{119m}Sn Mossbauer (mms^{-1}): I.S.=1.39; Q.S.=1.57.

Analysis (%): Found C 40.40; H 2.91; Calculated for $C_{36}H_{30}Se_3Sn_3$: C 40.96; H 2.86.

1,3-Dichloro-1,1,3,3-tetra-n-butyldistannoxane (**18**). A solution of di-n-butyltin dichloride (25g, 0.082 mole) in diethyl ether (300ml) was added dropwise to a solution of triethylamine (8.31g, 0.082 mole) in ethanol (100ml) at room temperature. On addition a dense white precipitate formed. Stirring was continued for a period of 2 hr. followed by *in vacuo* solvent removal. The crude product was purified using a chloroform/water extraction. The combined organic phase was dried over anhydrous sodium sulphate and after *in vacuo* solvent removal a white solid was obtained. The product was further purified by recrystallisation from ethanol. (17.43g, 38%) m.p. 109-111°C.
I.R. [(cm^{-1}) KBr disc]: 2970; 2940; 2870; 1465; 1420; 1380; 1165; 1090; 1035; 885; 690; 610; 595; 540; 285.

1,1,3,3-Tetra-i-propyl-1,3-dibromodistannoxane (**19**). The preparation of (**19**) followed the same synthetic route as for 1,3-dichloro-1,1,3,3-tetra-n-butyldistannoxane (**18**). The crude product obtained was recrystallised from chloroform/toluene. (18.43g, 57%) m.p. 206-207°C.
I.R. [(cm^{-1}), KBr disc]: 2950; 2900; 2875; 2820; 1460; 1380; 1365; 1200; 1155; 1085; 1000; 930; 875; 595; 510; 480; 415; 295.
^{1}H NMR [δ(ppm) $CDCl_3$ solution]: 1.49 [m,24H,$(CH_3)_2CH$]; 2.39 [m,4H, $(CH_3)_2CH$].
^{13}C NMR [δ(ppm) $CDCl_3$ solution]: 20.08 [$(CH_3)_2CH$]; 21.46 [$(CH_3)_2CH$]; 40.46 [$(CH_3)_2CH$]; $^{1}J[(CH_3)_2{}^{13}CH-{}^{117,119}Sn]$ 524.4 Hz (unresolved); $^{2}J[(^{13}CH_3)_2CH-{}^{117,119}Sn]$ 22.0 and 17.6 Hz (unresolved).
^{119}Sn NMR [δ(ppm) $CDCl_3$ solution]: -92.1; -143.6; $^{2}J[{}^{117}SnO-{}^{119}Sn]$ 100.2 Hz.

^{119m}Sn Mossbauer (mms^{-1}): I.S.=1.52; Q.S.=3.16.

Analysis (%): Found C 24.99; H 5.03; Calculated for $C_{12}H_{28}Br_2Sn_2$: C 24.62; H 4.82.

Mass Spectrum [(m/z) E.I.]: 619 [$(iPr_2SnO)_3$ - iPr]$^+$; 577; 491; 405; 321 [(iPr_2SnBr_2) - iPr]$^+$; 242; 199; 43.

1,3-dichloro-1,3-diphenyl-1,3-di[tris(trimethylsilyl)methyl]-distannoxane (**20**). The preparation of (**20**) followed the same synthetic route as for 1,3-dichloro-1,1,3,3-tetra-n-butyldistannoxane (**18**). Initially no apparent reaction occurred however after a brief induction period a heavy white precipitate formed. After 17 hr. stirring, *in vacuo* solvent removal yielded a white solid. The impure solid was redissolved in ethyl acetate and the inorganic residue removed by filtration. Recrystallisation from ethanol/toluene yielded colourless needle shaped crystals. (1.6g, 68%) m.p. 205-206°C.

I.R. [(cm^{-1}) KBr disc]: 3050; 2960; 2900; 1460; 1430; 1265; 1255; 1070; 1000; 850; 800; 790; 735; 715; 690; 680; 660; 625; 445; 430; 320.

^{1}H NMR [δ(ppm) $CDCl_3$ solution]: 0.39 (s,27H,[$(CH_3)_3Si]_3C$); 7.48 [m,3H, *m,p*-C_6H_5]; 7.80 [m,2H, *o*-C_6H_5]; $^2J[(C^1H_3)_3{-}^{29}Si]$ 6.1 Hz.

^{13}C NMR [δ(ppm) $CDCl_3$ solution]: 4.96 ([$(CH_3)_3Si]_3C$); 129.26 [*m*-C_6H_5]; 130.75 [*p*-C_6H_5]; 134.70 [*o*-C_6H_5]; 135.45 [*i*-C_6H_5]; $^1J[(^{13}CH_3)_3{-}^{29}Si]$ 52.9 Hz; $^3J([(^{13}CH_3)_3Si]_3C{-}^{117,119}Sn)$ 26.1 Hz (unresolved); $^2J[o{-}^{13}C_6H_5{-}^{117,119}Sn]$ 61.7 Hz (unresolved); $^3J[m{-}^{13}C_6H_5{-}^{117,119}Sn]$ 81.6 Hz (unresolved).

^{119}Sn NMR [δ(ppm) $CDCl_3$ solution]: 17.1.

^{119m}Sn Mossbauer (mms^{-1}): I.S.=1.21; Q.S.=2.18.

Analysis (%): Found C 40.87; H 7.00; Calculated for $C_{32}H_{64}Cl_2OSi_6Sn_2$: C 40.82; H 6.85.

Di-t-butylchlorotin Hydroxide. The preparation of di-t-butylchlorotin hydroxide followed the same synthetic route as for 1,3-dichloro-1,1,3,3-tetra-n-butyl-distannoxane (**18**). After 17 hr. stirring *in vacuo* solvent removal yielded a white solid. The impure solid was redissolved in boiling toluene and the inorganic residue filtered off. On cooling colourless needle shaped crystals formed from the toluene solution. (1.6g, 34%) m.p. 125-127°C.

I.R. [(cm^{-1}) KBr disc]: 3460; 2980; 2960; 2870; 1860; 1475; 1460; 1400; 1375; 1170; 1025; 975; 815; 535; 500; 405; 365; 290.

^{1}H NMR [δ(ppm) $CDCl_3$ solution]: 1.41 [s,18H,$(CH_3)_3C$]; ^3J[$(C'H_3)_3C$] 104.8 Hz (unresolved).

^{13}C NMR [δ(ppm) $CDCl_3$ solution]: 29.58 [$(CH_3)_3C$]; 42.10 [$(CH_3)_3C$].

^{119}Sn NMR [δ(ppm) $CDCl_3$ solution]: -31.6.

^{119m}Sn Mossbauer (mms^{-1}): I.S.=1.45; Q.S.=3.01.

Analysis (%): Found C 33.90; H 6.99; Calculated for $C_8H_{19}ClOSn$: C 33.67; H 6.71.

2,2,4,4-Tetra-n-butyl-1,3-oxathia-2,4-distannetane Monohydrate (**22**). A solution of sodium sulphide nonahydrate (2.36g, based on a 30% Na_2S content, 0.0091 mole) in water (50ml) was added dropwise to a solution of 1,1,3,3-tetra-n-butyl-1,3-dichloro-1,3-distannoxane (**18**) (5g, 0.0091 mole) in ethanol/toluene (350ml : 150ml) at room temperature.

The mixture was heated to reflux for 72 hr. After cooling *in vacuo* solvent removal yielded an impure white solid. The product was extracted using a toluene/water system followed by drying of the combined organic phases over anhydrous sodium sulphate. *In vacuo* solvent removal yielded a white solid that was further purified by recrystallisation from methanol. (1.18g, 25%), m.p. 95-98°C.

I.R. [(cm^{-1}) KBr disc]: 3460; 2970; 2940; 2880; 2860; 1465; 1420; 1380; 1345; 1185; 1160; 1085; 1030; 970; 890; 875; 690; 645; 580; 405; 370; 295.

^{1}H NMR [δ(ppm) $CDCl_3$ solution]: 0.93 [m,12H,$CH_3(CH_2)_3$]; 1.39 [m,16H, $CH_3(CH_2)_3$]; 1.69 [m,8H,$CH_3(CH_2)_3$].

^{13}C NMR [δ(ppm) $CDCl_3$ solution]: 13.52 and 13.59 [$CH_3(CH_2)_3$]; 25.72, 26.63, 26.82, 27.44 and 27.76 [$CH_3(CH_2)_3$].

^{119}Sn NMR [δ(ppm) $CDCl_3$ solution]: -158.2; $^{2}J[^{117,119}SnX\text{-}^{119}Sn]$ 216.6 Hz (unresolved); -174.6; $^{2}J[^{117,119}SnX\text{-}^{119}Sn]$ 195.3 Hz (unresolved) (for X = O or S).

^{119m}Sn Mossbauer (mms^{-1}): I.S.=1.17; Q.S.=2.78.

Analysis (%): Found C 36.00; H 7.24; Calculated for $C_{16}H_{36}O_2SSn_2$: C 36.12; H 7.20.

2,2,4,4-Tetra-t-butyl-1,3-oxathia-2,4-distannetane Dihydrate (23). The preparation of (23) followed the same synthetic route as for 2,2,4,4-tetra-n-butyl-1,3-oxathia-2,4-distannetane monohydrate (22). The impure solid obtained was recrystallised from ethanol. (0.29g, 24%), m.p. decomposed > 240°C.

I.R. [(cm^{-1}) KBr disc]: 3320; 2980; 2950; 2860; 1475; 1375; 1205;

1170; 1130; 1095; 1055; 1030; 1015; 995; 680; 605; 570; 450; 300.

^{119m}Sn Mossbauer (mms^{-1}): I.S.=1.29; Q.S.=2.71.

Analysis (%): Found C 35.20; H 7.39; Calculated for $C_{16}H_{40}O_3SSn_2$: C 34.95; H 7.46.

2,2,4,4-Tetra-i-propyl-1,3-oxathia-2,4-distannetane Monohydrate (**24**). The preparation of (**24**) followed the same synthetic route as for 2,2,4,4-tetra-n-butyl-1,3-oxathia-2,4-distannetane monohydrate (**22**). Extreme difficulties were encountered in the attempted isolation of the pure compound. Purification was attempted by recrystallisaton from either toluene or acetone and although products were obtained the exact nature of the species was inconsistent.

^{119m}Sn Mossbauer (mms^{-1}): I.S.=1.21; Q.S.=2.66.

The only product isolated from this reaction which was totally characterised was i-propylstannoic acid which was identified from the infra-red and ^{119}Sn nmr spectra.

2,4-Diphenyl-2,4-di[tris(trimethylsilyl)methyl]-1,3-oxathia-2,4-distannetane (**21**). The preparation of (**21**) followed the same synthetic route as for 2,2,4,4-tetra-n-butyl-1,3-oxathia-2,4-distannetane monohydrate (**18**). The impure solid was recrystallised from 60-80 petrol. (0.31g, 65%), m.p. decomposes > 300°C .

I.R. [(cm^{-1}) KBr disc]: 3060; 2980; 2960; 2910; 1485; 1440; 1265; 1260; 1075; 850; 790; 740; 710; 690; 670; 625; 465; 365; 330.

^{1}H NMR [δ(ppm) $CDCl_3$ solution]: 0.11 (s,54H,[$(CH_3)_3Si]_3C$); 7.37 [m,6H, *m,p*-C_6H_5]; 7.88 [m,4H,*o*-C_6H_5]; $^2J[(C'H_3)_3$-$^{29}Si]$ 6.23 Hz.

^{13}C NMR [δ(ppm) $CDCl_3$ solution]: 5.25 {[$(CH_3)_3Si]_3C$}; 128.05 [*m*-C_6H_5]; 128.86 [*p*-C_6H_5]; 136.10 [*o*-C_6H_5].

^{119}Sn NMR [δ(ppm) $CDCl_3$ solution]: 40.7; ^2J[^{117}*Sn*X-^{119}Sn] 125.1 Hz (for X = O or S); ^2J({[$(CH_3)_3$^{29}*Si*]$_3$C-^{119}Sn) 20.6 Hz.

^{119m}Sn Mossbauer (mms^{-1}): I.S.=1.14; Q.S.=1.63.

Analysis (%): Found C 42.20; H 7.25; Calculated for $C_{32}H_{64}OSSi_6Sn_2$: C 42.57; H 7.15.

2,2,4,4-Tetra[2,4,6-tri-i-propylphenyl]-1,3-oxathia-2,4-distannetane (**16**). A solution of sodium sulphide nonahydrate (4.1g, based on a 30% Na_2S content, 0.011 mole) in water (50ml) was added dropwise to a solution of impure 1,2-dichloro-1,1,2,2-tetra(tri-2,4,6-i-propylphenyl)distannane (4.5g, 0.0040 mole) in ethanol/toluene (300ml:150ml) at 40°C. On completion of additon the mixture was heated at reflux for 48 hr. After cooling, *in vacuo* solvent removal yielded a pale yellow solid. The product was extracted using a toluene/water system followed by the drying of the combined organic phases over anhydrous sodium sulphate. *In vacuo* solvent removal yielded an impure white solid. Further purification was achieved by recrystallisation from ethanol/hexane to yield a colourless crystalline material. (1.2g, 27%) m.p. 213-214°C.

I.R. [(cm^{-1}) KBr disc]: 3100; 2970; 2940; 2870; 1595; 1460; 1420; 1375; 1365; 1270; 1175; 1160; 1100; 885; 625; 615; 605; 550; 395; 295; 250.

^1H NMR [δ(ppm) $CDCl_3$ solution]: 1.05 [d,24H,$(CH_3)_2$CH]; 1.09 [s,24H,$(CH_3)_2$CH]; 1.20 [d,24H,$(CH_3)_2$CH]; 2.82 [m,4H,$(CH_3)_2CH$]; 3.36 [m,4H,

$(CH_3)_2CH$]; 3.51 [m,4H,$(CH_3)_2CH$]; 6.93 [s,8H,*m*-C_6H_2];

^4J[*m*-$C_6{}'H_2$-^{117,119}Sn] 28.2 Hz (unresolved).

^{13}C NMR [δ(ppm) $CDCl_3$]: 23.90, 23.97, 24.26, 24.78 and 25.30 [$(CH_3)_2CH$]; 34.28 and 36.55 [$(CH_3)_2CH$]; 121.83 [*m*-C_6H_2]; 142.39 [*i*-C_6H_2]; 150.43 [*p*-C_6H_2]; 154.42 and 154.52 [*o*-C_6H_2]; ^2J[*m*-$^{13}C_6H_2$-^{117,119}Sn] 44.0 Hz (unresolved).

^{119}Sn NMR [δ(ppm) $CDCl_3$ solution]: 11.4; ^2J[^{117}SnX-^{119}Sn] 136.9 Hz (for X = O or S).

^{119m}Sn Mossbauer (mms^{-1}): I.S.=1.20; Q.S.=1.90.

Analysis (%): Found C 65.30; H 8.49; Calculated for $C_{60}H_{92}OSSn_2$: C 65.58; H 8.44.

2,2'-Spirobi(4,4,6,6-tetra-t-butyl-1,3,5-trithia-2,4,6-tristanninane) (**25**). Di-t-butyltin dichloride (1.84g, 0.006 mole) was added to 2,2,4,4-tetra-t-butyl-1,3-dithia-2,4-distannetane (**10**) (1.6g, 0.003 mole) at room temperature. The reaction tube was flushed with nitrogen, cooled to -196°C and a partial vacuum applied prior to sealing. After attaining room temperature the mixture was heated to 180°C for 3 hr. resulting in the formation of a cloudy liquid. After cooling a beige solid remained. The residue was then dissolved in chloroform followed by filtration to remove any insoluble decomposition products. *In vacuo* solvent removal of the filtrate produced an off-white solid which on recrystallisation from 60-80 petrol yielded a highly crystalline product. (1.1g), m.p. 207-208°C. I.R. [(cm^{-1}) KBr disc]: 2980; 2940; 2930; 2860; 2730; 1465; 1370; 1165; 1020; 945; 810; 380; 330.

^{1}H NMR [δ(ppm) $CDCl_3$ solution]: 1.41 [s,72H,$(CH_3)_3C$]; ^3J[$(C^1H_3)_3C$-^{117,119}Sn] 95.1, 99.5 Hz.

^{13}C NMR [δ(ppm) $CDCl_3$ solution]: 30.55 [$(CH_3)_3C$]; 40.19 [$(CH_3)_3C$]; ^1J[$(CH_3)_3{}^{13}C$-^{117,119}Sn] 376.8, 394.4 Hz; ^2J[$(^{13}CH_3)_3C$-^{117,119}Sn] 70.5 Hz (unresolved).

^{119}Sn NMR [δ(ppm) $CDCl_3$ solution]: 66.5 [Sn^aS_4]; ^2J[$^{117,119}Sn^bS$-^{119}Sn] 317.4 Hz (unresolved); ^4J[$^{117,119}Sn^cSSnS$-^{119}Sn] 76.3 Hz (unresolved); 75.9 [Sn^bS_4]; ^2J[$^{117,119}Sn^{a,c}S$-^{119}Sn] 286.8 and 341.8 Hz (unresolved); 84.1 [SnS_4]; ^2J[$^{117,119}SnS$-^{119}Sn] 329.6 Hz (unresolved); 97.0 [tBu_2Sn^c]; 108.1 [tBu_2Sn].

^{119m}Sn Mossbauer (mms^{-1}): [Bu_2Sn] I.S.=1.59; Q.S.=1.96; [SnS_4] I.S.=1.22.

Analysis (%): Found C 31.00; H 6.03; Calculated for $C_{32}H_{72}S_6Sn_5$: C 30.93; H 5.84.

1,3-Dibromo-1,1,3,3-tetra-i-propyldistannathiane (27). The preparation of (27) followed the same synthetic route as for (25). In this instance the sealed tube was heated from room temperature and held at a constant 200°C for ½ hr. On cooling the resultant solid was dissolved in chloroform followed by filtration to remove any insoluble decomposition products. *In vacuo* solvent removal from the filtrate followed by recrystallisation from 40-60 petrol yielded colourless florets. (3.2g, 63%), m.p. 79-80°C.

A second preparation of (27) was undertaken using milder conditions. In this instance the reagents were dissolved in toluene (30ml) and heated to reflux for 1 hr. After cooling *in vacuo* solvent

removal yielded a solid product. Recrystallisation from 40-60 petrol generated the same product as in the previous preparation in approximately the same yield. (3.6g, 59%).

I.R. [(cm^{-1}) KBr disc]: 2970; 2960; 2880; 1465; 1395; 1375; 1200; 1160; 1095; 1010; 935; 875; 500; 410; 370; 330.

In the solution state nmr investigations it was concluded that a disproportionation reaction was taking place. This resulted in multiple peaks being observed in the spectra and a general overall decrease in the resolution. This was particularly noticeable in the ^1H nmr spectrum where the $^3J[(C^1H_3)_2CH-^{119}Sn]$ were observed but due to poor resolution no values were obtained.

^1H NMR [δ(ppm) $CDCl_3$ solution]: 1.43 [d,24H,$(CH_3)_2CH$]; 2.18 [m,4H, $(CH_3)_2CH$].

^{13}C NMR [δ(ppm) $CDCl_3$ solution]: 20.66 {[$(CH_3)_2CH$] [iPr_2SnBr_2 and $(iPr_2SnBr)_2S$]}; 21.02 {[$(CH_3)_2CH$] $(iPr_2SnS)_3$}; 27.15 {[$(CH_3)_2CH$] $(iPr_2SnS)_3$}; 30.49 {[$(CH_3)_2CH$] $(iPr_2SnBr)_2S$]; 31.30 {[$(CH_3)_2CH$] iPr_2SnBr_2).

^{119}Sn NMR [δ(ppm) $CDCl_3$ solution]: 94.3 (iPr_2SnBr_2); 116.3 [$(iPr_2SnS)_3$]; 128.2 [$(iPr_2SnBr)_2S$].

^{119m}Sn Mossbauer (mms^{-1}): I.S.=1.68; Q.S.=2.94.

Analysis (%): Found C 23.50; H 4.58; Calculated for $C_{12}H_{28}Br_2SSn_2$: C 23.96; H 4.69.

Attempted Preparation of 2,2-Di-t-butyl-4,4-di-i-propyl-1,3-oxathia-2,4-distannetane. Di-t-butyltin 'dihydroxide' (0.30g, 0.0011 mole) and 2,2,4,4,6,6-hexa-i-propyl-1,3,5-trithia-2,4,6-tristanninane (**14**)

(0.27g, 0.00036 mole) were heated at reflux in benzene (30ml) for a period of 17 hr. On cooling a white solid precipitated from solution. The solid was removed by filtration and the filtrate reduced in volume by *in vacuo* solvent removal to yield a white solid.

From the infra-red spectra of the two solids it would appear that the benzene soluble product is 2,2,4,4-tetra-t-butyl-1,3-dithia-2,4-distannetane (**10**) and the benzene insoluble product an impure sample of di-i-propyltin oxide.

2,4,6,9-Tetra-n-butyl-1,3,5,7,8,10-hexathia-2,4,6,9-tetrastanna-adamantane (**28**). A solution of sodium sulphide nonahydrate (2.1g, based on a 30% Na_2S content, 0.027 mole) in water (50ml) was added dropwise to n-butyltin trichloride (5g, 0.018 mole) at 0°C. On addition a white emulsion formed. On completion of addition the mixture was warmed to room temperature and stirring continued for 48 hr. Extraction with chloroform followed by drying over anhydrous sodium sulphate and *in vacuo* solvent removal yielded a white solid. Recrystallisation from ethyl acetate/60-80 petrol yielded a white powdery solid. (2.1g, 55%)

I.R. [(cm^{-1}) KBr disc]: 2960; 2930; 2870; 1460; 1380; 1250; 1175; 1145; 1080; 875; 715; 680; 380; 350.

^{1}H NMR [δ(ppm) $CDCl_3$ solution]: 0.90 [t,3H,$CH_3(CH_2)_3$]; 1.43 [m,2H, $CH_3(CH_2)_3$]; 1.77 [m,4H,$CH_3(CH_2)_3$].

^{13}C NMR [δ(ppm) $CDCl_3$ solution]: 13.47 [$CH_3(CH_2)_3$]; 25.89 [$CH_3(CH_2)_2CH_2$]; 26.96 [$CH_3CH_2CH_2CH_2$]; 29.88 [$CH_3CH_2(CH_2)_2$]; ^2J[$CH_3CH_2{}^{13}CH_2CH_2$-^{117,119}Sn] 39.6 Hz (unresolved).

^{119}Sn NMR [δ(ppm) $CDCl_3$ solution]: 142.6; $^{2}J[^{117}Sn-^{119}Sn]$ 201.8 Hz.

^{119m}Sn Mossbauer (mms^{-1}): I.S.=1.38; Q.S.=1.44.

Analysis (%): Found C 21.53; H 4.21; Calculated for $C_{16}H_{36}S_6Sn_4$: C 21.46; H 4.05.

2,4,6,9-Tetra-i-propyl-1,3,5,7,8,10-hexathia-2,4,6,9-tetrastanna-adamantane (29). A solution of sodium sulphide nonoahydrate (14.6g, based on a 30% Na_2S content, 0.057 mole) in water (100ml) was added dropwise to a solution of i-propyltin tribromide (15g, 0.037 mole) in ethanol/toluene (1200ml:600ml) at 40°C. On completion of addition the mixture was heated to reflux for a period of 48 hr. After cooling *in vacuo* solvent removal yielded an impure white solid. The crude product was purified firstly by extracting with an ethyl acetate/water system. The combined ethyl acetate washings were dried over anhydrous sodium sulphate followed by *in vacuo* solvent removal yielding a white solid. The product was recrystallised from either toluene or ethyl acetate to give colourless highly crystalline prisms. (4.9g, 63%), decomposes > 150°C.

I.R. [(cm^{-1}) KBr disc]: 2960; 2940; 2860; 1460; 1385; 1365; 1200; 1155; 1005; 510; 380; 350.

^{1}H NMR [δ(ppm) $CDCl_3$ solution]: 1.46 [d,6H,$(CH_3)_2CH$]; 2.22 [m,1H, $(CH_3)CH$]; $^{3}J[(CH_3)_2CH-^{117,119}Sn]$ 144.7, 159.4 Hz.

^{13}C NMR [δ(ppm) $CDCl_3$ solution]: 19.56 [$(CH_3)_2CH$]; 34.15 [$(CH_3)_2CH$]; $^{2}J[(^{13}CH_3)_2CH-^{117,119}Sn]$ 26.4 Hz (unresolved).

^{119}Sn NMR [δ(ppm) $CDCl_3$ solution]: 152.3.

^{119m}Sn Mossbauer (mms^{-1}): I.S.=1.46; Q.S.=1.40.

Analysis (%): Found C 17.47; H 3.53; Calculated for $C_{12}H_{26}S_6Sn_4$: C 17.17; H 3.36.

2,4,6,9-Tetra-n-butyl-1,5-dioxa-3,7,8,10-tetrathia-2,4,6,9-tetra-stannaadamantane (**30**). A slurry of n-butyldichlorotin hydroxide monohydrate[201,235] (1.27g, 0.0045 mole), sodium sulphide nonahydrate (1.17g, based on a 30% Na_2S content, 0.0045 mole) and ethanol (100ml) was heated to reflux for 36 hr. On cooling *in vacuo* solvent removal yielded an impure white solid. Recrystallisation from ethyl acetate/ toluene yielded a white powdery solid. (0.79g, 81%), decomposes > 170°C.

I.R. [(cm^{-1}) KBr disc]: 2960; 2930; 2870; 1460; 1380; 1245; 1175; 1145; 1080; 1020; 875; 710; 680; 630; 570; 520; 380; 340.

^{1}H NMR [δ(ppm) $CDCl_3$ solution]: 0.86 [t,3H,$CH_3(CH_2)_3$]; 1.37 [m,2H, $CH_3(CH_2)_3$]; 1.73 [m, 4H, $CH_3(CH_2)_3$].

^{13}C NMR [δ(ppm) $CDCl_3$ solution]: 13.49 [$CH_3(CH_2)_3$]; 25.88 [$CH_3(CH_2)_2CH_2$]; 26.99 [$CH_3CH_2CH_2CH_2$]; 29.90 [$CH_3CH_2(CH_2)_2$].

^{119}Sn NMR [δ(ppm) $CDCl_3$ solution]: 142.9; ^2J[^{117}*Sn*X-^{119}Sn] 201.4 Hz (for X = S or O).

^{119m}Sn Mossbauer (mms^{-1}): I.S.=0.90; Q.S.=2.28 and I.S.=1.04; Q.S.=0.93.

Analysis (%): Found C 22.28; H 4.36; Calculated for $C_{16}H_{36}O_2S_4Sn_4$: C 22.26; H 4.20.

CHAPTER 4.

SYNTHETIC APPROACHES FOR THE PREPARATION OF STANNYLBORONATES.

4.1 Introduction.

So far in this thesis the preparations of stannyl ring and cage structures have been discussed. The strategies involved in the syntheses were designed to manipulate the type of structures obtained by the use of either steric hindrance or by using heteroatom substituents of differing associative properties. In this chapter an attempt to incorporate organotin units into the ring and cage systems of compounds of other elements is described.

The classes of compounds chosen were the borates and boronates. For the borates, two different geometries are found at boron with both trigonal (BO_3) and tetrahedral (BO_4) species existing. In borate structural chemistry examples of both exclusive and mixed geometry arrays are found. For the trigonal units examples of cyclic [$(B_3O_6)^{3-}$ (**XIV**)], chain {[$(BO_2)^-]_n$ (**XV**)) and three-dimensional (B_2O_3) structures are available. Examples of tetrahedral units are known in chain {$Mg[B_2O(OH)_6]$ (**XVI**)), cyclic {$Na_2[B_2(O_2)_2(OH)_4].6H_2O$ (**XVII**)) and three-dimensional polynuclear ($Zn_4B_6O_{13}$) arrays. For the mixed tetrahedral/trigonal arrays similarly examples of ring [$CaB_3O_3(OH)_5.H_2O$ (**XVIII**)] and cage {$Na_2[B_4O_5(OH)_4].8H_2O$ (**XIX**)) structures are known. For the monoorganoboronates the structural types

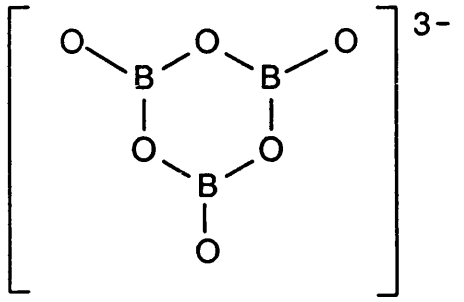

(XIV)

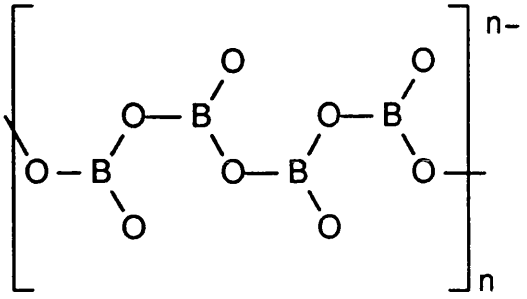

(XV)

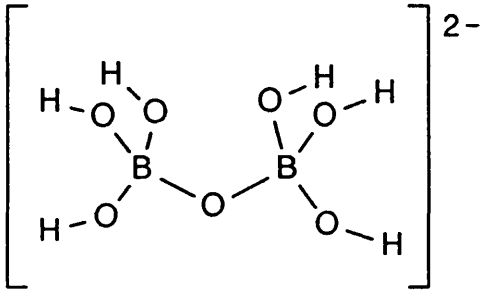

(XVI)

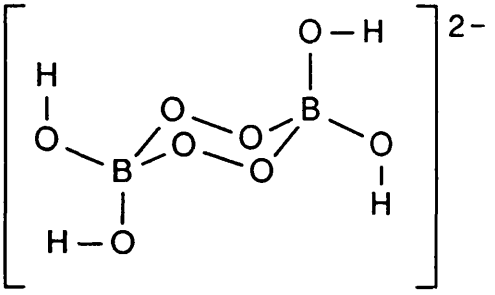

(XVII)

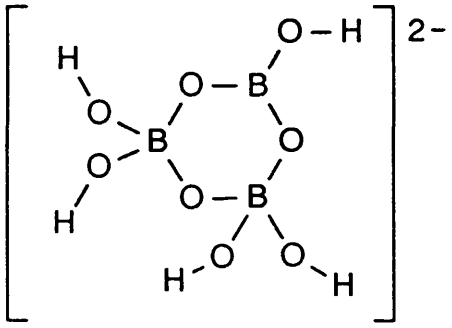

(XVIII)

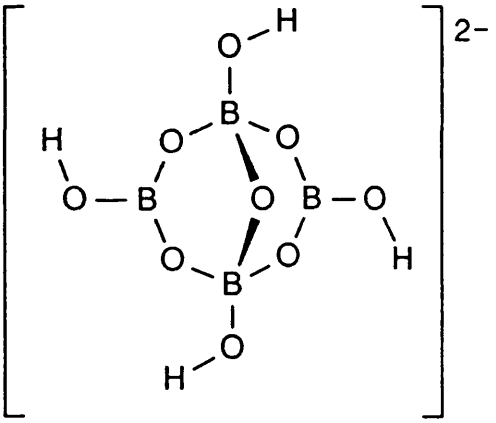

(XIX)

are restricted to either monomeric units for the boronic acids or trimeric ring arrays that occur on dehydration in the formation of oxaborinanes. By reaction of a ring or cage borate or boronate with an organotin unit it was hoped that the tin would be incorporated into the array.

In the literature only a limited amount of work has been reported on the investigation of organometallic borates.[236-239] Most of the examples cited are organosiloxy derived compounds although to a lesser extent organogermoxy and organostannoxy analogues are known. This observation, especially in the latter instance would seem surprising due to the extensive applications of both tin and boron compounds in the glass industry.[240-244]

Some of the more common methods used for the synthesis of these compounds are given in equations 93 to 103.

$$BX_3 + 3R_3SiOH + 3C_5H_5N \rightarrow (R_3SiO)_3B + 3C_5H_5NHX \quad (93)$$

$$BX_3 + 3R_3SiONa \rightarrow (R_3SiO)_3B + 3NaX \quad (94)$$

$$H_3BO_3 + 3Et_3GeH \rightarrow (Et_3GeO)_3B + 3H_2 \quad (95)$$

$$2H_3BO_3 + 3R_2SiCl_2 \rightarrow [B_2(OSiR_2O)_3] + 6HCl \quad (96)$$

$$H_3BO_3 + 3R_3MOH \rightarrow (R_3MO)_3B + 3H_2O \quad (97)$$

M = Si and Sn.

$$RB(OH)_2 + 2Me_3SiOH \rightarrow RB(OSiMe_3)_2 + 2H_2O \quad (98)$$

$$2H_3BO_3 + 3(R_3M)_2O \rightarrow 2(R_3MO)_3B + 3H_2O \quad (99)$$

M = Ge and Sn.

$$3B_2O_3 + 3(R_3M)_2O \rightarrow 2(OBOMR_3)_3 \quad (100)$$

M = Ge and Sn.

$$RBOH + EtOM(nBu)_3 \rightarrow RBOM(nBu)_3 + EtOH \quad (101)$$

R = -[O(CMe$_2$CH$_2$CHMe)O]-

M = Ge and Sn.

$$H_3BO_3 + 3R_3SiO_2CCH_3 \rightarrow (R_3SiO)_3B + 3CH_3CO(OH) \quad (102)$$

$$B(OR)_3 + nBu_3SnO_2CCH_3 \rightarrow (nBu_3SnO)_nB(OR)_{3-n} + CH_3CO(OR) \quad (103)$$

for n = 1 and 2.

As can be seen, a selection of methods are available for the inclusion of group IV metals into boroxy type species. So far the work reported has mainly dealt with the attempted formation of novel polymeric species capable of mimicking and possibly enhancing the properties of the currently known siloxane systems, resulting in most of the cited examples being siloxy derivatives. One known example of a crystalline cyclic boroxy group IV metal compound is 3,3,7,7-tetra-t-butyl-1-fluoro-5,5-dimethyl-cyclo-1-bora-3,5,7-trisila-2,4,6,8-tetraoxan (33) reported by Graalmann et al.[245]

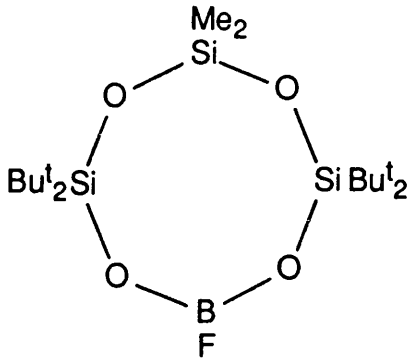

(33)

In the research detailed in this chapter the object has been to deviate from the polymeric type systems and to try to design synthetic routes for the preparation of discrete crystalline stannylboronates and related compounds, by utilising sterically hindered substituents on either tin or on both boron and tin. From these compounds it was hoped that interesting structural modifications might occur where tin and boron were incorporated into ring or cage systems.

4.2 Results and Discussion.

4.2.1 Condensation Reactions of Diorganotin Oxides and Organoboronic Acids.

The first synthetic methodology attempted in this work was similar to the reaction in equation 98 where instead of trimethylsilanol, a

diorganotin oxide was reacted in differing stoichiometries with an organoboronic acid in benzene and heated to reflux (equations 104 and 105).

$$nR_2SnO + nR'B(OH)_2 \rightarrow (R_2Sn[O(BR')O])_n + nH_2O \quad (104)$$

R = t-butyl, i-propyl, methyl and phenyl.

R' = phenyl and 2,4,6-trimethylphenyl (mesityl).

$$nR_2SnO + 2nR'B(OH)_2 \rightarrow (R_2Sn[O(BR')O]_2)_n + 2nH_2O \quad (105)$$

R = t-butyl.

R' = phenyl.

In the di-t-butyltin oxide instance good solubility was attained in hot benzene unlike the nearly insoluble methyl, i-propyl and phenyl substituted diorganotin oxides. The contrasting solubilities result from the different structures present in diorganotin oxides. For di-t-butyltin oxide the single crystal X-ray structure determination carried out by Puff et al.[151] reveals a discrete, trimeric, six-membered ring array which contrasts sharply with the highly associated polymeric systems present in the reduced steric hindrance examples. For the reactions using di-t-butyltin oxide, solid products were isolated and their structures investigated. For the other three tin oxides it would seem likely that their insolubility in benzene resulted in little if any reaction taking place and hence only low yields of impure materials were obtained. Due to the limited data available, no further comment will be made on these reactions.

For the reactions between di-t-butyltin oxide and either mesityl or phenylboronic acid, two products were obtained independent of the reaction stoichiometry (equation 106).

$$(tBu_2SnO)_3 + 3RB(OH)_2 \rightarrow [(34), (35)] + [(37), (38)] \quad (106)$$

[(34), (35)] = $tBu_2Sn[OB(R)(OH)]_2$ for R = phenyl and mesityl.

[(37), (38)] = $\{tBu_2Sn(OH)_2[(tBu_2SnO)_2OBR]\}$ for R = phenyl and mesityl.

Both (34) and (35) were isolated as highly crystalline solids. For the phenylboronic acid derived product a single crystal X-ray structure determination was carried out. The structure obtained for 3,3-di-t-butyl-1,5-dihydroxy-1,5-diphenyl-2,4-dioxa-3-stanna-1,5-diboronate (34) is a hydrogen-bonded, helical, polymeric system as can be seen in the ORTEP and PLUTO plots of the crystal structure given in figures 43 to 46. Selected bond lengths and angles are given in table 20 and full crystal data is available in Appendix VIII. The crystal sample used contained two independent molecules per asymmetric unit and monoclinic geometry in the unit cell with a $P2_1$ space group and c the unique axis.

The asymmetric unit of (34) contains two independent molecules with essentially the same structural features common to both. From the ORTEP plot (figure 43) it can be seen that a distorted *cis*-R_2SnX_3 five-coordinate geometry is accorded to tin. In the structure two phenylboronate units with different bonding characteristics are attached to tin. For one unit monodentate bonding is seen where the

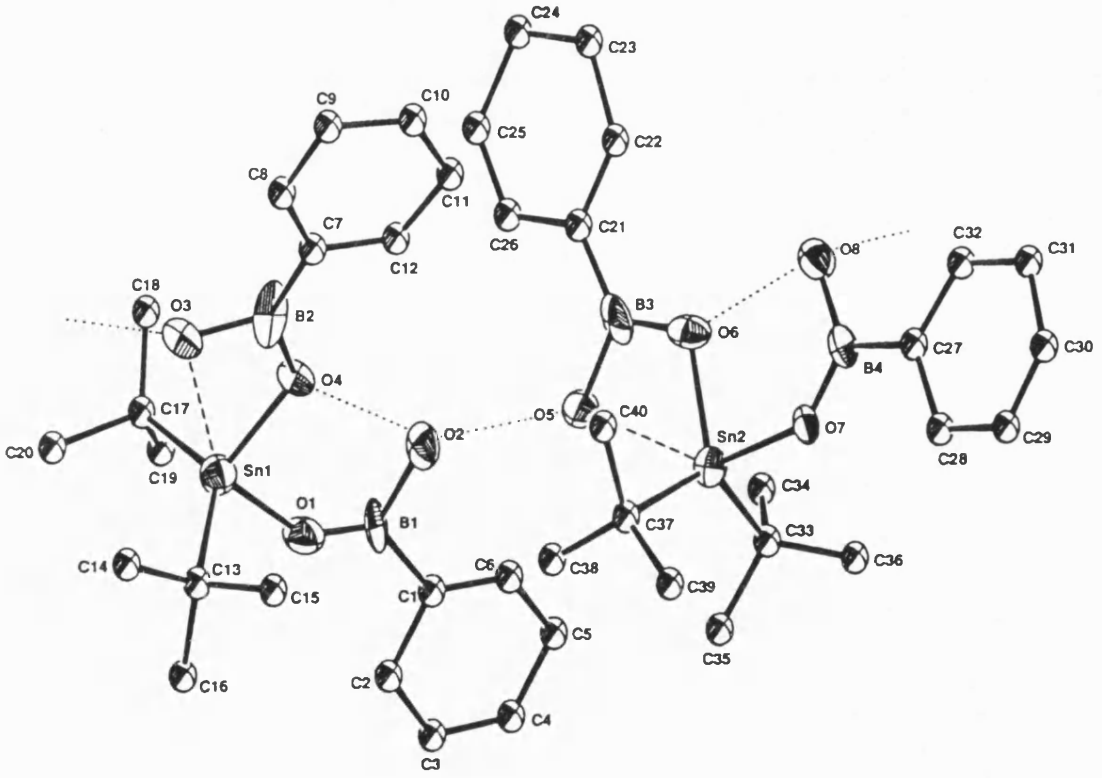

Figure 43: ORTEP Plot of 3,3-Di-t-butyl-1,5-dihydroxy-1,5-diphenyl-2,4-dioxa-3-stanna-1,5-diboronate (**34**). Hydrogen Bonding in the Molecule is Indicated by the Dotted Lines. Intramolecular Coordination Bonding is Represented by the Dashed Lines.

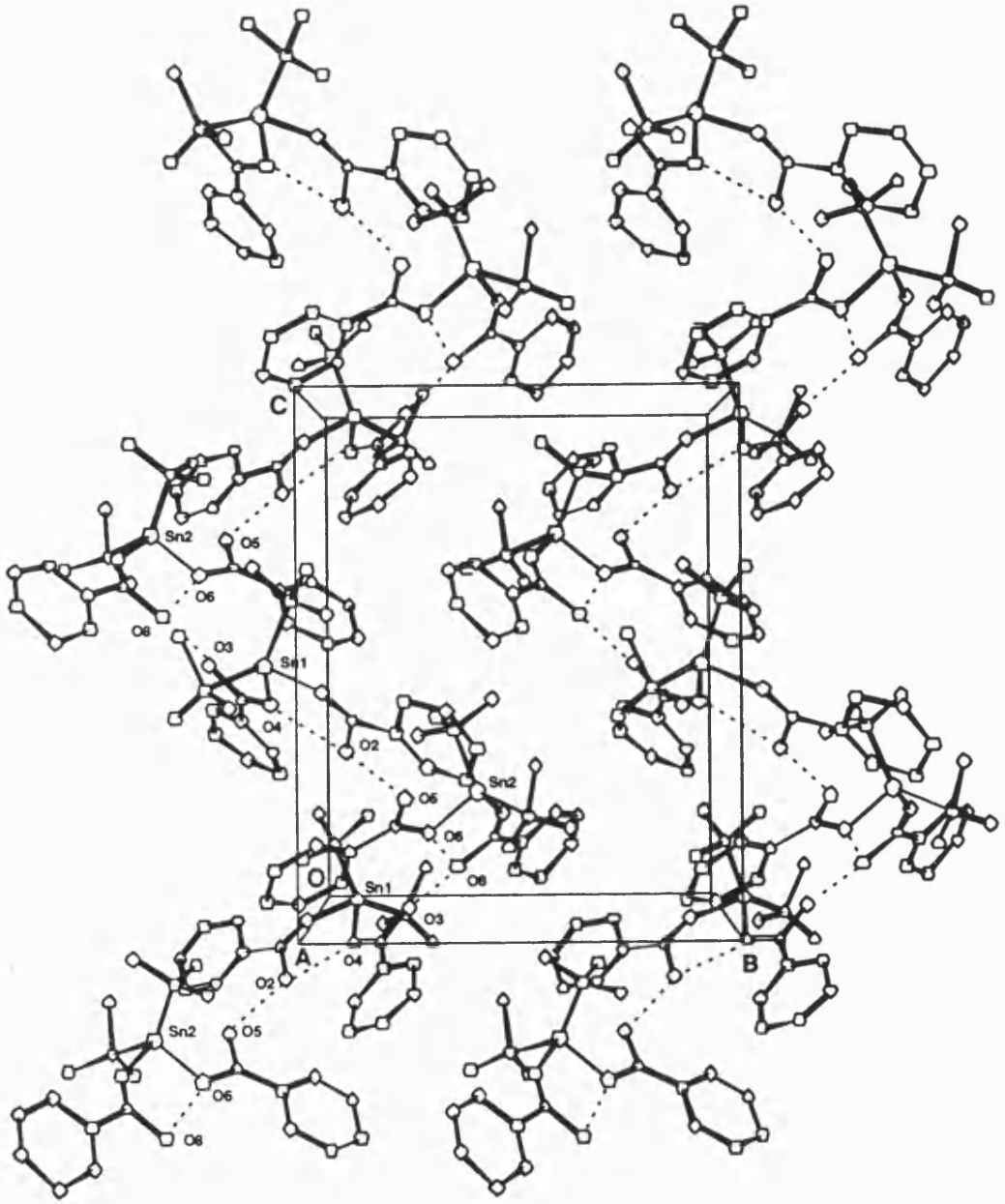

Figure 44: PLUTO Plot of 3,3-Di-t-butyl-1,5-dihydroxy-1,5-diphenyl-2,4-dioxa-3-stanna-1,5-diboronate (**34**) Viewed Down the x-axis Showing the Hydrogen-Bonding Present in the Helical Chain Structure. Hydrogen-Bonding is Indicated by the Dotted Lines.

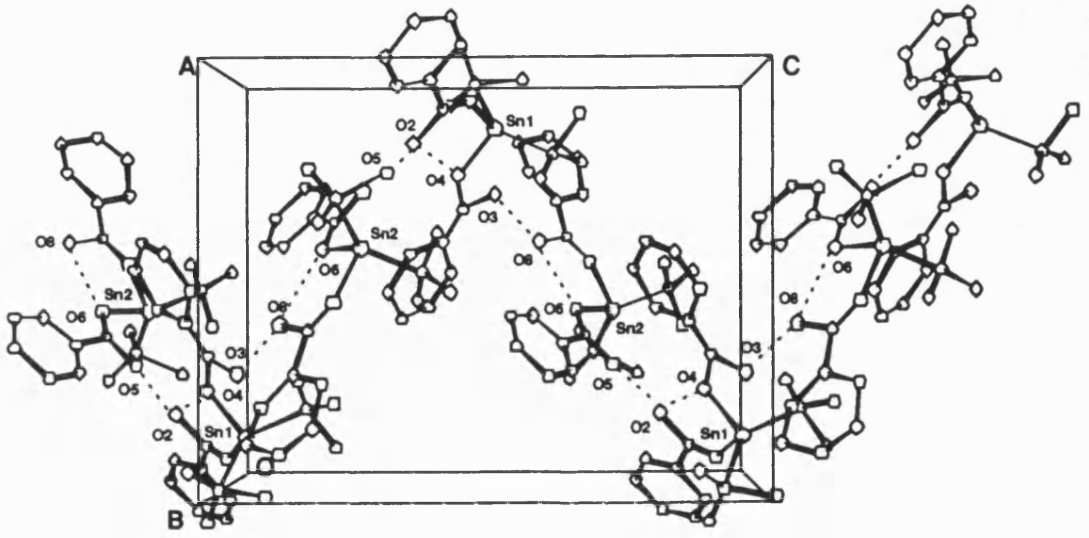

Figure 45: PLUTO Plot of 3,3-Di-t-butyl-1,5-dihydroxy-1,5-diphenyl-2,4-dioxa-3-stanna-1,5-diboronate (**34**) Viewed Down the y-axis Showing the Hydrogen-Bonding Present in the Helical Chain Structure. Hydrogen-Bonding is Indicated by the Dotted Lines.

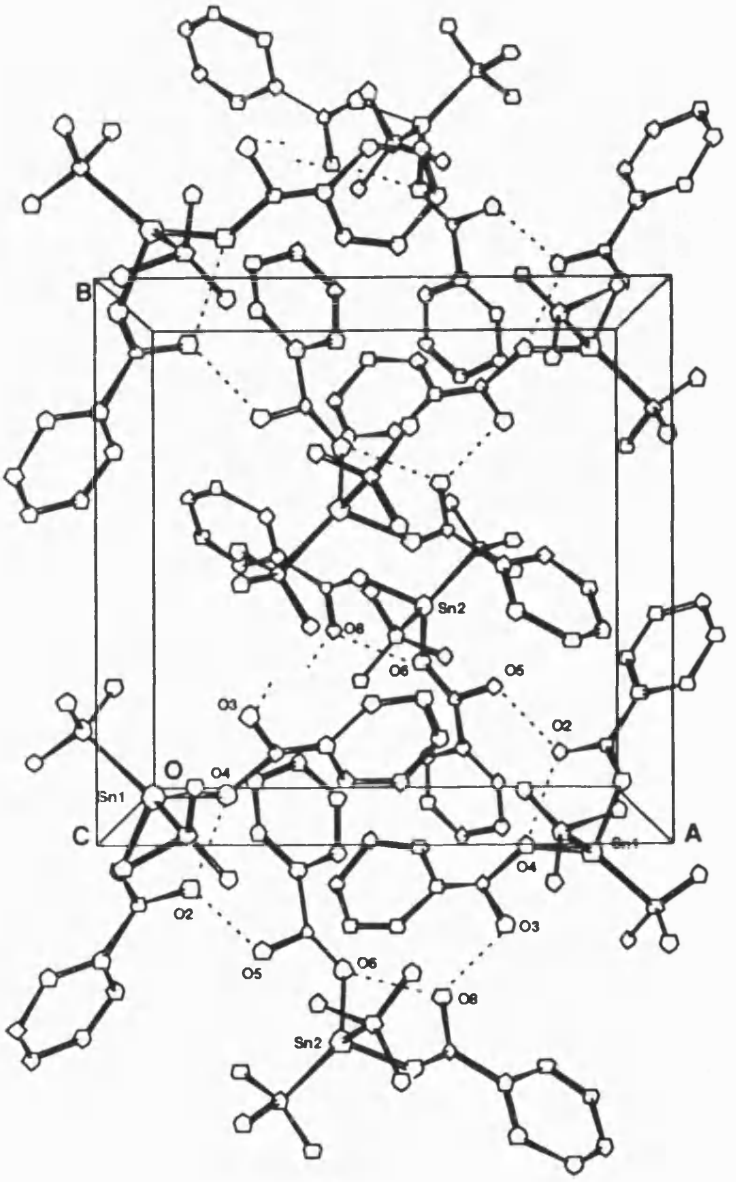

Figure 46: PLUTO Plot of 3,3-Di-t-butyl-1,5-dihydroxy-1,5-diphenyl-2,4-dioxa-3-stanna-1,5-diboronate (**34**) Viewed Down the z-axis Showing the Hydrogen-Bonding Present in the Helical Chain Structure. Hydrogen-Bonding is Indicated by the Dotted Lines.

Table 20: Bond Lengths[a] and Angles[b] for 3,3-Di-t-butyl-1,5-dihydroxy-1,5-diphenyl-2,4-dioxa-3-stanna-1,5-diboronate (**34**).

Sn1 -O1	1.99(2)	O3 -Sn1 -O1	146.3(6)
Sn1 -O3	2.78(2)	O4 -Sn1 -O1	92.0(7)
Sn1 -O4	1.97(2)	C13 -Sn1 -O1	101(1)
Sn1 -C13	2.16(4)	C17 -Sn1 -O1	101(1)
Sn1 -C17	2.18(3)	O4 -Sn1 -O3	54.6(6)
B1 -O1	1.20(3)	C13 -Sn1 -O3	87(1)
B1 -O2	1.47(4)	C17 -Sn1 -O3	96.0(9)
B1 -C1	1.61(4)	C13 -Sn1 -O4	107(1)
B2 -O3	1.48(4)	C17 -Sn1 -O4	111.4(9)
B2 -O4	1.43(4)	C17 -Sn1 -C13	135(1)
B2 -C7	1.36(5)	B1 -O1 -Sn1	140(2)
Sn2 -O5	2.75(2)	O2 -B1 -O1	120(3)
Sn2 -O6	1.97(2)	C1 -B1 -O1	129(3)
Sn2 -O7	1.99(2)	C1 -B1 -O2	111(2)
Sn2 -C33	2.19(3)	B2 -O3 -Sn1	82(2)
Sn2 -C37	2.19(4)	B2 -O4 -Sn1	120(2)
B3 -O5	1.41(4)	O4 -B2 -O3	103(3)
B3 -O6	1.38(4)	C7 -B2 -O3	124(3)
B3 -C21	1.52(4)	C7 -B2 -O4	133(3)
B4 -O7	1.28(3)	O7 -Sn2 -O5	145.7(6)
B4 -O8	1.39(3)	O7 -Sn2 -O6	90.0(7)
B4 -C27	1.51(4)	C33 -Sn2 -O7	102(1)
O2 -O5	2.70	C37 -Sn2 -O7	102(1)

O4	-O2	2.74	O6	-Sn2	-O5	55.9(6)
O6	-O8	2.70	C33	-Sn2	-O5	94.4(9)
O8	-O3'	2.67	C37	-Sn2	-O5	88(1)
			C33	-Sn2	-O6	110(1)
			C37	-Sn2	-O6	109(1)
			C37	-Sn2	-C33	133(1)
			B4	-O7	-Sn2	140(2)
			O8	-B4	-O7	118(2)
			C27	-B4	-O7	124(2)
			C27	-B4	-O8	118(2)
			B3	-O5	-Sn2	79(2)
			B3	-O6	-Sn2	114(2)
			O6	-B3	-O5	112(2)
			C21	-B3	-O5	120(3)
			C21	-B3	-O6	128(3)

▪ = Å.

▷ = °.

hydroxyl group is too far away from tin to be classed as being in the coordination sphere [Sn1-O2 3.46Å; Sn2-O8 3.47Å]. For the second unit bidentate chelation is seen with the hydroxyl group coordinating to tin in an axial manner. In (**34**) the two σ-bonded tin-oxygen bond lengths [Sn1-O1 1.99(2)Å, Sn1-O4 1.97(2)Å; Sn2-O6 1.97(2)Å, Sn2-O7 1.99(2)Å] are equivalent and are comparable with other tin-oxygen bonded systems exemplified by di-t-butyl- and di-t-amyltin oxides reported by Puff et al.[151] where the tin-oxygen bond lengths range between 1.95Å and 1.98Å. For the coordination bonded tin-hydroxyl system the tin-oxygen bond is considerably longer [Sn1-O3 2.78(2)Å; Sn2-O5 2.75(2)Å] indicating that the hydroxyl group is weakly coordinated to the tin.

The bond angles at tin confirm the structure as being a highly distorted *cis*-R_2SnX_3 with the 'axial' oxygens for the two molecules in the asymmetric unit displaying similar bond angles [O3-Sn1-O1 146.3(6)° and O7-Sn2-O5 145.7(6)°]. The reason for the axial oxygens not attaining a linear array is because the 'bite' size of the bidentate boronate unit is too small to bridge the required 90° axial-equatorial angle. The sum of the equatorial angles in the array [352° for Sn1 and 353° for Sn2] show that the structure is more akin to trigonal bipyramidal (360°) than to tetrahedral (328.4°) geometry. For (**34**) it can be seen that an expansion of the equatorial carbon-tin-carbon equatorial angle has occurred [C17-Sn1-C13 135(1)°; C37-Sn2-C33 133(1)°] compared to the 120° angle expected in a perfect sp^2 system. This angular expansion could have occurred for two reasons, the first being to relax the steric interactions of the bulky

t-butyl groups. The second reason could result from the increased *p* character present in the tin-oxygen bond compared to the tin-carbon bonds. The net result would be an increase in the *s* character of the tin-carbon bonds producing an expansion of the carbon-tin-carbon bond angle and a subsequent decrease in the carbon-tin-oxygen bond angles. These effects are in accordance with the rehybridisation arguments of Bent.[246] Comparison of the geometry about tin can be made with known structures containing similar chelating groups e.g. acetate. This is exemplified in the work of Harrison et al.[15] where the crystal structure of triphenyltin (2-hydroxy-5-methylphenylazobenzoate) is reported. In this compound an intramolecularly coordinated bidentate benzoate unit is present affording distorted trigonal bipyramidal geometry to tin. The carbonyl oxygen-tin coordination bond is 2.463(7)Å in length which is slightly shorter than the analogous bond present in (**34**). For this structure the sum of the equatorial angles is 340.7° indicating a greater tetrahedral nature to the structure than observed in (**34**).

In the boronate units considerable thermal motion is found in the structure resulting in large standard deviations in the geometric data. Because of this, precise assignment of structural features are made with caution. In both molecules in the asymmetric unit trigonal geometry is observed in the boronate groups. In the literature Farmer[247] describes boron-oxygen bond lengths for both trigonal BO_3 and tetrahedral BO_4 units. For the former, the bond lengths range between 1.28Å and 1.43Å while the latter are generally longer ranging from 1.43Å to 1.55Å. For the bidentate boronate unit the boron-oxygen

bond distances are equivalent [B2-O3 1.48(4)Å, B2-O4 1.43(4)Å; B3-O5 1.41(4)Å, B3-O6 1.38(4)Å]. These values are slightly larger than the comparable boron-oxygen bond lengths of between 1.36Å and 1.38Å found in the crystal structure of phenylboronic acid.[248] For the unidentate boronate unit asymmetry is observed in the boron-oxygen bond lengths [B1-O1 1.20(3)Å, B1-O2 1.47(4)Å; B4-O7 1.28(3)Å, B4-O8 1.39(3)Å]. As can be seen, for the hydroxyl boron-oxygen bond a standard bond length is found, but in the tin-oxygen-boron linkage considerable shortening is observed for the boron-oxygen bond indicating an increase in bond order. In the work of Akishin and Spiridonov[249] the gas phase structure of B_2O_3 was obtained from electron diffraction studies of boron oxide when heated to above 450°C. The molecular structure displays C_{2v} geometry with two slightly shorter than standard boron-oxygen single bonds and two boron-oxygen double bonds of length 1.36(2)Å and 1.20(3)Å respectively (figure 47).

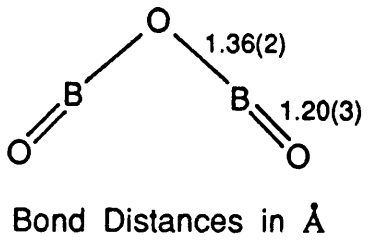

Figure 47: Molecular Structure of B_2O_3 in the Gas Phase.

The bond length of the boron-oxygen double bond in B_2O_3 is comparable in size with that observed in the tin-oxygen-boron linkage in the unidentate boronate group of (**34**).

In the structure of (34) the bond lengths of the axial and equatorially σ-bonded oxygens are equivalent. For an axial oxygen, *trans* disposed to the coordinating hydroxyl group it would be expected that the bond would elongate. Both of the above observations can be rationalised by the presence of a three centre *d-p-p* π-system operating in the tin-oxygen-boron linkage. To facilitate this effect, unfilled orbitals are available on both tin (d_{xz} or d_{yz}) and boron (p_z) for overlap with a filled lone pair *p* orbital on oxygen (figure 48).

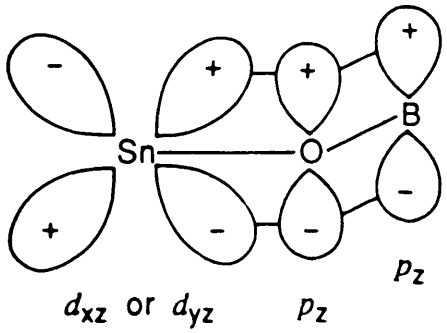

Figure 48: Orbital Arrangement Present in the Postulated Three Centre *d-p-p* π-system Present in the Tin-Oxygen-Boron Linkage.

The boron-oxygen bond length is uniquely short in this instance due to the fact that no hydrogen-bonding occurs through oxygen unlike the other three oxygen atoms present in each molecule. This results in increased lone pair electron density on the oxygen being directed into the three centre π-system.

For the boron-carbon bonds in the boronate units variations in the bond lengths occur. For the Sn1 based molecule the carbon-boron bond lengths are appreciably different [B1-C1 1.61(4)Å, B2-C7 1.36(5)Å],

however, for the Sn2 based molecule the bonds are equal in length [B3-C21 1.52(4)Å, B4-C27 1.51(4)Å]. In the structure of phenylboronic acid the boron-carbon bond length is 1.56Å. In the Sn2 based molecule standard bond lengths are observed while in the Sn1 based molecule one elongated and one shortened boron-carbon bond is seen. From this it may be surmised that a bond order increase in B2-C7 and a bond order decrease in B1-C1 has occurred. The increase of bond order in the boron-oxygen-tin linkage of the unidentate boronate group is attributed to the donation of electron density from an oxygen lone pair into the vacant *p* orbital on boron. Dependent on the planarity of the aryl ring with respect to the oxygen-boron-oxygen unit it can be surmised that for the aryl ring π-system, overlap with the vacant *p* orbital on boron can also occur. However, on analysis of the oxygen-boron-aryl ring dihedral angles in the two molecules [O1-B1-C1-C6 178.0°, O4-B2-C7-C8 179.6°; O6-B3-C21-C26 178.5°, O7-B4-C27-C32 176.2°] no drastic alteration from planarity is observed in any of the phenylboronate groups. Therefore, it would appear that another effect is in operation, possibly arising from crystal packing, resulting in a variation in the boron-carbon bond distances.

For the bond angles at boron general trends can be observed but exact structural details are hard to rationalise due to large standard deviations present in the data. For the bidentate boronate unit it is noticeable that the oxygen-boron-oxygen bond angle is below the 120° expected for a perfect sp^2 array [O4-B2-O3 103(3)°; O6-B3-O5 112(2)°]. This would be expected due to a reduction of the boronate bond angle caused by the intramolecular chelation at tin. For the unidentate

boronate groups the oxygen-boron-oxygen bond angle is equal to the expected 120° [O2-B1-O1 120(3)°; O8-B4-O7 118(2)°]. Considerable variation is found in the other angles at boron especially in the unidentate boronate group. However, a trend can be seen where the carbon-boron-oxygen bond angle is larger on the side of the boronate unit where the oxygen is σ-bonded to tin and smaller where the coordinating hydroxide unit is located.

The lattice structure of the compound as can be seen from the PLUTO plots is a helical, hydrogen-bonded, chain structure (figures 44 to 46). In the structure both intramolecular (O4-O2 2.74Å; O6-O8 2.70Å) and intermolecular (O2-O5 2.70Å; O8-O3' 2.67Å) hydrogen-bonding is observed. In the literature other examples are cited for structurally characterised hydrogen-bonded systems involving organotin units. In the structure of trimethyltin 2-pyridylcarboxylate monohydrate reported by Harrison and Philips[250] bond lengths for nitrogen-water (2.72Å to 2.88Å) and carbonyl-water (2.65Å to 2.79Å) hydrogen-bonding are quoted. Two other systems displaying hydrogen-bonding are tris(trimethyltin) chromate hydroxide[251] and trimethyltin nitrate monohydrate[252] which both display bond lengths (2.80Å and 2.72Å respectively) comparable with those observed in (**34**).

The extensive hydrogen-bonding present results in the molecular arrangement being drawn around into the observed helical chain structure found in the solid state. In the chain array four molecules of (**34**) are required to attain one complete turn of the helix. Although extensive inter- and intramolecular hydrogen-bonding occurs it can be seen that no interchain association occurs. For each

molecule three of the four oxygens are involved in the hydrogen-bonded network while the fourth is incorporated into the three centred tin-oxygen-boron π-system discussed above. It is apparent from the crystal data that the carbon-boron-oxygen bond angles in the unidentate boronate units are more distorted than in the bidentate units. To explain this it could be surmised that in the bidentate example the oxygens are held rigidly resulting from the additional coordination to tin restricting the possible angular distortions. However, for the unidentate case the hydroxyl group is pendular allowing sufficient mobility to enable maximum hydrogen-bonding to occur. This would result in a perturbation of the angles in the boronate group.

For (**34**) and the mesityl analogue (**35**) the solid state spectroscopic data are consistent with the X-ray determined molecular structure. In the infra-red spectrum broad bands are seen at 3250 and 3300 cm^{-1} respectively and are similar in shape to that observed for the hydrogen bonded hydroxyl group in phenylboronic acid. For the experimentally obtained elemental analysis values good agreement is found for both compounds with the theoretically derived figures based on the crystal structure of (**34**) [(**34**) Analysis (%): Found C 50.70; H 6.49; Calculated for $C_{20}H_{30}B_2O_4Sn$: C 50.60; H 6.37; (**35**) Analysis (%): Found 56.00; H 7.76; Calculated for $C_{26}H_{42}B_2O_4Sn$: C 55.87; H 7.57]. In the Mossbauer spectra of the two compounds broad doublets with similar isomer shift and quadrupole splitting values are obtained indicating geometry greater than four occurring in both instances [(**34**) I.S.= 1.46 mms^{-1} and Q.S.= 2.81 mms^{-1}; (**35**) I.S.= 1.37 mms^{-1} and Q.S.= 2.66 mms^{-1}].

In the solution state however, the picture is more complex. For (35) except for minor impurity peaks the ^{1}H, ^{13}C and ^{11}B nmr spectra are as expected. In the ^{119}Sn nmr spectrum two signals are seen at -106.7 ppm for the major component (84%) and -131.6 ppm for the minor component (16%). On this basis it would seem that the compound present in the solution state for (35) is mainly the same as that found in the solid state. In (34) however, the nmr spectra obtained displayed increased complexity. In the ^{119}Sn nmr spectrum of (34) as in (35), two peaks are observed. In this instance the minor component resides at -106.4 ppm (30%) and the major component at -127.8 ppm (70%), a reversal of the intensities observed for (35). In the ^{1}H and ^{13}C nmr spectra multiplicity of signals are observed. In both spectra two t-butyl signals are observed in approximately a 2:1 ratio. For the aryl signals two environments are seen for both the *ortho* and *para* carbons in the ^{13}C nmr spectrum as well as two environments for the *ortho* protons in the ^{1}H nmr spectrum.

From this evidence it can be concluded that two species are present in solution. From the observed ^{119}Sn nmr chemical shifts for (35), the minor product present in solution in (34) can be assigned to the species characterised by the X-ray structure determination. On this basis the smaller t-butyl signal at 1.46 ppm, the boron hydroxyl signal at 6.05 ppm, 20% of the *meta* and *para* multiplet at 7.44 ppm and the *ortho* proton multiplet at 7.87 ppm can all be assigned to the known structure of (34).

For the second product the integral ratio for the remaining *ortho* and the second t-butyl signals is 4:18. Therefore it would appear that

the second product contains one di-t-butyltin unit per two phenylboronate units as present in (**34**). However the boron hydroxyl signal in the ^{1}H nmr spectrum is totally accounted for by the presence of (**34**) indicating that the second component does not display boron hydroxyl groups. From the evidence presented it would seem reasonable to suggest that in solution the second product arises from a condensation reaction of (**34**) resulting in ring closure to form 2,2-di-t-butyl-4,6-diphenyl-1,3,5-trioxa-2-stanna-4,6-diborinane (**36**).

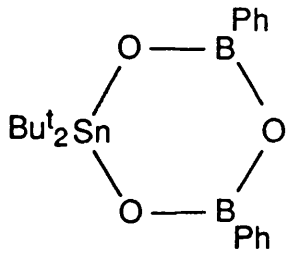

(**36**)

In the ^{1}H nmr spectrum of the analogous 2,4,6-triphenyl-1,3,5-trioxa-2,4,6-borinane formed from the dehydration of phenylboronic acid the *meta/para* and the *ortho* proton signals are at 7.4 and 8.2 ppm respectively. These values compare favourably with those observed for (**36**).

In the ^{1}H nmr spectrum even after subtraction of the second component the multiplet attributable to the *meta* and *para* protons in the two assigned species is not totally allocated. Due to the absence of any other spurious signals in the ^{1}H nmr spectrum it would appear that the additonal aryl species displays degenerate proton signals. In the ^{11}B nmr spectrum as well as the expected broad peak at 26.3 ppm

assignable to both (**34**) and (**36**) a sharp peak of low intensity is seen at -0.3 ppm. The chemical shift and shape of the peak are characteristic of a boron displaying tetrahedral geometry. These observations would seem to suggest that a small proportion of the compounds present in solution have degraded generating phenylboronic acid which has hydrolysed possibly to benzene and $B(OH)_4^-$ (^{11}B nmr: +1.1 ppm) (equations 107 and 108).

$$tBu_2Sn[OB(Ph)(OH)]_2 + H_2O \rightarrow tBu_2SnO + 2PhB(OH)_2 \quad (107)$$

$$PhB(OH)_2 + 3H_2O \rightarrow [PhB(OH)_3]^-[H_3O]^+ + H_2O \quad (108)$$

$$\downarrow$$

$$PhH + [B(OH)_4]^-[H_3O]^+$$

In the literature no precedent is reported for the hydrolysis of phenylboronic acid. Therefore, without further evidence only speculation as to the identities of the additional species present in the solution state can be made.

From the nmr investigation it would appear that the mesityl derivative (**35**) is far less susceptible to dehydration and resultant ring closure than the phenyl analogue (**34**). Without further investigation the exact reasons for the variation are unclear, however, it could be surmised that the increased hindrance of the mesityl group may impair the ring closure condensation.

As with (**34**) and (**35**) the second products yielded from the reactions between mesityl and phenylboronic acids and di-t-butyltin

oxide, (37) and (38), were obtained as highly crystalline solids. For (38) a single crystal X-ray structure determination was carried out. The structure obtained displayed pseudo tetragonal symmetry but on the basis of systematic absences no suitable tetragonal space group was found. By the use of the orthorhombic space group *Pnn2* for which the observed systematic absences are satisfied a preliminary structure can be reported, however symmetry related problems have currently precluded the complete refinement of the structure. The ORTEP plot given in figure 49 shows the totally planar tricyclo[3,1,1,1]nonane ring structure of the compound. Selected bond lengths and angles are given in table 21 and full crystal data is reported in Appendix IX. The crystal sample used contained four independent molecules per asymmetric unit. Due to the uncertainty in the space group assignment for the crystal structure high standard deviations are present in the data restricting structural analysis to a basic overview of the type of structure observed.

For all three tins present in the structure distorted *cis*-R_2SnX_3 arrays are seen. The five-coordinate array at Sn3 appears to be more highly distorted than those at Sn1 and Sn2. For Sn3 the axial angle is more perturbed from the ideal 180° than the analogous angles observed at Sn1 and Sn2 [O5-Sn1-O1 163.7(9)°; O4-Sn2-O2 163.3(9)°; O2-Sn3-O1 144.6(8)°]. The tin-oxygen bond lengths present in the structure appear to be of two distinct types. For Sn1-O3, Sn1-O5; Sn2-O3, Sn2-O4 and Sn3-O1, Sn3-O2, Sn3-O3, almost equal tin-oxygen bond lengths of 2.10(2)Å, 2.03(2)Å; 2.03(2)Å, 2.01(3)Å and 2.13(2)Å, 2.13(2)Å, 2.09(3)Å respectively, are observed. These bond distances are slightly

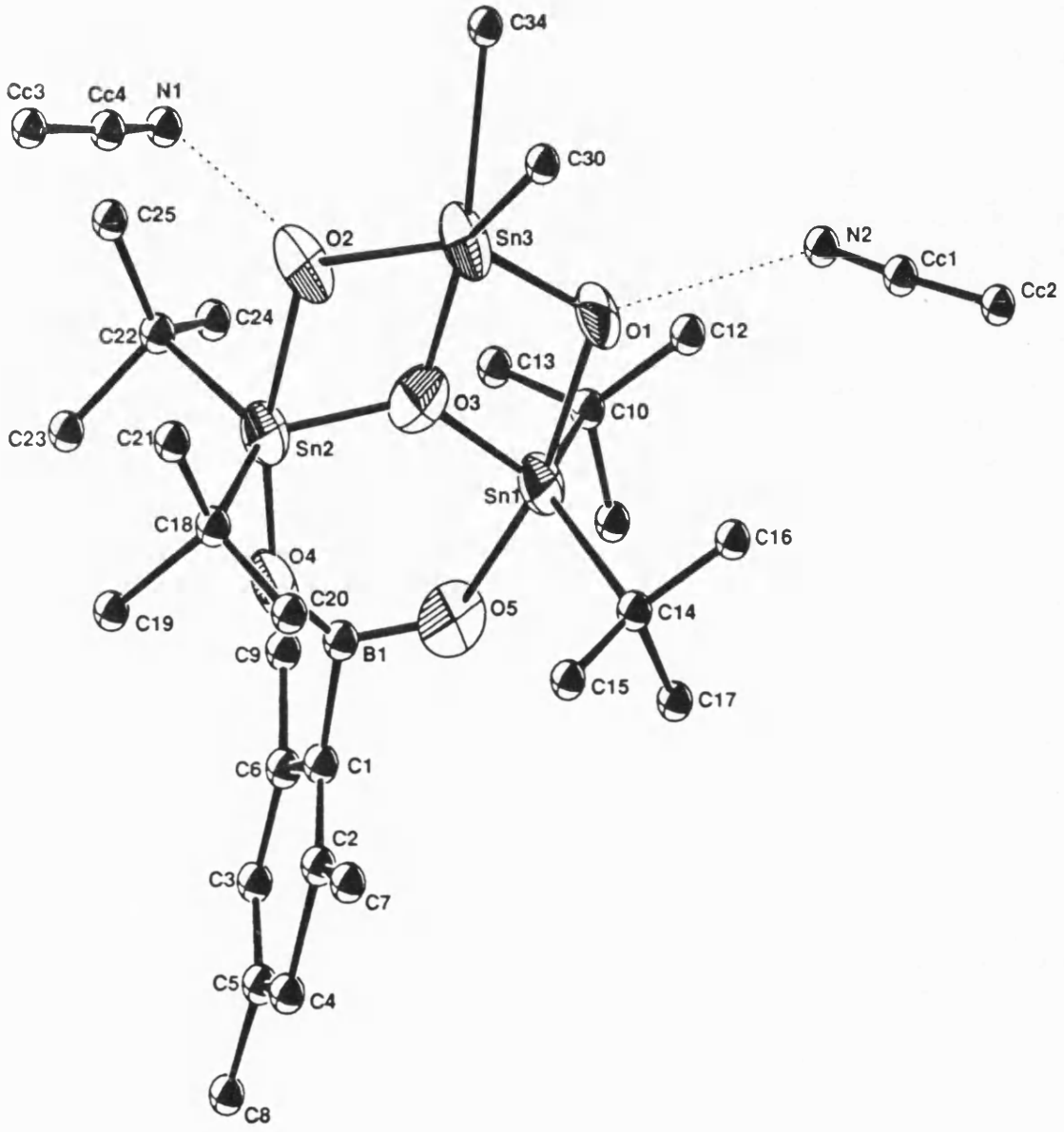

Figure 49: ORTEP plot of 2,4-Dihydroxy-1,1,3,3,5,5-hexa-t-butyl-7-mesityl-6,8,9-trioxa-1,3,5-tristanna-7-boratricyclo-[3,1,1,1]nonane (38). Only the α-Carbons of the t-Butyl Groups for Sn3 are Included due to Unresolved Disorder in this Part of the Molecule.

Table 21: Bond Lengths[a] and Angles[b] for 2,4-Dihydroxy-1,1,3,3,5,5-hexa-t-butyl-7-mesityl-6,8,9-trioxa-1,3,5-tristanna-7-boratricyclo[3,1,1,1]nonane (38).

Sn1 -O1	2.25(2)	O3 -Sn1 -O1	70.7(9)
Sn1 -O3	2.10(2)	O5 -Sn1 -O1	163.7(9)
Sn1 -O5	2.03(2)	O5 -Sn1 -O3	93(1)
Sn1 -C10	2.34(4)	C10 -Sn1 -O1	93(1)
Sn1 -C14	2.28(4)	C10 -Sn1 -O3	113(1)
Sn2 -O2	2.24(2)	C10 -Sn1 -O5	95(1)
Sn2 -O3	2.03(2)	C14 -Sn1 -O1	92(1)
Sn2 -O4	2.01(3)	C14 -Sn1 -O3	116(1)
Sn2 -C18	2.34(4)	C14 -Sn1 -O5	95(2)
Sn2 -C22	2.21(4)	C14 -Sn1 -C10	129(1)
Sn3 -O1	2.13(2)	O3 -Sn2 -O2	70.1(9)
Sn3 -O2	2.13(2)	O4 -Sn2 -O2	163.3(9)
Sn3 -O3	2.09(3)	O4 -Sn2 -O3	93(1)
Sn3 -C30	2.45(*)	C18 -Sn2 -O2	95(1)
Sn3 -C34	2.39(*)	C18 -Sn2 -O3	115(1)
O4 -B1	1.23(5)	C18 -Sn2 -O4	94(1)
O5 -B1	1.48(5)	C22 -Sn2 -O2	91(1)
B1 -C1	1.63(5)	C22 -Sn2 -O3	116(1)
N1 -O2	3.05	C22 -Sn2 -O4	95(1)
N2 -O1	3.06	C22 -Sn2 -C18	127(1)
		O2 -Sn3 -O1	144.6(8)
		O3 -Sn3 -O1	73.3(8)

O3 -Sn3 -O2	71.3(8)
C30 -Sn3 -O1	97(3)
C30 -Sn3 -O2	117(3)
C30 -Sn3 -O3	162(3)
C34 -Sn3 -O1	98(2)
C34 -Sn3 -O2	108(2)
C34 -Sn3 -O3	138(2)
C34 -Sn3 -C30	58(4)
Sn3 -O1 -Sn1	104.5(9)
Sn3 -O2 -Sn2	104.6(9)
Sn2 -O3 -Sn1	134(1)
Sn3 -O3 -Sn1	111(1)
Sn3 -O3 -Sn2	114(1)
B1 -O4 -Sn2	138(3)
B1 -O5 -Sn1	131(2)
O5 -B1 -O4	130(4)
C1 -B1 -O4	124(4)
C1 -B1 -O5	105(3)

* = Excessive errors are currently associated with these bond lengths due to disorder in this part of the molecule. See table 46 of Appendix IX for the standard deviations in the positional parameters for C30 and C34.

▪ = Å.

▹ = °.

elongated in comparison to the equivalent tin-oxygen bond lengths in di-t-butyl- and di-t-amyltin oxide (1.95Å-1.98Å).[151] A further increase in the tin-oxygen bond lengths is observed for Sn1-O1 and Sn2-O2 where distances of 2.25(2)Å and 2.24(2)Å respectively, are found.

In the structure two molecules of the recrystallisation solvent, acetonitrile are found per molecule of (**38**). The spatial arrangement of the acetonitrile groups adjacent to O1 and O2 implies the presence of hydrogen-bonding. This leads to the suggestion that O1 and O2 are hydroxyl groups. The hydrogen-bond lengths are relatively long (N1-O2 3.05Å and N2-O1 3.06Å) in comparison to those observed in (**34**) which ranged between 2.67Å and 2.74Å. The presence of hydroxyl groups for O1 and O2 accounts for the increase in the bond lengths of the Sn1-O1 and Sn2-O2 tin-oxygen bonds due to the presence of dative bonding as opposed to the σ-bonding found in a standard tin-oxygen bond.

By implication Sn3-O3 must also be a dative bond to maintain a valency of four at the metal, however in this instance a bond length of 2.09(3)Å is seen which is equal to the ring tin-oxygen bond distances. This phenomenon can be explained by the fact that due to hydrogen-bonding occurring for the hydroxyl groups O1 and O2, a decrease in the electron density at oxygen will reduce the donor properties to tin. By comparison, with O3 being a 'naked' oxygen, increased electron donation to tin can occur resulting in a comparative increase in the bond order for the dative bond and thus bond shortening. A schematic representation of the structure of (**38**) is given in figure 50. The formulation of (**38**) derived from the

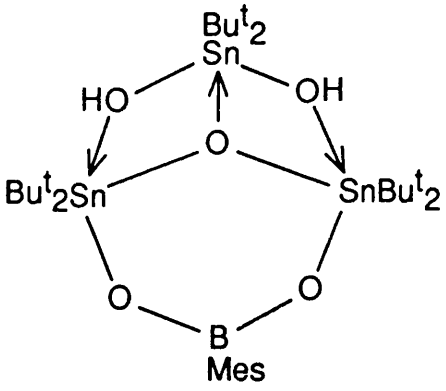

Figure 50: Schematic Representation of 2,4-Dihydroxy-1,1,3,3,5,5-hexa-t-butyl-7-mesityl-6,8,9-trioxa-1,3,5-tristanna-7-bora-tricyclo[3,1,1,1]nonane (**38**).

crystal structure satisfies the elemental analysis requirements of the compound [Analysis (%): Found C 44.80; H 7.55; N 2.99; Calculated for $C_{37}H_{73}BN_2O_5Sn_3$: C 44.75; H 7.41; N 2.82].

At boron two distinct boron-oxygen bond lengths are found. The B1-O5 bond length of 1.48(5)Å is of a magnitude normally found in tetrahedral BO_4 units.[247] For B1-O4 a very short bond of 1.23(5)Å is found which is comparable in length with a boron-oxygen double bond as found in B_2O_3 in the gas phase.[248] The high standard deviations present in this data impede the full explanation of this phenomenon. However, it could be suggested that for B1-O4-Sn2 a three centre π-system as postulated in (**34**) is in operation. This would increase the electron density present in the boron p_z orbital resulting in an increase in the bond order of the B1-O4 bond. If this occurred a consequent increase in the bond order of Sn2-O4 would be expected. This does not occur as Sn1-O5 and Sn2-O4 are of equal length. It would

therefore appear that the inequivalence of the boron-oxygen bond lengths result from a more localised effect probably resulting from a boron-oxygen two centre π-system. Before any further conclusions can be made a better refinement is required for the structure in order to reduce the standard deviations present in the data.

For compounds (37) and (38) the spectroscopic data obtained is consistent with the cyclic array in both the solid and solution states. For the di-t-butyltin units, in the ^{1}H nmr spectrum two sharp singlets are observed with a 2:1 intensity ratio. A similar observation is made for the ^{13}C nmr spectrum of (37), however only one environment is observed in the ^{13}C nmr spectrum of (38) which is presumed to occur as a result of a fortuitous overlap of signals. The ^{119}Sn nmr spectra of (37) and (38) also display doubling of signals in the same 2:1 ratio. This effect arises from the presence of two distinct environments for the di-t-butyltin moieties in the ring array of the two compounds.

From the chemical shifts of the peaks in the ^{119}Sn nmr spectra and the values of the quadrupole splitting in the Mossbauer spectra of (37) and (38) it can be seen that both tin environments display five-coordinate arrays. This results from the increased coordination at all three tin atoms resulting from dative bonding from either the hydroxyl groups or the ring oxygen as observed in the crystal structure. In the structure of (38) two molecules of acetonitrile are present in the lattice but do not coordinate to tin instead hydrogen-bonding to the hydroxyl groups occurs.

The structure of (37) and (38) is independent of the type of recrystallisation solvent used except for the absence of hydrogen-bonding for non-associating solvents. This is supported by the ^{119}Sn nmr spectral data observed for (37) when recrystallised from either a non-coordinating or a strongly associating solvent. For the former, if the degree of association in the array decreased a downfield shift for the signals would be expected. However, for both instances independent of the nature of the recrystallisation solvent the chemical shifts for the observed signals are unchanged.

For the mesityl and phenylboronate units the spectral data is consistent with the formulation of three di-t-butyltin units per boronate unit. In the ^1H nmr spectra no boron hydroxyl signals are present for either compound. This is consistent with the presence of a condensed cyclic array as opposed to an open chain system as in (34) and (35) where boron-hydroxyl groups are observed.

For (37) it is apparent that the infra-red spectra are dependent on the recrystallisation solvent. On comparison of the spectra for the samples recrystallised from non-coordinating solvents (60-80 petrol and chloroform) with those from associating solvents (acetonitrile and acetone) marked differences are found. For the former type a sharp band is observed at 3680 cm^{-1} as well as a strong band at 755 cm^{-1}. The former band is normally found in a system exemplified by trimethyltin hydroxide[125] resulting from an associated, non-hydrogen-bonded, O-H stretch. The latter band is in good agreement with an Sn-O-Sn asymmetric stretch as observed in di-t-butyltin oxide.[253] For (37) when recrystallised from associating solvents a broader band at

3510 cm^{-1} as well as weak, sharp bands at 3660 and 3640 cm^{-1} are observed. Additionally the strong band previously seen at 755 cm^{-1} diminishes in intensity.

This data is consistent with the observed crystal structure of (38) when recrystallised from acetonitrile. In the structure tin hydroxide groups hydrogen-bonded to acetonitrile were observed giving rise to the lower wavenumber broad O-H band. The observation of low intensity sharp bands at 3660 and 3640 cm^{-1} possibly arises from the loss of acetonitrile from the sample due to heating effects in the infra-red beam. If recrystallised from a non-coordinating solvent the hydrogen-bonding would be removed giving rise to an associated hydroxyl group with the infra-red active band as observed at 3680 cm^{-1}. The reason for the decrease in the Sn-O-Sn band at 755 cm^{-1} is unclear. However, if the association of the hydroxyl groups to tin is diminished as a result of hydrogen-bonding considerations the overall symmetry of the Sn-O-Sn linkage may change resulting in a conceivable alteration of the infra-red properties of the array.

In the literature the infra-red data for the parent di-t-butyltin oxide and the hydrated form, 'di-t-butyltin dihydroxide' is available.[263] In di-t-butyltin oxide an intense Sn-O-Sn band is observed at 755 cm^{-1}. For the hydrated form a sharp band is observed at 3680 cm^{-1} indicative as above of an associated hydroxyl group bonded to tin. Also the band at 755 cm^{-1} is replaced by bands at 790 cm^{-1} and 1650 cm^{-1} which are proposed to arise from associated water in the molecule. For di-t-butyltin oxide the structure is known to be a trimeric six-membered ring whereas for the hydrated form the exact

structure is not known. The authors suggest that the structure is trimeric based on molecular weight determinations in benzene and displays properties that are midway between 'di-t-butyltin dihydroxide' and di-t-butyltin oxide monohydrate.

Suggestions can be made as to the structure of 'di-t-butyltin dihydroxide' based on the similarity of its infra-red spectrum in comparison with the spectra observed for (37) and (38) when recrystallised from an associating solvent. From trimeric di-t-butyltin oxide the partial hydrolysis of the ring array could yield a dihydrated tricyclic species analogous to the structure of (38) incorporating both a tin-oxygen-tin σ-bonded skeleton as well as datively associated tin-dihydroxide units (figure 51).

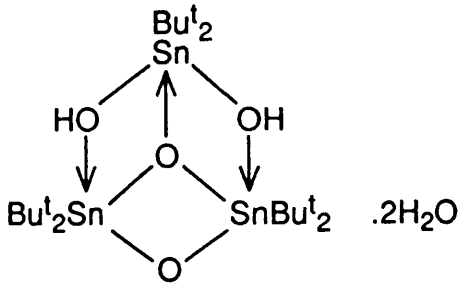

Figure 51: Postulated Tricyclic Species Present in the Structure of 'Di-t-butyltin Dihydroxide'.

The postulated array would satisfy the requirements of the infra-red spectroscopy, elemental analysis and molecular weight measurements quoted for the compound.

4.3 Experimental.

Di-t-butyltin oxide. Di-t-butyltin dichloride (5g, 0.016 mole), sodium hydroxide (20ml of a 5M solution in water) and diethyl ether (20ml) were shaken as a two-phase system for 3 hr. At this point a dense white precipitate was filtered off and washed with water until the filtrate was neutral by pH paper. The resultant white solid was then washed with methanol followed by diethyl ether and dried in a vacuum dessicator. (2.9g, 71%), m.p. 275°C (decomposes).

I.R. [(cm^{-1}) KBr disc]: 3450; 2960; 2940; 2875; 2850; 1470; 1365; 1175; 1020; 945; 815; 770; 560; 415; 380; 285.

^{119m}Sn Mossbauer (mms^{-1}): I.S.=1.20; Q.S.=1.81.

Analysis (%): Found C 38.60; H 7.56; Calculated for $C_8H_{18}OSn$: C 38.60; H 7.29.

Di-t-butyltin Dihydroxide. If the sample used for the above spectral determination is recrystallised from methanol colourless crystals are obtained which crumble on exposure to air. The spectral data obtained from this sample however is very different to that previously observed.

I.R. [(cm^{-1}) KBr disc]: 3650; 3220; 2960; 2940; 2875; 2850; 1540; 1475; 1375; 1340; 130; 1170; 1080; 1040; 1020; 950; 850; 815; 695; 600; 460; 420; 395; 315; 300.

^{119m}Sn Mossbauer (mms^{-1}): I.S.=1.24; Q.S.=2.54.

Analysis (%): Found C 36.40; H 7.66; Calculated for $C_8H_{20}O_2Sn$: C 36.00; H 7.55.

Mesitylboronic Acid. To prepare the mesityl Grignard reagent, mesityl bromide (30g, 0.151 mole) in dry diethyl ether (90ml) was added dropwise to previously activated magnesium turnings (3.7g, 0.152 mole) (0.2ml methyl iodide) in diethyl ether (10ml). The reaction rate at ambient temperatures was very sluggish and so gentle heating to 35°C (water bath) was implemented. After a period of 5 hr. at 35°C the excess magnesium was filtered off through a glass wool plug. To diethyl ether (200ml) at -78°C a simultaneous addition of the mesityl Grignard reagent and trimethylborate (15.6g, 0.150 mole) was made. After approximately 75% of the addition was completed a further 100ml of diethyl ether was added to the reaction mixture to enable efficient stirring to take place. On completion of addition the reaction mixture was allowed to warm to room temperature and stirring continued for 17 hr. To the stirred white slurry water was carefully added to hydrolyse the remaining methoxy groups present on the boron species in the reaction mixture. After extraction with diethyl ether the combined organic washings were dried over anhydrous sodium sulphate. *In vacuo* solvent removal yielded a white solid which was further purified by recrystallisation from chloroform/40-60 petrol to give a colourless crystalline solid. (8.1g, 33%), m.p. 177°C.

I.R. [(cm^{-1}) KBr disc]: 3320; 2970; 2920; 2860; 1615; 1560; 1440; 1345; 1190; 1165; 1105; 1020; 850; 835; 750; 700; 665; 580; 550; 435.

^1H NMR [δ(ppm) $CDCl_3$ solution]: 2.25 [s,3H, *p*-$(CH_3)_3C_6H_2$]; 2.32 [s,6H, *o*-$(CH_3)_3C_6H_2$]; 5.09 {s,2H,[$(CH_3)_3C_6H_2$]$B(OH)_2$}; 6.80 [s,2H, $(CH_3)_3C_6H_2$].

^{13}C NMR [δ(ppm) $CDCl_3$ solution]: 21.08 [*p*-$(CH_3)_3C_6H_2$]; 21.99 [*o*-$(CH_3)_3C_6H_2$]; 127.24 [*m*-C_6H_2]; 138.60 and 139.63 [*o,p*-C_6H_2].

^{11}B NMR [δ(ppm) $CDCl_3$ solution]: 29.6.

Analysis (%): Found C 65.20; H 8.02; Calculated for $C_9H_{13}BO_2$: C 65.91; H 7.99.

Reaction of Di-t-butyltin Oxide and Phenylboronic Acid. Di-t-butyltin oxide (1g, 0.004 mole) and phenylboronic acid (0.49g, 0.004 mole) in benzene (30ml) were heated to reflux in an apparatus fitted with a Dean and Stark head. Water was obtained from the reaction and heating continued for 17 hr. On cooling *in vacuo* benzene removal yielded a white solid. Recrystallisation from acetone produced colourless crystals that on exposure to air turned opaque and crumbled. m.p. 169-170°C.

From this reaction only one product was isolated, however, on repetition of the reaction using a variety of reaction stoichiometries, the above product was isolated as well as a second crystalline species. To purify the products different solvents were used for recrystallisation including 80-100 petrol and acetonitrile to try to reduce the tendency of the crystals to crumble on standing in air.

3,3-Di-t-butyl-1,5-dihydroxy-1,5-diphenyl-2,4-dioxa-3-stanna-1,5-diboronate (**34**).

In the solution state two assignable products are observed in a 10:3.6 ratio. The major component is assigned as the condensation product (**36**) and the minor as its open chain precursor (**34**). The ratio of products is based on the peak intensities found in the ^{119}Sn nmr

spectrum.

I.R. [(cm^{-1}) KBr disc]: 3250; 3080; 2960; 2930; 2880; 2860; 1605; 1495; 1465; 1440; 1395; 1345; 1295; 1270; 1210; 1160; 1115; 1070; 1030; 810; 770; 705; 645; 580; 565.

^{1}H NMR [δ(ppm) $CDCl_3$ solution]: 1.46 [s,18H,$(CH_3)_3C^{(34)}$]; 1.47 [s,18H,$(CH_3)_3C^{(36)}$]; 6.05 {s,2H,[OB(Ph)(OH)$^{(34)}$]); 7.44 {m,6H, [*m,p*-$C_6H_5^{(34)}$],[*m,p*-$C_6H_5^{(36)}$],[$C_6H_5^{(unknown)}$]); 7.87 {m,4H,[*o*-$C_6H_5^{(34)}$]); 8.11{m,4H,[*o*-$C_6H_5^{(36)}$]); $^{3}J[(C'H_3)_3C-^{117,119}Sn^{(34)}]$ 101.4, 104.8 Hz; $^{3}J[(C'H_3)_3C-^{117,119}Sn^{(36)}]$ 98.6, 102.9 Hz.

^{13}C NMR [δ(ppm) $CDCl_3$ solution]: 29.39 [$(CH_3)_3C^{(36)}$]; 29.45 [$(CH_3)_3C^{(34)}$]; 127.47 [*m*-$C_6H_5^{(36)}$]; 127.73 [*m*-$C_6H_5^{(34)}$]; 130.49 [*p*-$C_6H_5^{(34),(36)}$]; 134.22 [*o*-$C_6H_5^{(34)}$]; 135.06 [*o*-$C_6H_5^{(36)}$].

^{11}B NMR [δ(ppm) $CDCl_3$ solution]: 26.3 [(**34**) and (**36**); -0.3.

^{119}Sn NMR [δ(ppm) $CDCl_3$ solution]: -106.4 (**34**); -127.8 (**36**).

^{119m}Sn Mossbauer (mms^{-1}): I.S.=1.46; Q.S.=2.81.

Analysis (%): Found C 50.70; H 6.49; Calculated for $C_{20}H_{30}B_2O_4Sn$: C 50.60; H 6.37.

2,4-Dihydroxy-1,1,3,3,5,5-hexa-t-butyl-7-phenyl-6,8,9-trioxa-1,3,5-tristanna-7-boratricyclo[3,1,1,1]nonane (**37**).

In the infra-red of this compound variations in the spectra result from the use of different recrystallisation solvents.

I.R. [(cm^{-1}) KBr disc (from either acetonitrile or acetone)]: 3660; 3640; 3510; 3080; 3040; 2980; 2950; 2860; 2780; 2720; [2320 and 2280 (acetonitrile)]; [1715 (acetone)]; 1475; 1440; 1370; 1340; 1295; 1275; 1250; 1175; 1090; 1035; 1020; 820; 795; 765; 715; 670; 605; 500; 440;

305.

I.R. [(cm^{-1}) KBr disc (from either 80-100 petrol or chloroform)]:
3680; 3080; 3030; 2980; 2950; 2940; 2860; 2780; 2720; 1475; 1440;
1375; 1365; 1340; 1290; 1270; 1245; 1220; 1165; 1090; 1030; 1015; 805;
755; 700; 650; 585; 485; 425; 380; 290.

1H NMR [δ(ppm) $CDCl_3$ solution]: 1.38 [s,36H,$(CH_3)_3C^a$]; 1.39 [s,18H,
$(CH_3)_3C^b$]; 7.28 [m,3H,*m,p*-C_6H_5]; 7.94 [m,2H,*o*-C_6H_5]; $^3J[(C'H_3)_3C^a$-
$^{117,119}Sn]$ 100.2, 105.6 Hz; $^3J[(C'H_3)_3C^b$-$^{117,119}Sn]$ 99.7, 104.0 Hz.

^{13}C NMR [δ(ppm) $CDCl_3$ solution]: 30.75 [$(CH_3)_3C^a$]; 30.81 [$(CH_3)_3C^b$];
126.82 [*m*-C_6H_5]; 128.05 [*p*-C_6H_5]; 135.35 [*o*-C_6H_5].

^{11}B NMR [δ(ppm) $CDCl_3$ solution]: 25.0.

^{119}Sn NMR [δ(ppm) $CDCl_3$ solution]: -261.8; -277.8.

^{119m}Sn Mossbauer (mms^{-1}): I.S.=1.20; Q.S.=2.36

Analysis (%): Found C 42.80; H 7.20; N 2.75; Calculated for
$C_{34}H_{67}BN_2O_5Sn_3$: C 42.95; H 7.10; N 2.95.

Reaction of Di-t-butyltin Oxide and Mesitylboronic Acid. The reaction procedure employed in this reaction followed the same synthetic route as the analogous preparation using phenylboronic acid. As in the phenylboronic acid reaction two crystalline products were obtained independent of reaction stoichiometry. 80-100 petrol and acetonitrile were the respective recrystallisation solvents used in the purification of compounds (35) and (38).

3,3-Di-t-butyl-1,5-dihydroxy-1,5-dimesityl-2,4-dioxa-3-stanna-1,5-diboronate (**35**).

I.R. [(cm^{-1}) KBr disc]: 3300; 2970; 2950; 2930; 2870; 2710; 1615; 1540; 1435; 1380; 1365; 1350; 1320; 1255; 1235; 1170; 1105; 1075; 1020; 850; 845; 835; 745; 680; 615; 595; 550; 520; 395.

^{1}H NMR [δ(ppm) $CDCl_3$ solution]: 1.49 [s,18H,$(CH_3)_3C$]; 2.30 [s,6H, *p*-$(CH_3)_3C_6H_2$]; 2.39 [s,12H, *o*-$(CH_3)_3C_6H_2$]; 6.22 [s,2H,B(O*H*)]; 6.82 [s,4H, *m*-C_6H_2]; ^{3}J[$(C'H_3)_3C$-^{117,119}Sn] 99.6, 104.0 Hz.

^{13}C NMR [δ(ppm) $CDCl_3$ solution]: 21.05 [*p*-$(CH_3)_3C_6H_2$]; 22.41 [*o*-$(CH_3)_3C_6H_2$]; 29.42 [$(CH_3)_3C$]; 126.98 [*m*-C_6H_2]; 137.14 [*p*-C_6H_2]; 139.34 [*o*-C_6H_2].

^{11}B NMR [δ(ppm) $CDCl_3$ solution]: 28.0.

^{119}Sn NMR [δ(ppm) $CDCl_3$ solution]: -106.7; -131.6 (16% impurity see text).

^{119m}Sn Mossbauer (mms^{-1}): I.S.=1.37; Q.S.=2.66.

Analysis (%): Found C 56.00; H 7.76; Calculated for $C_{26}H_{42}B_2O_4Sn$: C 55.87; H 7.57.

2,4-Dihydroxy-1,1,3,3,5,5-hexa-t-butyl-7-mesityl-6,8,9-trioxa-1,3,5-tristanna-7-boratricyclo[3,1,1,1]nonane (**38**).

I.R. [(cm^{-1}) KBr disc]: 3670; 3480; 2970; 2950; 2930; 2870; 2840; 2710; [2290 and 2250 (acetonitrile)]; 1650; 1470; 1380; 1360; 1320; 1265; 1235; 1160; 1010; 935; 845; 805; 740; 680; 650; 585; 540; 505; 445; 355; 280.

^{1}H NMR [δ(ppm) $CDCl_3$ solution]: 1.33 [s,36H,$(CH_3)_3C^a$]; 1.39 [s,18H, $(CH_3)_3C^b$]; 1.95 [s,6H,CH_3CN]; 2.23 [s,3H,*p*-$(CH_3)_3C_6H_2$]; 2.49 [s,6H,

o-(CH_3)$_3$$C_6H_2$]; 6.73 [s,2H,($CH_3$)$_3$$C_6H_2$]; ^{3}J[($C'H_3$)$_3$$C^a$-^{117,119}Sn] 100.7, 104.4 Hz; ^{3}J[($C'H_3$)$_3$$C^b$-^{117,119}Sn] 99.6, 104.0 Hz.

^{13}C NMR [δ(ppm) $CDCl_3$]: 21.08 [*p*-(CH_3)$_3$$C_6H_2$]; 23.48 [*o*-($CH_3$)$_3$$C_6H_2$]; 30.72 [($CH_3$)$_3$C]; 39.15 [($CH_3$)$_3$*C*]; 126.53 [*m*-$C_6H_2$]; 134.38 [*p*-$C_6H_2$]; 139.67 [*o*-$C_6H_2$].

^{11}B NMR [δ(ppm) $CDCl_3$ solution]: 26.5.

^{119}Sn NMR [δ(ppm) $CDCl_3$ solution]: -260.3; -278.5.

^{119m}Sn Mossbauer (mms^{-1}): I.S.=1.16; Q.S.=2.31.

Analysis (%): Found C 44.80; H 7.55; N 2.99; Calculated for $C_{37}H_{73}BN_2O_6Sn_3$: C 44.75; H 7.41; N 2.82.

SUMMARY.

During the period of this research several methods have been attempted for the preparation of ring or cage/layer compounds. The preparation of ring arrays used diorganotin dihalides in reaction with a chalcogenating agent, e.g. sodium sulphide nonahydrate to produce compounds containing either exclusive or mixed chalcogen species. The structure of these compounds is dependent on the bulk of the organic substituents used as well as the nature of the chalcogen present, as reported in chapter one section 1.5. From the compounds produced it appears that the use of sterically restrictive organic substituents exerts a greater effect on the ring size than does the nature of the incorporated chalcogen species.

The diorganotin dihalide precursors were prepared by two routes. Dialkyltin dihalides were synthesised either by halogen cleavage of aryl groups from dialkyldiaryltin compounds or by direct stoichiometric addition of the carbanion of the alkyl group to an anhydrous tin(IV) halide. Diaryltin dihalides were prepared exclusively by use of the latter route as a result of limited selectivity for the halogen cleavage of mixed aryl substituted tin compounds.

By the use of sterically hindered oligomeric diorganotin oxides the preparation of associated chain and ring boronates was achieved (chapter four section 2.1). Only preliminary studies were made in this area but the results obtained indicate that incorporation of

sterically hindered tin units into oligomeric systems of other elements is possible.

Having proved the viability of diorgano substituted tin units for the synthesis of ring arrays of widely varying types, the work was extended to the preparation of cage/layer structures. The work carried out in this area was based upon sterically hindered monoorganotin trihalides as building blocks in an analogous synthetic methodology to that used in the preparation of the diorganotin ring systems. By this route adamantane cage structures were prepared, however due to the limited success achieved in the preparation of monoorganotin trihalides only low hindrance examples were investigated.

The synthesis of the monoorganotin trihalides has been attempted by the same methods as used to prepare the diorganotin dihalides detailed above. For the aryl cleavage reaction of alkyltriaryltin compounds using bromine it was found that for comparatively low hindrance examples the synthesis worked well. However, in more sterically hindered systems, the aryl cleavage conditions were insufficient to drive the reaction to completion (chapter two section 2.3). Under more vigorous conditions, reactions occurred at the substituent on the periphery of the molecule rather than directed at aryl group cleavage from tin. Use of aryl-magnesium or -lithium compounds again achieved only limited success. There were two reasons for this, firstly the problems incurred in restricting substitution at tin to mono- as opposed to bis-substitution. This can only be satisfactorily achieved by the use of substituents of a physical size large enough to prevent the bis-substitution. Secondly the formation of an alkyl halide side

product from the initial direct addition reaction resulting in reduction of the isolated yields of the required monoorganotin trihalide. This result together with the literature reported room temperature instability of mono-t-butytin trichloride[176] brings into question the overall stability of sterically hindered monoorganotin trihalides.

From the above work cage structures were obtained but the inability to reliably and reproducibly prepare sterically hindered monoorganotin trihalide precursors in good yield restricted the scope of the work. Further investigation to solve problems encountered in the preliminary synthetic stage is required before further progress in this area can be made.

APPENDIX I.

Synthesis and Preparation of Starting Materials.

I.1 Tin(IV) Reagents.

n-Butyltin trichloride, diphenyltin dichloride and triphenyltin chloride were all purchased from the Aldrich Chemical Company. Other tin reagents commercially purchased were dibenzyltin dichloride from Alfa Chemicals, anhydrous tin(IV) chloride from Fluka Chemicals and anhydrous tin(IV) bromide from BDH Chemicals. All of the above were used in synthesis without further purification.

I.2 Alkyl and Aryl Halides.

i-Propyl and mesityl bromides as well as t-butyl and neophyl chlorides were all purchased from the Aldrich Chemical Company. Only the t-butyl chloride was specially distilled prior to use, the others were used as received without further purification. 2,4,6-tri-i-propylphenyl bromide was purchased from Lancaster Synthesis and used without additional purification.

I.3 Arylboronic Acid Reagents.

Phenylboronic acid was purchased from the Aldrich Chemical Company. The preparation of mesitylboronic acid was achieved by the route cited in the literature by Khotinsky and Melamed[254] from the reaction between the mesityl Grignard reagent and trimethylborate followed by the hydrolysis of the intermediate bis(methoxy)mesitylborane (equations 109 and 110).

$$RMgBr + B(OMe)_3 \rightarrow RB(OMe)_2 + MgO + MeBr \quad (109)$$

$$RB(OMe)_2 + 2H_2O \rightarrow RB(OH)_2 + 2MeOH \quad (110)$$

R = 2,4,6-trimethylphenyl (mesityl)

The impure product was recrystallised from chloroform/60-80 petrol to give a colourless crystalline product with m.pt. 177°C.

I.4 Preparation of Tris(trimethylsilyl)methane (Tsi)H.

(Tsi)H was synthesised by the route cited by Merker and Scott[255] from the reaction between trimethylsilyl chloride, magnesium turnings and bromoform in a dry tetrahydrofuran solution (equation 111).

$$3Me_3SiCl + CHBr_3 + 3Mg \rightarrow (Me_3Si)_3CH + 3MgX_2 \quad (111)$$

From the reaction bis, tris and tetrakis trimethylsilyl substituted

methane products are obtained. To purify the product a multi-stage fractional distillation is employed generating a pure sample with b.pt. 108°C/20 mm.

I.5 Purification and Drying of Solvents.

In the research detailed in this thesis many references are made to the usage of dry diethyl ether and tetrahydrofuran. To dry these solvents a standard technique was employed whereby the solvent is refluxed in the presence of either sodium/lead alloy or sodium wire and benzophenone. Under dry conditions an intense blue colour is observed as a result of the benzophenone radical present in solution. On hydrolysis the radical is immediately quenched resulting in the disappearance of the blue coloration.

APPENDIX II.

CRYSTALLOGRAPHIC ANALYSIS AND STRUCTURAL REFINEMENT OF 1,2-DIBROMO-1,1,2,2-TETRA(2,4,6-TRI-i-PROPYLPHENYL)DISTANNANE (1).

II.1 Crystal Data.

$C_{60}H_{92}Br_2Sn_2$, M.W. = 1210.58, monoclinic, space group = $P2_1/n$.

a = 10.723(3)Å, b = 35.225(7)Å, c = 16.076(3)Å.

α = 90.0, β = 91.50(2), γ = 90.0.

U = 6070.46 Å^3, μ = 20.68 cm^{-1}, F(000) = 2448.

Radiation Mo-K$_\alpha$, λ = 0.71069Å, graphite monochromator.

For 4982 observed and unique reflections with $I > 3\sigma I$, R = 0.0562 and R_w = 0.0531.

II.2 Crystallographic Analysis.

A crystal of approximate dimensions 0.25 × 0.25 × 0.25 mm was glued to the top of a glass fibre and placed on a goniometer head. The same crystal was used for preliminary crystal analysis prior to the main data collection which was executed on a Hilger and Watts Y290 Automatic four circle diffractometer. The intensities of all reflections with $2^\circ < \theta < 22^\circ$ were measured. One reflection was used as a standard and its intensity monitored every fifty observed reflections. No significant crystal decay was observed.

II.3 Structure Solution and Refinement.

The crystal structure was solved using a Patterson search (SHELX86[256]) and refined by full matrix least-squares using SHELX76.[257] Data were corrected for Lorentz and polarisation effects but not for absorption. Hydrogen atoms were included in calculated positions. The tin and bromine atoms present in the molecule were refined anisotropically, while the remaining atoms were refined isotropically. The atomic scattering factors for hydrogen and non-hydrogen atoms and the anomolous dispersion correction factors for non-hydrogen atoms were taken from the literature.[258-260] The ORTEP program[261] was used for the drawing of the crystal structure (figure 17). The fractional atomic coordinates (Å) for the molecule are given in table 22, anisotropic thermal parameters (Å) in table 23 and the bond lengths (Å) and bond angles (°) are given in tables 24 and 25 respectively.

Table 22: Fractional Atomic Coordinates and Thermal Parameters (Å) for 1,2-Dibromo-1,1,2,2-tetra(2,4,6-tri-i-propylphenyl)-distannane (1).

Atom	x	y	z	Uiso or Ueq (***)	
Sn1	0.18129(7)	0.09039(2)	0.15218(4)	0.0436(5)	***
Sn2	0.31152(7)	0.12140(2)	0.01634(4)	0.0428(4)	***
Br1	-0.03538(11)	0.08346(4)	0.08457(7)	0.0643(8)	***
Br2	0.53182(12)	0.10671(3)	0.06806(8)	0.0658(8)	***
C1	0.1890(10)	0.0369(3)	0.2215(6)	0.050(3)	
C2	0.2767(10)	0.0094(3)	0.2085(6)	0.052(3)	
C3	0.2802(12)	-0.0230(3)	0.2616(7)	0.068(3)	
C4	0.1972(12)	-0.0263(3)	0.3225(8)	0.073(4)	
C5	0.1085(12)	0.0008(3)	0.3359(8)	0.074(4)	
C6	0.0999(11)	0.0334(3)	0.2848(7)	0.059(3)	
C7	0.3741(11)	0.0102(3)	0.1424(7)	0.064(3)	
C8	0.5059(12)	0.0157(4)	0.1786(8)	0.084(4)	
C9	0.3725(13)	-0.0255(4)	0.0884(8)	0.084(4)	
C10	0.2003(16)	-0.0609(5)	0.3812(11)	0.115(5)	
C11	0.1546(20)	-0.0945(5)	0.3531(12)	0.156(7)	
C12	0.2723(17)	-0.0559(4)	0.4578(9)	0.122(6)	
C13	-0.0010(11)	0.0618(3)	0.3024(7)	0.065(3)	
C14	-0.1299(12)	0.0444(4)	0.2919(8)	0.081(4)	
C15	0.0136(13)	0.0792(4)	0.3898(7)	0.078(4)	
C16	0.1923(10)	0.1346(3)	0.2489(6)	0.050(3)	
C17	0.1014(10)	0.1630(3)	0.2567(6)	0.053(3)	
C18	0.1035(11)	0.1851(3)	0.3302(7)	0.062(3)	
C19	0.1933(11)	0.1802(3)	0.3904(7)	0.063(3)	
C20	0.2837(11)	0.1538(3)	0.3805(7)	0.062(3)	

Table 22: Continued-

C21	0.2879(10)	0.1307(3)	0.3099(6)	0.052(3)
C22	0.0028(11)	0.1724(3)	0.1901(7)	0.067(3)
C23	0.0035(13)	0.2138(3)	0.1646(8)	0.081(4)
C24	-0.1248(13)	0.1607(4)	0.2176(8)	0.091(4)
C25	0.1910(14)	0.2053(4)	0.4684(8)	0.084(4)
C26	0.2735(15)	0.2381(4)	0.4598(9)	0.108(5)
C27	0.1812(18)	0.1867(5)	0.5440(10)	0.137(6)
C28	0.3957(10)	0.1031(3)	0.3022(7)	0.056(3)
C29	0.5221(12)	0.1235(3)	0.3008(7)	0.075(4)
C30	0.3988(12)	0.0729(3)	0.3726(7)	0.071(4)
C31	0.2600(10)	0.1819(3)	0.0137(6)	0.046(3)
C32	0.3281(10)	0.2091(3)	0.0640(6)	0.054(3)
C33	0.2978(11)	0.2483(3)	0.0511(7)	0.066(3)
C34	0.2069(11)	0.2586(3)	-0.0067(7)	0.065(3)
C35	0.1447(12)	0.2322(3)	-0.0513(7)	0.072(4)
C36	0.1710(11)	0.1931(3)	-0.0420(7)	0.058(3)
C37	0.4226(11)	0.1997(3)	0.1304(7)	0.060(3)
C38	0.5519(12)	0.2078(4)	0.1016(8)	0.085(4)
C39	0.4008(12)	0.2201(3)	0.2127(7)	0.075(4)
C40	0.1714(13)	0.3011(4)	-0.0177(8)	0.083(4)
C41	0.2807(13)	0.3238(4)	-0.0435(9)	0.096(4)
C42	0.1091(14)	0.3170(4)	0.0548(8)	0.101(5)
C43	0.0859(11)	0.1658(3)	-0.0911(7)	0.067(3)
C44	-0.0493(12)	0.1683(4)	-0.0666(8)	0.087(4)
C45	0.0959(14)	0.1697(4)	-0.1840(8)	0.092(4)
C46	0.3244(9)	0.1035(3)	-0.1129(6)	0.041(2)
C47	0.2399(10)	0.0758(3)	-0.1464(6)	0.047(3)
C48	0.2500(10)	0.0658(3)	-0.2295(6)	0.055(3)
C49	0.3364(11)	0.0824(3)	-0.2799(7)	0.057(3)
C50	0.4136(11)	0.1100(3)	-0.2475(7)	0.057(3)

Table 22: Continued-

C51	0.4092(10)	0.1213(3)	-0.1646(6)	0.053(3)
C52	0.1444(10)	0.0570(3)	-0.0940(6)	0.053(3)
C53	0.1882(13)	0.0192(3)	-0.0642(8)	0.081(4)
C54	0.0146(12)	0.0537(4)	-0.1372(7)	0.077(4)
C55	0.3408(12)	0.0722(4)	-0.3733(7)	0.073(4)
C56	0.3893(13)	0.0329(4)	-0.3863(8)	0.089(4)
C57	0.2151(15)	0.0741(5)	-0.4153(10)	0.121(6)
C58	0.4950(11)	0.1539(3)	-0.1341(7)	0.064(3)
C59	0.4652(13)	0.1907(4)	-0.1773(8)	0.086(4)
C60	0.6338(13)	0.1436(4)	-0.1455(9)	0.096(4)

Table 23: Anisotropic Thermal Parameters (Å) for 1,2-Dibromo-1,1,2,2-tetra(2,4,6-tri-i-propylphenyl)distannane (1).

Atom	U11	U22	U33	U23	U13	U12
Sn1	0.0507(5)	0.0379(4)	0.0421(4)	-0.0018(3)	-0.0011(3)	-0.0049(4
Sn2	0.0467(5)	0.0351(4)	0.0466(4)	0.0008(3)	-0.0026(3)	-0.0026(4)
Br1	0.054(1)	0.079(1)	0.060(1)	-0.011(1)	-0.003(1)	-0.010(1)
Br2	0.055(1)	0.065(1)	0.078(1)	0.005(1)	-0.011(1)	0.006(1)

Table 24: Bond Lengths (Å) for 1,2-Dibromo-1,1,2,2-tetra(2,4,6-tri-i-propylphenyl)distannane (1).

Sn1 -Sn2	2.841(1)	Sn1 -Br1	2.551(1)
Sn1 -C1	2.191(10)	Sn1 -C16	2.202(10)
Sn2 -Br2	2.537(1)	Sn2 -C31	2.201(10)
Sn2 -C46	2.179(9)	C1 -C2	1.369(14)
C1 -C6	1.419(14)	C2 -C3	1.426(14)
C2 -C7	1.509(14)	C3 -C4	1.345(15)
C4 -C5	1.369(16)	C4 -C10	1.540(19)
C5 -C6	1.415(15)	C6 -C13	1.506(15)
C7 -C8	1.527(16)	C7 -C9	1.525(15)
C10 -C11	1.356(20)	C10 -C12	1.447(19)
C13 -C14	1.517(16)	C13 -C15	1.537(15)
C16 -C17	1.403(14)	C16 -C21	1.408(14)
C17 -C18	1.415(14)	C17 -C22	1.521(15)
C18 -C19	1.358(15)	C19 -C20	1.358(15)
C19 -C25	1.534(16)	C20 -C21	1.398(14)
C21 -C28	1.517(14)	C22 -C23	1.515(15)
C22 -C24	1.506(17)	C25 -C26	1.464(17)
C25 -C27	1.388(17)	C28 -C29	1.534(15)
C28 -C30	1.553(14)	C31 -C32	1.441(14)
C31 -C36	1.351(14)	C32 -C33	1.433(14)
C32 -C37	1.489(14)	C33 -C34	1.377(15)
C34 -C35	1.342(15)	C34 -C40	1.551(16)
C35 -C36	1.414(15)	C36 -C43	1.531(15)
C37 -C38	1.501(16)	C37 -C39	1.529(15)
C40 -C41	1.487(17)	C40 -C42	1.469(17)
C43 -C44	1.515(17)	C43 -C45	1.507(15)
C46 -C47	1.427(13)	C46 -C51	1.396(13)

Table 24: Continued-

C47 -C48	1.389(13)	C47 -C52	1.496(14)
C48 -C49	1.377(14)	C49 -C50	1.371(14)
C49 -C55	1.545(15)	C50 -C51	1.392(13)
C51 -C58	1.545(15)	C52 -C53	1.489(14)
C52 -C54	1.543(15)	C55 -C56	1.496(16)
C55 -C57	1.493(18)	C58 -C59	1.500(15)
C58 -C60	1.546(18)		

Table 25: Bond Angles (°) for 1,2-Dibromo-1,1,2,2-tetra(2,4,6-tri-i-propylphenyl)distannane (1).

Br1	-Sn1	-Sn2	99.8(1)	C1 -Sn1 -Sn2	135.2(3)
C1	-Sn1	-Br1	99.0(3)	C16 -Sn1 -Sn2	104.6(3)
C16	-Sn1	-Br1	113.6(3)	C16 -Sn1 -C1	104.4(4)
Br2	-Sn2	-Sn1	98.2(1)	C31 -Sn2 -Sn1	105.0(3)
C31	-Sn2	-Br2	115.8(3)	C46 -Sn2 -Sn1	131.8(3)
C46	-Sn2	-Br2	99.9(3)	C46 -Sn2 -C31	106.5(4)
C2	-C1	-Sn1	123.2(8)	C6 -C1 -Sn1	114.9(8)
C6	-C1	-C2	122(1)	C3 -C2 -C1	119(1)
C7	-C2	-C1	126(1)	C7 -C2 -C3	115(1)
C4	-C3	-C2	120(1)	C5 -C4 -C3	122(1)
C10	-C4	-C3	121(1)	C10 -C4 -C5	117(1)
C6	-C5	-C4	121(1)	C5 -C6 -C1	117(1)
C13	-C6	-C1	125(1)	C13 -C6 -C5	118(1)
C8	-C7	-C2	112.6(9)	C9 -C7 -C2	113(1)
C9	-C7	-C8	108(1)	C11 -C10 -C4	119(1)
C12	-C10	-C4	115(1)	C12 -C10 -C11	125(2)
C14	-C13	-C6	111.6(9)	C15 -C13 -C6	112(1)
C15	-C13	-C14	109(1)	C17 -C16 -Sn1	122.8(8)
C21	-C16	-Sn1	116.5(7)	C21 -C16 -C17	120.2(9)
C18	-C17	-C16	118(1)	C22 -C17 -C16	124(1)
C22	-C17	-C18	117(1)	C19 -C18 -C17	121(1)
C20	-C19	-C18	120(1)	C25 -C19 -C18	119(1)
C25	-C19	-C20	121(1)	C21 -C20 -C19	122(1)
C20	-C21	-C16	118(1)	C28 -C21 -C16	123.3(9)
C28	-C21	-C20	119(1)	C23 -C22 -C17	113(1)
C24	-C22	-C17	111(1)	C24 -C22 -C23	111(1)
C26	-C25	-C19	111(1)	C27 -C25 -C19	117(1)

Table 25: Continued-

C27 -C25 -C26	121(1)	C29 -C28 -C21	112.1(9)
C30 -C28 -C21	112.4(9)	C30 -C28 -C29	109.2(9)
C32 -C31 -Sn2	120.7(7)	C36 -C31 -Sn2	118.0(8)
C36 -C31 -C32	121(1)	C33 -C32 -C31	117(1)
C37 -C32 -C31	125(1)	C37 -C32 -C33	118(1)
C34 -C33 -C32	120(1)	C35 -C34 -C33	121(1)
C40 -C34 -C33	120(1)	C40 -C34 -C35	119(1)
C36 -C35 -C34	122(1)	C35 -C36 -C31	119(1)
C43 -C36 -C31	124(1)	C43 -C36 -C35	116(1)
C38 -C37 -C32	111(1)	C39 -C37 -C32	113(1)
C39 -C37 -C38	110(1)	C41 -C40 -C34	111(1)
C42 -C40 -C34	113(1)	C42 -C40 -C41	113(1)
C44 -C43 -C36	113(1)	C45 -C43 -C36	113(1)
C45 -C43 -C44	110(1)	C47 -C46 -Sn2	120.1(7)
C51 -C46 -Sn2	119.7(7)	C51 -C46 -C47	120.0(9)
C48 -C47 -C46	118.1(9)	C52 -C47 -C46	121.9(9)
C52 -C47 -C48	120.0(9)	C49 -C48 -C47	122(1)
C50 -C49 -C48	119(1)	C55 -C49 -C48	121(1)
C55 -C49 -C50	120(1)	C51 -C50 -C49	122(1)
C50 -C51 -C46	119(1)	C58 -C51 -C46	122.5(9)
C58 -C51 -C50	119(1)	C53 -C52 -C47	111(1)
C54 -C52 -C47	113.8(9)	C54 -C52 -C53	110(1)
C56 -C55 -C49	112(1)	C57 -C55 -C49	112(1)
C57 -C55 -C56	107(1)	C59 -C58 -C51	112(1)
C60 -C58 -C51	111(1)	C60 -C58 -C59	110(1)

APPENDIX III.

CRYSTALLOGRAPHIC ANALYSIS AND STRUCTURAL REFINEMENT OF DIBENZYL[TRIS-(TRIMETHYLSILYL)METHYL][TRIMETHYLSILOXY]STANNANE (8).

III.1 Crystal Data.

$C_{27}H_{50}OSi_4Sn$ M.W. = 621.63, monoclinic, space group = $P2_1/a$.

a = 17.037(3)Å, b = 11.566(2)Å, c = 18.423(4)Å.

α = 90.0, β = 112.06(2), γ = 90.0.

U = 3364.79 $Å^3$, μ = 8.73 cm^{-1}, F(000) = 1552.

Radiation Mo-K_α, λ = 0.71069 Å, graphite monochromator.

For 2699 observed and unique reflections with $I > 3\sigma I$, R = 0.0685 and R_w = 0.0685.

III.2 Crystallographic Analysis.

A crystal of approximate dimensions 0.2 × 0.4 × 0.2 mm was used for both the preliminary crystal analysis and the main data collection. The intensities of all reflections with $2° < \theta < 22°$ were measured. One reflection was used as a standard and its intensity monitored every fifty observed reflections. No significant crystal decay was observed.

III.3 Structure Solution and Refinement.

The crystal structure was solved using a Patterson search (SHELX86[256]) and refined by full matrix least-squares using SHELX76.[257] Data were corrected for Lorentz and polarisation effects and for absorption.[262] Hydrogen atoms were included in calculated positions. The tin and silicon atoms present in the molecule were refined anisotropically, while the remaining atoms were refined isotropically. The atomic scattering factors for hydrogen and non-hydrogen atoms and the anomolous dispersion correction factors for non-hydrogen atoms were taken from the literature.[258-260] The ORTEP program[261] was used for the drawing of the crystal structure (figure 19). The fractional atomic coordinates (Å) for the molecule are given in table 26, anisotropic thermal parameters (Å) in table 27 and the bond lengths (Å) and bond angles (°) are given in tables 28 and 29 respectively.

Table 26: Fractional Atomic Coordinates and Thermal Parameters (Å) for Dibenzyl[tris(trimethylsilyl)methyl]trimethylsiloxystannane (8).

Atom	x	y	z	Uiso or Ueq (***)	
Sn1	0.00421(6)	0.04127(8)	0.22010(6)	0.0441(5)	***
Si1	0.18384(3)	0.06764(4)	0.37423(3)	0.0663(3)	***
Si2	0.03777(3)	0.24328(4)	0.35740(3)	0.0652(3)	***
Si3	0.13293(3)	0.25987(4)	0.24260(3)	0.0710(3)	***
Si4	-0.04695(4)	-0.20536(4)	0.30392(3)	0.0790(4)	***
C25	-0.11050(12)	-0.29202(16)	0.21763(11)	0.1008(16)	***
C26	-0.11238(22)	-0.16372(22)	0.35463(20)	0.3483(50)	***
C27	0.03374(19)	-0.29337(21)	0.36820(15)	0.1912(31)	***
O1	-0.0050(7)	-0.0930(9)	0.2789(7)	0.069(3)	
C1	0.0944(8)	0.1568(12)	0.3027(8)	0.048(3)	
C2	0.2837(11)	0.1509(17)	0.4227(11)	0.094(6)	
C3	0.1562(11)	0.0010(16)	0.4550(11)	0.091(6)	
C4	0.2135(11)	-0.0563(16)	0.3228(11)	0.089(6)	
C5	0.1841(11)	0.3949(15)	0.2962(11)	0.084(5)	
C6	0.0470(10)	0.3029(15)	0.1485(10)	0.079(5)	
C7	0.2131(11)	0.1911(17)	0.2056(11)	0.091(6)	
C8	-0.0306(11)	0.3637(15)	0.2975(10)	0.083(5)	
C9	0.1132(11)	0.3133(16)	0.4474(10)	0.087(6)	
C10	-0.0344(10)	0.1502(14)	0.3885(10)	0.071(5)	
C11	0.0404(9)	-0.0235(13)	0.1267(9)	0.060(4)	
C12	0.0192(9)	-0.1474(13)	0.1059(9)	0.054(4)	
C13	-0.0594(9)	-0.1786(13)	0.0519(9)	0.058(4)	

Table 26: Continued-

C14	-0.0785(11)	-0.2946(15)	0.0331(10)	0.073(5)
C15	-0.0195(10)	-0.3791(16)	0.0655(10)	0.077(5)
C16	0.0576(11)	-0.3493(17)	0.1176(11)	0.083(5)
C17	0.0791(10)	-0.2342(14)	0.1381(10)	0.069(5)
C18	-0.1238(9)	0.1092(15)	0.1739(10)	0.074(5)
C19	-0.1777(8)	0.0604(12)	0.0941(8)	0.046(3)
C20	-0.2342(10)	-0.0264(15)	0.0890(10)	0.075(5)
C21	-0.2856(11)	-0.0757(16)	0.0159(11)	0.084(5)
C22	-0.2790(12)	-0.0292(19)	-0.0470(12)	0.098(6)
C23	-0.2267(11)	0.0553(17)	-0.0471(11)	0.084(5)
C24	-0.1757(10)	0.1026(14)	0.0226(10)	0.068(4)

Table 27: Anisotropic Thermal Parameters (Å) for Dibenzyl[tris-(trimethylsilyl)methyl]trimethylsiloxystannane (8).

Atom	U11	U22	U33	U23	U13	U12
Sn1	0.040(1)	0.043(1)	0.049(1)	-0.004(1)	0.016(1)	0.000(1)
Si1	0.054(3)	0.081(3)	0.064(3)	0.001(3)	0.006(2)	0.007(2)
Si2	0.058(3)	0.064(3)	0.073(3)	-0.017(2)	0.025(2)	-0.006(2)
Si3	0.070(3)	0.063(3)	0.079(4)	-0.002(3)	0.031(3)	-0.016(2)
Si4	0.126(5)	0.061(3)	0.050(3)	0.000(2)	0.034(3)	-0.026(3)
C25	0.129(18)	0.080(14)	0.093(16)	-0.017(11)	0.047(13)	-0.031(12)
C26	0.506(65)	0.100(21)	0.439(63)	-0.107(29)	0.414(58)	-0.144(32)
C27	0.322(45)	0.086(20)	0.165(29)	0.025(19)	-0.077(29)	-0.039(25)

Table 28: Bond Lengths (Å) for Dibenzyl[tris(trimethylsilyl)methyl]-trimethylsiloxystannane (8).

Sn1 -Si3	3.270(5)	Sn1 -O1	1.933(11)
Sn1 -C1	2.170(14)	Sn1 -C11	2.167(15)
Sn1 -C18	2.169(15)	Si1 -C1	1.901(14)
Si1 -C2	1.865(18)	Si1 -C3	1.886(18)
Si1 -C4	1.888(19)	Si2 -C1	1.918(14)
Si2 -C8	1.884(17)	Si2 -C9	1.859(17)
Si2 -C10	1.879(16)	Si3 -C1	1.903(15)
Si3 -C5	1.878(17)	Si3 -C6	1.869(17)
Si3 -C7	1.914(18)	Si4 -O1	1.631(11)
Si4 -C25	1.847(17)	Si4 -C26	1.769(24)
Si4 -C27	1.762(24)	C11 -C12	1.491(20)
C12 -C13	1.384(19)	C12 -C17	1.395(20)
C13 -C14	1.393(21)	C14 -C15	1.368(21)
C15 -C16	1.349(22)	C16 -C17	1.395(23)
C18 -C19	1.519(20)	C19 -C20	1.370(20)
C19 -C24	1.417(20)	C20 -C21	1.421(23)
C21 -C22	1.319(24)	C22 -C23	1.324(24)
C23 -C24	1.366(22)		

Table 29: Bond Angles (°) for Dibenzyl[tris(trimethylsilyl)methyl]-trimethylsiloxystannane (8).

O1	-Sn1	-Si3	137.9(3)	C1	-Sn1	-Si3	33.9(4)
C1	-Sn1	-O1	106.7(5)	C11	-Sn1	-Si3	89.5(4)
C11	-Sn1	-O1	105.9(5)	C11	-Sn1	-C1	115.6(5)
C18	-Sn1	-Si3	107.3(5)	C18	-Sn1	-O1	103.3(6)
C18	-Sn1	-C1	113.3(6)	C18	-Sn1	-C11	111.0(6)
C2	-Si1	-C1	113.6(8)	C3	-Si1	-C1	113.3(7)
C3	-Si1	-C2	106.6(8)	C4	-Si1	-C1	111.1(8)
C4	-Si1	-C2	105.3(8)	C4	-Si1	-C3	106.2(9)
C8	-Si2	-C1	113.6(8)	C9	-Si2	-C1	112.3(7)
C9	-Si2	-C8	105.6(8)	C10	-Si2	-C1	112.2(7)
C10	-Si2	-C8	105.7(8)	C10	-Si2	-C9	106.8(8)
C1	-Si3	-Sn1	39.5(4)	C5	-Si3	-Sn1	150.0(6)
C5	-Si3	-C1	114.1(8)	C6	-Si3	-Sn1	80.4(6)
C6	-Si3	-C1	112.7(7)	C6	-Si3	-C5	108.3(8)
C7	-Si3	-Sn1	99.7(6)	C7	-Si3	-C1	113.3(8)
C7	-Si3	-C5	106.3(8)	C7	-Si3	-C6	101.3(8)
C25	-Si4	-O1	111.5(8)	C26	-Si4	-O1	111.3(9)
C26	-Si4	-C25	109(1)	C27	-Si4	-O1	110(1)
C27	-Si4	-C25	109(1)	C27	-Si4	-C26	107(2)
Si4	-O1	-Sn1	159.2(7)	Si1	-C1	-Sn1	108.9(6)
Si2	-C1	-Sn1	109.0(6)	Si2	-C1	-Si1	110.4(7)
Si3	-C1	-Sn1	106.6(7)	Si3	-C1	-Si1	112.4(7)
Si3	-C1	-Si2	109.3(7)	C12	-C11	-Sn1	115(1)
C13	-C12	-C11	121(1)	C17	-C12	-C11	121(1)

Table 29: Continued-

C17 -C12 -C13	118(1)	C14 -C13 -C12	120(1)
C15 -C14 -C13	121(2)	C16 -C15 -C14	119(2)
C17 -C16 -C15	121(2)	C16 -C17 -C12	120(2)
C19 -C18 -Sn1	113(1)	C20 -C19 -C18	119(1)
C24 -C19 -C18	124(1)	C24 -C19 -C20	117(1)
C21 -C20 -C19	122(2)	C22 -C21 -C20	116(2)
C23 -C22 -C21	126(2)	C24 -C23 -C22	119(2)
C23 -C24 -C19	120(2)		

APPENDIX IV.

CRYSTALLOGRAPHIC ANALYSIS AND STRUCTURAL REFINEMENT OF 1,1-BIS-(TRIMETHYLSILYL)-3-(DIBENZYL[TRIS(TRIMETHYLSILYL)METHYL]STANNYL)-PROP-1-ENE (9).

IV.1 Crystal Data.

$C_{33}H_{62}Si_6Sn$, M.W. = 718.00, triclinic, space group = $P\bar{1}$.

a = 9.478(3)Å, b = 12.932(3)Å, c = 17.512(4)Å.

α = 98.07(1), β = 98.26(2), γ = 103.39(2).

U = 2032.54 Å^3, μ = 7.20 cm^{-1}, F(000) = 760.00.

Radiation Mo-K$_\alpha$, λ = 0.71069 Å, graphite monochromator.

For 3395 observed and unique reflections with $I > 3\sigma I$, R = 0.0843 and R_w = 0.0837.

IV.2 Crystallographic Analysis.

A crystal of approximate dimensions 0.25 × 0.25 × 0.30 mm was used for both the preliminary crystal analysis and the main data collection. The intensities of all reflections $2^\circ < \theta < 22^\circ$ were measured. One reflection was used as a standard and its intensity monitored every fifty observed reflections. No significant crystal decay was observed.

IV.3 Structure Solution and Refinement.

The crystal structure was solved using a Patterson search (SHELX86[256]) and refined by full matrix least-squares using SHELX76.[257] Data were corrected for Lorentz and polarisation effects but not for absorption. Hydrogen atoms were included in calculated positions. The tin, silicon and some of the carbons present in the molecule (C1 - C20 inclusive and C27) were refined anisotropically, while the remaining atoms were refined isotropically. The atomic scattering factors for hydrogen and non-hydrogen atoms and the anomolous dispersion correction for non-hydrogen atoms were taken from the literature.[258-260] The ORTEP program[261] was used for the drawing of the crystal structure (figure 20). The fractional atomic coordinates (Å) for the molecule are given in table 30, the anisotropic thermal parameters (Å) in table 31 and the bond lengths (Å) and bond angles (°) are given in tables 32 and 33 respectively.

Table 30: Fractional Atomic Coordinates and Thermal Parameters (Å) for 1,1-Bis(trimethylsilyl)-3-{dibenzyl[tris(trimethylsilyl)-methyl]stannyl}prop-1-ene (**9**).

Atom	x	y	z	Uiso or Ueq (***)	
Sn1	0.25065(12)	0.14056(8)	0.21837(6)	0.0454(6)	***
Si1	0.13447(9)	-0.12839(4)	0.19388(3)	0.1139(5)	***
Si2	0.22563(8)	-0.00135(5)	0.36364(3)	0.1097(5)	***
Si3	-0.06465(8)	0.00869(6)	0.26035(5)	0.1495(6)	***
Si4	0.72613(5)	0.46190(4)	0.40440(3)	0.0690(3)	***
Si5	0.47682(5)	0.55775(3)	0.31228(3)	0.0694(3)	***
C1	0.33214(22)	-0.16286(16)	0.22649(15)	0.1420(19)	***
C2	0.12985(21)	-0.11737(14)	0.09058(9)	0.0838(13)	***
C3	-0.00148(21)	-0.25211(13)	0.20025(12)	0.0947(14)	***
C4	0.16528(33)	0.10730(16)	0.43865(11)	0.1519(21)	***
C5	0.16806(23)	-0.12975(15)	0.40077(11)	0.1075(15)	***
C6	0.42304(24)	0.04543(16)	0.38431(12)	0.1141(17)	***
C7	-0.08256(21)	0.14538(14)	0.28045(12)	0.0993(15)	***
C8	-0.16147(24)	-0.07497(16)	0.32559(13)	0.1273(18)	***
C9	-0.18050(22)	-0.05276(19)	0.15103(12)	0.1263(19)	***
C10	0.13192(16)	-0.00266(10)	0.26309(7)	0.0539(9)	***
C11	0.29397(16)	0.29507(10)	0.29881(8)	0.0558(9)	***
C12	0.44564(17)	0.33996(11)	0.34160(7)	0.0517(9)	***
C13	0.53706(16)	0.43948(11)	0.34959(7)	0.0543(9)	***
C14	0.76134(24)	0.55617(15)	0.49884(10)	0.1035(16)	***
C15	0.75868(22)	0.33470(15)	0.43087(13)	0.1104(16)	***
C16	0.85865(22)	0.50919(20)	0.34356(13)	0.1378(21)	***
C17	0.52894(25)	0.56987(17)	0.21435(11)	0.1247(18)	***
C18	0.56741(25)	0.68633(13)	0.38157(12)	0.1128(17)	***
C19	0.27822(21)	0.55151(14)	0.30279(13)	0.1154(17)	***

Table 30: Continued-

C27	0.11891(20)	0.15228(12)	0.10691(8)	0.0737(11) ***
C21	0.5171(18)	0.1795(13)	0.1318(9)	0.070(4)
C22	0.4873(21)	0.1271(15)	0.0562(10)	0.088(5)
C23	0.5317(21)	0.1804(15)	-0.0049(11)	0.093(5)
C24	0.6047(21)	0.2871(15)	0.0129(11)	0.095(6)
C25	0.6337(22)	0.3411(17)	0.0869(11)	0.100(6)
C26	0.5954(20)	0.2893(14)	0.1486(11)	0.087(5)
C28	0.1287(18)	0.2676(13)	0.0933(9)	0.069(4)
C29	0.0371(22)	0.3209(15)	0.1171(10)	0.090(5)
C30	0.0400(24)	0.4285(16)	0.1031(11)	0.106(6)
C31	0.1439(23)	0.4728(17)	0.0634(11)	0.105(6)
C32	0.2359(26)	0.4213(17)	0.0387(12)	0.115(7)
C33	0.2419(22)	0.3156(15)	0.0528(10)	0.094(6)

Table 31: Anisotropic Thermal Parameters (Å) for 1,1-Bis(trimethylsilyl)-3-(dibenzyl[tris(trimethylsilyl)methyl]stannyl)-prop-1-ene (**9**).

Atom	U11	U22	U33	U23	U13	U12
Sn1	0.046(1)	0.043(1)	0.048(1)	0.013(1)	0.009(1)	0.007(1)
Si1	0.190(7)	0.063(3)	0.088(4)	0.001(3)	0.047(4)	-0.010(4)
Si2	0.128(6)	0.105(4)	0.095(4)	0.057(4)	-0.003(4)	-0.012(4)
Si3	0.094(5)	0.114(5)	0.241(9)	0.077(5)	0.092(5)	0.028(4)
Si4	0.056(3)	0.076(3)	0.075(3)	0.000(2)	0.001(2)	0.005(2)
Si5	0.068(3)	0.053(3)	0.088(3)	0.019(2)	0.007(2)	0.005(2)
C1	0.090(17)	0.102(16)	0.234(25)	0.077(17)	0.070(16)	0.068(13)
C2	0.091(14)	0.079(12)	0.081(12)	0.001(9)	0.007(10)	0.020(10)
C3	0.086(15)	0.056(11)	0.142(17)	0.011(11)	0.007(12)	0.010(10)
C4	0.278(34)	0.105(17)	0.073(13)	-0.001(12)	0.078(18)	-0.005(19)
C5	0.117(17)	0.108(15)	0.098(13)	0.060(12)	0.022(12)	0.027(13)
C6	0.141(21)	0.098(15)	0.103(15)	0.047(12)	-0.016(14)	0.006(14)
C7	0.069(14)	0.105(15)	0.125(16)	0.003(12)	0.034(12)	0.028(11)
C8	0.119(19)	0.096(15)	0.167(20)	0.030(14)	0.086(16)	-0.005(13)
C9	0.060(14)	0.160(22)	0.159(21)	0.039(17)	-0.037(13)	-0.037(14)
C10	0.076(11)	0.033(8)	0.052(8)	0.002(6)	0.014(7)	-0.010(7)
C11	0.068(11)	0.034(8)	0.066(9)	0.003(7)	0.016(8)	0.007(7)
C12	0.069(11)	0.044(9)	0.041(8)	-0.007(6)	0.001(7)	-0.007(8)
C13	0.063(11)	0.053(9)	0.047(8)	0.000(7)	0.008(7)	0.010(8)
C14	0.121(19)	0.105(15)	0.085(13)	-0.014(11)	-0.026(12)	0.027(13)
C15	0.077(16)	0.098(15)	0.156(19)	-0.011(13)	-0.034(13)	0.040(12)
C16	0.058(15)	0.215(28)	0.141(19)	0.040(18)	0.021(13)	0.029(15)
C17	0.120(19)	0.132(18)	0.122(16)	0.070(14)	0.025(13)	0.061(15)
C18	0.130(19)	0.062(12)	0.146(19)	0.018(12)	-0.013(15)	0.001(12)
C19	0.102(17)	0.068(12)	0.177(21)	0.039(13)	0.051(15)	0.035(11)
C20	0.067(12)	0.066(10)	0.077(10)	0.016(8)	0.026(9)	0.022(8)
C27	0.111(14)	0.061(10)	0.049(9)	0.021(8)	-0.010(9)	0.023(9)

Table 32: Bond Lengths (Å) for 1,1-Bis(trimethylsilyl)-3-(dibenzyl-[tris(trimethylsilyl)methyl]stannyl)prop-1-ene (**9**).

Sn1 -C10	2.237(13)	Sn1 -C11	2.193(12)
Sn1 -C20	2.235(15)	Sn1 -C27	2.205(14)
Si1 -C1	2.046(19)	Si1 -C2	1.829(17)
Si1 -C3	1.836(17)	Si1 -C10	1.894(14)
Si2 -C4	2.024(21)	Si2 -C5	1.861(16)
Si2 -C6	1.794(22)	Si2 -C10	1.851(15)
Si3 -C7	1.805(18)	Si3 -C8	1.872(18)
Si3 -C9	2.017(21)	Si3 -C10	1.897(17)
Si4 -C13	1.845(15)	Si4 -C14	1.849(17)
Si4 -C15	1.851(18)	Si4 -C16	1.816(20)
Si5 -C13	1.916(15)	Si5 -C17	1.869(18)
Si5 -C18	1.857(17)	Si5 -C19	1.847(19)
C11 -C12	1.465(19)	C12 -C13	1.351(18)
C20 -C21	1.478(20)	C21 -C22	1.358(20)
C21 -C26	1.409(21)	C22 -C23	1.412(23)
C23 -C24	1.363(23)	C24 -C25	1.340(23)
C25 -C26	1.397(23)	C27 -C28	1.528(20)
C28 -C29	1.304(21)	C28 -C33	1.440(23)
C29 -C30	1.442(24)	C30 -C31	1.352(25)
C31 -C32	1.299(25)	C32 -C33	1.435(25)

Table 33: Bond Angles (°) for 1,1-Bis(trimethylsilyl)-3-(dibenzyl-[tris-(trimethylsilyl)methyl]stannyl)prop-1-ene (9).

C11 -Sn1 -C10	114.5(5)	C20 -Sn1 -C10	110.7(6)
C20 -Sn1 -C11	106.4(6)	C27 -Sn1 -C10	108.9(6)
C27 -Sn1 -C11	108.2(6)	C27 -Sn1 -C20	107.8(6)
C2 -Si1 -C1	103.6(9)	C3 -Si1 -C1	103.3(9)
C3 -Si1 -C2	108.9(9)	C10 -Si1 -C1	107.5(9)
C10 -Si1 -C2	116.6(7)	C10 -Si1 -C3	115.3(8)
C5 -Si2 -C4	103.4(9)	C6 -Si2 -C4	102(1)
C6 -Si2 -C5	109.4(9)	C10 -Si2 -C4	108.2(9)
C10 -Si2 -C5	114.7(8)	C10 -Si2 -C6	117.0(8)
C8 -Si3 -C7	110(1)	C9 -Si3 -C7	105(1)
C9 -Si3 -C8	105(1)	C10 -Si3 -C7	114.6(8)
C10 -Si3 -C8	112.0(9)	C10 -Si3 -C9	108.8(9)
C14 -Si4 -C13	112.5(8)	C15 -Si4 -C13	111.0(8)
C15 -Si4 -C14	105.0(9)	C16 -Si4 -C13	109.7(9)
C16 -Si4 -C14	111(1)	C16 -Si4 -C15	107(1)
C17 -Si5 -C13	109.8(8)	C18 -Si5 -C13	110.5(8)
C18 -Si5 -C17	109(1)	C19 -Si5 -C13	116.0(8)
C19 -Si5 -C17	108(1)	C19 -Si5 -C18	104(1)
Si1 -C10 -Sn1	107.7(6)	Si2 -C10 -Sn1	109.4(6)
Si2 -C10 -Si1	110.9(8)	Si3 -C10 -Sn1	106.4(7)
Si3 -C10 -Si1	110.2(7)	Si3 -C10 -Si2	112.1(8)
C12 -C11 -Sn1	116(1)	C13 -C12 -C11	130(1)
Si5 -C13 -Si4	119.4(8)	C12 -C13 -Si4	117(1)
C12 -C13 -Si5	123(1)	C21 -C20 -Sn1	112(1)
C22 -C21 -C20	120(1)	C26 -C21 -C20	121(1)
C26 -C21 -C22	118(2)	C23 -C22 -C21	122(2)
C24 -C23 -C22	119(2)	C25 -C24 -C23	121(2)

Table 33: Continued-

C26 -C25 -C24	121(2)	C25 -C26 -C21	119(2)
C28 -C27 -Sn1	115(1)	C29 -C28 -C27	121(2)
C33 -C28 -C27	118(2)	C33 -C28 -C29	121(2)
C30 -C29 -C28	123(2)	C31 -C30 -C29	116(2)
C32 -C31 -C30	122(2)	C33 -C32 -C31	124(2)
C32 -C33 -C28	113(2)		

APPENDIX V.

CRYSTALLOGRAPHIC ANALYSIS AND STRUCTURAL REFINEMENT OF 2,4-DIPHENYL-2,4-DI[TRIS(TRIMETHYLSILYL)METHYL]-1,3-DITHIA-2,4-DISTANNETANE (12).

V.1 Crystal Data.

$C_{32}H_{64}S_2Si_6Sn_2$, M.W. = 918.90, triclinic, space group = $P\bar{1}$.

a = 9.662(5)Å, b = 10.001(3)Å, c = 12.061(3)Å.

α = 96.12(2), β = 106.76(3), γ = 95.04(3).

U = 1101.00 Å^3, μ = 12.97 cm^{-1}, F(000) = 472.

Radiation Mo-K$_\alpha$, λ = 0.71069 Å, graphite monochromator.

For 1677 observed and unique reflections with $I > 3\sigma I$, R = 0.0962 and R_w = 0.0962 (unit weights).

V.2 Crystallographic Analysis.

A crystal of approximate dimensions 0.3 × 0.3 × 0.4 mm was used for both the preliminary crystal analysis and the main data collection. The intensities of all reflections with $2^\circ < \theta < 22^\circ$ were measured. One reflection was chosen as a standard and its intensity monitored every fifty observed reflections. No significant crystal decay was observed.

V.3 Structure Solution and Refinement.

The crystal structure was solved using a Patterson search (SHELX86[256]) and refined by full matrix least-squares using SHELX76.[257] Data were corrected for Lorentz and polarisation effects but not for absorption. Hydrogen atoms were not included in calculated positions. The tin, sulphur and silicon atoms present in the molecule were refined anisotropically, while the remaining atoms were refined isotropically. The atomic scattering factors and the anomolous dispersion correction factors for non-hydrogen atoms were taken from the literature.[258-260] The crystal used although not immediately apparent during preliminary crystal analysis was determined in the final structural refinement to be slightly 'twinned' giving rise to comparatively high R values for the final structure.

The ORTEP program[261] was used for the drawing of the crystal structure (figure 24). The fractional atomic coordinates for the molecule are given in table 34, the anisotropic thermal parameters (Å) in table 35 and the bond lengths (Å) and bond angles (°) are given in tables 36 and 37 respectively.

Table 34: Fractional Atomic Coordinates and Thermal Parameters (Å) for 2,4-Diphenyl-2,4-di[tris(trimethylsilyl)methyl]-1,3-dithia-2,4-distannetane (**12**).

Atom	x	y	z	Uiso or Ueq (***)	
Sn1	0.37541(2)	-0.12498(2)	0.91919(1)	0.0287(1)	***
S1	0.38919(7)	0.12314(6)	0.93505(5)	0.0337(4)	***
Si1	0.25180(9)	-0.40782(7)	0.74007(7)	0.0452(5)	***
Si2	0.22359(10)	-0.12991(8)	0.63442(6)	0.0491(5)	***
Si3	0.52874(11)	-0.23917(8)	0.71446(8)	0.0612(6)	***
C2	0.0827(18)	-0.1551(16)	0.9762(13)	0.043(7)	
C3	-0.0129(18)	-0.1912(16)	1.0384(13)	0.048(7)	
C4	0.0312(18)	-0.2662(16)	1.1308(13)	0.097(12)	
C5	0.1710(18)	-0.3050(16)	1.1610(13)	0.083(11)	
C6	0.2666(18)	-0.2689(16)	1.0988(13)	0.067(9)	
C1	0.2225(18)	-0.1940(16)	1.0064(13)	0.033(6)	
C7	0.3576(29)	-0.2302(24)	0.7410(21)	0.039(6)	
C8	0.0482(33)	-0.4102(28)	0.7174(25)	0.053(7)	
C9	0.2641(36)	-0.5306(31)	0.6118(27)	0.061(8)	
C10	0.3303(34)	-0.4851(28)	0.8760(25)	0.054(8)	
C11	0.0772(34)	-0.0664(28)	0.6932(25)	0.054(8)	
C12	0.1314(36)	-0.2363(30)	0.4885(27)	0.060(8)	
C13	0.3397(41)	0.0219(35)	0.6068(31)	0.076(10)	
C14	0.6675(37)	-0.0799(32)	0.7639(28)	0.065(9)	
C15	0.4961(44)	-0.2840(37)	0.5500(33)	0.084(11)	
C16	0.6458(42)	-0.3715(36)	0.7940(32)	0.080(10)	

Table 35: Anisotropic Thermal Parameters (Å) for 2,4-Diphenyl-2,4-di[tris(trimethylsilyl)methyl]-1,3-dithia-2,4-distannetane (12).

Atom	U11	U22	U33	U23	U13	U12
Sn1	0.030(1)	0.027(1)	0.029(1)	0.002(1)	0.007(1)	-0.001(1)
S1	0.035(4)	0.029(3)	0.037(3)	0.001(3)	0.001(3)	-0.002(3)
Si1	0.058(6)	0.037(4)	0.041(4)	0.002(3)	0.000(4)	0.001(4)
Si2	0.063(6)	0.047(4)	0.037(4)	0.010(3)	0.006(4)	0.006(4)
Si3	0.070(7)	0.046(5)	0.068(6)	-0.004(4)	0.036(5)	-0.002(4)

Table 36: Bond Lengths (Å) for 2,4-Diphenyl-2,4-di[tris(trimethylsilyl)methyl]-1,3-dithia-2,4-distannetane (12).

Sn1 -S1	2.457(6)	Sn1 -Si1	3.273(7)
Sn1 -C1	2.153(17)	Sn1 -C7	2.242(25)
Sn1 -Sn1	3.323(3)	Si1 -C7	1.968(25)
Si1 -C8	1.90(3)	Si1 -C9	1.91(3)
Si1 -C10	1.87(3)	Si2 -C7	1.97(3)
Si2 -C11	1.88(3)	Si2 -C12	1.89(3)
Si2 -C13	1.92(4)	Si3 -C7	1.78(3)
Si3 -C14	1.91(3)	Si3 -C15	1.91(4)
Si3 -C16	1.97(4)	C2 -C3	1.395(1)
C2 -C1	1.395(1)	C3 -C4	1.395(1)
C4 -C5	1.395(1)	C5 -C6	1.395(1)
C6 -C1	1.395(1)		

Table 37: Bond Angles (°) for 2,4-Diphenyl-2,4-di[tris(trimethylsilyl)methyl]-1,3-dithia-2,4-distannetane (12).

Si1	-Sn1	-S1	144.2(2)	C1 -Sn1 -S1	107.6(5)
C1	-Sn1	-Si1	85.1(5)	C7 -Sn1 -S1	114.8(6)
C7	-Sn1	-Si1	36.0(6)	C7 -Sn1 -C1	118.8(8)
C7	-Si1	-Sn1	42.1(7)	C8 -Si1 -Sn1	100.2(9)
C8	-Si1	-C7	115(1)	C9 -Si1 -Sn1	149(1)
C9	-Si1	-C7	109(1)	C9 -Si1 -C8	104(1)
C10	-Si1	-Sn1	82.5(9)	C10 -Si1 -C7	113(1)
C10	-Si1	-C8	108(1)	C10 -Si1 -C9	107(1)
C11	-Si2	-C7	114(1)	C12 -Si2 -C7	111(1)
C12	-Si2	-C11	108(1)	C13 -Si2 -C7	107(1)
C13	-Si2	-C11	109(1)	C13 -Si2 -C12	107(1)
C14	-Si3	-C7	117(1)	C15 -Si3 -C7	109(1)
C15	-Si3	-C14	106(2)	C16 -Si3 -C7	115(1)
C16	-Si3	-C14	100(1)	C16 -Si3 -C15	108(2)
C1	-C2	-C3	120.0(1)	C4 -C3 -C2	120.0(1)
C5	-C4	-C3	120.0(1)	C6 -C5 -C4	120.0(1)
C1	-C6	-C5	120.0(1)	C2 -C1 -Sn1	119.9(3)
C6	-C1	-Sn1	119.9(3)	C6 -C1 -C2	120.0(1)
Si1	-C7	-Sn1	102(1)	Si2 -C7 -Sn1	104(1)
Si2	-C7	-Si1	108(1)	Si3 -C7 -Sn1	114(1)
Si3	-C7	-Si1	114(1)	Si3 -C7 -Si2	115(1)

APPENDIX VI.

CRYSTALLOGRAPHIC ANALYSIS AND STRUCTURAL REFINEMENT OF 2,2,4,4-TETRA-(2,4,6-TRI-i-PROPYLPHENYL)-1,3-OXATHIA-2,4-DISTANNETANE (16).

VI.1 Crystal Data.

$C_{60}H_{92}OSSn_2$, M.W. = 1098.84, monoclinic, space group = $P2_1/n$.

a = 14.383(4)Å, b =21.031(4)Å, c = 20.562(7)Å.

α = 90.0, β = 91.845(2), γ = 90.0.

U = 6216.67 Å^3, μ =7.90 cm^{-1}, F(000) = 2304.

Radiation Mo-K_α, λ = 0.71069 Å, graphite monochromator.

For 3806 observed and unique reflections with $I > 3\sigma I$, R = 0.0665 and R_w = 0.0663.

VI.2 Crystallographic Analysis.

A crystal of approximate dimensions 0.2 × 0.2 × 0.2 mm was used for both the preliminary crystal analysis and the main data collection. The intensities of all reflections with $2^\circ < \theta < 22^\circ$ were measured. One reflection was used as a standard and its intensity monitored every fifty observed reflections. No significant crystal decay was seen.

VI.3 Structure Solution and Refinement.

The crystal structure was solved using a Patterson search (SHELX86[256]) and refined using blocked full matrix least-squares using SHELX76.[257] Data were corrected for Lorentz and polarisation effects but not for absorption. Hydrogen atoms were not included in calculated positions. The tin, sulphur, oxygen and i-propyl carbon atoms were refined anisotropically, while the remaining atoms in the molecule were refined isotropically. The atomic scattering factors and the anomolous dispersion correction factors for non-hydrogen atoms were taken from the literature.[258-260] The ORTEP program[261] was used for the drawing of the crystal structure (figure 25). The fractional atomic coordinates are given for the molecule in table 34, the anisotropic thermal parameters (Å) in table 35 and the bond lengths (Å) and bond angles (°) are given in tables 36 and 37 respectively.

Table 34: Fractional Atomic Coordinates and Thermal Parameters (Å) for 2,2,4,4-Tetra(2,4,6-tri-i-propylphenyl)-1,3-oxathia-2,4-distannetane (**16**).

Atom	x	y	z	Uiso or Ueq (***)
Sn1	0.05618(7)	0.21821(5)	0.48569(5)	0.0660(6) ***
Sn2	0.19322(7)	0.24733(4)	0.37277(4)	0.0606(6) ***
S1	0.19832(3)	0.16416(2)	0.45522(2)	0.0798(3) ***
O1	0.07293(6)	0.27921(4)	0.40968(3)	0.0663(6) ***
C7	-0.11982(19)	0.21196(14)	0.36406(13)	0.1656(24) ***
C8	-0.10749(22)	0.17324(16)	0.30159(14)	0.2153(31) ***
C9	-0.20220(21)	0.26091(14)	0.36341(16)	0.2119(31) ***
C10	-0.32112(21)	0.04548(17)	0.46780(16)	0.2310(33) ***
C11	-0.37408(27)	0.05288(23)	0.52257(20)	0.3455(50) ***
C12	-0.30528(16)	-0.01482(13)	0.43729(17)	0.1965(28) ***
C13	-0.01471(12)	0.10867(8)	0.58388(8)	0.0984(14) ***
C14	-0.05834(15)	0.12221(9)	0.65227(9)	0.1332(17) ***
C15	0.03558(15)	0.04292(10)	0.58694(11)	0.1489(20) ***
C22	0.20222(10)	0.21221(8)	0.62300(8)	0.0877(12) ***
C23	0.19261(14)	0.17812(9)	0.69232(8)	0.1231(16) ***
C24	0.30441(11)	0.22871(9)	0.60676(11)	0.1281(17) ***
C25	0.12935(21)	0.42598(11)	0.71620(13)	0.1829(25) ***
C26	0.17899(30)	0.47756(19)	0.67873(18)	0.4153(54) ***
C27	0.05780(27)	0.45517(14)	0.74439(17)	0.2620(37) ***
C28	-0.07008(12)	0.33861(8)	0.52456(9)	0.1043(14) ***
C29	-0.06349(16)	0.39979(9)	0.47838(11)	0.1441(19) ***
C30	-0.16400(13)	0.33417(13)	0.55993(11)	0.1667(21) ***
C37	0.21334(11)	0.40033(7)	0.43545(8)	0.0859(12) ***
C38	0.23021(14)	0.41231(8)	0.50779(8)	0.1154(15) ***

Table 34: Continued-

C39	0.17816(14)	0.46203(8)	0.40079(10)	0.1308(17) ***
C40	0.54745(14)	0.44141(9)	0.37739(12)	0.1265(17) ***
C41	0.55461(16)	0.46696(13)	0.30893(13)	0.1936(25) ***
C42	0.62487(20)	0.42306(18)	0.40963(20)	0.3016(41) ***
C43	0.40433(11)	0.22397(7)	0.32874(8)	0.0865(11) ***
C44	0.46875(16)	0.18441(9)	0.37608(14)	0.1692(22) ***
C45	0.43740(17)	0.22295(9)	0.25921(10)	0.1638(20) ***
C52	0.21223(14)	0.10409(7)	0.29082(9)	0.1061(14) ***
C53	0.13300(21)	0.05761(11)	0.30966(13)	0.2171(28) ***
C54	0.28981(20)	0.06763(9)	0.25390(11)	0.1797(22) ***
C55	0.07528(19)	0.17377(12)	0.07499(11)	0.1555(22) ***
C56	0.08168(26)	0.22790(13)	0.02846(10)	0.2290(30) ***
C57	-0.02145(19)	0.13440(13)	0.07547(14)	0.1827(26) ***
C58	0.11400(13)	0.33683(7)	0.25968(7)	0.0915(13) ***
C59	0.00921(17)	0.35896(10)	0.24932(13)	0.1743(23) ***
C60	0.18316(20)	0.37832(9)	0.22266(11)	0.1810(23) ***
C1	-0.0660(11)	0.1584(7)	0.4765(8)	0.087(5)
C2	-0.1282(13)	0.1646(8)	0.4273(9)	0.105(5)
C3	-0.2151(15)	0.1231(10)	0.4219(11)	0.139(7)
C4	-0.2212(14)	0.0828(9)	0.4772(11)	0.121(6)
C5	-0.1616(13)	0.0749(8)	0.5285(10)	0.114(6)
C6	-0.0805(11)	0.1162(7)	0.5290(8)	0.086(5)
C16	0.0714(10)	0.2787(7)	0.5706(7)	0.072(4)
C17	0.1424(11)	0.2709(7)	0.6183(8)	0.080(4)
C18	0.1555(11)	0.3222(8)	0.6640(8)	0.093(5)
C19	0.1006(12)	0.3733(8)	0.6618(9)	0.098(5)
C20	0.0294(11)	0.3819(7)	0.6181(8)	0.087(5)
C21	0.0147(10)	0.3303(7)	0.5714(8)	0.080(4)
C31	0.3109(9)	0.3130(6)	0.3794(6)	0.062(3)
C32	0.3009(10)	0.3754(6)	0.4038(7)	0.072(4)

Table 34: Continued-

C33	0.3829(10)	0.4157(7)	0.4023(7)	0.080(4)
C34	0.4616(11)	0.3949(7)	0.3751(8)	0.088(5)
C35	0.4722(10)	0.3325(7)	0.3526(7)	0.080(4)
C36	0.3934(9)	0.2924(6)	0.3533(6)	0.062(4)
C46	0.1584(9)	0.2206(6)	0.2741(6)	0.064(3)
C47	0.1683(10)	0.1580(6)	0.2500(7)	0.069(4)
C48	0.1415(10)	0.1442(7)	0.1839(8)	0.085(4)
C49	0.1055(11)	0.1906(8)	0.1470(9)	0.098(5)
C50	0.0947(11)	0.2521(8)	0.1698(8)	0.091(5)
C51	0.1212(10)	0.2667(6)	0.2332(7)	0.075(4)

Table 35: Anisotropic Thermal Parameters (Å) for 2,2,4,4-Tetra(2,4,6-tri-i-propylphenyl)-1,3-oxathia-2,4-distannetane (**16**).

Atom	U11	U22	U33	U23	U13	U12
Sn1	0.068(1)	0.078(1)	0.052(1)	0.006(1)	0.005(1)	-0.017(1)
Sn2	0.071(1)	0.058(1)	0.053(1)	-0.001(1)	0.010(1)	-0.009(1)
S1	0.089(3)	0.079(3)	0.071(3)	0.017(2)	0.010(2)	0.000(2)
O1	0.084(6)	0.086(6)	0.029(5)	-0.004(4)	0.005(5)	-0.031(5)
C7	0.156(22)	0.208(27)	0.133(24)	0.058(19)	-0.054(19)	-0.076(21)
C8	0.209(29)	0.318(40)	0.119(24)	0.009(23)	0.038(24)	-0.042(26)
C9	0.199(27)	0.220(30)	0.217(35)	0.077(24)	-0.092(24)	0.017(22)
C10	0.191(28)	0.261(35)	0.240(35)	-0.091(28)	0.068(26)	-0.186(27)
C11	0.240(38)	0.532(70)	0.265(43)	-0.132(44)	0.118(36)	-0.264(44)
C12	0.135(20)	0.153(23)	0.302(40)	-0.039(24)	-0.020(22)	-0.069(17)
C13	0.111(14)	0.118(15)	0.066(12)	0.033(9)	-0.004(11)	-0.036(11)
C14	0.178(20)	0.147(18)	0.075(14)	0.000(11)	0.010(14)	-0.039(14)
C15	0.151(19)	0.132(18)	0.164(22)	0.015(15)	0.022(17)	0.054(15)
C22	0.077(11)	0.118(13)	0.068(12)	0.007(9)	-0.012(9)	-0.012(10)
C23	0.151(17)	0.159(18)	0.060(13)	0.021(11)	-0.029(13)	-0.019(13)
C24	0.067(11)	0.151(18)	0.166(22)	-0.003(13)	-0.012(12)	-0.012(11)
C25	0.229(29)	0.120(19)	0.200(27)	-0.089(18)	0.091(23)	-0.061(18)
C26	0.517(67)	0.382(49)	0.346(47)	-0.279(42)	0.320(51)	-0.363(53)
C27	0.316(43)	0.192(28)	0.278(40)	-0.152(28)	0.098(35)	-0.103(28)
C28	0.094(13)	0.120(15)	0.099(15)	-0.015(11)	0.013(12)	-0.009(10)
C29	0.174(20)	0.118(16)	0.140(20)	0.025(14)	0.023(17)	0.034(14)
C30	0.072(13)	0.292(30)	0.137(21)	-0.007(18)	0.035(14)	0.009(15)
C37	0.093(11)	0.072(11)	0.093(13)	-0.007(9)	0.034(10)	0.010(8)
C38	0.151(17)	0.131(15)	0.064(12)	-0.010(10)	0.041(12)	-0.021(12)
C39	0.150(18)	0.093(14)	0.150(19)	0.022(12)	0.045(15)	0.043(12)
C40	0.081(14)	0.142(17)	0.156(21)	0.036(14)	0.026(14)	-0.065(12)

Table 35: Continued-

C41	0.160(21)	0.254(29)	0.168(26)	0.108(21)	-0.062(19)	-0.128(20)
C42	0.142(23)	0.354(45)	0.409(55)	0.226(39)	-0.148(29)	-0.181(27)
C43	0.103(12)	0.067(10)	0.090(12)	-0.007(8)	0.033(11)	0.009(9)
C44	0.174(21)	0.099(16)	0.234(30)	-0.024(16)	-0.074(20)	0.057(15)
C45	0.251(27)	0.120(15)	0.121(17)	-0.037(12)	0.109(19)	-0.020(16)
C52	0.148(16)	0.062(11)	0.108(15)	0.009(10)	-0.001(13)	0.004(11)
C53	0.305(35)	0.141(20)	0.205(28)	0.096(19)	-0.034(25)	-0.126(22)
C54	0.313(34)	0.113(16)	0.113(16)	-0.013(13)	0.040(21)	0.105(19)
C55	0.212(25)	0.191(24)	0.063(15)	-0.056(14)	-0.058(17)	0.001(20)
C56	0.425(49)	0.200(26)	0.062(15)	0.011(15)	0.005(23)	0.154(29)
C57	0.173(24)	0.184(24)	0.191(30)	-0.040(20)	-0.013(21)	-0.005(19)
C58	0.133(15)	0.071(11)	0.070(12)	0.008(8)	0.015(11)	0.012(10)
C59	0.168(21)	0.117(17)	0.238(30)	-0.048(17)	-0.006(20)	0.067(15)
C60	0.309(33)	0.088(15)	0.147(21)	0.013(13)	0.088(22)	-0.042(17)

Table 36: Bond Lengths (Å) for 2,2,4,4-Tetra(2,4,6-tri-i-propyl-phenyl)-1,3-oxathia-2,4-distannetane (**16**).

Sn1 -Sn2	3.154(1)	Sn1 -S1	2.439(4)
Sn1 -O1	2.042(8)	Sn1 -C1	2.164(15)
Sn1 -C16	2.166(14)	Sn2 -S1	2.435(4)
Sn2 -O1	2.026(8)	Sn2 -C31	2.186(13)
Sn2 -C46	2.148(13)	C1 -C2	1.336(25)
C1 -C6	1.419(23)	C2 -C3	1.52(3)
C2 -C7	1.65(3)	C3 -C4	1.42(3)
C4 -C5	1.35(3)	C4 -C10	1.64(4)
C5 -C6	1.454(24)	C6 -C13	1.457(24)
C7 -C8	1.54(4)	C7 -C9	1.57(4)
C10 -C11	1.39(5)	C10 -C12	1.44(5)
C13 -C14	1.58(3)	C13 -C15	1.56(3)
C16 -C17	1.402(21)	C16 -C21	1.357(20)
C17 -C18	1.438(22)	C17 -C22	1.507(22)
C18 -C19	1.334(23)	C19 -C20	1.352(24)
C19 -C25	1.62(3)	C20 -C21	1.460(21)
C21 -C28	1.539(23)	C22 -C23	1.606(24)
C22 -C24	1.557(23)	C25 -C26	1.52(5)
C25 -C27	1.35(5)	C26 -C27	2.29(6)
C28 -C29	1.60(3)	C28 -C30	1.56(3)
C31 -C32	1.413(19)	C31 -C36	1.388(18)
C32 -C33	1.452(20)	C32 -C37	1.529(21)
C33 -C34	1.352(22)	C34 -C35	1.402(21)
C34 -C40	1.574(25)	C35 -C36	1.414(19)
C36 -C43	1.535(19)	C37 -C38	1.521(23)
C37 -C39	1.557(24)	C40 -C41	1.51(4)
C40 -C42	1.34(4)	C43 -C44	1.56(3)

Table 36: Continued-

C43 -C45	1.52(3)	C46 -C47	1.415(19)
C46 -C51	1.382(19)	C47 -C48	1.430(22)
C47 -C52	1.535(22)	C48 -C49	1.331(23)
C49 -C50	1.386(24)	C49 -C55	1.57(3)
C50 -C51	1.381(22)	C51 -C58	1.576(20)
C52 -C53	1.56(3)	C52 -C54	1.57(3)
C55 -C56	1.49(3)	C55 -C57	1.62(4)
C58 -C59	1.59(3)	C58 -C60	1.54(3)

Table 37: Bond Angles (°) for 2,2,4,4-Tetra(2,4,6-tri-i-propylphenyl)-1,3-oxathia-2,4-distannetane (**16**).

S1	-Sn1	-Sn2	49.6(1)	O1	-Sn1	-Sn2	39.0(2)
O1	-Sn1	-S1	88.6(3)	C1	-Sn1	-Sn2	125.0(5)
C1	-Sn1	-S1	113.1(4)	C1	-Sn1	-O1	114.4(5)
C16	-Sn1	-Sn2	115.5(4)	C16	-Sn1	-S1	114.7(4)
C16	-Sn1	-O1	103.7(4)	C16	-Sn1	-C1	118.2(6)
S1	-Sn2	-Sn1	49.7(1)	O1	-Sn2	-Sn1	39.4(2)
O1	-Sn2	-S1	89.1(2)	C31	-Sn2	-Sn1	125.3(3)
C31	-Sn2	-S1	113.9(3)	C31	-Sn2	-O1	115.9(4)
C46	-Sn2	-Sn1	120.8(3)	C46	-Sn2	-S1	118.0(4)
C46	-Sn2	-O1	105.3(4)	C46	-Sn2	-C31	112.4(5)
Sn2	-S1	-Sn1	80.6(1)	Sn2	-O1	-Sn1	101.7(4)
C2	-C1	-Sn1	122(1)	C6	-C1	-Sn1	116(1)
C6	-C1	-C2	122(1)	C3	-C2	-C1	122(2)
C7	-C2	-C1	126(2)	C7	-C2	-C3	112(2)
C4	-C3	-C2	111(2)	C5	-C4	-C3	130(2)
C10	-C4	-C3	105(2)	C10	-C4	-C5	124(2)
C6	-C5	-C4	115(2)	C5	-C6	-C1	120(1)
C13	-C6	-C1	123(1)	C13	-C6	-C5	116(1)
C8	-C7	-C2	111(2)	C9	-C7	-C2	109(2)
C9	-C7	-C8	117(2)	C11	-C10	-C4	111(3)
C12	-C10	-C4	109(2)	C12	-C10	-C11	123(3)
C14	-C13	-C6	114(1)	C15	-C13	-C6	114(1)
C15	-C13	-C14	109(1)	C17	-C16	-Sn1	123(1)
C21	-C16	-Sn1	116(1)	C21	-C16	-C17	121(1)
C18	-C17	-C16	116(1)	C22	-C17	-C16	123(1)
C22	-C17	-C18	121(1)	C19	-C18	-C17	121(1)
C20	-C19	-C18	124(2)	C25	-C19	-C18	113(2)
C25	-C19	-C20	123(2)	C21	-C20	-C19	115(1)

Table 37: Continued-

C20 -C21 -C16	122(1)	C28 -C21 -C16	123(1)
C28 -C21 -C20	115(1)	C23 -C22 -C17	111(1)
C24 -C22 -C17	110(1)	C24 -C22 -C23	113(1)
C26 -C25 -C19	105(2)	C27 -C25 -C19	115(2)
C27 -C25 -C26	106(3)	C27 -C26 -C25	34(2)
C26 -C27 -C25	40(2)	C29 -C28 -C21	114(1)
C30 -C28 -C21	112(1)	C30 -C28 -C29	113(2)
C32 -C31 -Sn2	121.5(9)	C36 -C31 -Sn2	116.6(9)
C36 -C31 -C32	122(1)	C33 -C32 -C31	116(1)
C37 -C32 -C31	124(1)	C37 -C32 -C33	119(1)
C34 -C33 -C32	121(1)	C35 -C34 -C33	123(1)
C40 -C34 -C33	117(1)	C40 -C34 -C35	120(1)
C36 -C35 -C34	117(1)	C35 -C36 -C31	121(1)
C43 -C36 -C31	121(1)	C43 -C36 -C35	118(1)
C38 -C37 -C32	111(1)	C39 -C37 -C32	110(1)
C39 -C37 -C38	110(1)	C41 -C40 -C34	106(2)
C42 -C40 -C34	118(2)	C42 -C40 -C41	119(2)
C44 -C43 -C36	111(1)	C45 -C43 -C36	111(1)
C45 -C43 -C44	112(2)	C47 -C46 -Sn2	123(1)
C51 -C46 -Sn2	118(1)	C51 -C46 -C47	119(1)
C48 -C47 -C46	120(1)	C52 -C47 -C46	123(1)
C52 -C47 -C48	118(1)	C49 -C48 -C47	119(1)
C50 -C49 -C48	122(2)	C55 -C49 -C48	118(2)
C55 -C49 -C50	120(2)	C51 -C50 -C49	120(1)
C50 -C51 -C46	120(1)	C58 -C51 -C46	118(1)
C58 -C51 -C50	121(1)	C53 -C52 -C47	108(2)
C54 -C52 -C47	112(1)	C54 -C52 -C53	110(2)
C56 -C55 -C49	114(2)	C57 -C55 -C49	109(2)
C57 -C55 -C56	118(2)	C59 -C58 -C51	107(1)
C60 -C58 -C51	108(1)	C60 -C58 -C59	113(2)

APPENDIX VII.

CRYSTALLOGRAPHIC ANALYSIS AND STRUCTURAL REFINEMENT OF 2,2'-SPIROBI-(4,4,6,6-TETRA-t-BUTYL-1,3,5-TRITHIA-2,4,6-TRISTANNINANE) (25).

VII.1 Crystal Data.

$C_{32}H_{72}S_6Sn_5$, M.W. = 1242.74, triclinic, space group = $P\bar{1}$.

a = 14.223(2)Å, b = 14.190(2)Å, c = 16.362(4)Å.

α = 90.03(1), β = 113.59(2), γ = 119.89(1).

U = 2359.3 Å^3, μ = 24.92 cm^{-1}, F(000) = 1220.0.

Radiation Mo-K$_\alpha$, λ = 0.71069 Å, graphite monochromator.

For 4508 observed and unique reflections with $I > 3\sigma I$, R = 0.0541 and R_w = 0.0541.

VII.2 Crystallographic Analysis.

A crystal of approximate dimensions 0.3 × 0.3 × 0.3 mm was used for both the preliminary crystal analysis and the main data collection. The intensities of all reflections with $2^\circ < \theta < 22^\circ$ were measured. One reflection was used as a standard and its intensity monitored every fifty observed reflections. No significant crystal decay was observed.

VII.3 Structure Solution and Refinement.

The crystal structure was solved using a Patterson search (SHELX86[266]) and refined by full matrix least-squares using SHELX76.[257] Data were corrected for Lorentz and polarisation effects and for absorption.[262] Hydrogen atoms were included in calculated positions. The tin and sulphur atoms present in the molecule were refined anisotropically, while the remaining atoms were refined isotropically. The atomic scattering factors and the anomolous dispersion correction factors for both hydrogen and non-hydrogen atoms were taken from the literature.[258-260] From the structural refinement of this compound it became apparent that the structural geometry of the molecule was very similar to that reported by Puff et al.[215] even though the sample used in this instance was quoted as possessing a unit cell with monoclinic symmetry and a *C2/c* space group. To obtain the crystalline samples in each case different solvent systems were used in the recrystallisation process. This is thought to have brought about a difference in the packing in the crystal lattice resulting in the observed differences in the geometries of the unit cells.

The ORTEP program[261] was used for the drawing of the crystal structure (figure 52). The fractional atomic coordinates (Å) for the molecule are given in table 38, the anisotropic thermal parameters (Å) in table 39 and the bond lengths (Å) and bond angles (°) are given in tables 40 and 41 respectively.

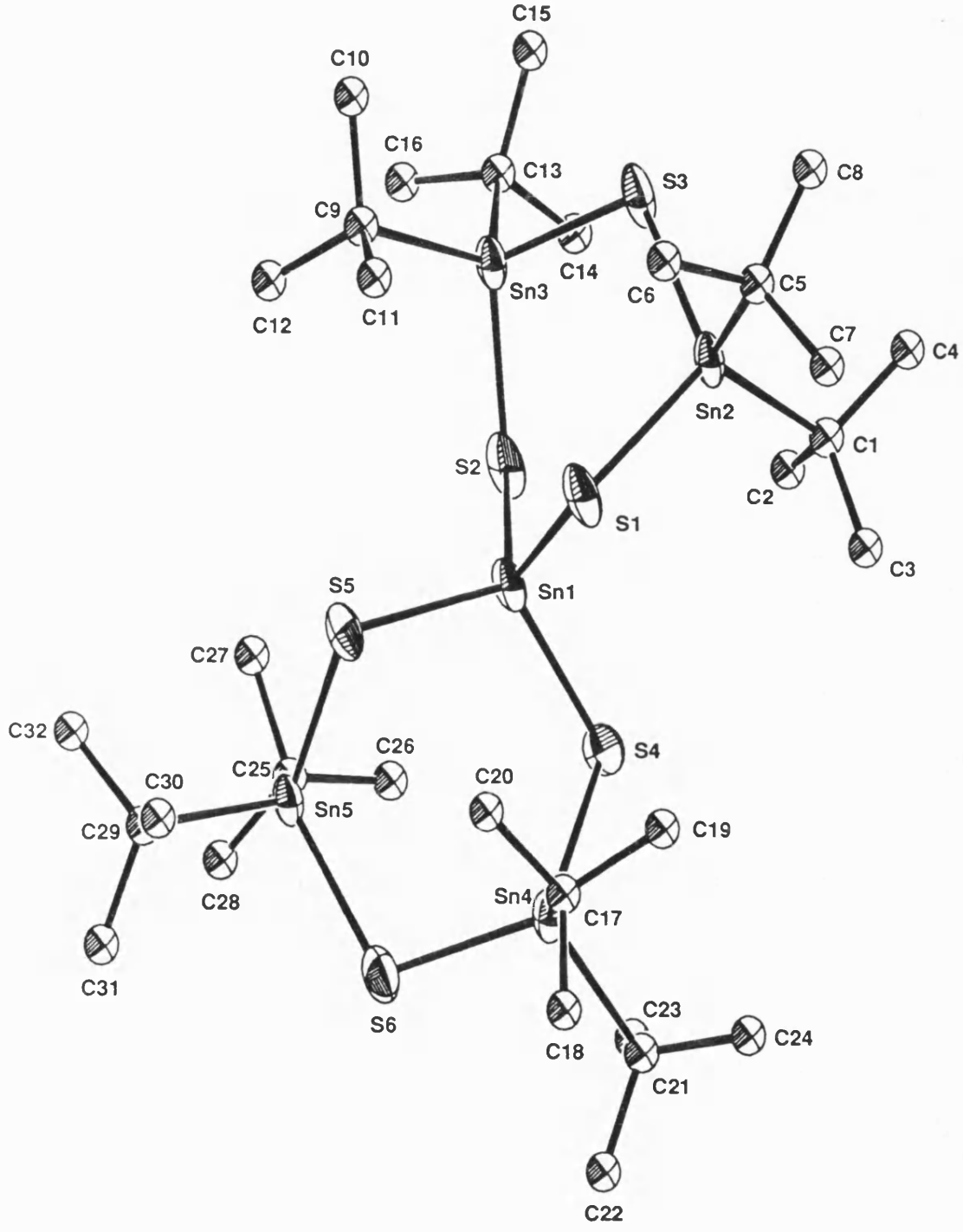

Figure 52: ORTEP Plot of 2,2'-Spirobi(4,4,6,6-tetra-t-butyl-1,3,5-trithia-2,4,6-tristanninane) (25).

Table 38: Fractional Atomic Coordinates and Thermal Parameters (Å) for 2,2'-Spirobi(4,4,6,6-tetra-t-butyl-1,3,5-trithia-2,4,6-tristanninane) (25).

Atom	x	y	z	Uiso or Ueq (***)	
Sn1	-0.00003(11)	0.62754(9)	0.25007(8)	0.0518(7)	***
Sn2	0.16179(10)	0.94646(9)	0.35513(8)	0.0449(7)	***
Sn3	-0.16180(10)	0.78465(9)	0.14489(8)	0.0450(7)	***
Sn4	0.17664(10)	0.47704(9)	0.31815(8)	0.0482(7)	***
Sn5	-0.17672(10)	0.30038(9)	0.18179(8)	0.0453(7)	***
S1	0.08709(4)	0.76294(3)	0.38712(3)	0.0621(3)	***
S2	-0.08696(4)	0.67593(4)	0.11248(3)	0.0654(3)	***
S3	-0.00045(4)	0.96546(3)	0.25044(3)	0.0559(3)	***
S4	0.14995(4)	0.61004(4)	0.23355(4)	0.0770(3)	***
S5	-0.14996(4)	0.46011(3)	0.26598(3)	0.0676(3)	***
S6	-0.00007(4)	0.28830(4)	0.25047(4)	0.0709(3)	***
C1	0.2938(15)	0.9949(14)	0.3037(12)	0.059(4)	
C2	0.2352(18)	0.9299(16)	0.2064(14)	0.079(6)	
C3	0.3890(22)	0.9722(21)	0.3585(18)	0.114(8)	
C4	0.3506(20)	1.1178(17)	0.3071(16)	0.093(7)	
C5	0.2269(16)	1.0498(14)	0.4862(13)	0.065(5)	
C6	0.1329(18)	0.9877(17)	0.5237(15)	0.082(6)	
C7	0.3492(18)	1.0716(17)	0.5584(15)	0.086(6)	
C8	0.2391(21)	1.1605(18)	0.4744(17)	0.099(7)	
C9	-0.2268(17)	0.8235(15)	0.0143(14)	0.072(5)	
C10	-0.1372(18)	0.8504(17)	-0.0246(15)	0.083(6)	
C11	-0.3484(19)	0.7231(18)	-0.0589(16)	0.095(7)	
C12	-0.2348(21)	0.9238(18)	0.0241(16)	0.096(7)	
C13	-0.2951(14)	0.7000(13)	0.1972(12)	0.053(4)	
C14	-0.2326(19)	0.6958(17)	0.2972(14)	0.087(6)	

Table 38: Continued-

C15	-0.3862(23)	0.5815(19)	0.1471(18)	0.116(8)
C16	-0.3510(20)	0.7678(18)	0.1921(16)	0.095(7)
C17	0.2288(16)	0.5228(14)	0.4616(13)	0.061(4)
C18	0.1232(21)	0.5054(20)	0.4757(18)	0.111(8)
C19	0.2872(26)	0.4654(23)	0.5106(21)	0.138(10)
C20	0.3204(23)	0.6506(20)	0.4987(19)	0.122(9)
C21	0.3074(16)	0.4729(14)	0.2824(13)	0.063(5)
C22	0.2627(20)	0.4602(18)	0.1794(15)	0.093(7)
C23	0.4288(21)	0.5823(18)	0.3316(17)	0.105(7)
C24	0.3179(22)	0.3764(18)	0.3094(17)	0.104(7)
C25	-0.2278(16)	0.2953(14)	0.0375(12)	0.060(4)
C26	-0.1244(22)	0.3772(20)	0.0242(19)	0.117(8)
C27	-0.3196(23)	0.3279(22)	0.0012(19)	0.122(9)
C28	-0.2893(24)	0.1780(20)	-0.0094(19)	0.125(9)
C29	-0.3081(15)	0.1654(14)	0.2174(12)	0.059(4)
C30	-0.2632(21)	0.1959(19)	0.3195(15)	0.097(7)
C31	-0.4296(21)	0.1524(20)	0.1682(18)	0.109(8)
C32	-0.3174(21)	0.0570(17)	0.1943(17)	0.097(7)

Table 39: Anisotropic Thermal Parameters (Å) for 2,2'-Spirobi(4,4,6,6-tetra-t-butyl-1,3,5-trithia-2,4,6-tristannınane) (25).

Atom	U11	U22	U33	U23	U13	U12
Sn1	0.061(1)	0.042(1)	0.053(1)	0.016(1)	0.030(1)	0.033(1)
Sn2	0.045(1)	0.043(1)	0.047(1)	0.008(1)	0.018(1)	0.024(1)
Sn3	0.045(1)	0.043(1)	0.047(1)	0.011(1)	0.017(1)	0.024(1)
Sn4	0.044(1)	0.050(1)	0.050(1)	0.015(1)	0.022(1)	0.028(1)
Sn5	0.045(1)	0.040(1)	0.051(1)	0.010(1)	0.022(1)	0.020(1)
S1	0.079(3)	0.046(2)	0.061(3)	0.013(2)	0.028(2)	0.035(2)
S2	0.078(3)	0.057(3)	0.061(3)	0.016(2)	0.031(2)	0.046(2)
S3	0.055(3)	0.045(2)	0.068(3)	0.002(2)	0.004(2)	0.030(2)
S4	0.081(3)	0.062(3)	0.088(4)	0.039(2)	0.058(3)	0.050(3)
S5	0.081(3)	0.050(2)	0.072(3)	0.023(2)	0.053(3)	0.036(2)
S6	0.061(3)	0.050(3)	0.103(4)	0.019(2)	0.032(3)	0.033(2)

Table 40: Bond Lengths (Å) for 2,2'-Spirobi(4,4,6,6-tetra-t-butyl-1,3,5-trithia-2,4,6-tristanninane) (25).

Sn1 -S1	2.378(5)	Sn1 -S2	2.385(5)
Sn1 -S4	2.382(4)	Sn1 -S5	2.378(4)
Sn2 -S1	2.424(4)	Sn2 -S3	2.406(4)
Sn2 -C1	2.165(18)	Sn2 -C4	2.987(22)
Sn2 -C5	2.159(18)	Sn3 -S2	2.425(4)
Sn3 -S3	2.406(4)	Sn3 -C9	2.157(20)
Sn3 -C13	2.192(16)	Sn3 -C16	2.986(22)
Sn4 -S4	2.433(4)	Sn4 -S6	2.403(5)
Sn4 -C17	2.147(18)	Sn4 -C19	2.95(3)
Sn4 -C21	2.188(18)	Sn5 -S5	2.429(4)
Sn5 -S6	2.403(5)	Sn5 -C25	2.164(18)
Sn5 -C27	3.00(3)	Sn5 -C28	2.93(3)
Sn5 -C29	2.193(17)	C1 -C2	1.499(25)
C1 -C3	1.48(3)	C1 -C4	1.501(24)
C5 -C6	1.56(3)	C5 -C7	1.527(25)
C5 -C8	1.515(25)	C9 -C10	1.53(3)
C9 -C11	1.53(3)	C9 -C12	1.497(25)
C13 -C14	1.536(25)	C13 -C15	1.47(3)
C13 -C16	1.507(24)	C17 -C18	1.51(3)
C17 -C19	1.46(3)	C17 -C20	1.54(3)
C21 -C22	1.52(3)	C21 -C23	1.50(3)
C21 -C24	1.498(25)	C25 -C26	1.45(3)
C25 -C27	1.50(3)	C25 -C28	1.46(3)
C29 -C30	1.50(3)	C29 -C31	1.49(3)
C29 -C32	1.511(24)		

Table 41: Bond Angles (°) for 2,2'-Spirobi(4,4,6,6-tetra-t-butyl-1,3,5-trithia-2,4,6-tristannınane) (25).

S2	-Sn1 -S1	113.6(2)	S4	-Sn1 -S1	111.9(2)
S4	-Sn1 -S2	103.2(2)	S5	-Sn1 -S1	103.6(2)
S5	-Sn1 -S2	111.8(2)	S5	-Sn1 -S4	113.1(1)
S3	-Sn2 -S1	112.7(2)	C1	-Sn2 -S1	114.5(5)
C1	-Sn2 -S3	108.5(5)	C4	-Sn2 -S1	142.2(4)
C4	-Sn2 -S3	95.1(4)	C4	-Sn2 -C1	28.6(6)
C5	-Sn2 -S1	100.8(5)	C5	-Sn2 -S3	103.8(5)
C5	-Sn2 -C1	116.0(7)	C5	-Sn2 -C4	96.5(6)
S3	-Sn3 -S2	112.9(2)	C9	-Sn3 -S2	100.9(5)
C9	-Sn3 -S3	103.8(5)	C13	-Sn3 -S2	114.5(4)
C13	-Sn3 -S3	108.0(4)	C13	-Sn3 -C9	116.1(7)
C16	-Sn3 -S2	142.5(4)	C16	-Sn3 -S3	94.7(4)
C16	-Sn3 -C9	96.1(7)	C16	-Sn3 -C13	29.0(6)
S6	-Sn4 -S4	112.9(2)	C17	-Sn4 -S4	113.9(5)
C17	-Sn4 -S6	109.3(5)	C19	-Sn4 -S4	139.2(5)
C19	-Sn4 -S6	100.1(6)	C19	-Sn4 -C17	28.1(7)
C21	-Sn4 -S4	98.9(5)	C21	-Sn4 -S6	103.5(5)
C21	-Sn4 -C17	117.7(7)	C21	-Sn4 -C19	96.1(7)
S6	-Sn5 -S5	112.6(2)	C25	-Sn5 -S5	113.5(5)
C25	-Sn5 -S6	109.5(5)	C27	-Sn5 -S5	91.3(5)
C27	-Sn5 -S6	137.0(5)	C27	-Sn5 -C25	28.3(6)
C28	-Sn5 -S5	138.8(5)	C28	-Sn5 -S6	100.9(5)
C28	-Sn5 -C25	28.6(6)	C28	-Sn5 -C27	47.5(7)
C29	-Sn5 -S5	99.0(5)	C29	-Sn5 -S6	103.4(5)
C29	-Sn5 -C25	118.2(7)	C29	-Sn5 -C27	107.6(7)
C29	-Sn5 -C28	95.5(7)	Sn2	-S1 -Sn1	108.5(2)
Sn3	-S2 -Sn1	108.1(2)	Sn3	-S3 -Sn2	107.6(2)

Table 41: Continued-

Sn4	-S4	-Sn1	108.3(2)	Sn5	-S5	-Sn1	108.6(2)
Sn5	-S6	-Sn4	107.3(2)	C2	-C1	-Sn2	112(1)
C3	-C1	-Sn2	112(1)	C3	-C1	-C2	106(2)
C4	-C1	-Sn2	108(1)	C4	-C1	-C2	109(2)
C4	-C1	-C3	111(2)	C1	-C4	-Sn2	43.7(9)
C6	-C5	-Sn2	109(1)	C7	-C5	-Sn2	112(1)
C7	-C5	-C6	107(2)	C8	-C5	-Sn2	110(1)
C8	-C5	-C6	109(2)	C8	-C5	-C7	110(2)
C10	-C9	-Sn3	109(1)	C11	-C9	-Sn3	113(1)
C11	-C9	-C10	104(2)	C12	-C9	-Sn3	112(1)
C12	-C9	-C10	108(2)	C12	-C9	-C11	111(2)
C14	-C13	-Sn3	111(1)	C15	-C13	-Sn3	112(1)
C15	-C13	-C14	104(2)	C16	-C13	-Sn3	106(1)
C16	-C13	-C14	110(2)	C16	-C13	-C15	113(2)
C13	-C16	-Sn3	44.8(9)	C18	-C17	-Sn4	111(1)
C19	-C17	-Sn4	108(2)	C19	-C17	-C18	116(2)
C20	-C17	-Sn4	109(1)	C20	-C17	-C18	102(2)
C20	-C17	-C19	109(2)	C17	-C19	-Sn4	44(1)
C22	-C21	-Sn4	109(1)	C23	-C21	-Sn4	109(1)
C23	-C21	-C22	108(2)	C24	-C21	-Sn4	109(1)
C24	-C21	-C22	111(2)	C24	-C21	-C23	111(2)
C26	-C25	-Sn5	112(1)	C27	-C25	-Sn5	108(1)
C27	-C25	-C26	106(2)	C28	-C25	-Sn5	106(1)
C28	-C25	-C26	117(2)	C28	-C25	-C27	108(2)
C25	-C27	-Sn5	43(1)	C25	-C28	-Sn5	45(1)
C30	-C29	-Sn5	109(1)	C31	-C29	-Sn5	109(1)
C31	-C29	-C30	109(2)	C32	-C29	-Sn5	110(1)
C32	-C29	-C30	107(2)	C32	-C29	-C31	111(2)

APPENDIX VIII.

CRYSTALLOGRAPHIC ANALYSIS AND STRUCTURAL REFINEMENT OF 3,3-DI-t-BUTYL-1,5-DIHYDROXY-1,5-DIPHENYL-2,4-DIOXA-3-STANNA-1,5-DIBORONATE (34).

VIII.1 Crystal Data.

$C_{20}H_{30}B_2O_4Sn$, M.W. = 474.77, monoclinic, space group = $P2_1$, c = unique axis.

a = 12.403(2)Å, b = 12.407(3)Å, c = 15.800(7)Å.

α = 90.0, β = 90.0, γ = 89.99(1).

U = 2428.52Å^3, μ = 9.75 cm^{-1}, F(000) = 968.

Radiation Mo-K$_\alpha$, λ = 0.71069Å, graphite monochromator.

For 3020 observed and unique reflections with $I > 3\sigma I$, R = 0.0718 and R_w = 0.0718.

VIII.2 Crystallographic Analysis.

A crystal of approximate dimensions 0.3 × 0.3 × 0.25 mm was used for both the preliminary crystal analysis and the main data collection. The intensities of all reflections $2^\circ < \theta < 22^\circ$ were measured. One reflection was used as a standard and its intensity monitored every fifty observed reflections. Significant crystal decay was observed for prolonged exposure to the X-ray beam.

VIII.3 Structure Solution and Refinement.

The crystal structure was solved using a Patterson search (SHELX86[256]) and refined by full matrix least-squares using SHELX76.[257] Data were corrected for Lorentz and polarisation effects and for absorption.[262] Hydrogen atoms were included in calculated positions. The tin, boron and oxygen atoms present in the molecule were refined anisotropically, while the remaining atoms in the molecule were refined isotropically. The atomic scattering factors for hydrogen and non-hydrogen atoms and the anomolous dispersion correction factors for non-hydrogen atoms were taken from the literature.[258-260] The ORTEP program[261] was used for the drawing of the crystal structure (figure 44) and the cell packing diagrams were obtained using PLUTO (figures 45 to 47). The fractional atomic coordinates (Å) for the molecule are given in table 42, the anisotropic thermal parameters (Å) in table 43 and the bond lengths (Å) and bond angles (°) are given in tables 44 and 45 respectively.

Table 42: Fractional Atomic Coordinates and Thermal Parameters (Å) for 3,3-Di-t-butyl-1,5-dihydroxy-1,5-diphenyl-2,4-dioxa-3-stanna-1,5-diboronate (34).

Atom	x	y	z	Uiso or Ueq (***)
Sn1	0.09662(15)	0.08154(12)	0.00000	0.0668(11) ***
B1	0.05446(27)	-0.12078(25)	-0.10002(19)	0.0655(24) ***
B2	0.30466(34)	0.15428(32)	-0.07217(26)	0.0970(32) ***
O1	0.03656(15)	-0.05473(13)	-0.04604(11)	0.0837(14) ***
O2	0.14601(15)	-0.10611(12)	-0.15766(11)	0.0739(14) ***
O3	0.26799(12)	0.22592(12)	-0.00278(12)	0.0708(11) ***
O4	0.21865(13)	0.07825(12)	-0.08022(9)	0.0557(11) ***
Sn2	0.41844(15)	-0.40326(12)	-0.24968(15)	0.0672(11) ***
B3	0.34842(38)	-0.20367(29)	-0.31575(19)	0.0944(31) ***
B4	0.62457(26)	-0.44156(22)	-0.35507(16)	0.0501(20) ***
O5	0.27541(14)	-0.23414(11)	-0.25200(13)	0.0859(12) ***
O6	0.42340(14)	-0.28382(13)	-0.33143(10)	0.0736(13) ***
O7	0.55266(14)	-0.46365(10)	-0.29912(10)	0.0666(12) ***
O8	0.60731(15)	-0.35229(13)	-0.40673(11)	0.0791(14) ***
C1	-0.0122(24)	-0.2283(20)	-0.1225(18)	0.076(8)
C2	-0.0937(25)	-0.2504(23)	-0.0608(19)	0.099(9)
C3	-0.1535(30)	-0.3422(26)	-0.0767(23)	0.126(12)
C4	-0.1322(27)	-0.4082(27)	-0.1404(21)	0.105(11)
C5	-0.0541(28)	-0.3875(26)	-0.2012(22)	0.120(11)
C6	0.0106(26)	-0.2975(22)	-0.1812(18)	0.092(9)
C7	0.4015(23)	0.1648(18)	-0.1122(15)	0.056(6)
C8	0.4797(26)	0.2421(23)	-0.0982(19)	0.091(9)
C9	0.5738(27)	0.2467(23)	-0.1417(18)	0.100(9)
C10	0.6060(33)	0.1680(25)	-0.1975(21)	0.121(12)
C11	0.5301(33)	0.0839(32)	-0.2194(27)	0.158(16)
C12	0.4325(29)	0.0898(25)	-0.1713(19)	0.104(10)

Table 42: Continued-

C13	0.1581(32)	0.0272(28)	0.1207(23)	0.121(12)
C14	0.1871(32)	0.1172(29)	0.1732(25)	0.162(17)
C15	0.2343(30)	-0.0507(29)	0.0995(24)	0.164(15)
C16	0.0641(30)	-0.0272(29)	0.1637(26)	0.140(16)
C17	-0.0263(27)	0.1969(24)	-0.0397(18)	0.094(9)
C18	0.0164(31)	0.2695(28)	-0.0975(24)	0.165(15)
C19	-0.1193(28)	0.1442(27)	-0.0662(22)	0.141(13)
C20	-0.0383(31)	0.2602(29)	0.0527(21)	0.147(14)
C21	0.3352(22)	-0.0967(18)	-0.3612(16)	0.069(7)
C22	0.4098(24)	-0.0704(20)	-0.4210(16)	0.081(8)
C23	0.4090(30)	0.0272(25)	-0.4736(23)	0.132(13)
C24	0.3301(27)	0.1031(28)	-0.4572(20)	0.121(11)
C25	0.2576(22)	0.0731(19)	-0.3867(16)	0.078(8)
C26	0.2582(23)	-0.0198(19)	-0.3466(17)	0.078(8)
C27	0.7258(23)	-0.5074(19)	-0.3687(16)	0.069(7)
C28	0.7487(25)	-0.5942(20)	-0.3160(19)	0.095(9)
C29	0.8461(27)	-0.6542(25)	-0.3285(21)	0.112(10)
C30	0.9085(27)	-0.6321(22)	-0.3909(19)	0.102(10)
C31	0.8857(30)	-0.5565(26)	-0.4500(23)	0.129(13)
C32	0.8001(27)	-0.4920(26)	-0.4327(20)	0.109(11)
C33	0.2980(28)	-0.5230(24)	-0.2886(19)	0.103(10)
C34	0.2282(27)	-0.4835(25)	-0.3514(21)	0.125(12)
C35	0.2378(38)	-0.5423(36)	-0.2085(27)	0.228(25)
C36	0.3582(26)	-0.6220(23)	-0.3203(20)	0.120(11)
C37	0.4734(32)	-0.3459(28)	-0.1259(23)	0.132(12)
C38	0.3799(27)	-0.3058(27)	-0.0747(23)	0.141(14)
C39	0.5300(29)	-0.4375(27)	-0.0853(24)	0.130(15)
C40	0.5441(27)	-0.2538(24)	-0.1453(21)	0.130(12)

Table 43: Anisotropic Thermal Parameters (Å) for 3,3-Di-t-butyl-1,5-dihydroxy-1,5-diphenyl-2,4-dioxa-3-stanna-1,5-diboronate (34).

Atom	U11	U22	U33	U23	U13	U12
Sn1	0.062(1)	0.068(1)	0.070(1)	-0.008(1)	0.005(1)	-0.001(1)
B1	0.041(29)	0.089(22)	0.067(20)	0.032(16)	0.014(18)	-0.023(19)
B2	0.054(34)	0.097(30)	0.139(34)	0.072(26)	-0.033(27)	-0.016(26)
O1	0.094(17)	0.084(12)	0.073(13)	-0.037(10)	0.022(11)	0.002(10)
O2	0.081(17)	0.077(11)	0.064(13)	-0.016(8)	-0.005(11)	-0.022(10)
O3	0.069(13)	0.096(11)	0.047(9)	-0.008(11)	0.002(11)	0.003(9)
O4	0.022(13)	0.081(10)	0.064(11)	-0.016(8)	0.008(9)	0.004(9)
Sn2	0.071(1)	0.061(1)	0.070(1)	0.007(1)	0.007(1)	0.000(1)
B3	0.137(46)	0.103(27)	0.042(20)	-0.016(17)	0.009(22)	-0.103(29)
B4	0.040(27)	0.072(18)	0.038(16)	0.001(13)	-0.010(15)	-0.017(17)
O5	0.080(15)	0.063(9)	0.115(13)	-0.012(12)	0.051(14)	0.008(9)
O6	0.072(15)	0.080(11)	0.069(11)	-0.041(9)	0.002(9)	0.012(10)
O7	0.091(16)	0.058(9)	0.051(10)	0.026(7)	0.022(10)	0.001(9)
O8	0.076(16)	0.087(12)	0.075(13)	0.011(10)	0.017(11)	0.013(11)

Table 44: Bond Lengths (Å) for 3,3-Di-t-butyl-1,5-dihydroxy-1,5-diphenyl-2,4-dioxa-3-stanna-1,5-diboronate (**34**).

Sn1 -O1	1.985(17)	Sn1 -O4	1.974(16)
Sn1 -C13	2.16(4)	Sn1 -C17	2.18(3)
B1 -O1	1.20(3)	B1 -O2	1.47(4)
B1 -C1	1.61(4)	B2 -O3	1.48(4)
B2 -O4	1.43(4)	B2 -C7	1.36(5)
C1 -C2	1.43(4)	C1 -C6	1.30(4)
C2 -C3	1.38(4)	C3 -C4	1.32(5)
C4 -C5	1.39(5)	C5 -C6	1.41(4)
C7 -C8	1.38(4)	C7 -C12	1.37(4)
C8 -C9	1.35(5)	C9 -C10	1.37(4)
C10 -C11	1.45(5)	C11 -C12	1.43(5)
C13 -C14	1.44(5)	C13 -C15	1.39(5)
C13 -C16	1.51(5)	C17 -C18	1.39(5)
C17 -C19	1.39(5)	C17 -C20	1.66(4)
Sn2 -O6	1.966(16)	Sn2 -O7	1.985(17)
Sn2 -C33	2.19(3)	Sn2 -C37	2.19(4)
B3 -O5	1.41(4)	B3 -O6	1.38(4)
B3 -C21	1.52(4)	B4 -O7	1.28(3)
B4 -O8	1.39(3)	B4 -C27	1.51(4)
C21 -C22	1.36(4)	C21 -C26	1.37(4)
C22 -C23	1.47(4)	C23 -C24	1.38(5)
C24 -C25	1.48(4)	C25 -C26	1.31(3)
C27 -C28	1.39(4)	C27 -C32	1.38(4)
C28 -C29	1.43(4)	C29 -C30	1.28(5)
C30 -C31	1.35(4)	C31 -C32	1.36(5)
C33 -C34	1.40(5)	C33 -C35	1.49(5)
C33 -C36	1.52(4)	C37 -C38	1.50(5)
C37 -C39	1.48(5)	C37 -C40	1.47(5)

Table 45: Bond Angles (°) for 3,3-Di-t-butyl-1,5-dihydroxy-1,5-diphenyl-2,4-dioxa-3-stanna-1,5-diboronate (**34**).

O4	-Sn1 -O1	92.0(7)	C13	-Sn1 -O1	101(1)
C13	-Sn1 -O4	107(1)	C17	-Sn1 -O1	101(1)
C17	-Sn1 -O4	111.4(9)	C17	-Sn1 -C13	135(1)
O2	-B1 -O1	120(3)	C1	-B1 -O1	129(3)
C1	-B1 -O2	111(2)	O4	-B2 -O3	103(3)
C7	-B2 -O3	124(3)	C7	-B2 -O4	133(3)
B1	-O1 -Sn1	140(2)	B2	-O4 -Sn1	120(2)
C2	-C1 -B1	112(2)	C6	-C1 -B1	126(3)
C6	-C1 -C2	121(3)	C3	-C2 -C1	114(3)
C4	-C3 -C2	123(3)	C5	-C4 -C3	123(3)
C6	-C5 -C4	113(3)	C5	-C6 -C1	124(3)
C8	-C7 -B2	128(3)	C12	-C7 -B2	120(3)
C12	-C7 -C8	112(3)	C9	-C8 -C7	123(3)
C10	-C9 -C8	123(3)	C11	-C10 -C9	118(3)
C12	-C11 -C10	113(3)	C11	-C12 -C7	129(3)
C14	-C13 -Sn1	111(2)	C15	-C13 -Sn1	104(2)
C15	-C13 -C14	121(3)	C16	-C13 -Sn1	105(2)
C16	-C13 -C14	106(3)	C16	-C13 -C15	109(3)
C18	-C17 -Sn1	110(2)	C19	-C17 -Sn1	111(2)
C19	-C17 -C18	115(3)	C20	-C17 -Sn1	97(2)
C20	-C17 -C18	108(3)	C20	-C17 -C19	114(3)
O7	-Sn2 -O6	90.0(7)	C33	-Sn2 -O6	110.3(9)
C33	-Sn2 -O7	102(1)	C37	-Sn2 -O6	109(1)
C37	-Sn2 -O7	102(1)	C37	-Sn2 -C33	133(1)
O6	-B3 -O5	112(2)	C21	-B3 -O5	120(3)
C21	-B3 -O6	128(3)	O8	-B4 -O7	118(2)
C27	-B4 -O7	124(2)	C27	-B4 -O8	118(2)
B3	-O6 -Sn2	114(2)	B4	-O7 -Sn2	140(2)
C22	-C21 -B3	118(3)	C26	-C21 -B3	127(3)

Table 45: Continued-

C26 -C21 -C22	115(2)	C23 -C22 -C21	126(3)
C24 -C23 -C22	117(3)	C25 -C24 -C23	114(3)
C26 -C25 -C24	125(3)	C25 -C26 -C21	122(3)
C28 -C27 -B4	120(2)	C32 -C27 -B4	126(2)
C32 -C27 -C28	114(3)	C29 -C28 -C27	119(3)
C30 -C29 -C28	120(3)	C31 -C30 -C29	123(3)
C32 -C31 -C30	116(3)	C31 -C32 -C27	126(3)
C34 -C33 -Sn2	112(2)	C35 -C33 -Sn2	102(2)
C35 -C33 -C34	110(3)	C36 -C33 -Sn2	108(2)
C36 -C33 -C34	110(3)	C36 -C33 -C35	113(3)
C38 -C37 -Sn2	110(2)	C39 -C37 -Sn2	106(2)
C39 -C37 -C38	113(3)	C40 -C37 -Sn2	105(2)
C40 -C37 -C38	108(3)	C40 -C37 -C39	114(3)

APPENDIX IX.

CRYSTALLOGRAPHIC ANALYSIS AND STRUCTURAL REFINEMENT OF 2,4-DIHYDROXY-1,1,3,3,5,5-HEXA-t-BUTYL-7-MESITYL-6,8,9-TRIOXA-1,3,5-TRISTANNA-7-BORATRICYCLO[3,1,1,1]NONANE (38).

IX.1 Crystal Data.

$C_{37}H_{73}BN_2O_5Sn_3$, M.W. = 992.88, orthorhombic, space group = *Pnn2*.

a = 16.456(2)Å, *b* = 16.448(3)Å, *c* = 18.411(2)Å.

α = 90.0, β = 90.0, γ = 90.0.

U = 4983.25Å^3, μ = 14.03 cm^{-1}, F(000) = 2064.

Radiation Mo-K$_\alpha$, λ = 0.71069Å, graphite monochromator.

For 1210 observed and unique reflections with $I > 3\sigma I$, R = 0.0718 and R_w = 0.0718.

IX.2 Crystallographic Analysis.

A crystal of approximate dimensions 0.3 × 0.2 × 0.2 mm was used for both the preliminary crystal analysis and the main data collection. The intensities of all reflections $2^\circ < \theta < 22^\circ$ were measured. One reflection was used as a standard and its intensity monitored every fifty observed reflections. Significant crystal decay was observed for prolonged exposure to the X-ray beam possibly due to acetonitrile loss.

IX.3 Structure Solution and Refinement.

Distinct problems were encountered for the refinement of the structure by the application of orthorhombic symmetry parameters. Two space groups, *Pnn2* and *Pnnm*, appeared suitable as all the observed systematic absences were satisfied. For the latter the space group would be centrosymmetric, however, based upon the mean absolute $[E^2-1]$ statistics this does not appear to be the case. Also, from the Patterson search in *Pnnm* too many tin positions were found in the unit cell for the analytically predicted stoichiometry. Using *Pnn2* the structure refined with difficulty probably resulting from the strong pseudo symmetry observed in the crystal from mirror planes observed both for the ring plane and perpendicular to the ring plane through Sn3, O3 and B1. Possibly as a consequence of this the t-butyl groups on Sn3 appear highly dissordered resulting in very high thermal parameters present in the data.

The crystal used, diplayed pseudo tetragonal symmetry where $a = b \neq c$ and $\alpha, \beta, \gamma = 90°$. The most suitable tetragonal space group available for the crystal is $P4_2nm$ which encompasses most of the systematic absences observed in the data when compared with the other available tetragonal space groups. However, not all are used as the h 0 l, h+l = 2n+1 systematic absence is not required in this instance. Even taking this into account the symmetry present in the structure appears higher than orthorhombic indicating that refinement using the $P4_2m$ even with the misgivings over the systematic absences may effect a better refinement of the structure. This attempted refinement is

currently taking place.

The crystal structure was solved using a Patterson search (SHELX86[256]) and refined by blocked matrix least-squares using SHELX76.[257] Data were corrected for Lorentz and polarisation effects but not for absorption. Hydrogen atoms were not included in calculated positions. The tin and oxygen atoms present in the molecule were refined anisotropically, while the remaining atoms in the molecule were refined isotropically. The atomic scattering factors and the anomolous dispersion correction factors for non-hydrogen atoms were taken from the literature.[258-260] The ORTEP program[261] was used for the drawing of the crystal structure (figure 49). The fractional atomic coordinates (Å) for the molecule are given in table 46, the anisotropic thermal parameters (Å) in table 47 and the bond lengths (Å) and bond angles (°) are given in tables 48 and 49 respectively.

Table 46: Fractional Atomic Coordinates and Thermal Parameters (Å) for 2,4-Dihydroxy-1,1,3,3,5,5-hexa-t-butyl-7-mesityl-6,8,9-trioxa-1,3,5-tristanna-7-boratricyclo[3,1,1,1]nonane (38).

Atom	x	y	z	Uiso or Ueq (***)
Sn1	0.20180(12)	0.13438(12)	0.00000	0.0671(11) ***
Sn2	0.36538(1)	0.29812(1)	-0.00027(2)	0.0672(1) ***
Sn3	0.28027(2)	0.21940(2)	-0.15700(2)	0.0916(2) ***
O1	0.19268(14)	0.13267(12)	-0.12183(11)	0.0767(14) ***
O2	0.36950(12)	0.30457(15)	-0.12185(11)	0.0826(14) ***
O3	0.28370(13)	0.21901(14)	-0.04350(15)	0.0934(16) ***
O4	0.33892(13)	0.26623(14)	0.10212(14)	0.0917(15) ***
O5	0.23268(15)	0.16168(14)	0.10403(13)	0.0936(16) ***
B1	0.2898(27)	0.2226(27)	0.1334(23)	0.103(13)
C1	0.2874(21)	0.2094(21)	0.2212(17)	0.084(9)
C2	0.2393(19)	0.2635(19)	0.2669(17)	0.077(9)
C3	0.3482(24)	0.1516(24)	0.3374(25)	0.124(13)
C4	0.2520(23)	0.2516(23)	0.3432(26)	0.122(13)
C5	0.3024(25)	0.1970(26)	0.3728(23)	0.124(14)
C6	0.3446(21)	0.1597(21)	0.2512(19)	0.092(10)
C7	0.1922(17)	0.3131(17)	0.2250(15)	0.071(8)
C8	0.3019(29)	0.1974(29)	0.4557(26)	0.155(18)
C9	0.3949(22)	0.1086(22)	0.2186(19)	0.106(12)
C10	0.2541(23)	0.0020(23)	0.0044(30)	0.131(12)
C11	0.1908(25)	-0.0239(26)	0.0777(22)	0.128(16)
C12	0.2165(31)	-0.0439(30)	-0.0594(28)	0.160(19)
C13	0.3309(26)	0.0039(26)	0.0332(22)	0.142(16)
C14	0.0708(23)	0.1775(24)	0.0110(31)	0.138(14)
C15	0.0735(23)	0.2626(24)	0.0255(21)	0.131(14)
C16	0.0258(29)	0.1334(30)	-0.0533(27)	0.151(18)

Table 46: Continued-

C17	0.0408(32)	0.1431(33)	0.0838(29)	0.169(21)
C18	0.3183(24)	0.4311(23)	0.0145(27)	0.136(14)
C19	0.3706(29)	0.4564(27)	0.0844(25)	0.142(17)
C20	0.2363(28)	0.4276(27)	0.0297(25)	0.160(18)
C21	0.3600(26)	0.4773(26)	-0.0563(24)	0.132(15)
C22	0.4928(22)	0.2565(22)	0.0038(29)	0.130(12)
C23	0.5281(24)	0.3052(25)	0.0798(22)	0.132(15)
C24	0.4979(23)	0.1723(24)	0.0221(22)	0.132(14)
C25	0.5428(34)	0.2806(34)	-0.0571(31)	0.205(24)
C30	0.2315(90)	0.2323(88)	-0.2820(70)	0.529(84)
C31	0.2335(39)	0.3706(41)	-0.2490(35)	0.226(26)
C32	0.1321(37)	0.2773(35)	-0.2362(33)	0.197(23)
C33	0.1451(36)	0.3491(37)	-0.1555(39)	0.234(26)
C34	0.4105(42)	0.0840(42)	-0.1783(41)	0.260(31)
C35	0.3374(60)	0.1428(61)	-0.2550(53)	0.316(43)
C36	0.3337(44)	0.0547(48)	-0.2561(42)	0.248(31)
C37	0.4445(43)	0.1618(42)	-0.2560(38)	0.241(29)
Cc1	0.4062(33)	0.4382(39)	0.2746(30)	0.169(20)
Cc2	0.4342(24)	0.3633(26)	0.2642(22)	0.120(13)
Cc3	0.6339(25)	0.4349(24)	0.7645(21)	0.114(12)
Cc4	0.5624(34)	0.4038(30)	0.7719(27)	0.150(17)
N1	0.4952(29)	0.3918(25)	0.7845(22)	0.169(15)
N2	0.3938(25)	0.5048(29)	0.2853(22)	0.165(15)

Table 47: Anisotropic Thermal Parameters (Å) for 2,4-Dihydroxy-1,1,3,3,5,5-hexa-t-butyl-7-mesityl-6,8,9- trioxa-1,3,5-tristanna-7-boratricyclo[3,1,1,1]nonane (38).

Atom	U11	U22	−U33	U23	U13	U12
Sn1	0.087(1)	0.080(1)	0.074(1)	0.004(2)	-0.006(2)	-0.028(1)
Sn2	0.082(1)	0.085(1)	0.075(1)	0.004(2)	0.001(2)	-0.027(1)
Sn3	0.131(2)	0.128(2)	0.070(1)	-0.006(2)	0.004(2)	-0.065(2)
O1	0.130(20)	0.083(16)	0.062(13)	-0.007(12)	-0.017(13)	-0.047(14)
O2	0.085(16)	0.158(23)	0.054(12)	0.017(13)	0.017(12)	-0.072(15)
O3	0.087(16)	0.096(17)	0.154(24)	0.018(16)	0.024(16)	0.017(14)
O4	0.083(16)	0.109(18)	0.138(20)	0.021(17)	-0.058(16)	-0.048(14)
O5	0.124(20)	0.098(18)	0.115(18)	0.059(16)	0.050(17)	-0.024(15)

Table 48: Bond Lengths (Å) for 2,4-Dihydroxy-1,1,3,3,5,5-hexa-t-butyl-7-mesityl-6,8,9-trioxa-1,3,5-tristanna-7-boratricyclo-[3,1,1,1]nonane (38).

Sn1 -O1	2.248(20)	Sn1 -O3	2.097(23)
Sn1 -O5	2.032(24)	Sn1 -C10	2.34(4)
Sn1 -C14	2.28(4)	Sn2 -O2	2.242(20)
Sn2 -O3	2.033(23)	Sn2 -O4	2.005(25)
Sn2 -C18	2.34(4)	Sn2 -C22	2.21(4)
Sn3 -O1	2.129(22)	Sn3 -O2	2.130(22)
Sn3 -O3	2.09(3)	Sn3 -C30	2.45(*)
Sn3 -C35	2.39(*)	O4 -B1	1.23(5)
O5 -B1	1.48(5)	B1 -C1	1.63(5)
C1 -C2	1.46(4)	C1 -C6	1.36(5)
C2 -C4	1.43(6)	C2 -C7	1.36(4)
C3 -C5	1.24(6)	C3 -C6	1.59(6)
C4 -C5	1.34(6)	C5 -C8	1.53(6)
C6 -C9	1.32(5)	C10 -C11	1.76(6)
C10 -C12	1.53(7)	C10 -C13	1.37(6)
C14 -C15	1.43(6)	C14 -C16	1.57(7)
C14 -C17	1.54(8)	C18 -C19	1.60(7)
C18 -C20	1.38(6)	C18 -C21	1.66(6)
C22 -C23	1.71(6)	C22 -C24	1.43(5)
C22 -C25	1.44(7)	C30 -C32	1.98(*)
C32 -C33	1.91(9)	C34 -C36	1.97(*)
C34 -C37	2.00(*)	C35 -C36	1.45(*)
C35 -C37	1.79(*)	Cc1 -Cc2	1.33(7)
Cc1 -N2	1.13(8)	Cc3 -Cc4	1.29(7)
Cc4 -N1	1.15(7)		

Table 49: Bond Angles (°) for 2,4-Dihydroxy-1,1,3,3,5,5-hexa-t-butyl-7-mesityl-6,8,9-trioxa-1,3,5-tristanna-7-boratricyclo-[3,1,1,1]nonane (**38**).

O3	-Sn1	-O1	70.7(9)	O5	-Sn1	-O1	163.7(9)
O5	-Sn1	-O3	93(1)	C10	-Sn1	-O1	93(1)
C10	-Sn1	-O3	113(1)	C10	-Sn1	-O5	95(1)
C14	-Sn1	-O1	92(1)	C14	-Sn1	-O3	116(1)
C14	-Sn1	-O5	95(2)	C14	-Sn1	-C10	129(1)
O3	-Sn2	-O2	70.1(9)	O4	-Sn2	-O2	163.3(9)
O4	-Sn2	-O3	93(1)	C18	-Sn2	-O2	95(1)
C18	-Sn2	-O3	115(1)	C18	-Sn2	-O4	94(1)
C22	-Sn2	-O2	91(1)	C22	-Sn2	-O3	116(1)
C22	-Sn2	-O4	95(1)	C22	-Sn2	-C18	127(1)
O2	-Sn3	-O1	144.6(8)	O3	-Sn3	-O1	73.3(8)
O3	-Sn3	-O2	71.3(8)	C30	-Sn3	-O1	97(3)
C30	-Sn3	-O2	117(3)	C30	-Sn3	-O3	162(3)
C35	-Sn3	-O1	98(2)	C35	-Sn3	-O2	108(2)
C35	-Sn3	-O3	138(2)	C35	-Sn3	-C30	58(4)
Sn3	-O1	-Sn1	104.5(9)	Sn3	-O2	-Sn2	104.6(9)
Sn2	-O3	-Sn1	134(1)	Sn3	-O3	-Sn1	111(1)
Sn3	-O3	-Sn2	114(1)	B1	-O4	-Sn2	138(3)
B1	-O5	-Sn1	131(2)	O5	-B1	-O4	130(4)
C1	-B1	-O4	124(4)	C1	-B1	-O5	105(3)
C2	-C1	-B1	120(3)	C6	-C1	-B1	118(3)
C6	-C1	-C2	120(3)	C4	-C2	-C1	114(3)
C7	-C2	-C1	110(3)	C7	-C2	-C4	136(3)
C6	-C3	-C5	117(4)	C5	-C4	-C2	125(4)
C4	-C5	-C3	124(4)	C8	-C5	-C3	122(4)
C8	-C5	-C4	114(4)	C3	-C6	-C1	119(3)
C9	-C6	-C1	129(3)	C9	-C6	-C3	112(3)
C11	-C10	-Sn1	92(2)	C12	-C10	-Sn1	106(3)
C12	-C10	-C11	103(3)	C13	-C10	-Sn1	109(3)

Table 49: Continued-

C13	-C10 -C11	105(4)		C13 -C10 -C12	133(4)
C15	-C14 -Sn1	107(3)		C16 -C14 -Sn1	104(3)
C16	-C14 -C15	127(4)	—	C17 -C14 -Sn1	105(3)
C17	-C14 -C15	102(4)		C17 -C14 -C16	110(4)
C19	-C18 -Sn2	99(2)		C20 -C18 -Sn2	108(3)
C20	-C18 -C19	112(4)		C21 -C18 -Sn2	101(2)
C21	-C18 -C19	107(3)		C21 -C18 -C20	126(4)
C23	-C22 -Sn2	102(2)		C24 -C22 -Sn2	111(2)
C24	-C22 -C23	104(4)		C25 -C22 -Sn2	115(3)
C25	-C22 -C23	108(3)		C25 -C22 -C24	115(4)
C32	-C30 -Sn3	84(5)		C33 -C32 -C30	118(5)
C37	-C34 -C36	79(4)		C36 -C35 -Sn3	121(6)
C37	-C35 -Sn3	108(5)		C37 -C35 -C36	102(7)
C35	-C36 -C34	74(5)		C35 -C37 -C34	67(4)
N2	-Cc1 -Cc2	170(6)		N1 -Cc4 -Cc3	166(5)

APPENDIX X.

INSTRUMENTATION DETAILS.

X.1 Infra-red Spectroscopy.

Infra-red spectra were recorded from prepared samples either as KBr discs or nujol mulls between KBr or CsI plates. The spectra were recorded on either Perkin Elmer 597 or 599B spectrometers in the 4000 - 200 cm^{-1} region. Calibration of the recorded spectra was with polystyrene film.

X.2 NMR Spectroscopy.

All ^{1}H and ^{13}C nmr spectra were recorded on a JEOL GX 270 spectrometer except for the 400 MHz ^{1}H and 90° 2d-COSY ^{1}H spectra of (1) which were recorded on a JEOL GX 400. In all ^{1}H and ^{13}C nmr spectra $(CH_3)_4Si$ (TMS) was used as the standard except for compounds containing the (Tsi) group when either $CHCl_3$, δ = 7.26 ppm or CH_2Cl_2, δ = 5.35 ppm was used. Proton decoupled ^{11}B, ^{29}Si, ^{77}Se and ^{119}Sn multinuclear nmr spectra were also recorded on the JEOL GX 400 spectrometer fitted with a multinuclear probe. The standards used in these instances were $BF_3.(CH_3CH_2)_2O$, $(CH_3)_4Si$, H_2SeO_3 and $(CH_3)_4Sn$ respectively.

X.3 Mass Spectrometry.

Mass spectra were collected on a V.G. 70-70E instrument interfaced with a DS2025 database. Ionisation techniques of electron ionisation (70 eV or low eV) or chemical ionisation using i-butene were implemented to obtain spectra.

X.4 Microanalysis.

Carbon, hydrogen and nitrogen were analysed for in solid and liquid samples using a Carlo Erba Strumentazione E.A. model 1106.

X.5 Mossbauer Spectroscopy.

Mossbauer spectra were recorded on a constant acceleration Cryophysics Mossbauer Spectrometer working in a sawtooth wave mode. For the tin spectra a 10 mCi calcium stannate (^{119m}Sn) source purchased from Amersham International, was used which in all instances was operated at ambient temperature. All the tin spectra were recorded at 78.5 ± 0.5 K except in the variable temperature experiments. The temperature of the sample was controlled using a constant flow liquid nitrogen cryostat interfaced to a DTC-2 digital variable temperature controller supplied by Oxford Instruments. All samples were either ran as finely ground powders or as frozen liquids. Calibration was equated to the six line magnetic hyperfine split spectrum of natural iron at room temperature. All the tin spectra obtained are quoted relative to

the singlet spectrum of SnO_2 at 78K (zero velocity). The spectra obtained were fitted to standard Lorenzian line shapes with a correction made for the parabolic base line curvature using a conventional least-squares fitting technique.

REFERENCES.

1. K.A. Kocheshkov, *Chem. Ber.* **62**, 996, 1926.
2. K. Moedritzer, *Organomet. Chem. Rev.* **1**, 179, 1966.
3. A.G. Davies, P.J. Smith, 'Comprehensive Organometallic Chemistry eds. G. Wilkinson; F.G.A. Stone; E.W. Abel, Pergamon Press, Oxford, (1982), P.519
4. H. Meyer, G. Baum, W. Massa, S.Berger and A. Berndt, *Angew. Chem. Int. ed.* **26**, 546, 1987.
5. K.D. Dobbs and W.J.Hehre, *Organometallics.* **5**, 2057, 1986.
6. I. Wharf and M.G. Simard, *J. Organomet. Chem.* **332**, 85, 1987.
7. P. Ganis, G. Valle, G. Tagliavini, W. Kitching, K.G. Penman and M.A. Jones, *J. Organomet. Chem.* **349**, 57, 1988.
8. D.K. Srivastava, V.D. Gupta, H. Noth and W. Rattay, *J. Chem. Soc. Dalton Trans.* 1533, 1988.
9. M. Weidenbruch, K. Schafers, S. Pohl, W. Saak, K. Peters and H.G. von Schnering, *J. Organomet. Chem.* **346**, 171, 1988.
10. J.S. Tse, M.J. Collins, F.L. Lee and E.J. Gabe, *J. Organomet. Chem.* **310**, 169, 1986.
11. R.S. Berry, *J. Chem. Phys.* 32, 933, 1960.
12. B. Jousseaume, P. Villeneuve, M. Drager, S. Roller and J.M Chezau, *J. Organomet. Chem.* **349**, C1, 1988.
13. T. Tahara, H. Imazaki, K. Aoki and H. Yamazaki, *J. Organomet. Chem.* **327**, 157, 1987.

14. R.O. Day, J.M. Holmes, S. Shafieezad, V. Chandrasekhar and R.R. Holmes, *J. Am. Chem. Soc.* **110**, 5377, 1988.

15. P.G. Harrison, K. Lambert, T.J. King and B. Majee, *J. Chem. Soc. Dalton Trans.* 363, 1983.

16. T.P. Lockhart, *Organometallics.* **7**, 1438, 1988.

17. M. Drager, *Z. Naturforsch.* **B36**, 437, 1981.

18. R.R. Holmes, S. Shafieezad, J.M Holmes and R.O. Day, *Inorg. Chem.* **27**, 1232, 1988.

19. S.W. Ng, C. Wei, V.G. Kumar Das and T.C.W. Mak, *J. Organomet. Chem.* **326**, C61, 1987.

20. V.G. Kumar Das, L.K. Mun and C. Wei, *Organometallics.* **6**, 10, 1987.

21. B.K. Nicholson, *J. Organomet. Chem.* **265**, 153, 1984.

22. K.C. Molloy, T.G. Purcell, K. Quill and I.W. Nowell, *J. Organomet. Chem.* **267**, 237, 1984.

23. G. Valle, A.S. Gonzalez, R. Ettorre and G. Plazzogna, *J. Organomet. Chem.* **348**, 49, 1988.

24. P. Ganis, V. Peruzzo and G. Valle. *J. Organomet. Chem.* **256**, 245, 1983.

25. D. Cunningham, T. Higgins, B. Kneafsey, P. McArdle and J. Simmie, *J. Chem. Soc. Chem. Commun.* 231, 1985.

26. D.K. Srivastava, V.D. Gupta, H. Noth and W. Rattay, *J. Chem. Soc. Dalton Trans.* 1533, 1988.

27. C. Pelizzi, G. Pelizzi and G. Predieri, *J. Organomet. Chem.* **263**, 9, 1984.

28. P.J. Smith and A.P. Tupciauskas, *Annu. Rev. NMR Spectrosc.* **8**, 291, 1978.

29. J.D. Kennedy and W. Mcfarlane, *Rev. Silicon, Germanium, Tin, Lead Compd.* **1**, 235, 1974.

30. V.S. Petrosyan, *Prog. Nucl. Magn. Reson. Spectrosc.* **11**, 115, 1977.

31. B. Wrackmeyer, *Annu. Rev. NMR Spectrosc.* **16**, 73, 1985.

32. R.K. Harris, J.D. Kennedy and W. Mcfarlane, in 'NMR and the Periodic Table', ed. R.K. Harris and B.E. Mann, Academic Press, London, 342, 1978.

33. 'Multinuclear NMR', ed. J. Mason, Plenum Press, New York, 1987.

34. M. Mehring, 'High Resolution NMR Spectroscopy in Solids', eds. P. Diehl, E. Fluck and R. Kosfeld, Springer-Verlag, New York, 11, 1976.

35. U. Haeberlen, *Adv. Magn. Resonance*, Suppl. 1. 1976.

36. E.R. Andrew, *Progr. NMR Spectrosc.* **8**, 1, 1971.

37. E.R. Andrew, in 'International Review of Science, Physical Chemistry, Series 2', ed. C.A. McDowell, Butterworths, London, **4**, 173, 1975.

38. R.G. Griffen, *Analyt. Chem.* **49**, 951A, 1977.

39. R.W. Vaughan, *Annu. Rev. Phys. Chem.* **29**, 397, 1978.

40. 'Nuclear Magnetic Resonance in Solids', *NATO Advanced Study Institute Series*, ed. L.W. Gerven, Plenum Press, New York, B22, 1974.

41. R.K. Harris and K.J. Packer, *European Spectrosc. News.* **21**, 37, 1978.

42. H.W. Spiess, 'Dynamic NMR Spectroscopy', in 'NMR Basic Principles and Progress', eds. P. Diehl, E. Fluck and R. Kosfeld, Springer-Verlag, New York, **15**, 1978.

43. J. Schaefer and E.D. Stejskal, 'High Resolution ^{13}C NMR of Solid Polymer' in 'Topics in Carbon-13 NMR Spectroscopy', ed. G.C. Levy, Wiley-Interscience, New York, **3**, 283, 1979.

44. D.A Torchia and D.L. VanderHart, 'High-Power Double-Resonance Studies of Fibrous Proteins, Proteoglycans and Model Membranes', in 'Topics in Carbon-13 NMR Spectroscopy', ed. G.C Levy, Wiley-Interscience, New York, **3**, 325, 1979.

45. N. Boden, 'NMR Studies of Plastic Crystals', in 'The Plastically Crystalline State', ed. J.N. Sherwood, John Wiley and Sons, New York, 147, 1979.

46. F.P. Miknis, V.J. Bartuska and G.E. Maciel, *Amer. Lab.* **Nov**, 19, 1979.

47. J.R. Lyerla, 'High Resolution Carbon-13 Studies of Bulk Polymers' , in 'Contempory Topics in Polymer Science', ed. M. Shen, Plenum Publishing Corp., New York, **3**, 143, 1979.

48. J. Schaefer, E.D. Stejskal, M.D. Sefcik and R.A. McKay, *Phil. Trans. Roy. Soc.* **A299**, 475, 1981.

49. A.N. Garroway, D.L. VanderHart and W.L. Earl, *Phil. Trans. Roy. Soc.* **A299**, 609, 1981.

50. G.E. Balimann, C.J. Groombridge, R.K. Harris, K.J. Packer, B.J. Say and S.F. Tanner, *Phil. Trans. Roy. Soc.* **A299**, 643, 1981.

51. S.J. Opella, J.G. Hexem, M.H. Frey and T.A. Cross, *Phil. Trans. Roy. Soc.* **A299**, 665, 1981.

52. B.C. Gerstein, 'High Resolution Nuclear Magnetic Resonance of Solids', in 'Magnetic Resonance in Colloid and Interface Science', eds. J.P. Fraissard and H.A. Resing, Reidel Publishing Company, 175, 1980.

53. R.E. Wsaylishen and C.A. Fyfe, 'High-Resolution NMR of Solids', in 'Annual Reports on NMR Spectroscopy', ed. G.A. Webb, Academic Press, **12**, 1982.

54. G.E. Maciel and D.W. Sindorf, *J. Am. Chem. Soc.* **102**, 7606, 1980.

55. J.M. Thomas and J. Klinowski, in 'Advances in Catalysis', eds. D.D. Eley, H. Pines and P.B. Weisz, Academic Press, **33**, 1985.

56. R.C. Mehrotra and R. Bohra, in 'Metal Carboxylates', Academic Press, London, 1983.

57. K.C. Molloy and J.J. Zuckerman, *Acc. Chem. Res.* **16**, 386, 1983.

58. T.P. Lockhart, W.F. Manders and J.J. Zuckerman, *J. Am. Chem. Soc.* **107**, 4546, 1985.

59. W.F. Manders and T.P. Lockhart, *J. Organomet. Chem.* **297**, 143, 1985.

60. R.K. Harris and A. Sebald, *J. Organomet. Chem.* **331**, C9, 1987.

61. K.C. Molloy, *Inorg. Chim. Acta.* **141**, 151, 1988.

62. A. Lycka, D. Snobl, K. Handlir, J. Holecek and M. Nadvornik, *Collection Czech. Chem. Commun.* **46**, 1383, 1981.

63. J. Holecek, M. Nadvornik, K. Handlir and A. Lycka, *J. Organomet. Chem.* **241**, 177, 1983.

64. J. Otera, A. Kusaba, T. Hinoishi and Y. Kawasaki, *J. Organomet. Chem.* **228**, 223, 1982.

65. R. Hulme, *J. Chem. Soc.* 1524, 1963.

66. W. Mcfarlane and R.J. Wood, *J. Organomet. Chem.* **40**, C17, 1972.

67. R.W. Taft Jr., in 'Steric Effects in Organic Chemistry', ed. M.S. Newman, Wiley, New York, 591, 1956.

68. P.J. Smith and L. Smith, in 'Inorg. Chim. Acta Rev.', ed. U. Croatto, **7**, 11, 1973.

69. A.P. Tupciauskas, C and Diss., Moscow State Univ. 1972

70. J.D. Kennedy, W. Mcfarlane, G.S. Pyne, P.L. Clarke and J.L. Wardell, *J. Chem. Soc. Perkin II*, 1234, 1975.

71. J.D. Kennedy, *J. Chem. Soc. Perkin II*, 242, 1977.

72. E.V. van den Berghe and G.P. van der Kelen, *J. Mol Struct.* **20**, 147, 1974.

73. B.K. Hunter and L.W. Reeves, *Can. J. Chem.* **46**, 1399, 1968.

74. P.G. Harrison, S.E. Ulrich and J.J. Zuckerman, *J. Am. Chem. Soc.* **93**, 5398, 1971.

75. J.D. Kennedy, W. Mcfarlane and G.S. Pyne, *Bull. Soc. Chim. Belge.* **84**, 289, 1975.

76. T.P. Lockhart and W.F. Manders, *Inorg. Chem.* **25**, 892, 1986.

77. T.P. Lockhart and W.F. Manders, *J. Am. Chem. Soc.*, **107**, 5863, 1985.

78. J. Holecek and A. Lycka, *Inorg. Chim. Acta.* **118**, L15, 1986.

79. R.L. Mossbauer, *Naturwissenschaften.* **45**, 538, 1958.

80. 'Mossbauer Effect Data Index', eds. A.H. Muir, K.J. Ando and H.M. Coogan, Wiley, New York, 1966.

81. 'An Introduction to Mossbauer Spectroscopy', ed. L. May, Plenum Press, New York, 1971.

82. 'Chemical Applications of Mossbauer Spectroscopy', eds. V.I. Goldanskii and R.H. Herber, Academic Press, New York, 1968.

83. H. Frauenfelder, in 'The Mossbauer Effect', Benjamin, New York, 1962.

84. T.C. Gibb and N.N. Greenwood, in 'Mossbauer Spectroscopy', Chapman and Hall, London, 1971.

85. V.I. Goldanskii, in 'The Mossbauer Effect And its Applications in Chemistry', Consultants Bureau, New York, 1964.

86. 'Mossbauer Effect Methodology', ed. I.J. Gruverman, Plenum Press, New York, 1-7, 1965-1971.

87. 'The Mossbauer Effect and its Applications in Chemistry', ed. R.F. Gould, Amer. Chem. Soc., Washington, D.C., 1967.

88. G.K. Wertheim, in 'Mossbauer Effect: Principles and Applications', Academic Press, New York, 1964.

89. G.M. Bancroft and R.H. Platt, *Adv. Inorg. Chem. Radiochem.* **15**, 59, 1972.

90. J.R. Devoe and J.J. Spijkerman, *Mossbauer Spectrometry, Anal. Chem. Ann. Rev.* **42**, 366R, 1970.

91. J.F. Duncan and R.M Golding, *Quart. Rev. Chem. Soc.* **19**, 36, 1965.

92. E. Fluck, *Adv. Inorg. Chem. Radiochem.* **6**, 433, 1964.

93. V.I. Goldanskii, V.V. Khrapov and R.A. Stukan, *Organometal. Chem. Rev. Sect. A.* **4**, 225, 1969.

94. N.N. Greenwood, *Chem. Brit.* **3**, 56, 1967.

95. R.H. Herber, *Progr. Inorg. Chem.* **8**, 1, 1966.

96. R.V. Parish, *Progr. Inorg. Chem.* **15**, 101, 1972.

97. P.J. Smith, *Organometal. Chem. Rev. Sect. A.* **5**, 373, 1970.

98. J.J. Zuckerman, *Adv. Organomet. Chem.* **9**, 21, 1970.

99. J.N.R. Ruddick, *Rev. Silicon, Germanium, Tin, Lead Compd.* 2, 115, 1976.

100. J.J. Zuckerman, in 'Chemical Mossbauer Spectroscopy', ed. R.H. Herber, Plenum Publishing Company, New York, 267, 1984.

101. J.D. Cotton, P.J. Davidson and M.F. Lappert, *J. Chem. Soc. Dalton Trans.* 2275, 1976.

102. D.E. Williams and C.W. Kocher, *J. Chem. Phys.* **52**, 1480, 1970.

103. N. Watanabe and E. Niki, *Bull. Chem. Soc. Japan.* **45**, 1, 1972.

104. P.A. Grutsch, M.V. Zeller and T.P. Fehlner, *Inorg. Chem.* **12**, 1431, 1973.

105. J. Devooght, M. Gielen and S. Lejeune, Private Communication. 1968.

106. M. Cordey-Hayes, *J. Inorg and Nucl. Chem.* **26**, 915, 1964.

107. R.H. Herber, H.A. Stockler and W.T. Reichle, *J. Chem. Phys.* **42**, 2447, 1965.

108. V.V. Khrapov, C and Diss., Inst. Chem. Phys., Acad. Sci. U.S.S.R., Moscow. 1965.

109. A.A. Petrov, B.I. Rogozev, C.M. Kristianskii and V.S. Zavgorodnii, *Zhur. Obshchei Khim.* **38**, 1196, 1968.

110. V.I. Goldanskii, E.F. Makarov, R.A. Stukhan, T.N. Sumakarova, V.A. Trukhtanov and V.V. Khrapov, *Doklady Phys. Chem.* **156**, 474, 1964.

111. H.A. Stockler and H. Sano, *Trans. Faraday Soc.* **64**, 577, 1968.

112. V.I. Goldanskii, E.F. Makarov, R.A. Stukhan, V.A. Trukhtanov and V.V. Khrapov, *Doklady Akad. Nauk. S.S.S.R., Phys. Chem. Sect.* **151**, 598, 1963.

113. M. Cordey-Hayes, R.D. Peacock and M. Vucelic, *J. Inorg. Nucl. Chem.* **29**, 1177, 1967.

114. W.B. Fitzsimmons, N.J. Seeley and A.W. Smith, *J. Chem. Soc. (A).* 890, 1968.

115. M.A. Mullins and C. Curran, *Inorg. Chem.* **7**, 2584, 1968.

116. R.V. Parish and R.H. Platt, *J. Chem. Soc. (A).* 2145, 1969.

117. T.K. Sham and G.M. Bancroft, *Inorg. Chem.* **14**, 2281, 1975.

118. K.C. Molloy and K. Quill, *J. Chem. Soc. Dalton Trans.* 1417, 1985.

119. R.H. Herber, *J. Chem. Phys.* **54**, 3755, 1971.

120. R.A. Cummins and P. Dunn, *The Infra-red Spectra of Organotin Compounds*, Austral. Defence Scientific Service, 1963.

121. R. Okawara and M. Wada, *Adv. Organomet. Chem.* **5**, 137, 1967.

122. T. Tanaka, *Organometal. Chem. Rev. Sect. A.* **5**, 1, 1970.

123. R. Okawara, D.E. Webster and E.G. Rochow, *J. Am. Chem. Soc.* **82**, 3287, 1965.

124. N. Kasai, K. Yasuda and R. Okawara, *J. Organomet. Chem.* **3**, 172, 1965.

125. R. Okawara and K. Yasuda, *J. Organomet. Chem.* **1**, 356, 1964.

126. M.C. Henry and J.G. Noltes, *J. Am. Chem. Soc.* **82**, 555, 1960.

127. R. Mathis-Noel, M. Lesbre and I. Seree de Roch, *C.R. Hebd. Seances Acad. Sci.* **243**, 257, 1956.

128. M.P. Brown, R. Okawara and E.G. Rochow, *Spectrochim. Acta.* **16**, 595, 1960.

129. R.C. Poller, *J. Inorg. Nucl. Chem.* **24**, 593, 1962.

130. E. Friebe and H. Kelker, *Z. Analyt. Chem.* **192**, 267, 1963.

131. R.C. Poller, *J. Chem. Soc.* 706, 1963.

132. H. Schumann, *Z. Anorg. Allg. Chem.* **354**, 192, 1967.

133. F.W. Behnke and C. Tamborski, A.S.T.I.A. AD.274995, Technical Documentary Report No. ASD-TDR-62-224. 1962.

134. P. Taimsalu and J.L. Wood, *Spectrochim. Acta.* **20**, 1043, 1964.

135. N.A.D. Carey and H.C. Clark, *J. Chem. Soc. Chem. Commun.* 292, 1967.

136. J.G. Noltes, M.C. Henry and M.J. Janssen, *Chem. and Ind.* 298, 1959.

137. M. Atoji and W.N. Lipscomb, *Acta Crystallogr.* **6**, 547, 1963.

138. A. Zalkin and D.E. Sands, *Acta Crystallogr.* **11**, 615, 1958.

139. D.W. Breck, in 'The Properties and Applications of Zeolites', ed. R.P. Townsend, The Chemical Society, London, 1980.

140. G.M. Sheldrick and R. Taylor, *Acta Crystallogr.* **B33**, 135, 1977.

141. R. Hengel, U. Kunze and J. Strahle, *Z. Anorg. Allg. Chem.* **423**, 35, 1976.

142. D. Ginderow and M.M. Huber, *Acta Crystallogr.* **B29**, 560, 1973.

143. N.W. Alcock and R.E. Timms, *J. Chem. Soc. (A).* 1873, 1968.

144. E.O. Schlemper and D. Britton, *Inorg. Chem.* **5**, 507, 1966.

145. N.W. Alcock and R.E. Timms, *J. Chem. Soc. (A).* 1876, 1968.

146. G.M. Sheldrick and W.S. Sheldrick, *J. Chem. Soc. (A).* 490, 1970.

147. N.W. Alcock and J.F. Sawyer, *J. Chem. Soc. Dalton Trans.* 1090, 1977.

148. S. Masamune, L.R. Sita and D.L.J. Williams, *J. Am. Chem. Soc.* **105**, 630, 1983.

149. W.V. Farrar and H.A. Skinner, *J. Organomet. Chem.* **1**, 434, 1964.

150. H. Puff, C. Bach, W. Schuh and R. Zimmer, *J. Organomet. Chem.* **312**, 313, 1986.

151. H. Puff, W. Shuh, R. Sievers, W. Wald and R. Zimmer, *J. Organomet. Chem.* **260**, 271, 1984.

152. U. Weber, N. Pauls, W. Winter and H.B. Stegmann, *Z. Naturforsch. B.* **37**, 1316, 1982.

153. H. Puff, R. Gattermeyer, R. Hundt and R. Zimmer, *Angew. Chem. Int. Ed. Engl.* **16**, 547, 1977.

154. B. Menzebach and P. Bleckmann, *J. Organomet. Chem.* **91**, 291, 1975.

155. H. Puff, I. Bung, E. Friedrichs and A. Jansen, *J. Organomet. Chem.* **254**, 23, 1983.

156. V. Chandrasekhar, C.G. Schmid, S.D. Burton, J.M. Holmes, R.O. Day and R.R. Holmes, *Inorg. Chem.* **26**, 1050, 1987.

157. R.R. Holmes, C.G. Schmid, V. Chandrasekhar, R.O. Day and J.M. Holmes, *J. Am. Chem. Soc.* **109**, 1408, 1987.

158. H. Berwe and A. Haas, *Chem. Ber.* **120**, 1175, 1987.

159. H. Schumann and H. Benda, *Angew. Chem. Int. Ed. Engl.* **7**, 813, 1968.

160. M. Drager and B. Mathiasch, *Angew. Chem. Int. Ed. Engl.* **20**, 1029, 1981.

161. M. Veith and R. Lisowsky, *Angew. Chem. Int. Ed. Engl.* **27**, 1087, 1988.

162. V. Chandrasekhar, R.O. Day and R.R. Holmes, *Inorg. Chem.* **24**, 1970, 1985.

163. R.O. Day, J.M. Holmes, V. Chandrasekhar and R.R. Holmes, *J. Am. Chem. Soc.* **109**, 940, 1987.

164. K. Yunlu, N. Hock and R.D. Fischer, *Angew. Chem. Int. Ed. Engl.* **24**, 879, 1985.

165. S. Masamune and L.R. Sita, *J. Am. Chem. Soc.* **107**, 6390, 1985.

166. C. Couret, J. Escudie and J. Satge, *J. Am. Chem. Soc.* **107**, 8280, 1985.

167. W.T. Reichle, *Inorg. Chem.* **5**, 87, 1966.

168. S.A. Kandil and A.L. Allred, *J. Chem. Soc. (A).* 2987, 1970.

169. S.D. Rosenberg, E. Debreczeni and E.L. Weinberg, *J. Am. Chem. Soc.* **81**, 972, 1959.

170. R.K. Ingham, S.D. Rosenberg and H. Gilman, *Chem. Rev.* **60**, 459, 1960.

171. H.C. Clark and C.J. Willis, *J. Am. Chem. Soc.* **82**, 1888, 1960.

172. A. Rahm and M. Pereyre, *J. Am. Chem. Soc.* **99**, 1672, 1977.

173. L.F. McGahey and F.R. Jensen, *J. Am. Chem. Soc.* **101**, 4397, 1979.

174. G.J.M. van der Kerk and J.G.A. Luijten, *J. Appl. Chem.* **6**, 56, 1956.

175. R.H. Prince, *J. Chem. Soc.* 1783, 1959.

176. D. Hanssgen, H. Puff and N. Beckermann, *J. Organomet. Chem.* **293**, 191, 1985.

177. H. Gilman, O.L. Marrs and S.-Y. Sim, *J. Org. Chem.* **27**, 4232, 1962.

178. B. Jousseaume and P. Villeneuve, *J. Chem. Soc. Chem. Commun.* 513, 1987.

179. H.G. Kuivila, T.J. Karol and K. Swami, *Organometallics.* **2**, 909, 1983.

180. E.V. van den Berghe and G.P. van der Kelen, *J. Organomet. Chem.* **26**, 207, 1971.

181. J.D. Kennedy, W. McFarlane, G.S. Pyne, P.L. Clarke and J.L. Wardell, *J. Chem. Soc. Perkin Trans. 2.* 1234, 1975.

182. H. Preut, H.-J. Haupt and F. Huber, *Z. Anorg. Allg. Chem.* **396**, 81, 1973.

183. S. Adams, M. Drager and B. Mathiasch, *Z. Anorg. Allg. Chem.* **532**, 81, 1986.

184. T.A.K. Al-Allaf, C. Eaborn, P.B. Hitchcock, M.F. Lappert and A. Pidcock, *J. Chem. Soc. Chem. Commun.* 548, 1985.

185. A.L. Spek, K.D. Bos, E.J. Bulten and J.G. Noltes, *Inorg. Chem.* **15**, 339, 1976.

186. S. Adams, M. Drager and B. Mathiasch, *J. Organomet. Chem.* **326**, 173, 1987.

187. N.W. Alcock and J.F. Sawyer, *J. Chem. Soc. Dalton Trans.* 1090, 1977.

188. F. Glockling, P. Harriott and W.-K. Ng, *J. Chem. Res.* (S) 12, (M) 275, 1979.

189. Z.H. Aiube and C. Eaborn, *J. Organomet. Chem.* **269**, 217, 1984.

190. R. Okawara, D.G. White, K. Fujitani and H. Sato, *J. Am. Chem. Soc.* **83**, 1342, 1961.

191. A.G. Davies, L. Smith, P.J. Smith and W. McFarlane, *J. Organomet. Chem.* **29**, 245, 1971.

192. P.G. Harrison, T.J. King, J.A. Richards and R.C. Phillips, *J. Organomet. Chem.* **116**, 307, 1976.

193. R. Okawara and M. Wada, *Adv. Organomet. Chem.* **5**, 164, 1967.

194. D. Seyferth and S.C. Vick, *J. Organomet. Chem.* **125**, C11, 1977.

195. P. Ganis, D. Furlani, D. Marton, G. Tagliavini and G. Valle, *J. Organomet. Chem.* **293**, 207, 1985.

196. R.D. Bach and P.A. Scherr, *Tetrahedron Lett.* 1099, 1973.

197. T.J. Barton and S.K. Hoekman, *J. Am. Chem. Soc.* **102**, 1584, 1980.

198. H.-J. Jacobsen and B. Krebs, *J. Organomet. Chem.* **136**, 333, 1977.

199. M. Drager, A. Blecher, H.-J. Jacobsen and B. Krebs, *J. Organomet. Chem.* **161**, 319, 1978.

200. A. Blecher and M. Drager, *Angew. Chem. Int. Ed. Engl.* **18**, 677, 1979.

201. R.R. Holmes, S. Shafieezad, V. Chandrasekhar, J.M. Holmes and R.O. Day, *J. Am. Chem. Soc.* **110**, 1174, 1988.

202. A.G. Davies, A.J. Price, H.M. Davies and M.B. Hursthouse, *J. Chem. Soc. Dalton Trans.* 297, 1986.

203. P.A. Bates, M.B. Hursthouse, A.G. Davies and S.D. Slater, *J. Organomet. Chem.* **325**, 129, 1987.

204. A.G. Davies, S.D. Slater, D.C. Povey and G.W. Smith, *J. Organomet. Chem.* **352**, 283, 1988.

205. E. W. Abel and D.A. Armitage, *Adv. Organomet. Chem.* **5**, 1, 1967.

206. M. Schmidt and H. Ruf, *Chem. Ber.* **96**, 784, 1963.

207. H. Schumann, R. Montachemi, H.J. Kroth and U. Frank, *Chem. Ber.* **106**, 2049, 1973.

208. G.S. Sasin, *J. Org. Chem.* **18**, 1142, 1953.

209. W.T. Reichle, *Inorg. Chem.* **1**, 650, 1962.

210. H. Kriegsmann and H. Hoffmann, *Z. Chem.* **3**, 268, 1963.

211. B. Mathiasch, *J. Organomet. Chem.* **194**, 37, 1980.

212. H. Puff, B. Breuer, W. Schuh, R. Sievers and R. Zimmer, *J. Organomet. Chem.* **332**, 279, 1987.

213. H. Puff, A. Bongartz, W. Schuh and R. Zimmer, *J. Organomet. Chem.* **248**, 61, 1983.

214. B. Mathiasch, *Z. Anorg. Allg. Chem.* **432**, 269, 1977.

215. H. Puff, E. Friedrichs, R. Hundt and R. Zimmer, *J. Organomet. Chem.* **259**, 79, 1983.

216. D.L. Klayman and T.S. Griffin, *J. Am. Chem. Soc.* **95**, 197, 1973.

217. D.N. Harpp and K. Steliou, *Synthesis*. 721, 1976.

218. S. Masamune, Y. Hanzawa, S. Murakami, T. Bally and J.F. Blount, *J. Am. Chem. Soc.* **104**, 1150, 1982.

219. A. Schafer, M. Weidenbruch, K. Peters and H.G. Schnering, *Angew. Chem. Int. Ed. Engl.* **23**, 302, 1984.

220. S. Masamune, Y. Hanzawa and D.J. Williams, *J. Am. Chem. Soc.* **104**, 6136, 1982.

221. W. Ando, Y. Hamada, A. Sekiguchi and K. Ueno, *Tetrahedron Lett.* **23**, 5323, 1982.

222. H.B. Yokelson, A.J. Millevolte, G.R. Gillette and R. West, *J. Am. Chem. Soc.* **109**, 6865, 1987.

223. W. Ando, Y. Hamada, A. Sekiguchi and K. Ueno, *Tetrahedron Lett.* **24**, 4033, 1983.

224. R. West, D.J. De Young and K.J. Haller, *J. Am. Chem. Soc.* **107**, 4942, 1985.

225. W. Ando and T. Tsumuraya, *Tetrahedron Lett.* **27**, 3251, 1986.

226. D.L. Alleston, A.G. Davies, M. Hancock and R.F.M. White, *J. Chem. Soc.* 5469, 1963.

227. H. Puff, E. Friedrichs and F. Visel, *Z. Anorg. Allg. Chem.* **477**, 50, 1981.

228. A.G. Davies and P.G. Harrison, *J. Chem. Soc. (C).* 2035, 1970.

229. W. Hoffmeister, Dissertation, Bonn 1976.

230. A.J. Gibbons, A.K. Sawyer and A. Ross, *J. Org. Chem.* **26**, 2304, 1961.

231. D. Kobelt, E.F. Paulus and H. Scherer, *Acta Crystallogr.* **B28**, 2323, 1972.

232. A.G. Davies, L. Smith and P.J. Smith, *J. Organomet. Chem.* **39**, 279, 1972.

233. J.G.A. Luijten, *Recl. Trav. Chim. Pays-Bas.* **85**, 873, 1966.

234. W.D. Honnick and J.J. Zuckerman, *Inorg. Chem.* **15**, 3034, 1976.

235. S.J. Blunden, P.J. Smith and D.G. Gillies, *Inorg. Chim. Acta.* **60**, 105, 1982.

236. S.K. Mehrotra, G. Srivastava and R.C. Mehrotra, *J. Organomet. Chem.* **73**, 277, 1974.

237. S.K. Mehrotra, G. Srivastava and R.C. Mehrotra, *J. Organomet. Chem.* **65**, 361, 1974.

238. S.K. Mehrotra, G. Srivastava and R.C. Mehrotra, *J. Organomet. Chem.* **65**, 367, 1974.

239. S.K. Mehrotra, G. Srivastava and R.C. Mehrotra, *J. Organomet. Chem.* **47**, 39, 1973.

240. C.J. Evans, *Glass.* **51**, 303, 1974.

241. T. Suzukawa, *Seramikkusu (Japan).* **4**, 852, 1969.

242. M.J. Fuller, *Tin Its Uses.* **103**, 3, 1975.

243. M & T Chemicals Inc., *U.S. Pat.* 4 130 673 (1978) (*Chem. Abstr.* **85**, 9632, 1976).

244. H.G. Faender, in 'Schott Guide to Glass', Van Nostrand Reinhold, New York, 1983.

245. O. Graalmann, U. Klingebiel, W. Clegg, M. Haase and G.M. Sheldrick, *Z. Anorg. Allg. Chem.* **519**, 87, 1984.

246. H.A. Bent, *Chem. Rev.* **61**, 275, 1961.

247. J.B. Farmer, *Adv. Inorg. Chem. Radiochem.* **25**, 187, 1982.

248. S.J. Rettig and J. Trotter, *Can. J. Chem.* **55**, 3071, 1977.

249. P.A. Akishin and V.P. Spiridonov, *Dokl. Akad. Nauk. SSSR.* **131**, 557, 1960.

250. P.G. Harrison and R.C. Philips, *J. Organomet. Chem.* **182**, 37, 1979.

251. A.M. Domingos and G.M. Sheldrick, *J. Chem. Soc. Dalton Trans.* 477, 1974.

252. R.E. Drew and F.W.B. Einstein, *J. Organomet. Chem.* **114**, 47, 1976.

253. C.K. Chu and J.D. Murray, *J. Chem. Soc. (A).* 360, 1971.

254. E. Khotinsky and M. Melamed, *Chem. Ber.* **42**, 3090, 1909.

255. R.L. Merker and M.J. Scott, *J. Am. Chem. Soc.* **85**, 2243, 1963.

256. G.M. Sheldrick, SHELX86 a computer program for crystal structure determination, University of Goetingen, 1986.

257. G.M. Sheldrick, SHELX76 a computer program for crystal structure determination, University of Cambridge, 1976.

258. D.T. Cromer and J.B. Mann, *Acta Crystallogr.* **A24**, 321, 1968.

259. R.F. Stewart, E.R. Davidson and W.T. Simpson, *J. Chem. Phys.* **42**, 3175, 1965.

260. D.T. Cromer and D.J. Liberman, *J. Chem. Phys.* **53**, 1891, 1970.

261. C.K. Johnson, ORTEP, Oak Ridge Natl. Lab (Rep) ORNL (US), 3794, 1965, revised 1971.

262. N. Walker and D.Stewart, DIFABS a computer program to correct for absorption effects in crystals, *Acta Crystallogr.* **A39**, 158, 1983.

NUMERICAL INDEX FOR COMPOUNDS INCLUDED IN THIS THESIS.

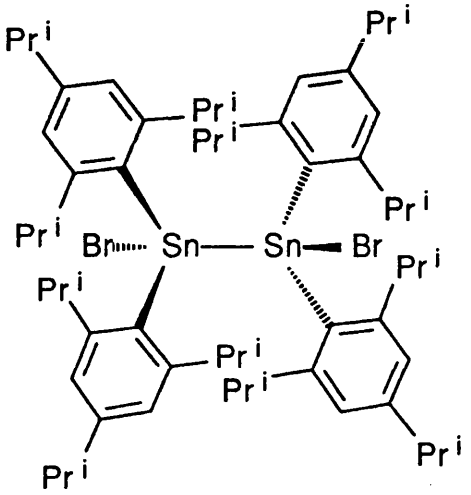

(1)

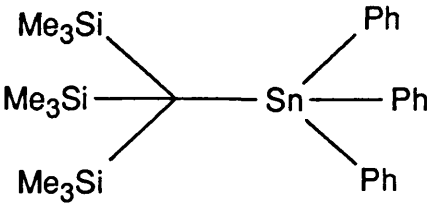

(2)

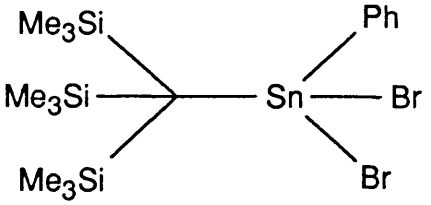

(3)

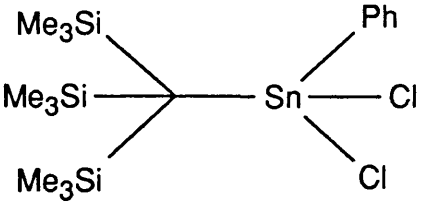

(4)

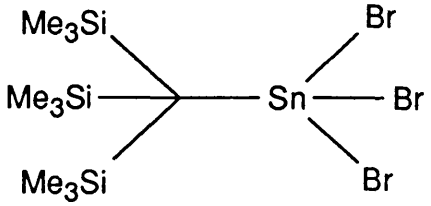

(5)

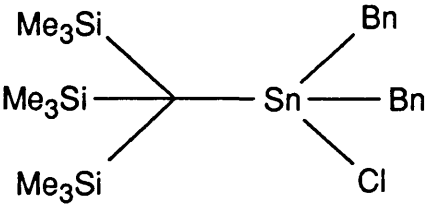

(6)

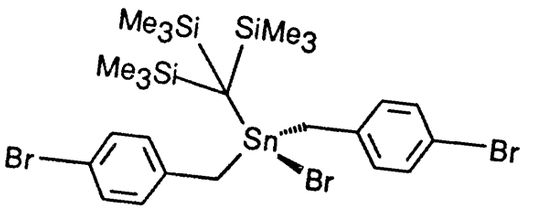
Me3Si
SiMe3
Me3Si
Sn
Br
Br
Br

(7)

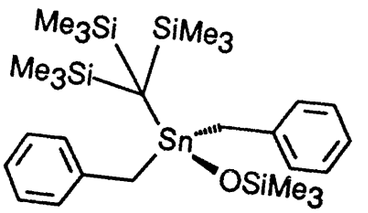
Me3Si
SiMe3
Me3Si
Sn
OSiMe3

(8)

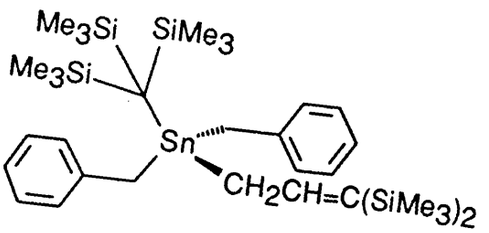
Me3Si
SiMe3
Me3Si
Sn
CH2CH=C(SiMe3)2

(9)

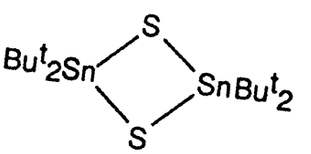
But2Sn
S
SnBut2
S

(10)

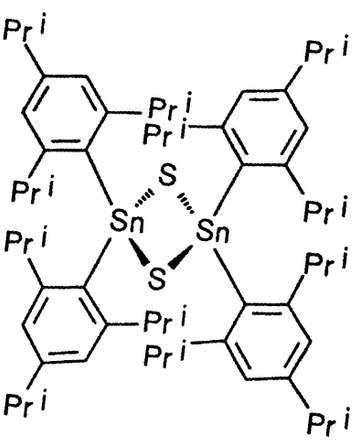
Pri
Pri
Pri
Pri
Pri
S
Sn
Sn
S
Pri
Pri
Pri
Pri
Pri
Pri
Pri

(11)

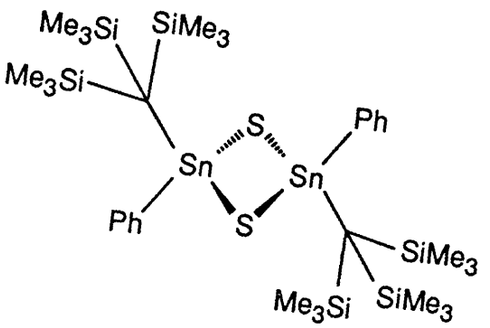
Me3Si
SiMe3
Me3Si
S
Ph
Sn
Sn
Ph
S
SiMe3
Me3Si
SiMe3

(12)

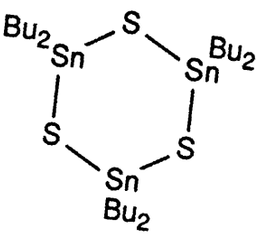
Bu2
Sn
S
Sn
Bu2
S
S
Sn
Bu2

(13)

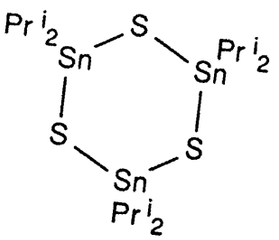
Pr i 2
Sn
S
Sn
Pr i 2
S
S
Sn
Pr i 2

(14)

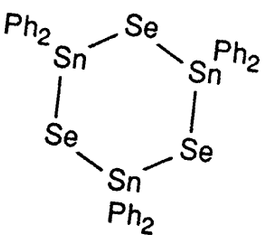
Ph2
Sn
Se
Sn
Ph2
Se
Se
Sn
Ph2

(15)

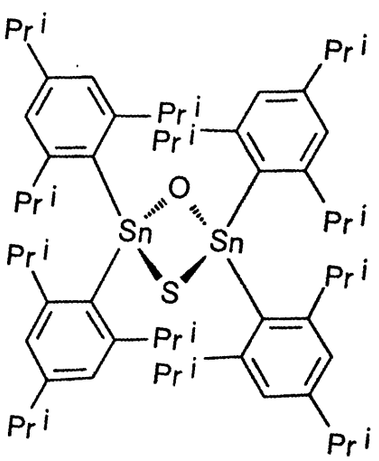
Pr i
Pr i
Pr i
Pr i
Pr i
O
Sn
Sn
Pr i
Pr i
S
Pr i
Pr i
Pr i
Pr i
Pr i

(16)

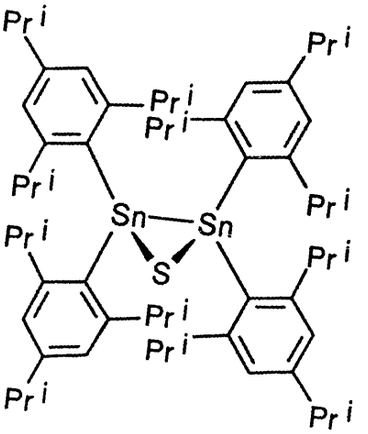
Pr i
Pr i
Pr i
Pr i
Pr i
Pr i
Pr i
Pr i
Pr i
Pr i
Pr i
Pr i
Sn
Sn
S

(17)

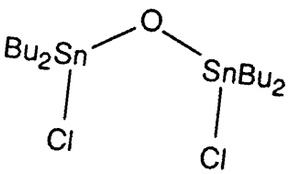
Bu2Sn
O
SnBu2
Cl
Cl

(18)

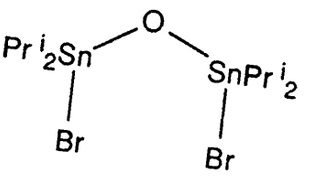
Pr i2Sn
O
SnPr i2
Br
Br

(19)

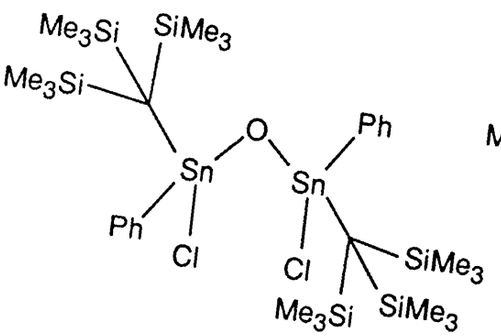
Me3Si
SiMe3
Me3Si
O
Ph
Sn
Sn
Ph
Cl
Cl
SiMe3
Me3Si
SiMe3

(20)

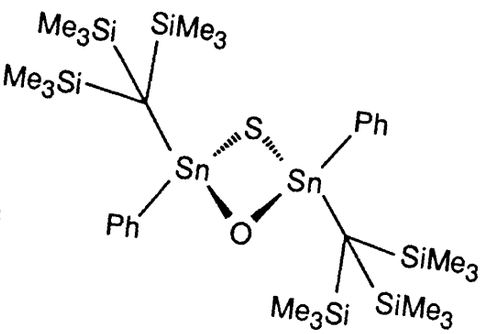
Me3Si
SiMe3
Me3Si
S
Ph
Sn
Sn
Ph
O
SiMe3
Me3Si
SiMe3

(21)

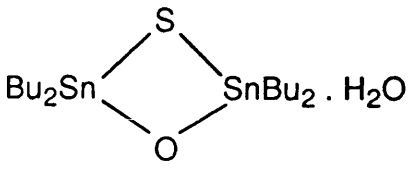
S
Bu2Sn
SnBu2 . H2O
O

(22)

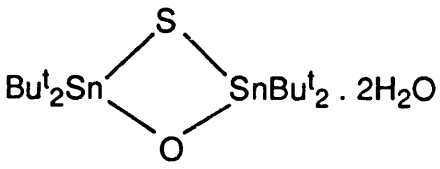
S
But2Sn
SnBut2 . 2H2O
O

(23)

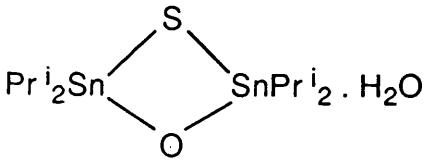
S
Pri2Sn
SnPri2 . H2O
O

(24)

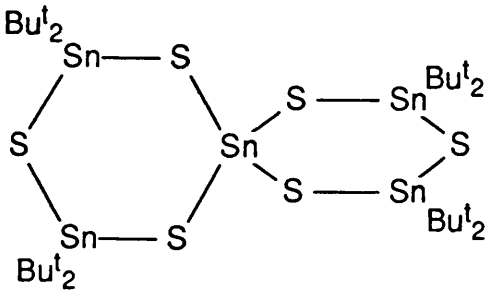
But2
Sn
S
S
Sn
S
Sn
But2
S
Sn
S
S
Sn
But2
But2

(25)

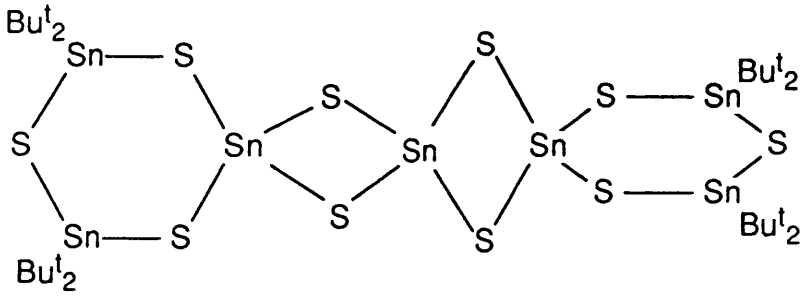
But2
Sn
S
S
Sn
S
S
Sn
S
S
Sn
But2
S
Sn
S
S
Sn
But2
But2

(26)

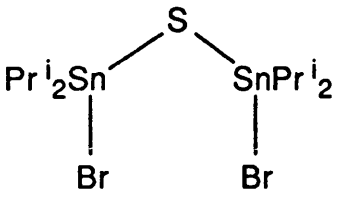

(27)

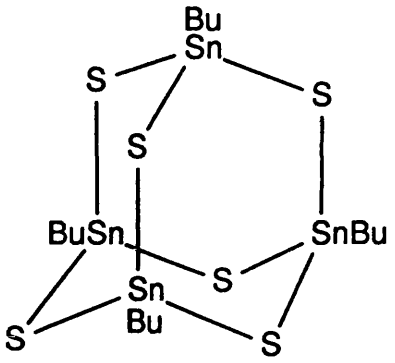

(28)

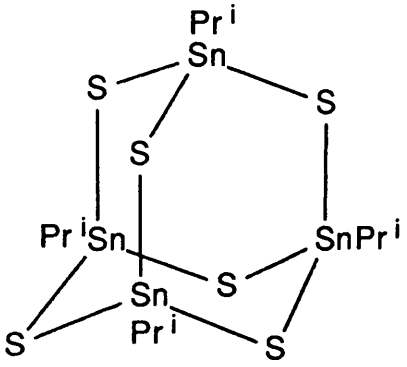

(29)

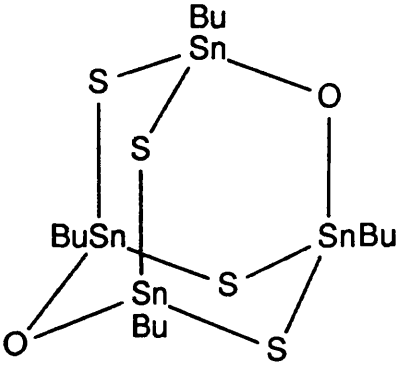

(30)

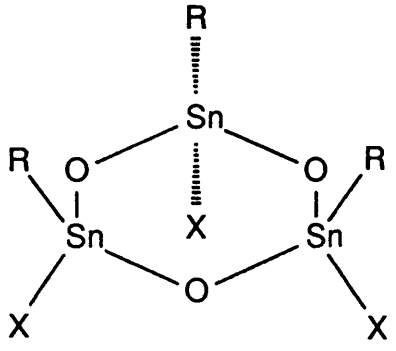

(31)

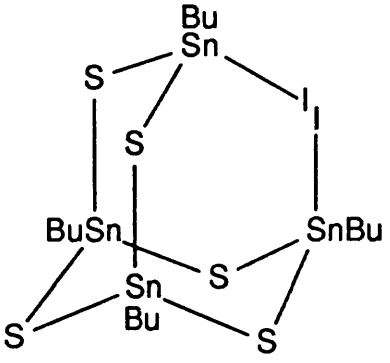

(32)

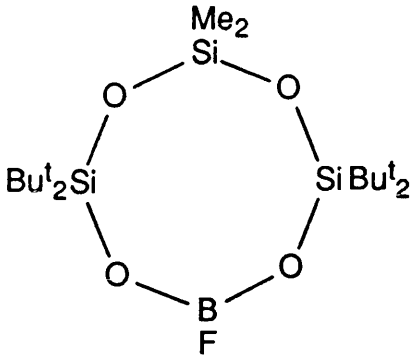

(33)

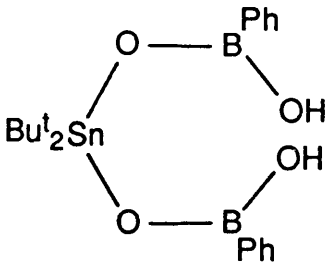

(34)

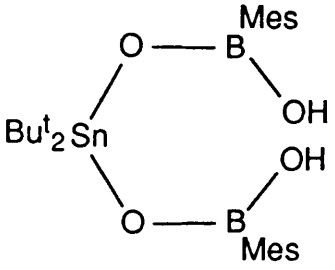

(35)

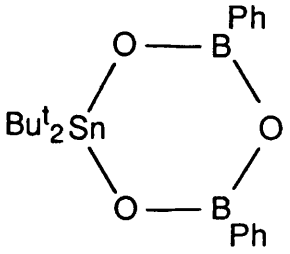

(36)

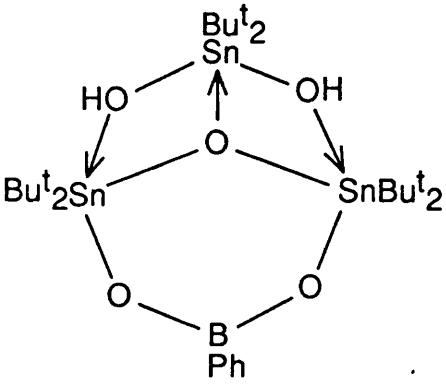

(37)

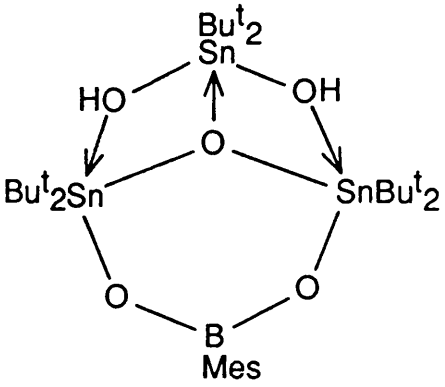

(38)